UNIVERSITY OF LIEGE
Faculty of Sciences
Department of Chemistry

Center for Education and
Research on Macromolecules (CERM)
Professor C. JEROME

Université de Liège

Tailor-made degradable copolymers for the design of advanced drug delivery systems

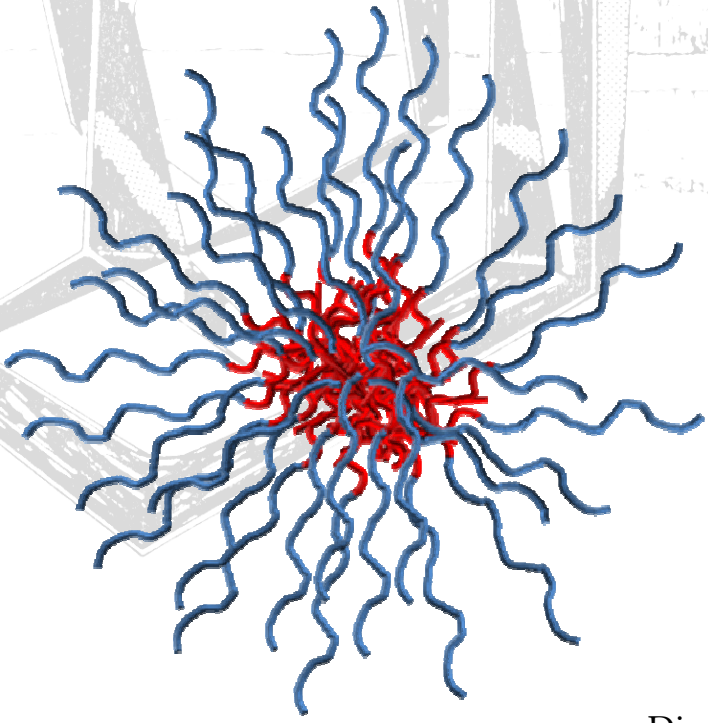

Dissertation presented by

Sébastien CAJOT

To obtain the grade of
Doctor in Sciences
Academic Year 2011-2012

Académie Universitaire Wallonie-Europe

Tailor-made degradable copolymers

for the design of advanced drug delivery systems

by Sébastien CAJOT

Over the last decades, polymer micelles have attracted an increasing interest in drug pharmaceutical research because they could be used as efficient drug delivery systems.

The goal of this thesis was centered on the design of new smart nanocarriers and more particularly on the basis of reversibly redox-cross-linked polymer micelles. The first part of that work was dedicated to the synthesis of new macromolecular architectures associating biodegradable hydrophobic polymers such as polyester (e.g. PCL), polycarbonate (e.g. PTMC) or also polyphosphate (e.g. PBODOP) and the water soluble poly(ethylene oxide) (PEO) frequently used due to its biocompatible properties. Well-defined block copolymers have been synthesized by ring-opening polymerization.

The second part of that work was focus on the cross-linking of the hydrophobic block in order to obtain well stabilized micelles. The copolymerization of α-chloro-ε-caprolactone (αClεCL) allows to easy functionalize the hydrophobic block in order to reversibly cross-link the future micelle core by the addition of a disulfide bearing cross-linker. The self assembly of theses copolymers and redox-dependent micellization behaviours have been studied by diffusion light scattering and transmission electronic microscopy.

Finally, the potential of these redox-sensitive micelles as active drug delivery system has been analysed by investigating their stealthy behaviours using the complement activation (CH50) test, their cytotoxicity, their cellular internalization and also the redox-sensitive profile of a hydrophobic dye.

Copolymères biodégradables sur mesure pour la conception de systèmes avancés d'administration des médicaments

par Sébastien CAJOT

Au cours de ces dernières décennies, la recherche pharmaceutique a marqué un intérêt croissant pour les micelles polymères puisqu'elles peuvent être utilisées comme des systèmes efficaces d'administration de médicaments.

L'objectif de cette thèse fut centré sur la conception de nouveaux nanovecteurs intelligents et plus particulièrement sur la base de micelles polymères à réticulation réversible selon le potentiel oxydo-réducteur. La première partie de ce travail fut consacrée à la synthèse de nouvelles architectures macromoléculaires associant des polymères hydrophobes biodégradables tels que les polyesters (ex. PCL), les polycarbonates (ex. PTMC) ou encore les polyphosphates (ex. PBODOP) ainsi que le polymère hydrosoluble, le poly(oxyde d'éthylène) (PEO), fréquemment utilisé en raison de son caractère biocompatible. Des copolymères séquencés bien définis ont été synthétisés par polymérisation d'ouverture de cycle.

La deuxième partie de ce travail a mis l'accent sur la réticulation de la séquence hydrophobe afin d'obtenir des micelles bien stabilisées. La copolymérisation d'α-chloro-ε-caprolactone (αClεCL) permet de fonctionnaliser facilement la séquence hydrophobe afin de réticuler de façon réversible le cœur des futures micelles par un agent réticulant porteur de ponts disulfures. L'auto-assemblage de ces copolymères ainsi que leur micellisation en fonction du potentiel oxydo-réducteur ont été étudiées par diffusion de la lumière et par microscopie électronique à transmission.

Enfin, le potentiel de ces micelles sensibles à l'environnement oxydo-réducteur en tant que système d'administration actif de médicaments a été analysé en examinant leur comportement furtif par l'intermédiaire du test d'activation du complément (CH50), leur cytotoxicité, leur internalisation cellulaire et également le profil de libération d'un colorant hydrophobe en fonction du potentiel oxydo-réducteur.

Je tiens vivement à remercier le Professeur Christine Jérôme pour m'avoir permis de réaliser ce projet de thèse et de la confiance qu'elle m'a accordée au cours de ces années. Merci pour ses conseils avisés et pour son soutien lors de mes moments de doute et de découragement malgré un emploi du temps surchargé. Par la même occasion, je tiens à remercier le Professeur Robert Jérôme pour m'avoir accueilli au CERM en 2007 afin de réaliser mon mémoire, mais également d'avoir contribué à la rédaction de ce manuscrit.

Je souhaite aussi remercier les différents partenaires liés de près ou de loin à la réalisation de cette thèse, à savoir le laboratoire du Professeur Jean-Pierre Benoît, l'INSERM U646 de l'Université d'Angers, et plus particulièrement les Docteurs Catherine Passirani, Emmanuel Garcion et Archibalt Paillard ainsi que Nolwenn Lautram pour leur accueil chaleureux au cours de mes deux séjours à Angers mais surtout pour leur disponibilité.
Merci à l'Université Catholique de Louvain qui, par l'intermédiaire du Professeur Véronique Préat, m'a ouvert les portes de son laboratoire afin de m'initier aux tests biologiques avec l'aide précieuse de Fabienne Danhier. Merci également aux Professeurs Jean-François Gohy et Charles André Fustin pour m'avoir permis d'accéder à la DLS.
Je remercie aussi le Professeur Marie-Claire De Pauw-Gillet ainsi que toute son équipe et plus particulièrement Daureen, Virginie et Mike pour l'aide apportée dans la réalisation des divers tests biologiques.

Merci à Valérie Collard ainsi qu'à Charlotte Dannemark pour leur contribution au cours des diverses synthèses réalisées ainsi que pour les injections tardives en GPC. Merci également à Martine Dejeneffe pour son aide en TEM.

Merci aux Professeurs Cameron Alexander, Véronique Préat, Marie-Claire De Pauw-Gillet, Christine Jérôme et aux docteurs Raphaël Riva et Kathy Van Butsele de me faire l'honneur d'être membre de mon jury de thèse mais également au Professeur Albert Demonceau d'avoir accepté la présidence de ce jury.

Toute ma reconnaissance va au « Fonds pour la Formation à la Recherche dans l'Industrie et dans l'Agriculture » (FRIA) pour leur apport financier au cours ce travail.

Merci à l'équipe de la Bibliothèque des Sciences pour leur disponibilité.

Je remercie également le docteur Raphaël Riva pour ses précieux conseils en ROP et « click chemistry » ainsi que pour sa participation aux différentes étapes de rédaction et de correction de cette thèse.

Je tiens aussi à remercier Justine Simon et Alexandre Ansias qui, en tant qu'étudiants, ont contribué à cette thèse de doctorat.

Un merci tout particulier à Kathy qui m'a suivi au cours de mon mémoire et qui m'a guidé et soutenu dans mes premiers pas en tant que doctorant.

Merci aux anciens collègues du +2 et +3 et tout particulièrement à Kathy, Emi, Valco, Chacha, Flogaga, Mika, Pierre, David, (Prince) Ali, Rachiiiiid (BOULA) et Sami. Votre présence ainsi que votre bonne humeur ont permis que les journées ne se ressemblent pas et que des moments inoubliables ponctuent la réalisation de cette thèse ! Merci également à toutes les personnes qui ont contribué de près ou de loin à la réalisation de cette thèse.

Toute ma sympathie va à Krystina, Enza et Sophie au vu de leur disponibilité et de l'aide qu'elles m'ont apportée.

Merci aux différents membres du Département de Chimie que j'ai eu l'occasion de côtoyer au cours de ce projet et plus particulièrement à Pierre C., Laurent, Cédric, Jennifer et Julie pour leur bonne humeur quotidienne.

Un clin d'œil tout particulier à ma petite bande de chimistes : Daureen, Jessica et Jérôme. Merci pour toutes ces années passées ensemble mais surtout pour toutes celles à venir !

Merci également à ma famille, à ma belle-famille et à mes amis pour leur présence lors des moments de découragement (et/ou de mauvaise humeur) ainsi que pour leur soutien tout au long de ces 4 années (presque 5). Merci à vous tous !

Enfin, merci à mon épouse, ma Crollette, d'être présente à mes côtés depuis plus de 5 ans maintenant et pour son soutien incessant. Merci d'avoir toujours su trouver les mots pour m'encourager et me pousser vers l'avant !

Liège, juillet 2012

Table of contents

List of figures, schemes and tables

Chapter I Novel amphiphilic mikto-arm star-shaped copolymers for the preparation of PLA-based nanocarriers

Chapter II Cross-linked Nanosystems as New Drug Delivery Systems

Chapter III Novel unsaturated polyphosphate containing amphiphilic block copolymer as promoter of core cross-linked micelles

Chapter IV Novel functional degradable block copolymers for the building of reactive micelles

Chapter VII Pegylated disulfide core cross-linked micelles based on poly(trimethylene carbonate) and functional poly(ε-caprolactone)

General conclusions and Perspectives

List of abbreviations

αClεCL	α-Chloro-ε-caprolactone
BODOP	2-(but-3-en-1-yloxy)-1,3,2 dioxaphospholane 2-oxide
CH50	Complement Haemolytic 50
$CDCl_3$	Deuterated chloroform
ClDOP	2-chloro-1,3,2-dioxaphospholane 2-oxide
CMC	Critical Micellar Concentration
CMT	Critical Micellar Temperature
CuAAC	Copper Azide-Alkyne Cycloaddition
D_h	Hydrodynamic diameter
DHBCP	Double Hydrophilic Block Copolymer
DLS	Dynamic Light Scattering
DMF	Dimethylformamide
DNA	Deoxyribonucleic acid
DOX	Doxorubicin
DP	Degree of Polymerization
DSC	Differential Scanning Calorimetry
DSDMA	bis(2-methacryloyloxyethyl)disulfide
DTT	Dithiothreitol
εCL	ε-caprolactone
EDTA	Ethylenediaminetetraacetic acid
EPR effect	Enhanced Permeability and Retention effect
FDA	Food and Drug Administration
GSH	Glutathione
HEMA	2-hydroxyethyl methacrylate
HLB	Hydrophilic lypophilic Balance
IR	Infrared
LCST	Lower Critical Solubilization Temperature

SEC	Size Exclusion Chromatography
M_n	Number average molecular weight
MPEO	Monomethoxy poly(ethylene oxide)
M_w	Weight average molecular weight
NHS	Normal Human Serum
NMR	Nuclear Magnetic Resonance
PAA	Poly(acrylic acid)
P(αClεCL)	Poly(α-chloro-ε-caprolactone)
P(αN_3εCL)	Poly(α-azido-ε-caprolactone)
PCL	Poly(ε-caprolactone)
PCMA	Poly(coumarin methacrylate)
PDI	Polydispersity index
PDEA	Poly(2-(diethylamino)ethyl methacrylate)
PDS	Pyridyldisulfide
PEEP	Poly(ethyl ethylene phosphate)
PEG	Poly(ethylene glycol)
PEO	Poly(ethylene oxide)
PGMA	Poly(glycerol monomethacrylate)
PLA	Poly(lactide)
PMAA	Poly(methacrylic acid)
PNAS	Poly(N-acryloxysuccinimide)
PNIPAAM	Poly(N-isopropylacrylamide)
PS	Poly(styrene)
PTMC	Poly(trimethylene carbonate)
ROP	Ring Opening Polymerization
SEC	Size Exclusion Chromatography
Sn(Oct)2	Tin octoate
TEM	Transmission Electron Microscopy
TGA	Thermogravimetry analysis
THF	Tetrahydrofuran
TMC	Trimethylene carbonate

AIM OF THE THESIS

Aim of the thesis

The aim of this thesis was to design new amphiphilic macromolecules in order to build well-defined nanocarriers in aqueous media able to drive hydrophobic drugs specifically to the targeted site, tumor tissues, with limited effects on healthy organs.

The **chapter I** is focused on the synthesis of three-arm (A_2B) and four-arm (A_2B_2) star-shaped copolymers based on blocks commonly used in drug delivery systems, i.e. the poly(ethylene oxide) (PEO) and the poly(ε-caprolactone) (PCL). With the aim to study the effect of the macromolecular architecture, these novel star copolymers have been compared to conventional diblock copolymers of PEO-*b*-PCL in their ability to form micelles and to stabilize PLA nanoparticles.

One of the major limitations of conventional self-assembled nanocarriers is their lack of stability towards high dilution, particularly occuring upon administration by i.v. injection. This leads to a premature release and precipitation of the encapsulated drug in non-targeted sites. The **chapter II** aims at reviewing advances made in the last decades in the development of stable nanocarriers based on cross-linked systems such as nanogels or cross-linked micelles.

The **chapter III** is dedicated to the synthesis of irreversibly core cross-linked micelles based on the synthesis of a new cyclic phosphate monomer bearing an unsaturated group. These vinylic side-groups along the polyphosphate backbone, allow the cross-linking of the micelle core by simple UV irradiation of the self-assembled structures.

After the accumulation of the nanocarriers in tumor cells by passive or active targeting, the encapsulated drugs need to be released intracellularly from the nanocarriers. This can be achieved by elaborating smart micelles able to dissociate in response to the

reductive environment of the cytoplasm. This essential aspect will be the topic of the **chapters IV** to **VII**.

To build such micelles, there is a need of reactive block copolymers easily functionalizable. These have been designed based on a hydrophilic block of PEO and a reactive hydrophobic block of PCL or poly(trimethylene carbonate) (PTMC). This hydrophobic block obtained by the random or sequential copolymerization of a functional lactone, the α-chloro-ε-caprolactone was easily derivatized further by click chemistry after substitution for an azide. The synthesis of these novel amphiphilic reactive copolymers, their self-assembly in aqueous media and the post-functionalization by various alkyne-dyes of their micelle core are described in the **chapter IV**.

Then, the cross-linking of such PCL based reactive micelles by a dedicated cross-linker bearing a disulfide bridge has been considered in the **chapter V** such as their stealthy behaviors. The **chapter VI** reports on the cytotoxicity, the cellular internalization and the glutathione-triggered drug release of these PCL-based core cross-linked micelles.

Finally, the **chapter VII** is focused on reversibly cross-linked micelles of the PTMC based copolymers. Their physico-chemical properties, their circulation life-time in the blood stream, their cytotoxicity and their cellular uptake are studied and compared to previous results obtained in the **chapter V** and **VI** for the PCL based cross-linked micelles.

CHAPTER I

Novel amphiphilic mikto-arm star-shaped copolymers for the preparation of PLA-based nanocarriers

S. Cajot, R. Riva, L. Billiet, F. Du Prez, M. Alexandre, P. Lecomte, C.Jérôme

Macromolecular Symposia, **2011**, 309/310, 111-122

Abstract

Three-arm (A_2B) and four-arm (A_2B_2) star-shaped copolymers based on biocompatible and biodegradable hydrophobic poly(ε-caprolactone) (PCL) (A arms) and biocompatible and bioeliminable hydrophilic poly(ethylene oxide) (PEO) (B arms) were synthesized by the coupling of an ω-azide terminated PEO chains with PCL chain bearing one (A_2B) or two (A_2B_2) alkyne functions at the middle of the chain by the copper mediated azide-alkyne cycloaddition (CuAAC). The amphiphilic behavior of these different stars was confirmed by micellization experiments in water followed by dynamic light scattering and transmission electron microscopy analyses. The efficiency to stabilize PLA nanoparticles was investigated in function of the stars structure.

1. Introduction

Nowadays, an increasing interest was paid to the use of nanoparticles for the development of new drug delivery systems. Polymer micelles are well known nanoparticles composed of biocompatible and biodegradable amphiphilic copolymers already used for drug encapsulation. Indeed, many new drugs are poorly soluble in water, which leads to their rapid elimination from the body by enzymatic degradation or by metabolization. Drug encapsulation in nanometric particles improves their solubility in water, increasing the action time by controlling the drug release. Moreover, nanoparticles prevent the chemical and enzymatic degradation of the active principle and, when it is necessary, decrease its toxicity[1,2].

Drug nanocarriers are characterized by colloidal suspensions of submicronic particles in an aqueous medium that can be directly injected in the blood stream[3]. They have to be composed of biocompatible polymers in order to prevent them from the effect of the stealth defense against foreign bodies. Various kinds of nanocarriers are described in the literature such like micelles [2,4,5], nanoparticles[6,7] and liposomes[8]. Polymer micelles are supramolecular shell-core structures with a diameter of ten nanometers and are composed of amphiphilic block copolymers. By their supramolecular structure, polymer micelles are able to encapsulate a hydrophobic drug into their core, which allows increasing concentration to be reached in water.

Polymer nanoparticles are another type of polymer based nanocarrier generally prepared starting from hydrophobic and biodegradable biocompatible polymer, in which the drug is encapsulated. Their sizes are generally around one hundred nanometers. The use of amphiphilic copolymers is then required to stabilize such nanoparticles in aqueous media.
Aliphatic polyesters, such as poly(ε-caprolactone) (PCL) or poly(lactide) (PLA), are highly reported in the literature for the preparation of these nanocarriers. These polyesters are easily degradable by hydrolysis of the ester bonds leading to a decrease of the molecular weight. Short polymer chains are then removed by solubilization in the biological fluids or by

phagocytosis. The degradation is catalyzed by acids or bases for PCL (PCL is known as an hydrolysable polymer) while enzymes catalyze the PLA degradation which is an actual biodegradable material [9,10].

The poly(ethylene oxide) (PEO) is frequently used as hydrophilic block of amphiphilic structures used in vectorisation [11,12]. PEO is a neutral, hydrophilic, highly flexible and biocompatible polymer and is approved by the Food and Drug Administration (FDA) for intravenous applications. Contrary to aliphatic polyesters, PEO is not (bio)degradable but bioeliminable by renal filtration when the molecular weight remains lower than 20000 g/mol. Moreover, the flexibility of the PEO, due to the absence of bulky substituent and the easy rotation of the ether bonds, disfavors the adsorption of plasmic proteins at the surface of the nanocarrier, leading to nanocarriers of second generation [13] exhibiting prolonged circulation in the blood stream. Such carrier thus can accumulate in tumors by the EPR effect (Enhanced permeability and Retention Effect) [14,15].

The synthesis and applications of amphiphilic diblock copolymers based on PEO and PCL for pharmaceutical application are largely described in the literature due to their ability to form stable micelles[16, 17] or to stabilize PLA nanoparticles in solution. Typically, when the molecular weight of the hydrophilic block (PEO) is higher than the hydrophobic block (PCL) (HLB > 10), the amphiphilic copolymers are generally prone to form spherical micelles. In contrast, when the molecular weight of the hydrophobic block is higher than the hydrophilic one (HLB<10), the copolymer is rather used for nanoparticles stabilization. As already reported, the stabilization efficiency appears not only to depend on the copolymer composition (or hydrophilic/lipophilic balance, HLB) but also on the architecture of the copolymer. For example, palm-tree copolymers of PEO and PCL have been found more efficient than diblock copolymers of the same HLB for the stabilisation of PLA nanoparticles[7].

In this paper, we focus on another type of architecture, i.e. star-shape copolymers with the aim to evidence another architecture effect on micellization and/or nanoparticles stabilization efficiency. Interestingly, these stars systems allow to vary the number of PEO arms (one or two) grafted on the mid-chain of a PCL backbone (Figure 1) and, to our

knowledge, have so far not yet been investigated for nanomedecine. For this purpose, a novel strategy to synthesize well-defined three- and four-arm star-shaped amphiphilic copolymers based on PEO and PCL (Figure 1) has been first investigated and is reported in the present paper. Then, the micellization so as the efficiency to stabilize PLA nanoparticle of these star copolymers, have been studied in order to highlight the potential of such architecture to be used in drug delivery systems. Particularly, the effect of these star architectures on the micelles size and shape and on the nanoparticles stabilization efficiency will be discussed based on comparison to more conventional diblock and graft copolymers.

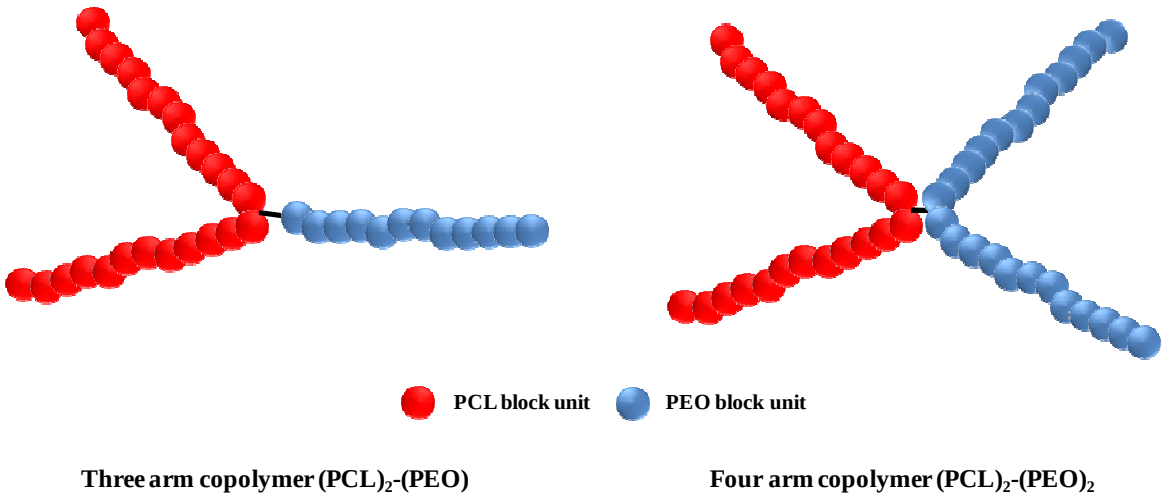

Figure 1. Structures of the three- and four-arm star-shaped copolymers

Such study requires first the careful synthesis of well-defined star copolymers. Two similar routes were developed for the synthesis of the three-arm (A_2B) (Scheme 1) and four-arm (A_2B_2) (Scheme 2) star-shaped copolymers based on the copper catalyzed coupling of ω-azido-poly(ethylene oxide) with a poly(ε-caprolactone) chain bearing one or two alkyne groups at the mid-chain.

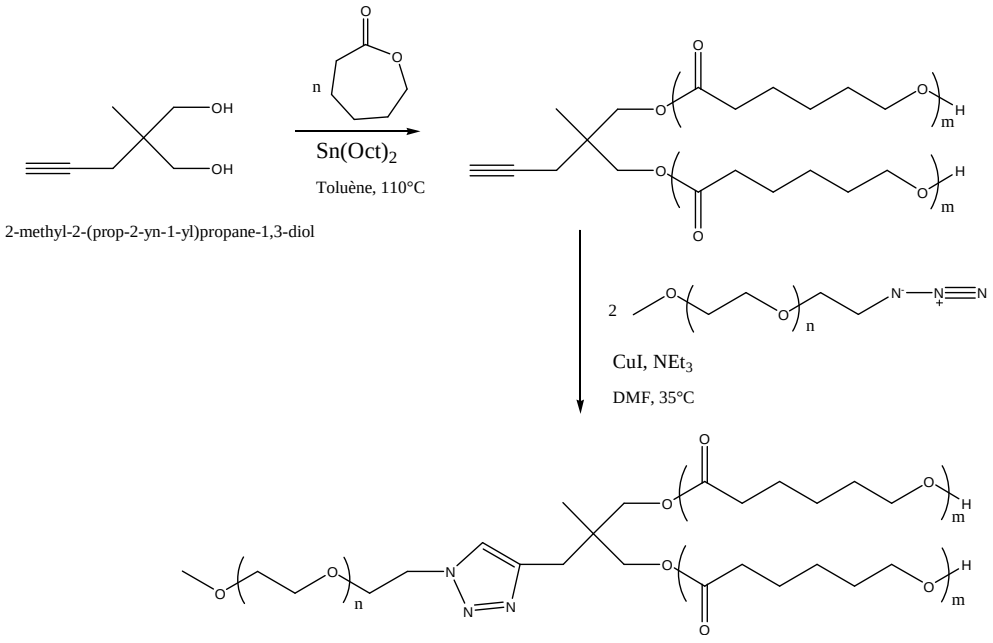

Scheme 1. Synthesis strategy for the A_2B star copolymers

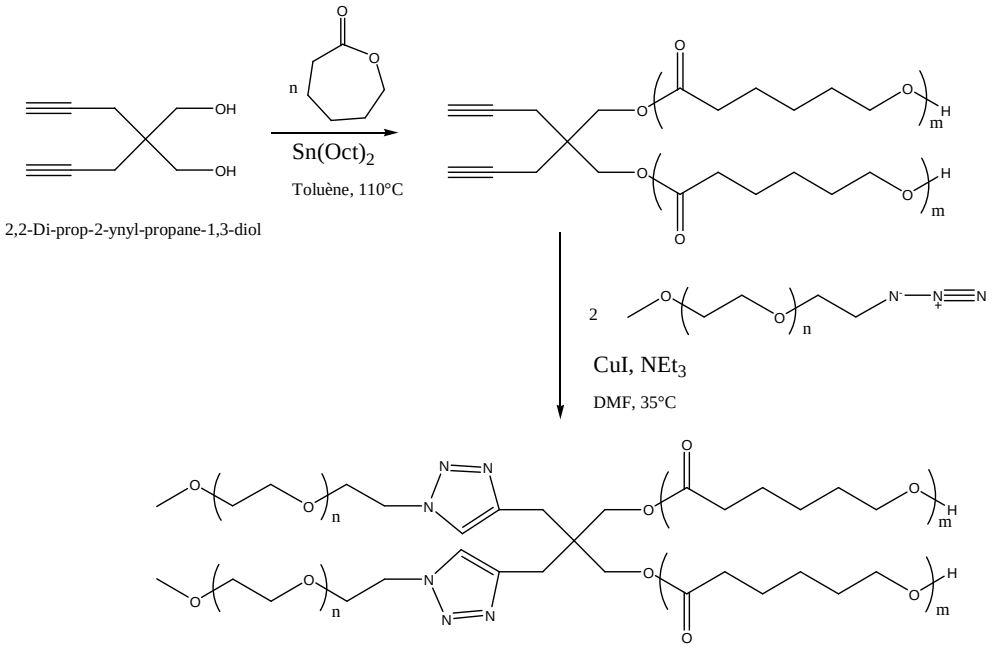

Scheme 2. Synthesis strategy for the A_2B_2 star copolymers

2. Materials and methods

Materials

Monomethoxy poly(ethylene oxide) (M_n = 1000 and 2000 g/mol, MPEO-OH, Aldrich), *N*,*N*-dimethylformamide (DMF, Aldrich), dimethylsulfoxide (DMSO, Aldrich) methanol (Chem-lab), dichloromethane (CH_2Cl_2, Chem-lab), heptane (Chem-lab), diethyl ether (Chem-Lab), triethylamine (NEt_3, Aldrich), tin 2-ethylhexanoate ($SnOct_2$, Fluka), sodium azide (Aldrich), copper(I) iodide (CuI, Aldrich), poly(D,L-lactide) (PLA, Purac) were used as received. The synthesis of 2-methyl-2-(prop-2-yn-1-yl)propane-1,3-diol and 2-methyl-2-(prop-2-yn-1-yl)propane-1,3-diol were reported elsewhere[18]. ε-caprolactone (ε-CL) (Aldrich) was dried over calcium hydride at room temperature for 48 h and distilled under reduced pressure just before use. Toluene and dichloromethane were dried on molecular sieves under nitrogen.

Synthesis of the alkyne bearing poly(ε-caprolactone)

The polymerization of ε-CL was carried out at 110 °C in toluene. Typically, 2-methyl-2-(prop-2-yn-1-yl)propane-1,3-diol or 2-methyl-2-(prop-2-yn-1-yl)propane-1,3-diol (0.304 g, 1.997 mmol) was transferred in a previously dried glass reactor. After three azeotropic distillations with toluene, εCL (4 mL, 35 mmol) and anhydrous toluene (10 mL) were sequentially added to the reactor through a rubber septum with a syringe equipped with a stainless steel capillary. The reactor was then thermostated at 110 °C before adding the catalyst (0.3 mL, 0.06 M $SnOct_2$ in toluene). After 5 h of polymerization, PCL was recovered by precipitation in cold heptane.[19]

PCL-(alkynes)$_1$: ^{1}H NMR($CDCl_3$) δ (ppm) = 1 (s, 3H, C-C***H***$_3$), 1.4 (m, 2H, CO-CH_2-CH_2-C***H***$_2$-CH_2-CH_2-O-), 1.6 (m, 4H, CO-CH_2-C***H***$_2$-CH_2-C***H***$_2$-CH_2-O-), 2 (m, 3H, ***H***C≡C-C***H***$_2$-), 2.4 (t, 2H, CO-C***H***$_2$-CH_2-CH_2-CH_2-CH_2-O-), 3.6 (t, 2H, terminated -C***H***$_2$-OH), 4.1 (t, 2H, CO-CH_2-CH_2-CH_2-CH_2-C***H***$_2$-O- and 2H, -C***H***$_2$-O-CO-).

PCL-(alkynes)$_2$: ^{1}H NMR ($CDCl_3$) δ (ppm) = 1.4 (m, 2H, CO-CH_2-CH_2-C***H***$_2$-CH_2-CH_2-O-), 1.6 (m, 4H, CO-CH_2-C***H***$_2$-CH_2-C***H***$_2$-CH_2-O-), 2 (m, 3H, ***H***C≡C-C***H***$_2$-), 2.4 (t, 2H, CO-C***H***$_2$-CH_2-CH_2-CH_2-CH_2-O-), 3.6 (t, 2H, terminated -C***H***$_2$-OH), 4.1 (t, 2H, CO-CH_2-CH_2-CH_2-CH_2-C***H***$_2$-O- and 2H, -C***H***$_2$-O-CO-).

Synthesis of the ω-azido terminated-poly(ethylene oxide)

Monomethoxy poly(ethylene oxide) (1.5 g, 1.2 10^{-3} mol, M_n = 1250 g/mol) was transferred in a previously dried glass reactor and dried by three azeotropic distillations with anhydrous toluene. 15 mL of anhydrous dichloromethane were then added with an excess of *p*-toluenesulfonyl chloride (0.02 g, 1.2 10^{-2} mol) and triethylamine (0.02 mL, 1.3 10^{-2} mol). The reaction was carried out at room temperature for 48 hours. The organic phase was washed two times with saturated solution of $NH_4^+Cl^-$, one time with water before to be dried on anhydrous $MgSO_4$. The polymer was recovered by precipitation in cold diethyl ether. The ω-tosyl-poly(ethylene oxide) (1.2 g, 9.6 10^{-4} mol, M_n = 1250 g/mol) was transferred in a previously dried glass reactor and dried by three azeotropic distillations of anhydrous toluene. 120 mL of *N*,*N*-dimethylformamide were added with an excess of sodium azide (0.09 g, 1.4 10^{-3} mol). The reaction was carried out overnight at 30°C. DMF was removed under reduce pressure. The polymer was dissolved in dichloromethane and was washed three times with water then, the ω-azido-PEO was extracted from the collected aqueous phases by using dichloromethane. Organic phases were combined and dried on anhydrous $MgSO_4$. The polymer was recovered by precipitation in cold diethyl ether.

ω-Tosyl-PEO: ^{1}H NMR ($CDCl_3$) δ (ppm) = 2.4 (s, 3H, C***H***$_3$-$C_6H_4SO_3$-), 3.4 (s, 3H, C***H***$_3$-O-), 3.6 (m, 4H, -C***H***$_2$-C***H***$_2$-O-), 4.1 (t, 2H, -C***H***$_2$-O-SO_2-), 7.3 – 7.8 (d, 4H, -SO_2-C_6***H***$_4$-CH_3).
ω-N_3-PEO: ^{1}H NMR ($CDCl_3$) δ (ppm) = 3.4 (s, 3H, C***H***$_3$-O-), 3.6 (m, 4H, -C***H***$_2$-C***H***$_2$-O-, -C***H***$_2$-N_3).

Synthesis of the copolymers A_2B and A_2B_2 by CuAAC

The coupling of the ω-azido-poly(ethylene oxide) (0.4 g, 3.2 10^{-4} mol, M_n= 1250

g/mol) with the poly(ε-caprolactone) bearing the alkyne(s) (e.g. for PCL-bis-alkyne: 0.77 g, 3.2 10^{-4} mol, M_n= 2400 g/mol) was carried out in a glass reactor containing THF. CuI (0.7 mg, 3.2 10^{-6} mol) and triethylamine (0.4 µL, 3.2 10^{-6} mol) were added to the polymer solution and let reacted at 35°C during 4 hours. The star copolymers were recovered by two precipitations in cold heptane.

Three-arm star-shaped copolymer $(PCL)_2$-*b*-PEO: ^{1}H NMR ($CDCl_3$) δ (ppm) = 1 (s, 3H, C-C***H***$_3$), 1.4 (m, 2H, CO-CH_2-CH_2-C***H***$_2$-CH_2-CH_2-O-), 1.6 (m, 4H, CO-CH_2-C***H***$_2$-CH_2-C***H***$_2$-CH_2-O-), 2 (m, 3H, ***H***C≡C-C***H***$_2$-), 2.4 (t, 2H, CO-C***H***$_2$-CH_2-CH_2-CH_2-CH_2-O-), 2.7 (s, 2H, triazole-C***H***$_2$-), 3.4 (s, 3H, CH_3-O-) 3.6 (m, 4H, PEO -C***H***$_2$-C***H***$_2$-O-), 3.9 (m, 2H, -C***H***$_2$-O-CO- and 2H, -C***H***$_2$-CH_2-triazole), 4.1 (t, 2H, CO-CH_2-CH_2-CH_2-CH_2-C***H***$_2$-O-), 4.5 (m, -CH_2-C***H***$_2$-triazole), 7.7 (s, 1H, triazole(***H***))

Four-arm star-shaped copolymer $(PCL)_2$-*b*-$(PEO)_2$: ^{1}H NMR ($CDCl_3$) δ (ppm) = 1.4 (m, 2H, CO-CH_2-CH_2-C***H***$_2$-CH_2-CH_2-O-), 1.6 (m, 4H, CO-CH_2-C***H***$_2$-CH_2-C***H***$_2$-CH_2-O-), 2 (m, 3H, ***H***C≡C-C***H***$_2$-), 2.4 (t, 2H, CO-C***H***$_2$-CH_2-CH_2-CH_2-CH_2-O-), 2.7 (s, 2H, triazole-C***H***$_2$-), 3.4 (s, 3H, CH_3-O-) 3.6 (m, 4H, PEO -C***H***$_2$-C***H***$_2$-O-), 3.9 (m, 2H, -C***H***$_2$-O-CO- and 2H, -C***H***$_2$-CH_2-triazole), 4.1 (t, 2H, CO-CH_2-CH_2-CH_2-CH_2-C***H***$_2$-O-), 4.5 (m, -CH_2-C***H***$_2$-triazole), 7.7 (s, 1H, triazole(***H***))

Micellisation in water

Aqueous micelle dispersions of the star copolymers were obtained by addition of water to an organic solution. A stock solution of star copolymer was prepared with a well-defined concentration (1%) in DMF. Then, 20 mL of water (Milli-Q) were added to 5 mL of the organic solution under vigorous stirring for two hours. The solutions were dialyzed against water by using a cellulose dialysis membrane (Spectrapor, cut-off 3500) overnight.

Formation of stabilized PLA nanoparticles in water

Nanoparticles of PLA were prepared by the nanoprecipitation technique[20] in presence of various amounts of three or four-arm star-shaped copolymers as already reported for

diblock and palm-tree copolymers based on PEO and PCL[7]. Two stock solutions of PLA (16 mg/mL) or star copolymers (16 mg/mL) were prepared in DMSO. Various amounts of the star solution (10, 20, 30, 40, 50, 60 and 70wt%) were added to 2 mL of PLA solution. Five volumes of phosphate buffer (pH=7.4) were then added to the organic mixture under vigorous stirring for two hours. The solutions were dialyzed against water by using a cellulose dialysis membrane (Spectrapor, cut-off 6000-8000) overnight.

Characterization techniques

Size exclusion chromatography (SEC) was carried out in THF at 45 °C at a flow rate of 1 mL/min with a SFD S5200 auto sampler liquid chromatograph equipped with a SFD refractometer index detector 2000. The PL gel 5 µm (10^5 Å, 10^4 Å, 10^3 Å, and 100 Å) columns were calibrated with polystyrene standards. For pure PCL samples, the molecular weights were corrected by Mark-Houwink relation: $M_n(PCL) = 0.259Mn(PS)^{1.073}$. ^1H NMR spectra were recorded in $CDCl_3$ at 400 MHz in the FT mode with a Bruker AN 400 apparatus at 25°C. The infrared spectra were recorded with a Perkin-Elmer FT-IR 1720X. The IR samples were prepared by slow evaporation of a star solution, in THF, onto NaCl windows. Dynamic light scattering measurements were performed using a Beckman Coulter Delsa Nano C Particle analyzer and the data were treated by the Delsa Nano UI 2.21 software. All the measurements were carried out at 25 °C at a measuring angle of 165°. The samples for transmission electron microscopy (TEM) were prepared by slow evaporation of the solutions after DLS analysis on a formvar-coated copper grid. The excess of solution was removed with a filter paper. The samples were analyzed with a Philips CM100 microscope equipped with an Olympus camera and transferred to a computer equipped with the Megaview system.

3. Results and discussion

2-methyl-2-(prop-2-yn-1-yl)propane-1,3-diol and 2-methyl-2-(prop-2-yn-1-yl)propane-1,3-diol are two diols already used in polyurethane chemistry so that their synthesis is already described in the literature[18]. These two diols have been used here as difunctional initiator for the ring opening polymerization of εCL in order to reach both targeted mono-alkyne-PCL (PCL-(alkyne)$_1$) and bis-alkyne-PCL (PCL-(alkyne)$_2$), respectively. The polymerization performed in anhydrous toluene at 110°C in presence of conventional tin 2-ethylhexanoate as catalyst with the same monomer to initiator ratio led to two poly(ε-caprolactone)s having the macromolecular characteristics reported in table 1.

Table 1. Macromolecular characteristics of the obtained PCL-(alkyne)$_1$ and PCL-(alkyne)$_2$

	DP_{th} [a]	**$M_{n,\,th}$ [b]**	**DP_{exp} (^{1}H NMR) [c]**	**$M_{n,\,exp}$ (^{1}H NMR) [d]**	**DP_{exp} (SEC) [e]**	**$M_{n,\,exp}$ (SEC) [f]**	**M_w/M_n (SEC) [g]**
PCL-(alkyne)$_1$	18	2000	18.5	2100	17	1900	1.10
PCL-(alkyne)$_2$	18	2000	21	2400	23	2600	1.17

[a] Theoretical value for the polymerization degree of PCL calculated by the [monomer] /[initiator] ratio,

[b] Theoretical value for the molecular weight (g/mol) of PCL

[c] Polymerization degree determined of PCL by ^{1}H NMR

[d] Molecular weight (g/mol) of PCL determined by ^{1}H NMR,

[e] Polymerization degree of PCL determined by SEC,

[f] Molecular weight (g/mol) of PCL measured by SEC (universal calibration),

[g] Polydispersity index determined by SEC.

As an example, the ^{1}H NMR spectrum for the bis-alkyne-PCL is shown in Figure 2 allowing determination of the molecular weight by the comparison of the intensity of the characteristic peaks of the alkyne at 2 ppm (peak **a** and **b**, Fig. 2) with the protons at 4.2 ppm of the εCL unit (peak **h**, Fig. 2) according to equation 1:

$$M_n = \frac{I_h/2}{I_{a\ and\ b}/3}\ x\ 114 \qquad (1)$$

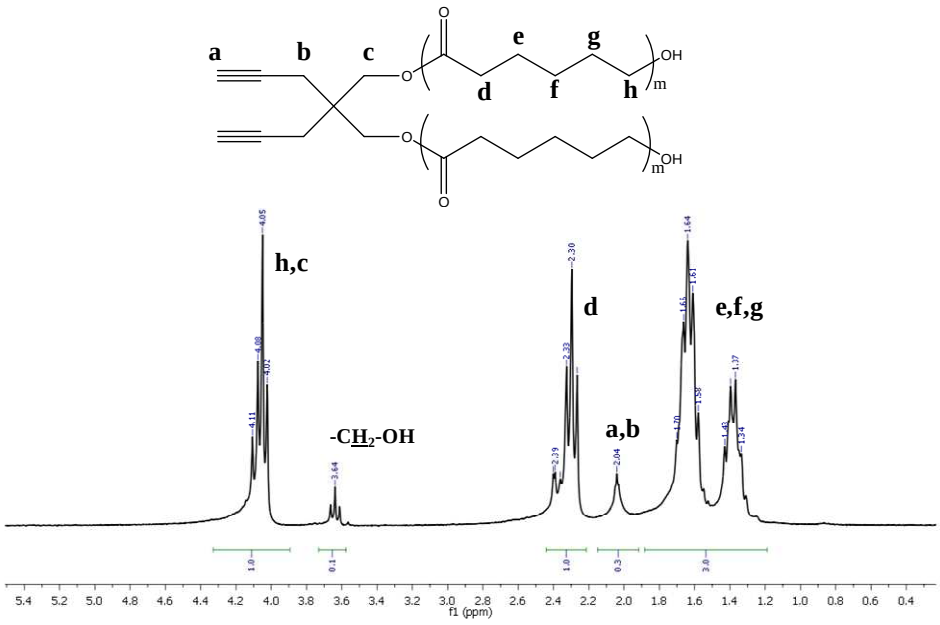

Figure 2. ^{1}H NMR spectrum of the PCL-(alkyne)$_2$ in $CDCl_3$

The ^{1}H NMR spectrum of PCL-(alkyne)$_1$ (not shown) is quite similar excepted the presence of an additional signal at 1 ppm corresponding to the CH_3 group present on the initiator and gives the data reported in table 1. For both polymers, a good agreement between the theoretical and experimental molecular weights is observed. Moreover, the polydispersity indexes as determined by SEC are very low. These PCLs exhibiting one or two alkyne groups at the middle of the chain will be used further to anchor one or two PEO arms by CuAAC to get the two targeted stars. This requires first the functionalization of PEO chain-end with an azide group.

The conversion of the hydroxyl chain end of two α-methoxy-ω-hydroxy-PEO ($M_n(PEO_A)$=1000 g/mol and $M_n(PEO_B)$=2000 g/mol) into azide was performed by a two-step reaction. First, the hydroxyl end-group was converted into tosylate, a better leaving group. The ^{1}H NMR spectrum corresponding to tosyl-PEO_A is shown Figure 3-**a.** The functionalization yield was determined by comparison of the intensity of the methoxy protons at 3.3 ppm and the protons of the tosyl group at 7.8 ppm. A quantitative conversion was

obtained with high yield (90%). Azide end-group was then obtained by reaction of the tosylate terminated PEO with an excess of sodium azide. A quantitative conversion was also confirmed by a complete disappearance of the signals of the aromatic protons of the tosyl group at 2.4, 7.3 and 7.8 ppm and of the -CH_2- protons at the α-position of the tosyl at 4.2 ppm. The presence of the azide group was confirmed by FTIR analysis by the appearance of a characteristic absorption band at 2106 cm^{-1} (Figure 3-**c**). Except for the chain-end functionality, the mild conditions used during both reactions kept unchanged the PEO chains as shown by the SEC elugrams recorded before and after reactions (Figure 3-**b)**. The same conclusions can be drawn for the functionalization of PEO_B even if the M_n is doubled.

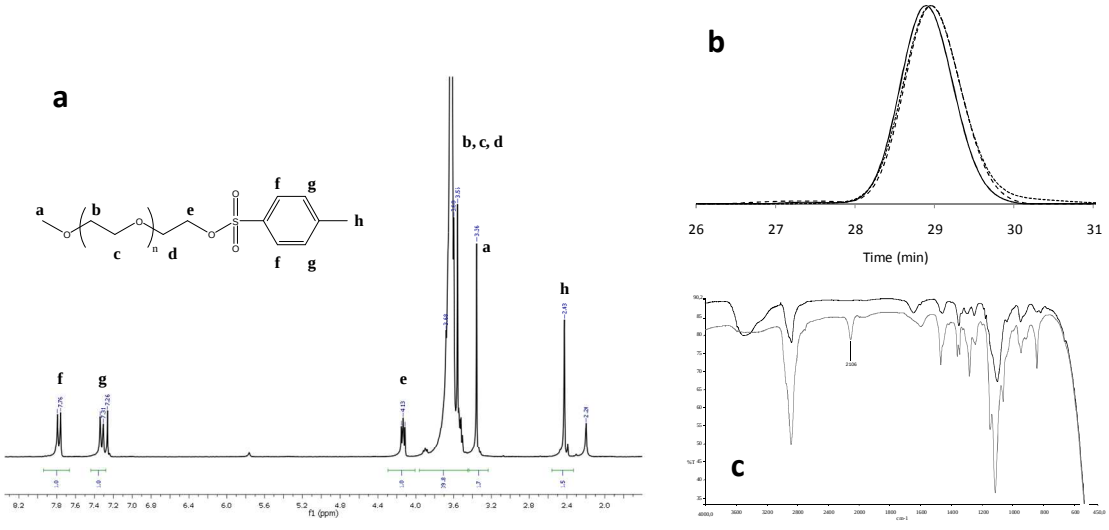

Figure 3. (**a**) ^{1}H NMR spectrum of the ω-tosyl-PEO_A (M_n = 1250 g/mol) in $CDCl_3$, (**b**) SEC traces in THF of ω-hydroxy-PEO_B (M_n = 2100 g/mol) (– –), ω-tosyl-PEO_B (——) and ω-azido-PEO_B (.....) and (**c**) FITR spectrum of ω-tosyl-PEO_B (black) and ω-azido-PEO_A (grey)

The coupling reaction between the PCL-$(alkyne)_1$ or PCL-$(alkyne)_2$ with the ω-azido-$PEO_{A\ or\ B}$ was performed by CuAAC in THF in presence of 10mol% of CuI and NEt_3. The progress of the reaction was followed by the decrease of the intensity of the azide band in the IR spectrum. After four hours of reaction, the intensity of the azide band was low and remained constant in time. This observation was explained by the presence of a small excess of ω-azido-PEO during the reaction even if reaction in stoechiometric conditions was

targeted. The star copolymer obtained after precipitation was first analyzed by SEC which confirmed by the shift of the SEC trace to lower elution volume after the coupling reaction, the quantitative conversion of PCL-(alkyne)$_1$ and PCL-(alkyne)$_2$ in star copolymers of expected three-arm (PCL)$_2$-PEO$_B$ (Figure 4-**c**) and four-arm (PCL)$_2$-(PEO)$_2$ (Figures 4-**a** and 4-**b**). A small amount of ω-azido-PEO was still detected after purification mainly from the catalyst by precipitation in cold heptane. Indeed, this solvent does not allowed the separation of the residual ω-azido-PEO from the star. Nevertheless, the presence of this small amount of free PEO chains in the star samples was not deleterious for the formation of micelles or nanoparticles as it will be shown later.

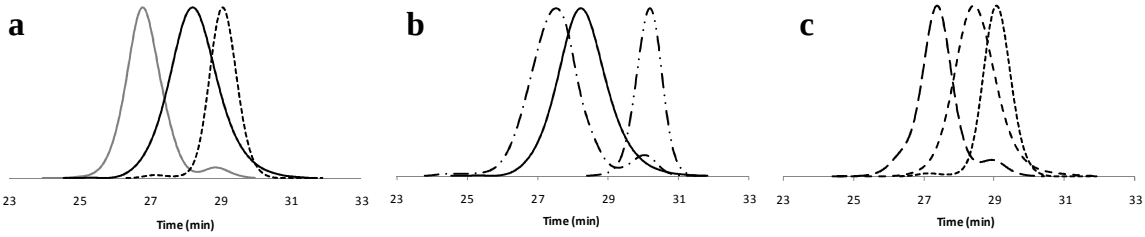

Figure 4: SEC traces recorded for the coupling between the PCL-(alkyne)$_1$ and PCL-(alkyne)$_2$ with ω-azido-PEO:

a: (PCL)$_2$-(PEO$_B$)$_2$ ——, PCL-(alkyne)$_2$ ——, ω-azido-PEO$_B$ (M_n=2100g/mol) .....

b: (PCL)$_2$-(PEO$_A$)$_2$ — . —, PCL-(alkyne)$_2$ ——, ω-azido-PEO$_A$ (M_n=1250g/mol) — . . .

c: (PCL)$_2$-PEO$_B$ — —, PCL-(alkyne)$_1$ – – – , ω-azido-PEO$_B$ (M_n = 2100 g/mol) .....,

^{1}H NMR also confirmed the coupling thanks to the appearance of a new signal at 7.7 ppm, characteristic of the proton of the triazole ring (peak f, Figure 5) and at 4.5 ppm and 2.7 ppm, corresponding to two CH_2 next to triazole ring (peak e and g, Figure 5). A ratio of 0.96 between the intensity of the two -CH_2- groups next to the triazole ring that belong to the PCL (peak g, Figure 5) and PEO arms (peak e, Figure 5), confirmed the quantitative coupling reaction. The excess of ω-azido-PEO could not be determined by ^{1}H NMR since the signal of the CH_2 next to the azide is covered by the large signal of the proton of the PEO.

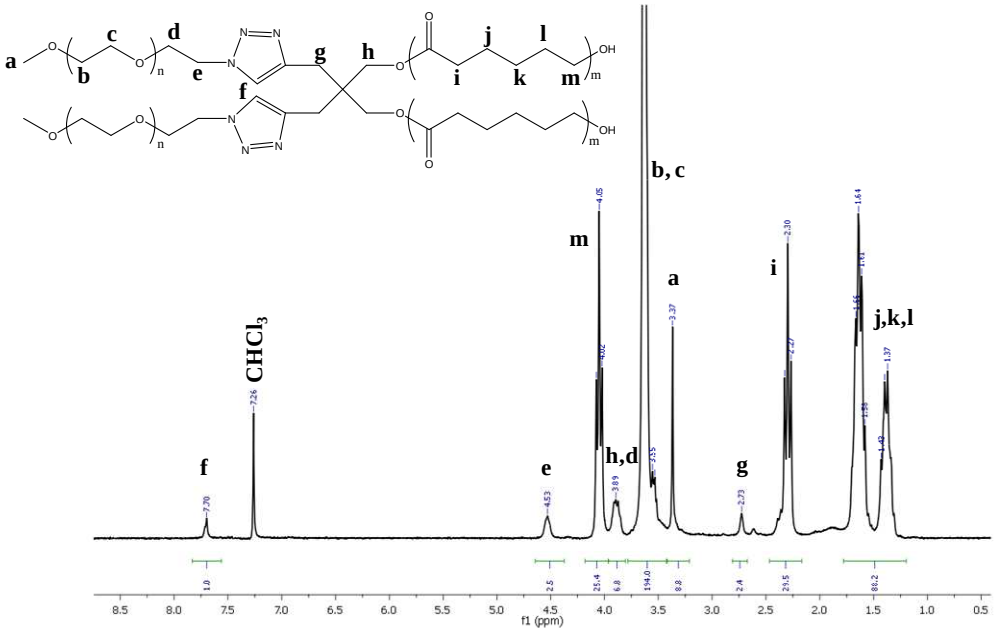

Figure 5. ^{1}H NMR spectrum of the $(PCL)_2$-$(PEO_A)_2$ amphiphilic copolymer in $CDCl_3$

The table 2 summarizes the different characteristics of the stars obtained by this coupling method and for which the behavior in aqueous media was investigated. For each copolymer, the length of the PCL chain remained constant. In order to keep the same HLB for the three-arm and four-arm stars, two azido-PEO of M_n = 2100 and 1250 g/mol, were respectively introduced to get the star. In addition, a third four-arm star copolymer has been synthesized with a higher HLB but with PEO arms of identical length to the three-arm star. The influence of the architecture and of the hydrophilic arms length of the star copolymers on the objects formed in solution was so studied.

Table 2. Characteristics of the stars synthesized by the developed strategy

Copolymers	PCL Arm content		PEO Arm content		M_w/M_n (SEC) [e]	HLB [f]
	DP_{exp} (^{1}H NMR)[a]	$M_{n,exp}$ (^{1}H NMR)[b]	DP_{exp} (^{1}H NMR)[c]	$M_{n,exp}$ (^{1}H NMR)[d]		
$(PCL)_2$-$(PEO_B)_1$	18.5	2100	48	2100	1.13	10
$(PCL)_2$-$(PEO_A)_2$	21	2400	56	2500	1.16	10.2
$(PCL)_2$-$(PEO_B)_2$	21	2400	96	4200	1.19	12.7

[a] Polymerization degree of PCL determined by ^{1}H NMR for PCL-$(alkyne)_1$ and PCL-$(alkyne)_2$ before coupling reaction

[b] Molecular weight (g/mol) of PCL determined by ^{1}H NMR for PCL-(alkyne)$_1$ and PCL-(alkyne)$_2$ before coupling reaction

[c] Polymerization degree of PEO determined by ^{1}H NMR for the ω-azido-PEO before coupling reaction

[d] Molecular weight (g/mol) of PEO determined by ^{1}H NMR for the ω-azido-PEO before coupling reaction

[e] Polydispersity index measured by SEC after coupling reaction

[f] Hydrophilic-Lypophilic Balance (HLB) determined by $20x(1 - \frac{M_n\ PCL}{M_n\ TOTALE\ (PCL+PEO}$)

The micellization of the well-defined star-shaped copolymers in water was achieved by dissolving the copolymer into DMF, a good solvent of all arms of the copolymer followed by the rapid addition of water, a selective solvent of the hydrophilic arms. After two hours of stirring, the solution was dialyzed against water to remove the DMF. The size and the polydispersity data of the objects in solution were collected by DLS and are listed in table 3. Small particles of around 20 nanometers are observed and no significant influence of the molecular weight or the architecture of the copolymers is underlined. The spherical morphology of the micelles was confirmed by TEM analysis (Figure 6).

Table 3. DLS data for micelles of the various copolymers in water

Copolymers	**$D_{h,\ app}$ (nm) [a]**	**PDI [b]**
$(PCL)_2$-$(PEO_B)_1$ – *4200 g/mol*	18.6 nm	0.15
$(PCL)_2$-$(PEO_A)_2$ – *4900 g/mol*	18.4 nm	0.17
$(PCL)_2$-$(PEO_B)_2$ – *6600 g/mol*	19.9 nm	0.13

Apparent hydrodynamic diameter [a] and PDI [b] determined by DLS

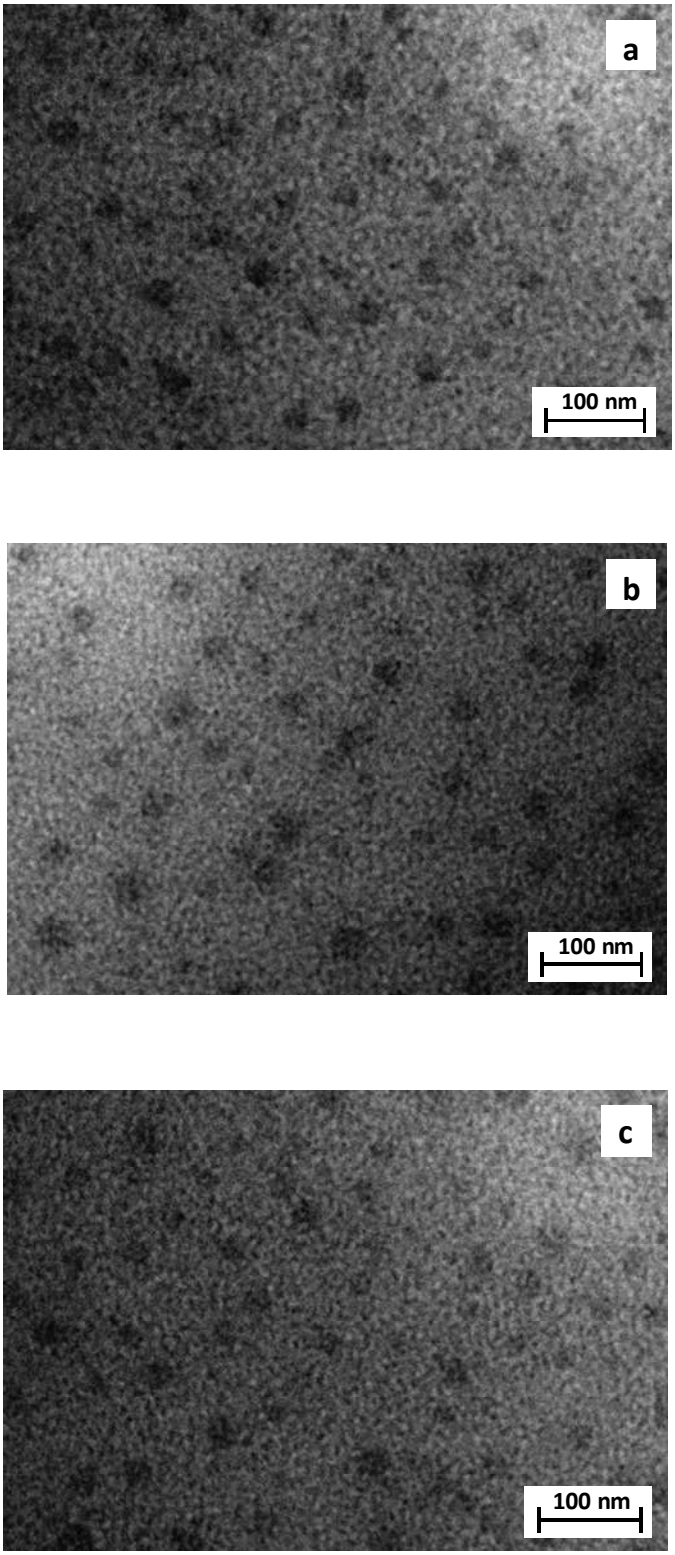

Figure 6. TEM images of micelles obtained for copolymers: **a** - $(PCL)_2$-PEO_B (HLB = 10), **b** - $(PCL)_2$-$(PEO_A)_2$ (HLB= 10.2) and **c** - $(PCL)_2$-$(PEO_B)_2$ (HLB=12.7)

Nanoparticles of PLA were prepared by the nanoprecipitation technique by the addition of increasing amounts of copolymers (from 10 to 70% in weight) to a constant volume of PLA in DMSO (concentration of 16 mg/mL). The efficiency of these copolymers to stabilize nanoparticles is presented in the table 4. For each copolymer synthesized in this work, a concentration of 30 %weight is required to stabilize the PLA nanoparticle solution. Nevertheless, the better stabilization was obtained with the four-arm star-shaped copolymer $(PCL)_2$-$(PEO_B)_2$ with the HLB of 12.7 (the most hydrophilic copolymer used), whose the longer PEO chains prevent the coalescence of the nanoparticles (Figure 7-**c**). For the two copolymers of the same HLB (about 10), the three-arm star-shaped copolymer (Figure 7-**a**) exhibited a less efficient stabilization of the PLA nanoparticles by comparison of the quantity of PLA precipitated for the three-arm and four-arm star-shaped copolymers (Figure 7-**b**). Indeed, as depicted on the drawings of table 4, the three-arm star-shaped copolymer could present a lower density of PEO chain at the surface of the PLA nanoparticles than the four-arm star-shaped copolymer with the same HLB. This observation is in line with already published results comparing diblock and palm-tree copolymers[7].

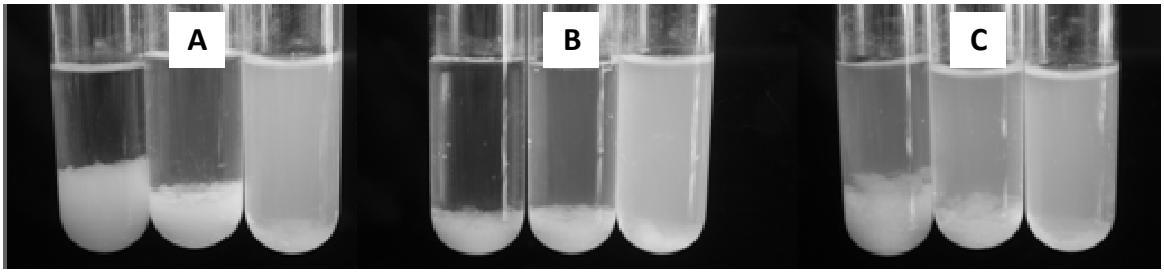

Figure 7. Co-precipitation of PLA with increasing amount of 10 wt%, 20 wt% and 30 wt% (from left to right) copolymers: **A** - $(PCL)_2$-PEO_B (HLB = 10), **B** - $(PCL)_2$-$(PEO_A)_2$ (HLB= 10.2) and **C** - $(PCL)_2$-$(PEO_B)_2$ (HLB=12.7).

Table 4. Characterization of the stabilized nanoparticles

Star Copolymers			Nanoparticles		
	$M_{n\ TOT}$	HLB	wt% copolymers [a]	$D_{h,\ app}$ (nm) [b]	PDI [c]
$(PCL)_2$-$(PEO_B)_1$	4200 g/mol	10	10	*PLA precipitation*	
			20	*PLA precipitation*	
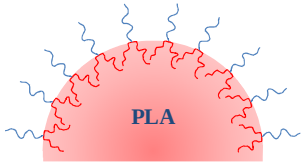			30	165±1	0.16
			40	163±1	0.16
			50	160±1	0.11
			60	152±2	0.13
			70	151±1	0.11
$(PCL)_2$-$(PEO_A)_2$	4900 g/mol	10.2	10	*PLA precipitation*	
			20	*PLA precipitation*	
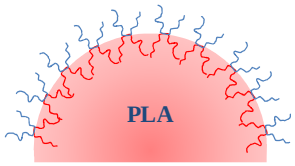			30	217±4	0.17
			40	207±2	0.19
			50	201±3	0.15
			60	198±1	0.13
			70	210±1	0.11
$(PCL)_2$-$(PEO_B)_2$	6600 g/mol	12.7	10	*PLA precipitation*	
			20	*PLA precipitation*	
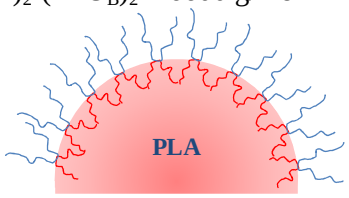			30	208±2	0.17
			40	191±1	0.18
			50	214±3	0.15
			60	196±1	0.14
			70	203±1	0.15

[a] wt% of copolymer in the (PLA + copolymer) mixture dissolved in DMSO (c = 16 mg/ml),

[b] Apparent diameter determined by DLS

[c] PDI determined by DLS

The star-shaped copolymers prepared during this work have a comparable efficiency to stabilize PLA nanoparticles, compared to graft amphiphilic copolymers PCL-*g*-PEO. Indeed, 33 wt% of graft copolymers are required to stabilize PLA nanoparticles solution but didn't require a high HLB (a HLB of 7.5 is enough to stabilized nanoparticles). However, amphiphilic diblock copolymers PEO-*b*-PCL are less efficient stabilizers compared to star-shaped copolymer since higher amount of copolymers (about 50 wt% for a HLB of 7.5) or higher HLB value (33wt% for a HLB of 13) are required to stabilize PLA. The results obtained for the star-shaped copolymer with the longer PEO chain are close to the results for the amphiphilic diblock copolymer. However, only the macromolecular architecture is compared but another point to take into account is the molecular weight. A higher molecular

weight will probably favor the stabilization of a PLA nanoparticles suspension. In case of the synthesized stars, low molecular weight appears to give efficient stabilization, while higher molecular weight of about 15 000 g/mol are rather required for the diblock copolymers[7].

As a rule, the nanoparticles have a diameter of about 150-200 nm, whatever the macromolecular architecture and the amount of polymeric stabilizer. The obtained sizes are comparable to those observed with graft or block copolymers based on PEO and PCL. For the three-arm star-shaped copolymers, the size of the PLA nanoparticles seemed to decrease when the amount of polymer increases. No significant improvement was observed with the increase of the HLB value for the four-arm star-shaped copolymers with an average size of 200 nm.

4. Conclusion

Well-defined three and four-arm star-shaped copolymers were successfully synthesized via an original pathway based on the coupling reaction between a PCL bearing one or two alkyne groups at the middle of the chain with an ω-azido-poly(ethylene oxide). Moreover, the synthesis strategy elaborated could be easily adapted to the synthesis of a variety of star-shaped copolymers by adapting the nature of the alkyne initiated monomer or/and the nature of ω-azido-functional polymer. The ability of these star copolymers to form micelles in aqueous solution was assessed by DLS and TEM which did not evidence a strong effect of the numbers and length of the hydrophilic arms on the size and shape of the micelles that remain spherical with a diameter around 20 nm. Besides micellization, the efficiency of these star copolymers to stabilize PLA nanoparticles has been studied and compared to more conventional diblock and graft copolymers. Star-shaped copolymers appeared to exhibit an intermediate behavior between these two other architectures in terms of PLA stabilization efficiency. These novel star copolymers, that were obtained via a quite simple synthesis route, have thus quite promising future in the elaboration of drug delivery systems.

5. References

1. Kataoka, K.; Harada, A.; Nagasaki, Y., Block copolymer micelles for drug delivery: design, characterization and biological significance. *Advanced Drug Delivery Reviews* **2001,** *47* (1), 113-131.

2. Kwon, G. S.; Okano, T., Polymeric micelles as new drug carriers. *Advanced Drug Delivery Reviews* **1996,** *21* (2), 107-116.

3. Barratt, G.; Couarraze, G.; Couvreur, P.; Dubernet, C.; Fattal, E.; Gref, R.; Labarre, D.; Legrand, P.; Ponchel, G.; Vauthier, C., Polymeric Micro- and Nanoparticles as Drug Carriers. *Polymeric Biomaterials* **2002**, 753-781.

4. Astafieva, I.; Zhong, X. F.; Eisenberg, A., Critical micellization phenomena in block polyelectrolyte solutions. *Macromolecules* **1993,** *26* (26), 7339-52.

5. Jones, M. C.; Leroux, J. C., Polymeric micelles - a new generation of colloidal drug carriers. *European Journal of Pharmaceutics and Biopharmaceutics* **1999,** *48* (2), 101-111.

6. Gautier, S.; Grudzielski, N.; Goffinet, G.; Henry De Hassonville, S.; Delattre, L.; Jérôme, R., Preparation of poly(D,L-lactide) nanoparticles assisted by amphiphilic poly(methyl methacrylate-co-methacrylic acid) copolymers. *Journal of Biomaterial Science Polymer Edition* **2001,** *12* (4), 429-450.

7. Rieger, J.; Passirani, C.; Benoit, J.-P.; Van Butsele, K.; Jerome, R.; Jerome, C., Synthesis of amphiphilic copolymers of poly(ethylene oxide) and poly(ε-caprolactone) with different architectures, and their role in the preparation of stealthy nanoparticles. *Advanced Functional Materials* **2006,** *16* (11), 1506-1514.

8. Forssen, E.; Willis, M., Ligand-targeted liposomes. *Advanced Drug Delivery Reviews* **1998,** *29* (3), 249-271.

9. Jerome, C.; Lecomte, P., Recent advances in the synthesis of aliphatic polyesters by ring-opening polymerization. *Adv. Drug Delivery Rev. FIELD Full Journal Title:Advanced Drug Delivery Reviews* **2008,** *60* (9), 1056-1076.

10. Albertsson, A.-C.; Varma, I. K., Aliphatic polyesters: synthesis, properties and applications. *Advances in Polymer Science* **2002,** *157* (Degradable Aliphatic Polyesters), 1-40.

11. Lee, J. H.; Lee, H. B.; Andrade, J. D., Blood compatibility of polyethylene oxide surfaces. *Progress in Polymer Science* **1995,** *20* (6), 1043-79.

12. Vermette, P.; Meagher, L., Interactions of phospholipid- and poly(ethylene glycol)-modified surfaces with biological systems: relation to physico-chemical properties and mechanisms. *Colloids Surf., B* **2003,** *28*, 153-198.

13. Couvreur, P., Drug vectorization or how to modulate tissular and cellular distribution of biologically active compounds. *Annales Pharmaceutiques Francaises* **2001,** *59* (4), 232-238.

14. Maeda, H.; Wu, J.; Sawa, T.; Matsumura, Y.; Hori, K., Tumor vascular permeability and the EPR effect in macromolecular therapeutics. A review. *Journal of Controlled Release* **2000,** *65* (1-2), 271-284.

15. Takakura, Y.; Hashida, M., Macromolecular drug carrier systems in cancer chemotherapy: macromolecular prodrugs. *Crit Rev Oncol Hematol FIELD Full Journal Title:Critical reviews in oncology/hematology* **1995,** *18* (3), 207-31.

16. Aliabadi, H. M.; Elhasi, S.; Mahmud, A.; Gulamhusein, R.; Mahdipoor, P.; Lavasanifar, A., Encapsulation of hydrophobic drugs in polymeric micelles through co-solvent evaporation: The effect of solvent composition on micellar properties and drug loading. *International Journal of Pharmaceutics* **2007,** *329* (1-2), 158-165.

17. Vangeyte, P.; Gautier, S.; Jerome, R., About the methods of preparation of poly(ethylene oxide)-b-poly(.vepsiln.-caprolactone) nanoparticles in water Analysis by dynamic light scattering. *Colloids and Surfaces, A: Physicochemical and Engineering Aspects* **2004,** *242* (1-3), 203-211.

18. Billiet, L.; Fournier, D.; Du Prez, F., Combining "click" chemistry and step-growth polymerization for the generation of highly functionalized polyesters. *Journal of Polymer Science, Part A: Polymer Chemistry* **2008,** *46* (19), 6552-6564.

19. Riva, R.; Lazzari, W.; Billiet, L.; Du Prez, F.; Jerome, C.; Lecomte, P., Preparation of pH-sensitive star-shaped aliphatic polyesters as precursors of polymersomes. *Journal of Polymer Science, Part A: Polymer Chemistry* **2011,** *49* (7), 1552-1563.

20. Fessi, H.; Puissieux, F.; Devissaguet, J.-P. Procédé de préparation de systèmes colloïdaux dispersibles d'une substance sous forme de nanocapsules. 0274961, 1988.

CHAPTER II

Cross-linked Nanosystems as New Drug Delivery Systems

S. Cajot, R. Jérôme, C.Jérôme

Abstract

The recent past has witnessed a huge research effort in order to overcome the intrinsic limitations of conventional drug administration, i.e. lack of selectivity and damages to healthy tissues. Among the new drug delivery systems that were devised until now, nano-systems, such as nanogels and micelles, are very promising because of good mechanical properties, tunable size in the range of tens nanometers and large surface area. This paper aims at reviewing the recent advances in the preparation of both nanogels and cross-linked-micelles. The cross-linking of these nanomaterials is the reason for significantly improved mechanical properties compared to traditional micelles prepared and tested earlier. Although the cross-linking strategies are similar, these two types of nanoparticles differ one from the other in a way that will be discussed hereafter.

1. Introduction

Nanogels are tridimensional nanostructures (typically < 100 nm) consisting of cross-linked hydrophilic macromolecules. They thus belong to the large family of hydrogels together with macro- and microgels, which are however out of the scope of this review. High water content, biocompatibility and good mechanical properties make them candidates of choice for biomedical applications, among which drug delivery systems, tissue engineering and implants may be mentioned. Hydrogels have a high affinity for water which accounts for their biocompatibility, but also requires the cross-linking of the constitutive chains for them to resist water dissolution[1-3]. Actually, two types of hydrogels have to be distinguished depending whether the cross-linking is physical, thus based on non-covalent chain interactions or chemical[4-5]:

- *Physical cross-linking approach*. In this case, the structure and composition of the hydrophilic chains are such that they associate spontaneously into a tridimensional network in water. The interchain bonding is reversible and may operate though a variety of interactions, exemplified by electrostatic forces, hydrophobic interactions, Van der Waals forces, hydrogen bonds, complexation and host guest interactions. The stability of this first type of nanogels directly depends on the strength of the interchain bonding in close relation to the environmental conditions. Once their structure is properly designed (nature and content of the interacting moieties), chains can self-associate in water into hydrogels endowed with adjustable characteristics, particularly the swelling degree.
- *Chemical cross-linking approach*. Compared to the former case, an additional chemical reaction is required for the constitutive chains to be part of a permanent tridimensional network. As a rule, the original chains must contain chemical groups reactive toward a bi-or multifunctional reagent, such that a typical organic reaction (esterification, amidation…) can be carried out. Whenever chain synthesis and cross-linking can be conducted simultaneously, thus in one pot, a one step process is

possible. Step-growth reactions and radical chain reactions are currently reported in the scientific literature. Although the chemical cross-linking is known as non reversible, the chemical interaction bonding may be selected for sensitivity to external stimuli, e.g. hydrazone or ester sensitive to the pH and disulfide sensitive to redox agents. Then, reversibility can be triggered on purpose under specific conditions.

- A typical process followed to reduce the size of these hydrogels to nanometric dimensions is the use of reverse mini-emulsions. For example, polymerization in the aqueous phase of an inverse mini-emulsion of the hydrogel precursors (monomer(s), cross-linker, initiator...) (Figure 1A) leads to hydrogels with a size controlled by the water nanodroplets of the mini-emulsion, i.e. in the range of tens of nanometers [6-7].

Besides this strategy that requires significant amounts of surfactants, self-assembly of amphiphilic copolymers is a quite straightforward approach to build well-defined nanocarriers below 100 nm diameter. The major difference between nanogel and micelle nanosystems has to be found in the original chemical structure of the chains, which are amphiphilic macromolecules when micelles are concerned. In water the micelles are stabilized by a hydrophobic core surrounded by a hydrophilic shell. How far the hydrophobic interactions in the core, added with the core-water repulsion, outmatch the shell-water interactions is the deciding parameter on the micelle stability. It is thus clear that the chemical cross-linking of the core is the way to provide micelles with high if not permanent stability. Micelles are typically smaller (tens of nanometers) than nanogels whose size may reach a few hundred nanometers and their structure is dual as result of the intimate combination of two components of opposite hydrophilicity. Nevertheless, hybrids of nanogels and cross-linked micelles are known as transient structures in the preparation of nanogels (Figure 1B). Indeed, micelles of amphiphiles are first prepared, followed by the cross-linking of either the core or the shell. In the final step known as hydrophilic transition, the originally hydrophobic core is converted into a hydrophilic component such that the whole system becomes hydrophilic as a nanogel must be. The so-prepared nanogels have of course a size typical of micelles [8].

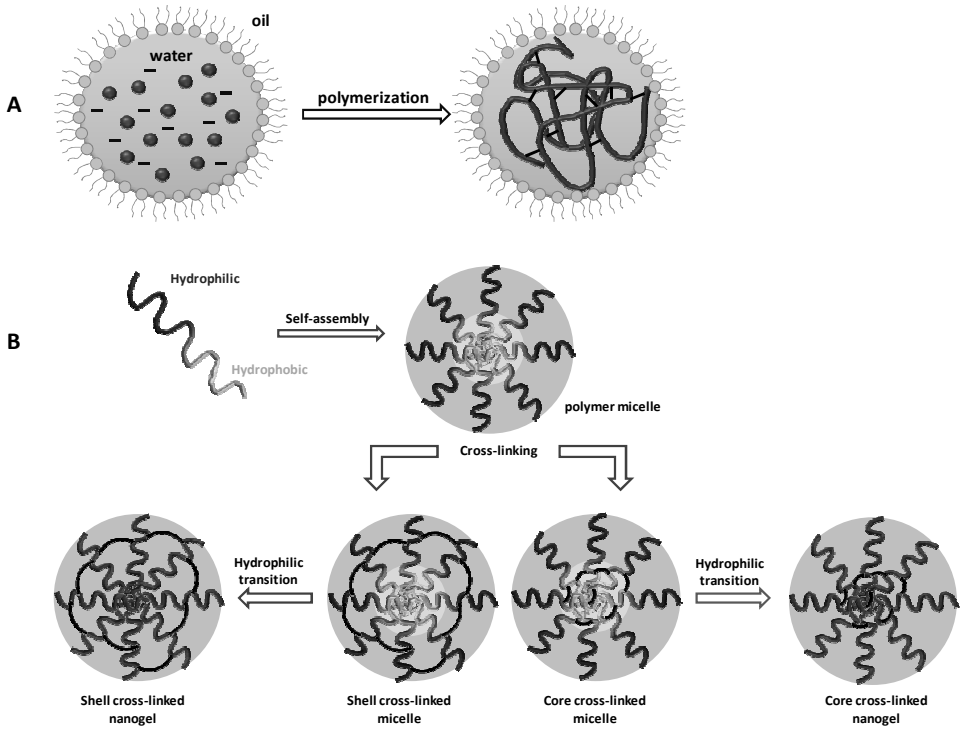

Figure 1. Nanogel formation by (**A**) reverse mini-emulsion process and (**B**) micelle template

Hereafter, recent advances in the design of nanogels and cross-linked micelles will be overviewed within the prospect of finalizing very effective drug delivery systems. A special attention will be paid to stimuli responsive systems of these advanced nanomaterials.

2. Nanogels

When poured in water, cross-linked hydrophilic nanoparticles swell rather than to be dissolved. Therefore, any drugs pre-dissolved in water can penetrate the nanoparticles which are then nothing but a container and a potential vehicle for them. The degree of cross-linking of the constitutive chains, together with their affinity for water, regulates the drug loading and the kinetics of drug release. Of course, any specific drug-chain segment interactions can modify these characteristic features, that would be improved in case of attractive interactions (high loading, slower release, restricted burst effect)[9-10]. In addition to the drug loading and release, the possible targeting of specific tissues is of the utmost importance for the therapeutic activity of the drug to be optimum. It is thus clear that a series of stringent criteria

have to be met for nanogels to be effective drug delivery systems [5]. In addition to the criteria of high loading and sustained release at predetermined targets, biocompatibility and stealthiness of the nanogels are additional major concerns for the lifetime of the nanogels in the bloodstream to be as long as possible. For this purpose, poly(ethylene oxide) (PEO) is the polymer the most frequently used in vectorisation [11-12]. Indeed, it is a neutral, hydrophilic, highly flexible and biocompatible polymer approved by the Food and Drug Administration (FDA) for intravenous applications. Moreover, the flexibility of the PEO, due to the absence of bulky substituent and the easy rotation of the ether bonds, disfavor the adsorption of plasmatic proteins at the surface of the nanocarrier exhibiting prolonged circulation in the bloodstream [13]. The stimuli responsiveness of the nanogels may not be ignored as a trick for triggering the drug release at the right place. These preliminary comments emphasize how challenging is the design of nanogels to be used in therapeutic applications. Let us discuss now how nanogels can be endowed with stimuli-responsiveness.

Non covalent stimuli responsive nanogels

Various kinds of polymers have been described in the literature as suitable materials for hydrogel formation due to their ability to self-assemble in aqueous media by physical cross-links, such as hydrogen bonds, which might be reversible depending on external conditions such as temperature or pH. In order to obtain a nanogel of these materials, a specific attention needs to be paid to the process of self-assembly which might already occur during the polymerization. Reverse mini-emulsions might also advantageously used to control the nanogel size.

Ionic polymers of the polyacrylate type as poly(acrylic acid) (PAA), poly(methacrylic acid) (PMAA) form a first class of polymers used in nanogel formation [9]. The degree of swelling of these nanogels is directly governed by the ionization of the weak carboxylic acid substituents, thus by the pH of the surrounding aqueous phase [2,14]. At low pH, mutual interactions of the protonated acidic side-groups by hydrogen bonding are responsible for cross-linking. Upon increasing the pH, the carboxylic acids are increasingly deprotonated, which results in ionic repulsions, less effective cross-linking and thus higher degree of

swelling. A difference in the concentration of the counterions within the nanogels and the external solution triggers an osmotic pressure that also controls the swelling of the nanogels. Such pH-responsive nanogels are effective in protecting drug against acidic degradation in the stomach in case of oral administration. Indeed, under acidic conditions, the drug is protected by encapsulation within a collapsed nanogel. Further in the digestive tract at a higher pH, the nanogel is expanded (deprotonation) and the non degraded drug is released [14-16].

Most attention is however paid to temperature-responsive nanogel in the scientific literature. Particularly, poly(N-isopropylamide) (PNIPAM) exhibiting a temperature induced sol-gel transition that can be adjusted close to the body temperature, is considered as an interesting candidate to achieve temperature triggered drug delivery systems. More precisely, PNIPAM modified by a few percentage (of about 12% wt) of acrylic acid was reported to be a biocompatible material that exhibits a lower critical solution temperature (LCST) higher than 50°C at pH 7.4. This LCST however decreases as the pH is decreased. As illustrated in Figure 2, the copolymer is solvated by water at 37°C and pH 7.4 (physiological conditions) but it self-associates into a typical nanogel through hydrogen bonding at lower pH. Under hyperthermia conditions (43°C), although the nanogel remains stable at the characteristic pH of normal cells (7.4), it collapses at the lower pH of cancer cells (6.8) which allow it to penetrate the endosomes and to expel pre-encapsulated compounds in the right place. In an improved version of this system, an anticancer drug has been covalently attached to the polyacrylamide chains through pH-sensitive bonds, e.g., hydrazones. At the low pH of the endosomes (5.3), the drug, doxorubicin (DOX) is released in situ, which makes the treatment highly selective [17]. The former nanogels exhibit sizes of 150 to 375 nm depending on the temperature and allowed to specifically release DOX from them at pH lower than 5.3. Significant decreased of the cell viability was already observed *in vitro* at pH 6.8 and at 43°C compared to physiological conditions. The proper tailoring of the dual temperature-pH sensitivity imparted to a biocompatible nanogel makes thus possible high performances in the treatment of tumor. Moreover, the addition of ligands at the surface of the nanogel, i.e. folic acid, may induced a specific targeting of the tumor cells that over-express folate receptors [18].

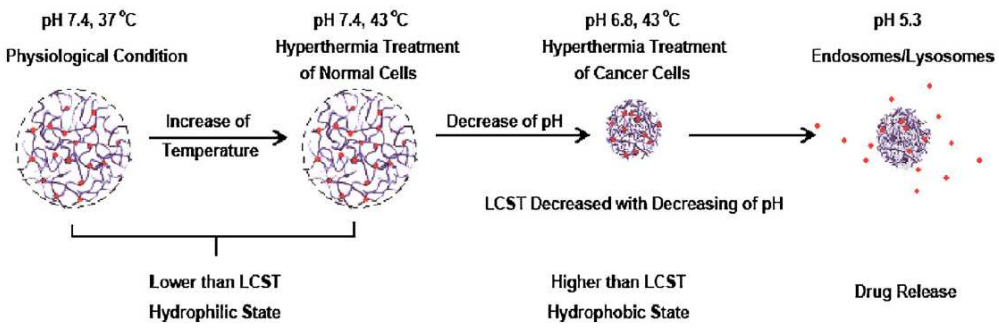

Figure 2. Phase transition of a poly(N-isopropylacrylamide-*co*-acrylic acid) nanogels

Covalently cross-linked nanogels

Photochemical reactions are very well-suited to the chemical cross-linking of hydrogels since they advantageously do not necessarily require the synthesis and reaction of mutually reactive groups attached to hydrophilic chains with an additional cross-linker. As an example, Wang et *al.* reported on a template free strategy to prepare biocompatible nanogels based on the photo cross-linking of the hydrophobic core of micelles followed by hydrophilic transition as schematized in Figure 1B. A BAB triblock copolymer based on poly(ethylene glycol) (PEG) (A) and poly(ethyl ethylene phosphate) (PEEP) (B) was functionalized by acrylate (Acr) as end-groups, (Acr-PEEP-*b*-PEG-*b*-PEEP-Acr) and dissolved in water. Salt addition triggered the collapse and self-association of the B block, locating the acrylate groups in the core of the accordingly formed flower-like assemblies, which were then permanently cross-linked by UV irradiation at 365 nm. The hydrophilicity of the B block was restored by eliminating the salt by dialysis. The resulting nanogel was drug loaded (DOX) and targeted to hepatocellular carcinoma cells with the assistance of a Latosyl end group attached at the end of the A block of a diblock copolymer of PEG and PEEP (AB) (Acr-PEEP-*b*-PEG-Lac) added to the system (Figure 3). By this process, the size of the nanogels could be adjusted between 70 to 550 nm by tuning the concentration of polymer and/or salt. A constantly accelerated drug released of the encapsulated drug was observed in the presence of the enzyme phosphodiesterase I, present in mammalian cells, which catalyzes the degradation of the phosphoester linkages [19].

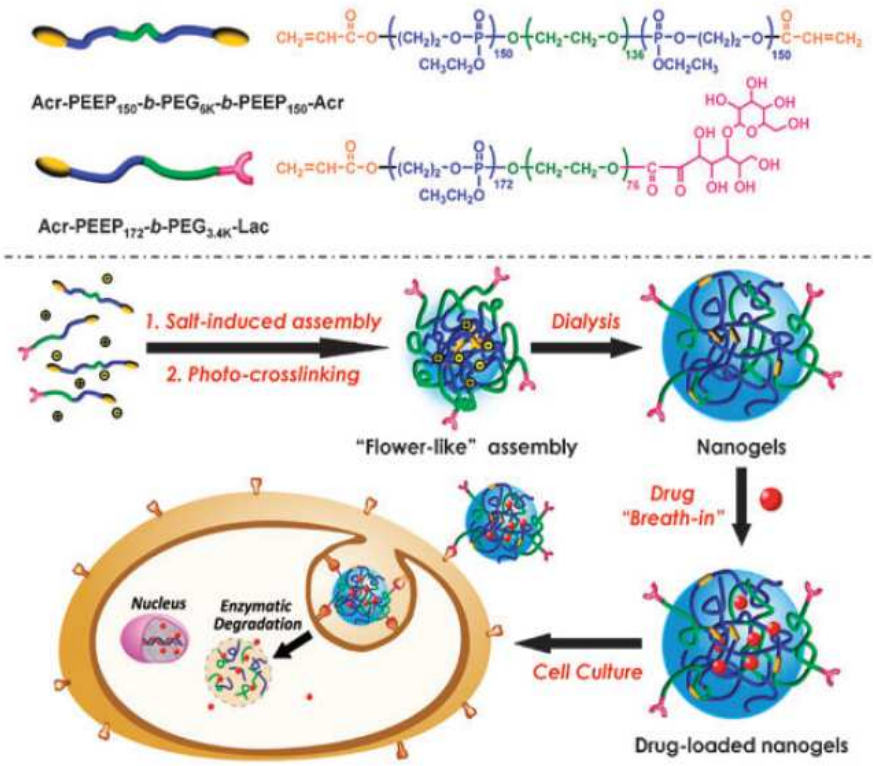

Figure 3. Nanogels engineering by photo-cross-linking of salt induced polymer micelles based on poly(ethyl ethylene phosphate) and poly(ethylene glycol)

Kabanov et *al*. exploited the same concept with a hydrophilic diblock copolymer of poly(ethylene oxide) (PEO) and partially ionized poly(methacrylic acid) (PMAA). The self-assembly into micelles was caused by the addition of divalent cations, such as Ca^{2+} (or Ba^{2+} and Sr^{2+}) that collapsed the ionic block into a micellar core which was chemically cross-linked by reaction of part of the carboxylic acid groups with 1,2-ethylenediamine. Finally, the metal cations were complexed with ethylenediaminetetraacetic acid (EDTA) and removed by dialysis, such that the micellar structure was converted into a nanogel as a result of the so-called hydrophilic transition. Former nanoparticles exhibited size change from 170 to 290 nm which is governed by the pH but also by variation of the ionic strength. Encapsulation of Cisplatin, an anticancer drug, significantly decreases the particle size from 290 nm to 125 nm probably due to the contraction of the cross-linked PMAA core by the neutralization of the PMA segments by the added drug [20]. Preparing nanogels by this transient assistance of

polymeric micelles bypasses the emulsion polymerization and its drawbacks (contamination by surfactants, unreacted monomers, initiator residues), thus the key step of the classical method of nanogels preparation.

Biopolymer-based nanogels

The advantage of preparing nanogels with natural polymers such as polysaccharides (hyaluronic acid, chitosan, heparin, dextran…, whose structure is shown in Scheme 1) and proteins, e.g. collagen, has to be found in their unique hydrophilicity and self-assembling properties hardly achieved with synthetic polymers [21-22]. In addition, they were found quite biocompatible with a low toxicity. Moreover, they are made available from renewable and more abundant sources than synthetic polymers. Their compositions and structures might also be largely varied or adjusted.

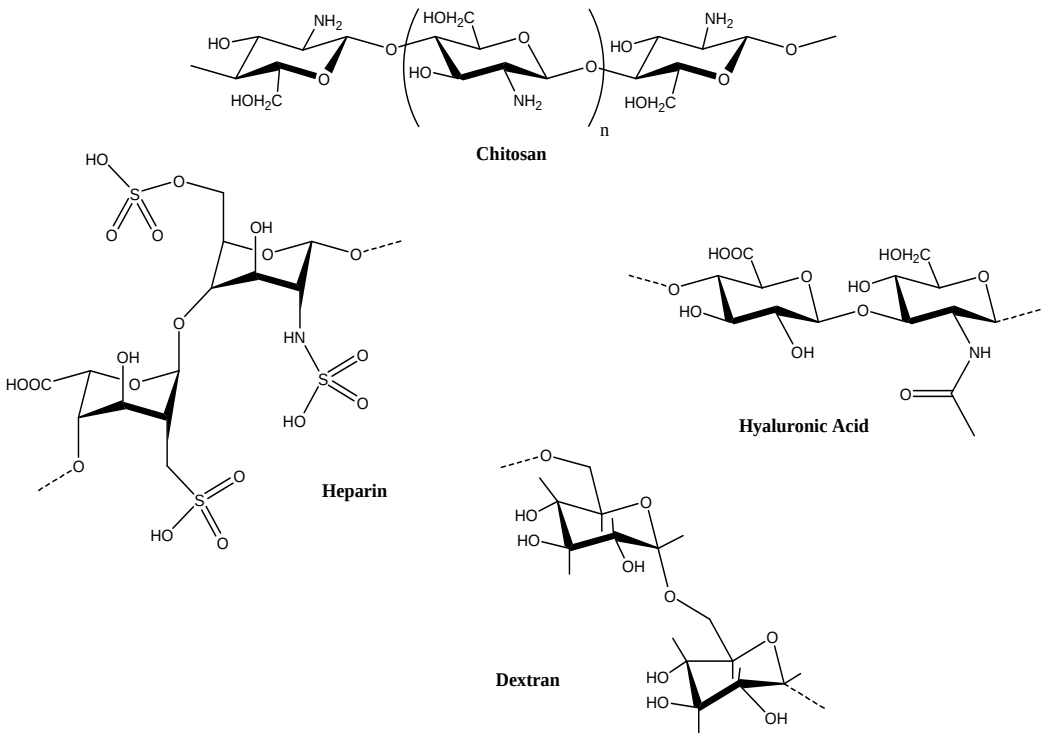

Scheme 1. Chemical structures of polymers from renewable resources

Hyaluronic acid is a glucosaminoglycan made of repeated disaccharide units commonly used in medical applications because of non-toxicity, non-immunogenicity and

non-inflammatory properties. Its nanogel formation generally relies on chemical cross-linking in several steps. Purposely, the polymer is aminated by reaction of the acid units with a diamine [23] or hydrazine [24-25]. The side amino groups are then reacted with a difunctional compound, such as dialdehydes [26], diepoxides [27] or carboxylic diacids [28]. It must be noted that modification by hydrazine has the advantage to impart pH sensitivity to the polymer [24-25]. Interestingly enough, esterification of the alcohols of the disaccharide units by methacrylic anhydride is a way to make the polymer photo cross-linkable [29].

Similar strategies are also applicable to chitosan, a linear polysaccharide that contains a primary amine in the repeating units. This biopolymer obtained by hydrolysis of chitin, can be degraded in the lysosomes which makes it a good candidate for the development of drug delivery systems [26].

Quite an interesting nanogel was prepared by Park et *al*. from a thiolated heparin (glycosaminoglycan composed of repeating units of pyranosyluronic acid and glucosamine residues) known for anti-tumor properties. Such thiolated version of heparin interacts by hydrogen bonding with repeating ether-oxide units of e.g., poly(ethylene oxide) [30] and Pluronic [31], which leads to a physically cross-linked nanogel. Upon oxidation of the thiols, disulfide bridges are formed (chemical cross-linking) and the complexing agent (at the origin of the physical cross-linking) is eliminated by dialysis under sonication (Figure 4). Disulfide cross-linked heparin nanogels were produced with an hydrodynamic diameter of about 200 nm. These nanogels which are redox-sensitive, (equation 1)

$$\text{-S-S-} + 2\,H^+ + 2\,e^- \underset{\text{Oxy}}{\overset{\text{Red}}{\rightleftharpoons}} 2\,\text{-SH} \qquad (1)$$

can be internalized into cells, where the disulfide units are rapidly reduced into thiols by the tripeptide glutathione (GSH), available at high concentration (10 mM) in the intracellular compartment (compared to 10µM in the extracellular compartment). The nanogel is accordingly destroyed and the heparin released in situ. *In vitro* studies highlighted a triggered release of heparin at high concentration of GSH. Almost 65% of free heparin was released from the nanogels at 5mM of GSH while less than 3% was released in the absence of GSH.

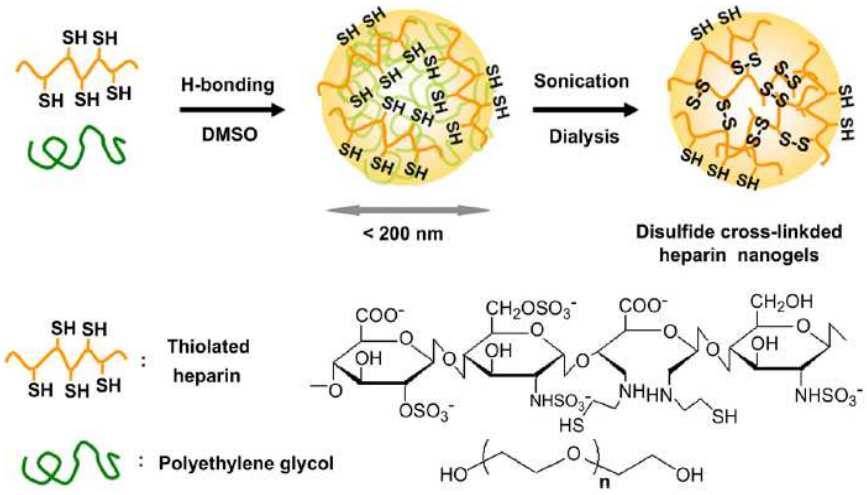

Figure 4. Formation of disulfide cross-linked heparin nanogels

3. Cross-linked micelles

Whenever amphiphiles form micelles above the so-called Critical Micellar Concentration (CMC), a dynamic equilibrium is established between unimers (non associated molecules) and micelles. Dilution of such a micellar self-assembly causes a displacement of this equilibrium towards the unimers. Because this phenomenon occurs when micelles are injected in the bloodstream, part of the micelles disappear and release their content (drug) at the expense of the expected controlled delivery activity [32-35]. An efficient way to prevent micelles from being dissociated upon dilution is to have them chemically cross-linked within either the shell or the core depending on which constitutive block is better suited to chemical modification.

Non-reversibly cross-linked micelles

As mentioned earlier, photochemistry is a very convenient approach to have micelles cross-linked. UV-induced [2+2] cycloaddition reaction of cinnamates is a typical illustration of that concept whenever one of the block of diblock [36-38] or triblock [39-40] used as precursors of micelles, are grafted by cinnamate groups. That strategy was also reported for the cross-linking of spherical nanocapsules made of vinyl containing phospholipids [41]. Straightforward

cross-linking without the need of additional reagent (cross-linker, initiator) is the major advantage of the process.

Nevertheless, less direct photo cross-linking was reported that required the addition of a difunctional low molecular weight reagent. J. S. Kim et *al*. reported on the cross-linking of the core of PEG-*b*-P(HEMA-*co*-MMA) micelles in the presence of molecules containing two benzophenone groups (BPD in Figure 5) under UV irradiation. A radical-radical combination between the excited benzophenone units and the labile hydrogen atoms of HEMA (2-hydroxyethyl methacrylate) units both located in the hydrophobic block mainly based on PMMA, actually occurs (Figure 5) [42]. Along this strategy based on the addition of multifunctional cross-linking agents, traditional chemistry was also used instead of photochemistry, such as click chemistry [43] and amidation reaction [44].

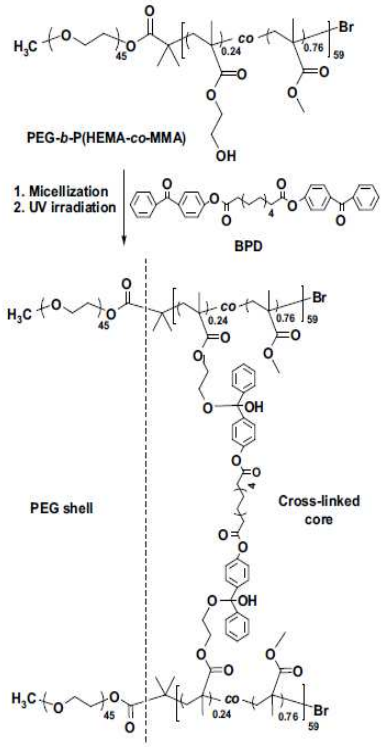

Figure 5. Formation of core-cross-linked micelles from PEG-*b*-P(HEMA-*co*-MMA) block copolymer

In another strategy, macromonomer polymerization was extended to the chemical cross-linking of micelles, as exemplified by the radical polymerization of vinyl groups at the

free end of the hydrophobic block of PEG-lipid amphiphiles initiated by AIBN (2,2'-azo-isobutyronitrile) (Figure 6) [45]. First, a branched hydrophobic domain was prepared by acylation of 2,2-bis(hydroxymethyl)propionic acid (DMAP) with 10-undecanoyl chloride and conjugated to monohydroxyl poly(ethylene glycol) to form the branched polymer amphiphile. Then, radical polymerization of the peripherical ends of the 10-undecanoyl acid chains was investigated as a model reaction for the cross-linking of the hydrophobic core of the PEG-lipid micelles. Well-defined cross-linked micelles were obtained with a size range of 15-20 nm whose the stability is maintained under various solvents and temperate up to 75°C. The drug loaded capacity was investigated by the efficient encapsulation of triclosan, a hydrophobic bactericide. This method is however limited to the cross-linking of micellar cores by the selective polymerization of the unsaturated end-groups of the hydrophobic subchains.

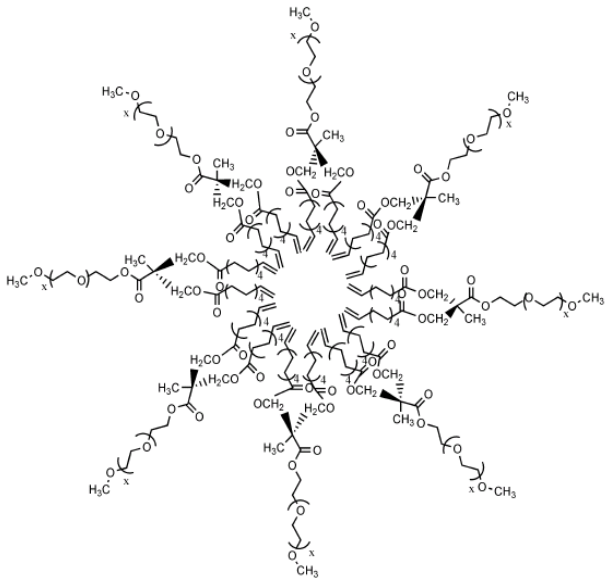

Figure 6. Core Cross-linkable core of micelles of PEG-lipid amphiphiles

Other monomers as MAC (5-methyl-5-allyloxycarbonyl-1,3-dioxan-2-one) [46] would also afford the cross-linking of the micellar core due to its pendant vinyl functions. Let also mention the synthesis of macromonomers as PDMA (poly(2-(N,N-dimethylamino)ethyl methacrylate)) whose copolymerization with a hydrophobic macromonomer as i.e. poly(ε-

caprolactone) allows the formation of core-surface cross-linked micelles of amphiphilic brush copolymers. Instead of the core, the shell of micelles can be cross-linked in order to stabilize them. Wooley et *al*. engaged themselves in this direction and introduced the concept of "nanoscale cage-like structure" in the case of copolymers consisting of a poly(acrylic acid-*co*-acrylamide) hydrophilic block and either a poly(1,4-isoprene) or a poly(ε-caprolactone) hydrophobic block. In a further step, hollow nanoparticles were prepared as result of the degradation of the hydrophobic core, including ozonolysis (Figure 7) [47-49]. The ultimate purpose is to have hydrophilic guests sequestrated within the nanocage. The shell cross-linking was carried out by covalent reaction of acrylic acid units with a diamino cross-linker, a 2,2'-(ethylenedioxy)bis(ethylamine). Due to the carboxylic acid groups of acrylic acid units, the size of these hollow particles is pH dependent. Indeed, increasing the pH induces significant volume expansion from about 80 nm at pH 5 to 100 nm at pH 9. Moreover, the degradation of the hydrophobic core leaves ketone and aldehyde functionalities lining the nanocage which may be used for the attachment of specific guests within the cage.

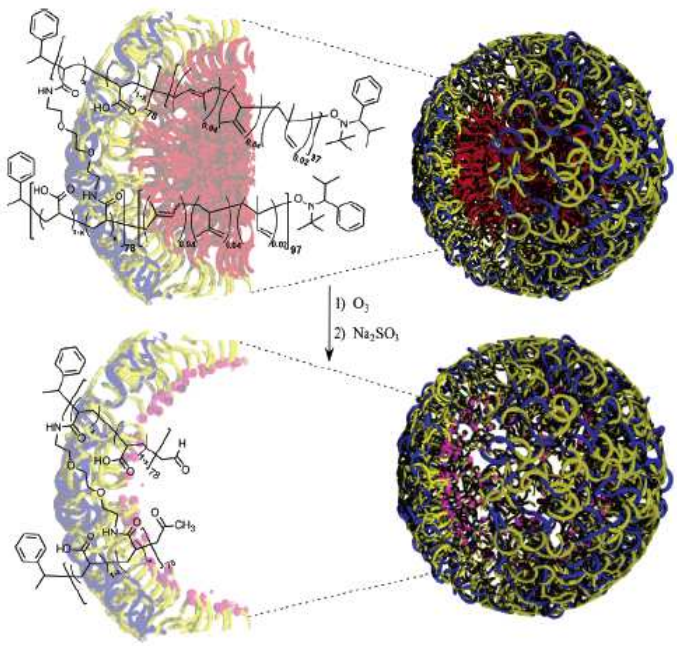

Figure 7. Production of nanocages resulting from the ozonolytic degradation of the poly(isoprene) core of shell cross-linked polymer micelle template

Reversibly and stimuli responsive cross-linked micelles

The interest of having drugs encapsulated within cross-linked micelles is only justified whether they can be released when desired in answer to external stimuli such as a change in pH, temperature or chemical composition (e.g. in presence of an oxidizing agent or a reductant).

Acid-labile cross-linking was searched for with the purpose to have micelles stable under physiological conditions and prone to destabilization by hydrolysis of the cross-linking bonds in more acidic media followed by de-association below the CMC. Because the environmental pH of tumor cells is lower (about 6.5) compared to the physiological conditions, drugs might be released preferentially in the surrounding of these cells. Whenever this type of micelles is internalized in targeted cells, the chance for them to be destabilized and drug to be released in the endosomes or lysosomes is much higher because of a local pH as low as about 5. The pH lability of cross-links against pH is thus of a crucial importance. Labile acetal [50-51] and ester [43] bonds were mainly considered in the scientific literature.

As previously discussed, disulfides are redox-sensitive cross-linkers that can be cleaved by reduction into thiols (e.g. by reaction with glutathione). Various strategies were reported on how to promote disulfide bridging, e.g. by polymerization of β-benzyloxycarbonyl-L-cysteine [52] and by grafting of cystamine groups [53] or pyridyldisulfide (PDS) ones [54-55]. Illustrative of this type of stimulus (Figure 8), Murthy et *al*. [56] designed core cross-linked micelles of poly(ethylene glycol) and poly(L-lysine) modified by disulfides, i.e. thiopyridal group (I) diblock copolymers as a robust and simple strategy for the development delivery vehicles of about 50 nm for vaccine peptides. The copolymer self-assembly was carried out in the presence of an immunostimulator (ISS-DNA) that was accordingly encapsulated. Cross-linking was the result of an exchange redox reaction between the disulfide groups and a tetrathiol, i.e. a cystein-modified antigenic peptide (II). After phagocytosis by antigen-presenting cells (APCs), the peptides cross-linked micelles were de-assembled by disulfide reduction (cleavage) with glutathione (GSH) and both the immunostimulatory molecules and the peptide antigens were released in situ. High peptide release level (close to one hundred

percents) was observed in presence of 50 mM of GSH while only 10 % of release was measured in absence of glutathione.

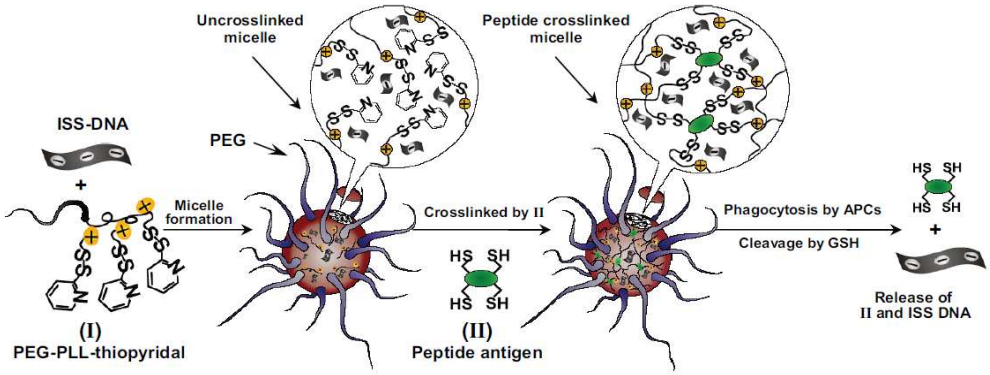

Figure 8. Peptide disulfide core-cross-linked micelles self-assembled by DNA complexation

Redox sensitivity was imparted to polymer micelles by different routes of reversible cross-linking by disulfide bridges [53,57-58]. For instance, the hydrophobic block of an amphiphilic diblock was synthesized by ring-opening copolymerization of ε-caprolactone (εCL) with an azido-substituted εCL. The core of the former micelles of PEO-*b*-P(αN_3-*co*-ε-CL) was cross-linked by reaction of the side azido groups with a bis-alkyne disulfide by click chemistry (Figure 9). Stable micelles of about 40 nm were obtained upon dilution and also in a non selective solvent while the presence of dithiothreitol (DTT), as a reducing agent, leads to the destabilization of the micelle structure [57].

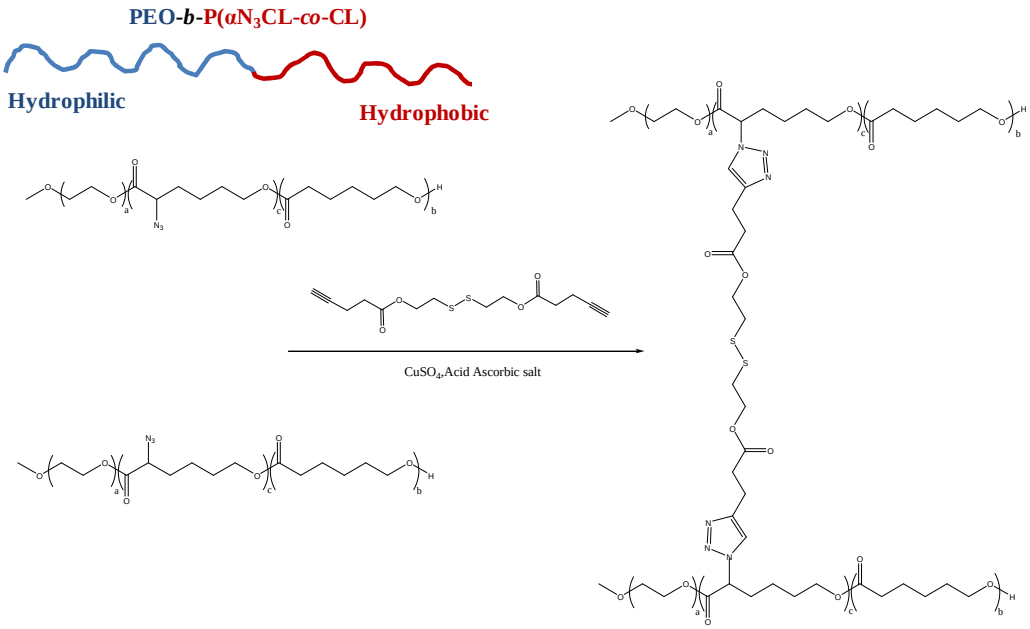

Figure 9. Synthesis of core cross-linked micelles of PEO-*b*-P(αN_3εCL-*co*-εCL)

In another example, core cross-linking of poly(polyethylene glycol methyl ether methacrylate)-*b*-poly(5'-O-methacryloyluridine) (PPEGMEMA-*b*-PMAU) micelles was achieved by radical copolymerization (RAFT mechanism) of the core side of methacrylate groups and bis(2-methacryloyloxyethyl)disulfide (DSDMA) (Figure 10). These cross-linked micelles exhibited sizes of about one hundred nanometer in water. In reductive environment, these ones loose their stability but are permanently cross-linked to a small extend due to the presence of chain transfer reaction to the disulfide groups. Nevertheless, high release rate of about 60-70% are reached after 7 hours of incubation with DTT at a concentration of 0.65 mM [58].

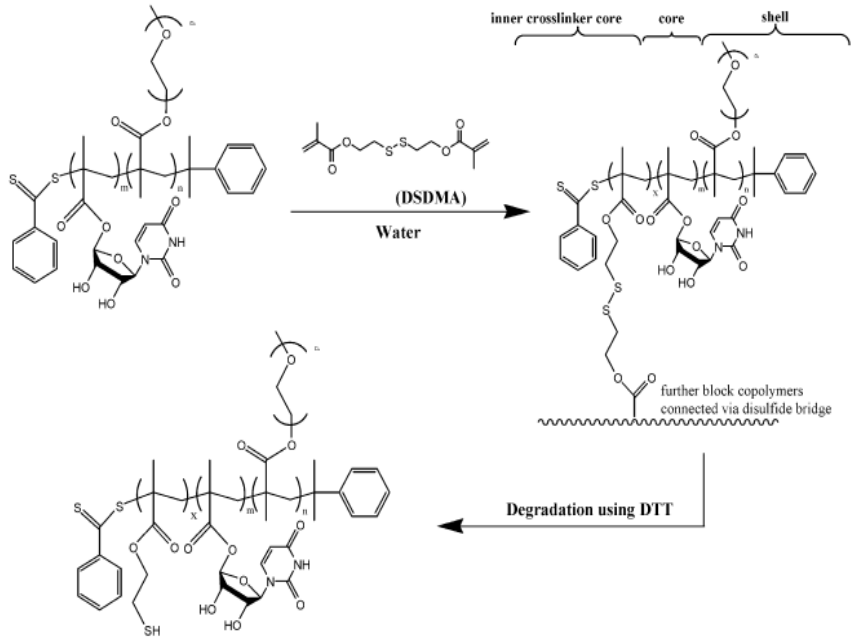

Figure 10. Synthesis and degradation of core cross-linked micelles of PPEGMEMA-*b*-PMAU

As already mentioned above, photochemistry is here again an attractive approach to induce cross-linking. Most of the photo cross-linking reactions used result in irreversible covalent bonds by [2+2] cycloaddition. An exception may however be found in the controlled dimerization of coumarin. Jiang et *al*. synthesized block copolymers of hydrophilic poly(ethylene oxide) and hydrophobic poly(coumarin methacrylate) (PCMA) and poly(methylmethacrylate) (PMMA). Micelles were cross-linked by photodimerization of the coumarin groups at $\lambda > 310$ nm. The accordingly formed cyclobutane bridges can be cleaved by UV irradiation at 260 nm and consequently the micelle destabilization can be triggered by external UV irradiation. Micelles of about 130 nm were obtained with this system from which the release of a hydrophobic dye, the Nile Red, was investigated by comparing uncross-linked micelles, photo cross-linked micelles with various degree of cross-linking and photo de-cross-linked micelles. As expected, the release rate decreased as the percentage of cross-linking (dimerization) is increased. After de-cross-linking by changing the wavelength of irradiation, the rate of release was increased again though without recovering the initial rate of the starting uncross-linked micelles. That effect could be explained by an incomplete photocleavage of

coumarin dimers, since a photostationary state can be reached due to some dimerization reactions under used irradiation wavelength ($\lambda < 260$ nm) [59].

4. Double hydrophilic block copolymers (DHBCP) as precursors of cross-linked micelles and nanogels

Block copolymers that consist of a hydrophilic block associated to a smart block whose philicity can be reversibly switched from hydrophilic to hydrophobic under an external stimulation, have great potential in the design of drug delivery nanoparticles. Indeed, when amphiphilic, these copolymers spontaneously form micelles in water. A second prerequisite is however that the micelle core is covalently cross-linkable. Then, the switching of the core forming block of the cross-linked micelles from hydrophobic to hydrophilic, causes the transition from cross-linked micelles to nanogels and the faster release of in-core encapsulated drug.

In an alternative version, the shell of the micelles is covalently cross-linked, whereas the hydrophobic (and switchable) core is pH-sensitive. As a result, the protonation of an aminated core by reducing the pH makes it hydrophilic and allows the core content to be released. Accordingly, Jiang et *al*. synthesized triblock copolymers of poly(ethylene oxide) (PEO), poly(glycerol monomethacrylate) (PGMA) and poly(2-(diethylamino)ethyl methacrylate) (PDEA) (PEO-*b*-PGMA-*b*-PDEA). The micelles shell was made photo cross-linkable by the grafting of cinnamoyl groups onto PGMA (PCGMA units). At low pH, the hydrophobic PDEA block was protonated, the micelle core was swollen and the size of the micelles increased from about 24 to 39 nm allowing the release of the encapsulated drug (Figure 11) [40].

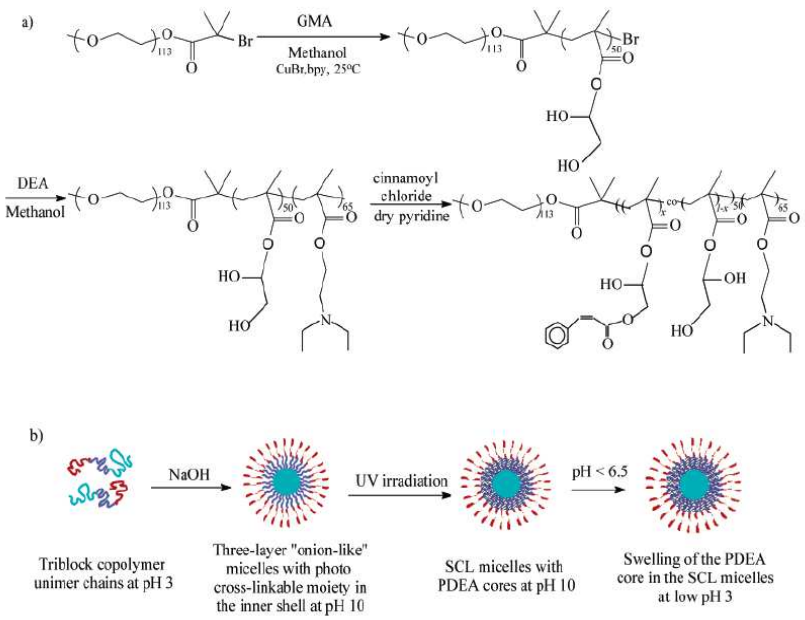

Figure 11. UV shell cross-linking (SCL) and pH dependence of triblock copolymers of PEO-*b*-(PGMA$_x$-*co*-PCGMA$_{1-x}$)-*b*-PDEA

A lower critical solution temperature (LCST) makes PNIPAM switchable from water soluble (below LCST) to collapsed in water (above LCST). Liu et *al*. investigated the synthesis of poly(N,N'-dimethylacrylamide)-*b*-poly(N-isopropylacrylamide-*co*-3-azidopropylacrylamide) diblock (PDMA-*b*-P(NIPAM-*co*-AzPAM)) copolymers as precursors of either core cross-linked micelles (T>LCST) or nanogels (T<LCST). The switchable block was covalently cross-linked by click chemistry, thus by the addition of a dialkyne (propargyl ether) onto the azide groups. The temperature dependence of the size of the core cross-linked micelles was followed by dynamic light scattering. A significant variation of the micelle size occurs within the temperature range of 30-35°C. At 45°C, an average hydrodynamic diameter of 50 nm was observed, whereas at 25°C, the swelling of the core cross-linked micelles by the solubilization of the PNIPAM block leads to the formation of nanogels with an average hydrodynamic diameter of 68 nm [60].

Similarly block copolymers of poly(ethylene oxide) and poly(N-isopropylacrylamide-*co*-N-acryloxysuccinimide) (PEO-*b*-P(NIPAM-*co*-NAS)) form thermally reversible micelles as a consequence of the LCST of the PNIPAM block [61]. The core can be cross-linked by reaction of cystamine, a disulfide containing primary diamine, with the NAS side groups.

Upon decreasing temperature below the LCST of PNIPAM, nanogels are formed at the expense of the cross-linked micelles. The cross-linking is however reversible upon addition of DTT (Figure 12). When this addition occurs below the LCST of PNIPAM, the micelles are then destabilized. The thermoresponsive micellization behavior was evaluated at 25 and 40°C. At the lower temperature, an average hydrodynamic diameter of about 6 nm was measured corresponding to unimers of the diblock copolymers. Above the critical micellar temperature (CMT) of 40°C, well-defined micelles of 26 nm were observed. After the addition of cystamine, effective core cross-linked micelles were observed by the preservation of the micelle structure at 25°C.

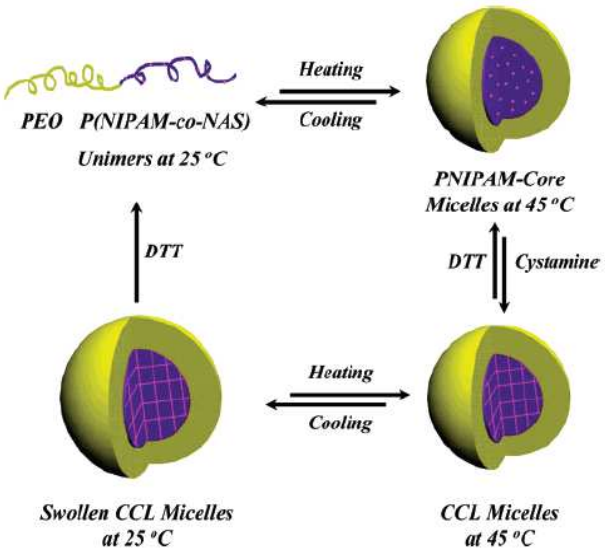

Figure 12. Reversible core cross-linked micelles and nanogels based on the double hydrophilic block copolymer PEO-b-P(NIPAM-co-NAS)

Zhao et *al*. proposed a general strategy to prepare core cross-linked micelles and nanogels from a double hydrophilic block copolymer of poly(ethylene oxide) and poly[2-(2-methoxyethoxy) ethyl methacrylate-*co*-4-methyl-[7-(methacryloyl)oxyethyloxy]coumarin] (PEO-*b*-P(MEOMA-*co*-CMA)). Micelles were formed at T > LCST of the P(MEOMA-*co*-CMA) block followed by their cross-linking by dimerization of the coumarin groups of the PMEOMA block at 310 nm with an average hydrodynamic diameter of 35 nm. Nanogels resulting from the cooling of the cross-linked micelles at T < LCST with a D_h of about 40 nm

were thus observed. Under irradiation at 260 nm, dimerization was partially reversible leading to an extra swelling of the nanogels up to 49 nm by the reduced cross-linking density (Figure 13). The release of an encapsulated dye could be achieved by either direct photo de-cross-linking of the nanogel or by tuning the cross-linking degree when preparing the nanogel [62].

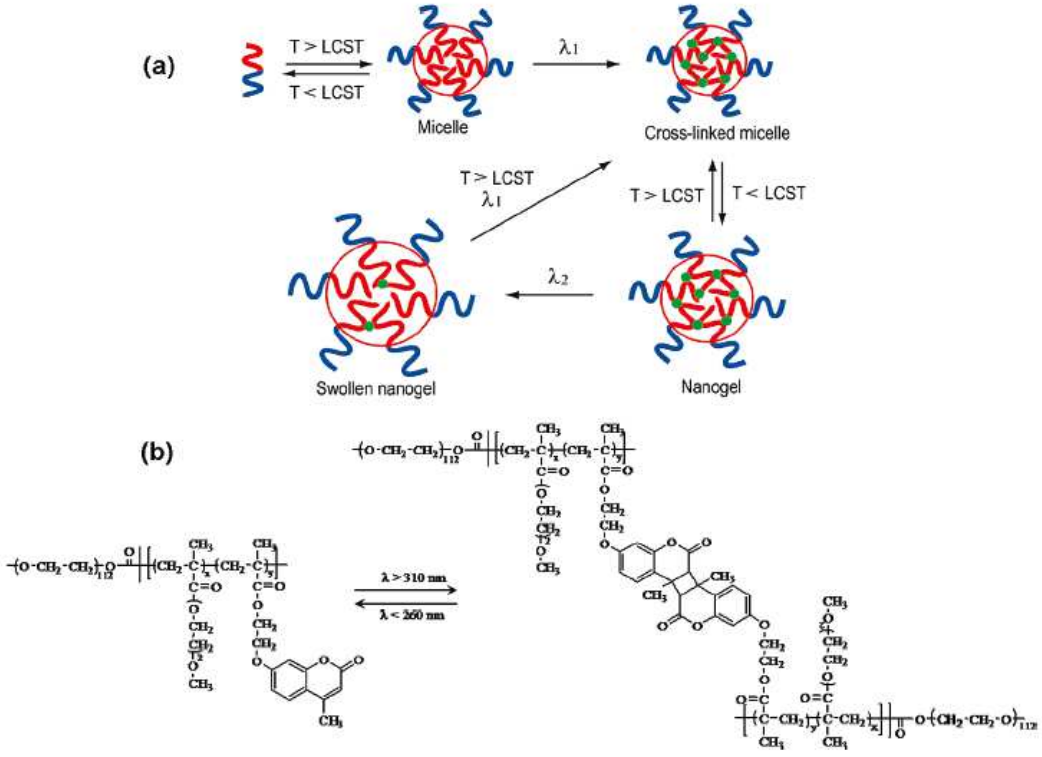

Figure 13. Preparation of core cross-linked micelles and photo-controlled volume change of PEO-*b*-P(MEOMA-*co*-CMA) nanogels

Both core and shell cross-linked micelles and nanogels were prepared from double hydrophilic copolymers of poly[N,N-dimethylacrylamide-*co*-4-methyl-[7-(methacryloyl)oxyethyloxy]coumarin] and poly[N-isopropylacrylamide-*co*-4-methyl-[7-(methacryloyl)oxyethyloxy]coumarin] (P(DMA-*co*-CMA)-*b*-P(NIPAM-*co*-CMA)) as a new thermal- and photoresponsive core-shell particles. The shell and the core blocks may be both cross-linked due to the presence of coumarin units while the PNIPAM units located in the core of the micelles insure thermal transition between cross-linked micelles and nanogels [63].

Finally, Ji et *al*. prepared core or shell photo cross-linked micelles and nanogels with a double responsive behavior (pH and thermal) from poly(butanedioic acid, 1-[3[(2-methyl-1-oxo-2-propen-1-yl)oxy]propyl] ester)-*b*-poly(methoxydi(-ethylene glycol) methacrylate-*co*-4-methyl-[7-(methacryloyl)oxyethyloxy] coumarin) (PSPMA-*b*-P(DEGMMA-*co*-CMA)). Micellization can be triggered by a change in either temperature or pH. Although soluble in water at 20°C and pH 10, the P(DEGMMA-*co*-CMA) block collapses when the temperature is increased up to 35°C at constant pH. Conversely, the PSPMA block forms the micelle core when the pH is decreased down to 3 at constant temperature. Partially reversible cross-linking of the micelles is achieved by the dimerization of the coumarin units under UV irradiation. Nanogels are finally prepared by making the core forming block hydrophilic by the proper adjustment of pH or temperature (Figure 14) [64].

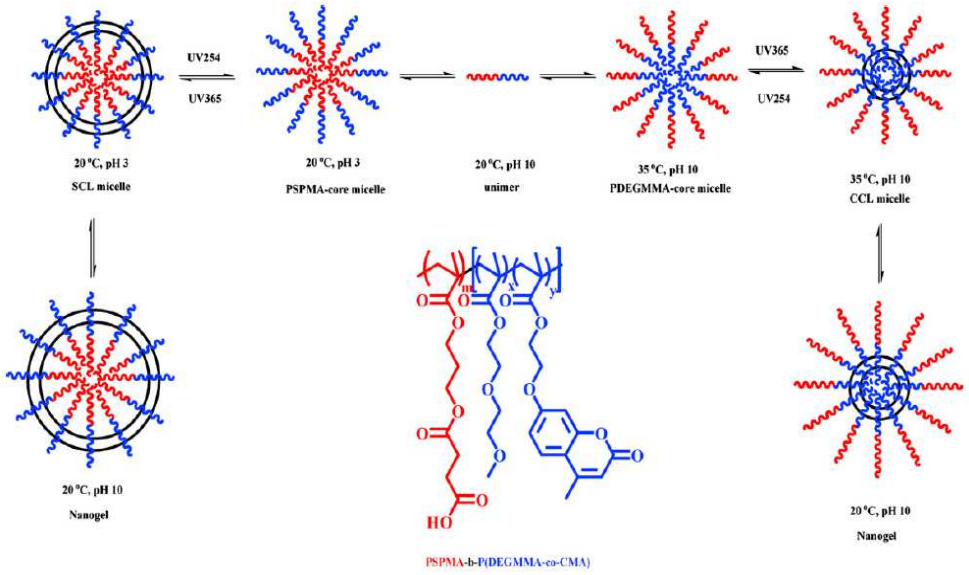

Figure 14. Thermo- and pH-responsive micellization and photo cross-linking of PSPMA-*b*-P(DEGMMA-*co*-CMA) block copolymer

5. Conclusions

In the recent past, the design of drug delivery systems with steadily increasing performances has been a great concern particularly with the advent of nanotechnologies. Although the potential of nanoparticles as nanovehicles has been extensively investigated, how to control on demand the nanoparticle stability remains a key issue for drug delivery to be a very selective and highly effective process. This paper has reviewed the most representative achievements in the synthesis of cross-linked nanoparticles, with a special emphasis on nanogels and micelles. The cross-linking of these particles formed in water is very instrumental for improving both the stability and the mechanical properties. The most remarkable progress results however from the possible reversibility of the cross-linking and its triggering off by stimuli responsive mechanisms.

6. References

1. Hamidi, M.; Azadi, A.; Rafiei, P. *Advanced Drug Delivery Reviews* **2008**, *60*, 1638.
2. Peppas, N. A.; Bures, P.; Leobandung, W.; Ichikawa, H. *European Journal of Pharmaceutics and Biopharmaceutics* **2000**, *50*, 27.
3. Hoffman, A. S. *Advanced Drug Delivery Reviews* **2002**, *54*, 3.
4. Clark, A. H.; Ross-Murphy, S. B. *Adv. Polym. Sci.* **1987**, *83*, 57.
5. Oh, J. K. *Can. J. Chem.* **2010**, *88*, 173.
6. Oh, J. K.; Drumright, R.; Siegwart, D. J.; Matyjaszewski, K. *Progress in Polymer Science* **2008**, *33*, 448.
7. Raemdonck, K.; Demeester, J.; De Smedt, S. *Soft Matter* **2009**, *5*, 707.
8. Sasaki, Y.; Akiyoshi, K. *Chem. Rec.* **2010**, *10*, 366.
9. Peppas, N. A.; Hilt, J. Z.; Khademhosseini, A.; Langer, R. *Advanced Materials (Weinheim, Germany)* **2006**, *18*, 1345.
10. Lee, K. Y.; Rowley, J. A.; Eiselt, P.; Moy, E. M.; Bouhadir, K. H.; Mooney, D. J. *Macromolecules* **2000**, *33*, 4291.
11. Barratt, G.; Couarraze, G.; Couvreur, P.; Dubernet, C.; Fattal, E.; Gref, R.; Labarre, D.; Legrand, P.; Ponchel, G.; Vauthier, C. *Polymeric Biomaterials* **2002**, 753.
12. Astafieva, I.; Zhong, X. F.; Eisenberg, A. *Macromolecules* **1993**, *26*, 7339.
13. Couvreur, P. *Annales Pharmaceutiques Francaises* **2001**, *59*, 232.
14. Argentiere, S.; Blasi, L.; Morello, G.; Gigli, G. *Journal of Physical Chemistry C* **2011**, *115*, 16347.
15. Lally, S.; Mackenzie, P.; LeMaitre, C. L.; Freemont, T. J.; Saunders, B. R. *Journal of Colloid and Interface Science* **2007**, *316*, 367.
16. Kim, J. O.; Sahay, G.; Kabanov, A. V.; Bronich, T. K. *Biomacromolecules* **2010**, *11*, 919.
17. Xiong, W.; Wang, W.; Wang, Y.; Zhao, Y.; Chen, H.; Xu, H.; Yang, X. *Colloids and Surfaces, B: Biointerfaces* **2011**, *84*, 447.

18. Soppimath, K. S.; Liu, L.-H.; Seow, W. Y.; Liu, S.-Q.; Powell, R.; Chan, P.; Yang, Y. Y. *Advanced Functional Materials* **2007**, *17*, 355.

19. Wang, Y.-C.; Wu, J.; Li, Y.; Du, J.-Z.; Yuan, Y.-Y.; Wang, J. *Chem. Commun. (Cambridge, U. K.)* **2010**, *46*, 3520.

20. Bronich, T. K.; Keifer, P. A.; Shlyakhtenko, L. S.; Kabanov, A. V. *Journal of the American Chemical Society* **2005**, *127*, 8236.

21. Lee, K. Y.; Mooney, D. J. *Chemical Reviews (Washington, D. C.)* **2001**, *101*, 1869.

22. Coviello, T.; Matricardi, P.; Marianecci, C.; Alhaique, F. *Journal of Controlled Release* **2007**, *119*, 5.

23. Maroda, M.; Bodnar, M.; Berko, S.; Bako, J.; Eros, G.; Csanyi, E.; Szabo-Revesz, P.; Hartmann, J. F.; Kemeny, L.; Borbely, J. *Carbohydr. Polym.* **2011**, *83*, 1322.

24. Vercruysse, K. P.; Marecak, D. M.; Marecek, J. F.; Prestwich, G. D. *Bioconjugate Chemistry* **1997**, *8*, 686.

25. Prestwich, G. D.; Marecak, D. M.; Marecek, J. F.; Vercruysse, K. P.; Ziebell, M. R. *Journal of Controlled Release* **1998**, *53*, 93.

26. Monteiro, O. A. C., Jr.; Airoldi, C. *International Journal of Biological Macromolecules* **1999**, *26*, 119.

27. Qin, C.; Ling, X.; Du, Y.; Shi, X.; Chen, J. *Reactive & Functional Polymers* **2002**, *50*, 165.

28. Bodnar, M.; Hartmann, J. F.; Borbely, J. *Biomacromolecules* **2006**, *7*, 3030.

29. Burdick, J. A.; Chung, C.; Jia, X.; Randolph, M. A.; Langer, R. *Biomacromolecules* **2005**, *6*, 386.

30. Bae, K. H.; Mok, H.; Park, T. G. *Biomaterials* **2008**, *29*, 3376.

31. Nguyen, D. H.; Choi, J. H.; Joung, Y. K.; Park, K. D. *Journal of Bioactive and Compatible Polymers* **2011**, *26*, 287.

32. Jones, M. C.; Leroux, J. C. *European Journal of Pharmaceutics and Biopharmaceutics* **1999**, *48*, 101.

33. Gohy, J.-F. *Advances in Polymer Science* **2005**, *190*, 65.

34. Van Butsele, K.; Jerome, C. *Chimie Nouvelle* **2007**, *25*, 8.

35. Kwon, G. S.; Okano, T. *Advanced Drug Delivery Reviews* **1996**, *21*, 107.

36. Sandholzer, M.; Bichler, S.; Stelzer, F.; Slugovc, C. *Journal of Polymer Science, Part A: Polymer Chemistry* **2008**, *46*, 2402.

37. Jamroz-Piegza, M.; Walach, W.; Dworak, A.; Trzebicka, B. *Journal of Colloid and Interface Science* **2008**, *325*, 141.

38. Yusa, S.-i.; Sugahara, M.; Endo, T.; Morishima, Y. *Langmuir* **2009**, *25*, 5258

39. Kim, J. S.; Jeon, H. J.; Park, M. S.; You, Y. C.; Youk, J. H. *European Polymer Journal* **2009**, *45*, 1918.

40. Jiang, X.; Luo, S.; Armes, S. P.; Shi, W.; Liu, S. *Macromolecules* **2006**, *39*, 5987.

41. Lawson, G. E.; Lee, Y.; Singh, A. *Langmuir* **2003**, *19*, 6401.

42. Kim, J. S.; Youk, J. H. *Polymer* **2009**, *50*, 2204.

43. Garg, S. M.; Xiong, X.-B.; Lu, C.; Lavasanifar, A. *Macromolecules (Washington, DC, United States)* **2011**, *44*, 2058.

44. O'Reilly, R. K.; Joralemon, M. J.; Wooley, K. L.; Hawker, C. J. *Chemistry of Materials* **2005**, *17*, 5976.

45. Tian, L.; Yam, L.; Wang, J.; Tat, H.; Uhrich, K. E. *Journal of Materials Chemistry* **2004**, *14*, 2317.

46. Hu, X.; Chen, X.; Wei, J.; Liu, S.; Jing, X. *Macromolecular Bioscience* **2009**, *9*, 456.

47. Zhang, Q.; Remsen, E. E.; Wooley, K. L. *Journal of the American Chemical Society* **2000**, *122*, 3642.

48. Huang, H.; Remsen, E. E.; Kowalewski, T.; Wooley, K. L. *Journal of the American Chemical Society* **1999**, *121*, 3805.

49. Turner, J. L.; Wooley, K. L. *Nano Letters* **2004**, *4*, 683.

50. Chan, Y.; Wong, T.; Byrne, F.; Kavallaris, M.; Bulmus, V. *Biomacromolecules* **2008**, *9*, 1826.

51. Zhang, L.; Bernard, J.; Davis, T. P.; Barner-Kowollik, C.; Stenzel, M. H. *Macromolecular Rapid Communications* **2008**, *29*, 123.

52. Sun, J.; Chen, X.; Lu, T.; Liu, S.; Tian, H.; Guo, Z.; Jing, X. *Langmuir* **2008**, *24*, 10099.

53. Lv, L.-P.; Xu, J.-P.; Liu, X.-S.; Liu, G.-Y.; Yang, X.; Ji, J. *Macromolecular Chemistry and Physics* **2010**, *211*, 2292.

54. Ryu, J.-H.; Chacko, R. T.; Jiwpanich, S.; Bickerton, S.; Babu, R. P.; Thayumanavan, S. *Journal of the American Chemical Society* **2010**, *132*, 17227.

55. Jia, Z.; Wong, L.; Davis, T. P.; Bulmus, V. *Biomacromolecules* **2008**, *9*, 3106.

56. Hao, J.; Kwissa, M.; Pulendran, B.; Murthy, N. *International Journal of Nanomedicine* **2006**, *1*, 97.

57. Cajot, S.; Lautram, N.; Passirani, C.; Jerome, C. *Journal of Controlled Release* **2011**, *152*, 30.

58. Zhang, L.; Liu, W.; Lin, L.; Chen, D.; Stenzel, M. H. *Biomacromolecules* **2008**, *9*, 3321.

59. Jiang, J.; Qi, B.; Lepage, M.; Zhao, Y. *Macromolecules* **2007**, *40*, 790.

60. Jiang, X.; Zhang, J.; Zhou, Y.; Xu, J.; Liu, S. *Journal of Polymer Science, Part A: Polymer Chemistry* **2008**, *46*, 860.

61. Zhang, J.; Jiang, X.; Zhang, Y.; Li, Y.; Liu, S. *Macromolecules (Washington, DC, United States)* **2007**, *40*, 9125.

62. He, J.; Tong, X.; Zhao, Y. *Macromolecules (Washington, DC, United States)* **2009**, *42*, 4845.

63. He, J.; Yan, B.; Tremblay, L.; Zhao, Y. *Langmuir* **2011**, *27*, 436.

64. Jin, Q.; Liu, X.; Liu, G.; Ji, J. *Polymer* **2010**, *51*, 1311.

CHAPTER III

Novel unsaturated polyphosphate containing amphiphilic block copolymers as promoter of core cross-linked micelles

S. Cajot, R. Riva, A. Ansias, B. Grignard, R. Jérôme, C. Jérôme

Abstract

A new amphiphilic block copolymer consisting of two biocompatible blocks, i.e. polyethylene oxide and polyphosphate, was synthesized for potential as drug carrier. Stability was imparted to the micelles formed in water, even at high dilution, by cross-linking of the hydrophobic polyphosphate core. Typically, an unsaturated side group was attached to the phosphate monomer in a one-step reaction. Polymerization of this 2-(but-3-en-1-yloxy)-1,3,2 dioxaphospholane 2-oxide monomer was initiated by a polyethylene oxide macroinitiator. Micelles formed in water by the accordingly prepared diblock copolymer were analyzed (size and morphology) by dynamic light scattering and transmission electron microscopy. They were then UV irradiated in order to induce the core cross-linking by polyaddition of the unsaturated side groups. Effectiveness of the cross-linking was evaluated from the stability of the micelles in DMF, a good solvent for the both constitutive blocks.

1. Introduction

Double affinity for water and hydrophobic media makes amphiphilic block copolymers highly specialized macromolecules. Indeed, they are prone to self-organize in water with formation of nanometric well-defined structures [1-2]. Among the variety of the possible supramolecular assemblies, spherical micelles, with a hydrophobic core surrounded by a hydrophilic shell, are most commonly observed [2]. Nevertheless, depending on the molecular architecture of the block copolymers (linear, star-shaped, comb-shaped…) the number of block and their relative length, much more elaborated nanostructures can be formed, including crew-cut, flower-like and vesicular micelles [2-4]. It is thus justified to speak about engineering of micelles, which is an exciting task for the polymer chemist.

A major incentive to design micelles with a well-defined morphology has to be found in the need for nanocarriers for hydrophobic poorly soluble drugs in water. Indeed, the encapsulation of drugs in an effective way is a need to provide protection against degradation in a hostile environment and to improve its usually low biodisponibility[5-7]. According to their structural complexity and thus performances, nanovehicles are ranked in terms of generation. Nanovectors of the first generation are liposomes - vesicles composed of a lipid bilayer-, basically intended to liver pathology because of their fast recognition by macrophages[8]. Nanovectors of the second generation were designed for restricting rapid elimination by the immune system. Their coating by a flexible and hydrophilic polymer, typically poly(ethylene oxide) (PEO), is actually a break to the adsorption of plasmic proteins responsible for recognition as foreign body[9]. Moreover, a proper control of their size allows them to penetrate the tumor cells more rapidly than normal cells according to the so-called enhanced permeability and retention (EPR) effect[10]. The third generation of nanovectors has the capacity of targeting specific tissues because of the availability of recognition molecules at their surface. These pilot molecules recognize a receptor typical of the targeted cells, which enhances the nanovector endocytosis and thus the delivery of the drug within the cytoplasm[11].

It is needless to say that the polymeric constituent of nanovectors must be biocompatible and biodegradable or bioeliminable whenever pharmaceutical or biomedical applications are concerned. For nanovectors to comply with the stealthiness, the hydrophilic block of amphiphilic block copolymers is usually a biocompatible and bioeliminable short length poly(ethylene oxide) (PEO). Biocompatible and biodegradable aliphatic polyesters, such as poly(ε-caprolactone) (PCL) and polylactides (PLA) [12] are preferably used as the hydrophobic block[13]. PEO-*b*-PCL copolymer is one of the amphiphilic block copolymers most studied worldwide for nanovector applications[14-16].

An important issue is however the unstability of all the micellar systems, thus including the micellar nanovectors because of the establishment of an equilibrium between unimers and micelles. Actually, below the critical micellar concentration (CMC), only unimers persist and any pre-encapsulated drug is released. The only way of preventing this damage from occurring in the bloodstream just after injection is to have the shell or the core of the micelles cross-linked[17-20]. Although making PEO cross-linkable is quite a problem, synthesis of aliphatic polyesters modified by side reactive groups has been reported[21], which offers opportunities of cross-linking. Nevertheless, the hydrolytic degradation of PCL and PLA has an impact on the local pH, which is decreased. This acidification may have undesirable side effect on living tissues.

This work aims at reporting on the synthesis of a new amphiphilic block copolymer for the design of core cross-linked micelles potentially applicable as nanovectors of the second generation. PEO is the hydrophilic block, whereas the choice of polyphosphate has been made as the hydrophobic block. Indeed, polyphosphates, which are biocompatible and biodegradable, are increasingly used in the biomedical field[22-23]. Their degradation does not change significantly the local pH and they are easily synthesized by ring-opening polymerization (ROP) of cyclic phosphates. Moreover, the synthesis of a new polyphosphate based copolymer bearing a functional side-group allowing further cross-linking is targeted. For this purpose, the choice of a polyphosphate block bearing an unsaturation prone to be cross-linked under UV irradiation, appears straightforward from literature investigations[24].

The strategy consists of the addition of a functional alcohol (F-R-OH) onto 2-chloro-1,3,2-dioxaphospholane 2-oxide as shown in Scheme 1, followed by coordinative ring-opening polymerization (ROP) of the cyclic phosphate.

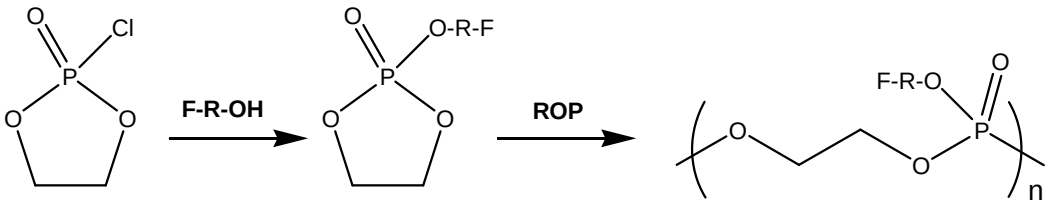

Scheme 1. General synthesis of polyphosphates by ring-opening polymerization

Synthesis of the amphiphilic PEO-*b*-polyphosphate block copolymer envisioned in this work relies on the initiation of ROP of an alkene substituted cyclic phosphate by a monomethoxy poly(ethylene oxide) macroinitiator in the presence of a catalytic amount of FDA approved tin octoate ($SnOct_2$) (Scheme 2).

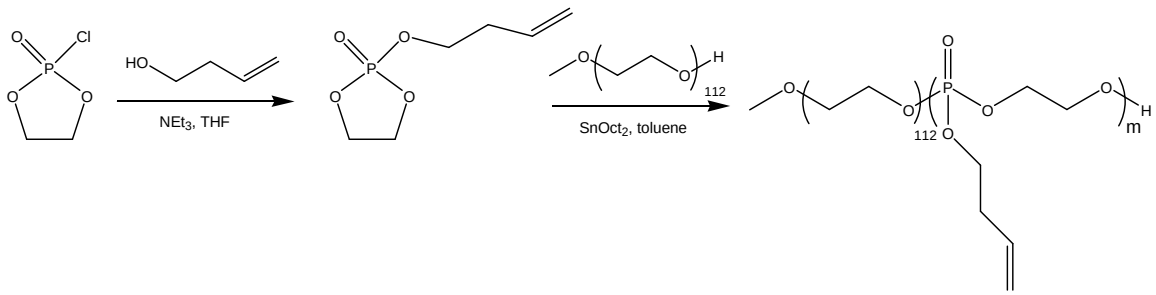

Scheme 2. Proposed strategy for the synthesis of poly(ethylene oxide)-*b*-poly(2-(but-3-en-1-yloxy)-1,3,2 dioxaphospholane 2-oxide) (PEO-*b*-PBODOP) amphiphilic copolymer

Micelles of this novel copolymer will be prepared in water and characterized by dynamic light scattering (DLS) and transmission electron microscopy (TEM). Finally, the cross-linking effectiveness of the micelle core under UV irradiation will be evaluated from the stability of the cross-linked micelles in a good solvent of both blocks.

2. Materials and Methods

Materials

2-chloro-1,3,2-dioxaphospholane 2-oxide (ClDOP, Acros), monomethoxy poly(ethylene oxide) (MPEO, M_n = 5000 g/mol, Aldrich), triethylamine (Aldrich) and diethyl ether (VWR) were used as received. 3-buten-1-ol (Aldrich), tetrahydrofuran (THF) and toluene (Chem-Lab) were flown over molecular sieves in order to remove water. $SnOct_2$ (Alfa Aesar) was dissolved in anhydrous toluene (0.5M) and stored under nitrogen.

Synthesis of 2-(but-3-en-1-yloxy)-1,3,2 dioxaphospholane 2-oxide (BODOP)

5.3 mL of 3-buten-ol (55 mmol) and 8.3 mL of triethylamine (55 mmol) were dissolved in 50 mL of anhydrous THF in a flame dried glass reactor of 250 mL under nitrogen at 0°C. 5.2 mL of 2-chloro-1,3,2-dioxaphospholane 2-oxide (61 mmol) were dissolved in 50 mL of anhydrous THF and added dropwise to the previous solution under stirring over a period of 3 h. After one additional hour of stirring at room temperature, triethylamine hydrochloride was filtered out, and the solvent was evaporated under reduced pressure. The final product was purified by fractionated distillation under reduced pressure (bp = 75°C, 0.1 Torr) and kept at -20°C under nitrogen.

^{1}H NMR ($CDCl_3$): δ (ppm): 5.75 (m, 1H, CH_2=C**H**-CH_2), 5.12 (m, 2H, C**H$_2$**=CH-CH_2), 4.38 (m, 4H, $(RO)_2P(O)O$-C**H$_2$**-C**H$_2$**-O(O)P$(OR)_2$), 4.15 (m, 2H, $(RO)_2$-P(O)-O-C**H$_2$**-CH_2), 2.46 (m, 2H, CH_2-C**H$_2$**-CH=CH_2).

^{13}C NMR ($CDCl_3$): δ (ppm): 132.7 (**C**H_2=CH-CH_2), 117.9 (CH_2=**C**H-CH_2), 65.7 (CH_2-**C**H_2-O), 34.7 (CH_2=**C**H-CH_2).

^{31}P NMR ($CDCl_3$): δ (ppm): 17.5 ppm

Synthesis of poly(BODOP)

Typically, 1.1 g of BODOP (6.2 mmol) was dried in a glass reactor by three azeotropic distillations of anhydrous toluene. 0.1 mL of the 0.5 M solution of $SnOct_2$ and 0.5 mL of a 0.2 M solution of benzyl alcohol solution in toluene (0.1 mmol) were added through a rubber septum via a stainless steel capillary. The solution was then stirred at 55°C. After 24 hours of polymerization, a drop of pure acetic acid was added, and the copolymer was recovered by precipitation in cold diethyl ether.

^{1}H NMR($CDCl_3$): δ (ppm): 7.38 (m, $C_6\mathbf{H_5}$-$CH_2O(O)P$) 5.75 (m, CH_2=C**H**-CH_2), 5.12 (m, C$\mathbf{H_2}$=CH-CH_2), 4.26 (m, $(RO)_2P(O)O$-C$\mathbf{H_2}$-C$\mathbf{H_2}$-$O(O)P(OR)_2$, 4.15 (m, $(RO)_2$-P(O)-O-C$\mathbf{H_2}$-CH_2), 3.79 (m, C_6H_5-C$\mathbf{H_2}$O(O)P), 2.46 (m, CH_2-C$\mathbf{H_2}$-CH=CH_2).
^{13}C NMR($CDCl_3$): δ (ppm): 133 (s, CH_2=**C**H), 118 (s, CH=**C**H_2), 77 (m, CH_2-**C**H_2-O), 66 (m, C-**C**H_2-O), 34 (s, CH_2-**C**H_2-CH)

Synthesis of MPEO-*b*-poly(BODOP)

Typically, 2 g of MPEO (0.4 mmol of OH end-group) and 0.9 g of BODOP (5 mmol) were separately dried in a glass reactor by three azeotropic distillations of anhydrous toluene. In the BODOP containing reactor, 5 ml of anhydrous toluene was added, and the monomer solution was transferred into the MPEO containing glass reactor through a freshly flamed stainless capillary. 0.1 mL of the 0.5 M solution of $SnOct_2$ (0.5 mmol) was added through a rubber septum via a stainless steel capillary, and the temperature was increased up to 55°C. After 24 h of polymerization, a drop of pure acetic acid was added, and the copolymer was recovered by precipitation in cold diethyl ether.

^{1}H NMR ($CDCl_3$): δ (ppm) : 5.75 (m, CH_2=C**H**-CH_2), 5.12 (m, C$\mathbf{H_2}$=CH-CH_2), 4.26 (m, $(RO)_2P(O)O$-C$\mathbf{H_2}$-C$\mathbf{H_2}$-$O(O)P(OR)_2$, 4.15 (m, $(RO)_2$-P(O)-O-C$\mathbf{H_2}$-CH_2), 3.64 (m, O-C$\mathbf{H_2}$-C$\mathbf{H_2}$-O), 2.46 (m, CH_2-C$\mathbf{H_2}$-CH=CH_2).

Characterization methods

Size exclusion chromatography (SEC) was carried out in THF at 45°C at a flow rate of 1 mL/min with a SFD S5200 auto sampler liquid chromatograph equipped with a SFD refractometer index detector 2000. The PL gel 5 µm (10^5, 10^4, 10^3, and 100 Å) columns were calibrated with polystyrene standards. ^{1}H NMR spectra were recorded in $CDCl_3$ at 400 MHz in the FT mode with a Bruker AN 400 apparatus at 25°C. The infrared spectra were recorded with a Perkin-Elmer FT-IR 1720X. The IR samples were prepared by slow evaporation of a polymer solution in THF, onto NaCl windows. Differential scanning calorimetry (DSC) was carried out with a TA DSC Q 100 thermal analyzer calibrated with indium. Glass transition and melting temperatures were measured, after a first cooling (- 80°C) and heating (100°C) cycle. Thermograms were recorded during the second heating cycle at 10°C/min. Thermogravimetric analysis (TGA) was carried out with a TA Q 500 thermal analyzer under nitrogen atmosphere at 10°C/min.

Micellization

Micelles of the amphiphilic MPEO-*b*-poly(BODOP) block copolymers were prepared by a co-solvent process. A 1% stock solution of the copolymer was prepared in DMF added with a catalytic amount of benzophenone. 20 mL of Milli-Q water were added to 5 mL of this organic solution under vigorous stirring for 2 h. Micelles were purified by dialysis overnight against 1L of water with a cellulose dialysis membrane (Spectrapor, cut-off 3500). The cross-linking reaction proceeded under UV irradiation (Lot Oriel, Hg vapor, 200 Watts) of a degassed micellar solution for 4 h.

Micelles characterization methods

Dynamic light scattering (DLS) was carried out with a Beckman Coulter Delsa Nano C Particle analyzer, and the data were treated by the Delsa Nano UI 2.21 software. All the measurements were carried out at 25°C at an angle of 165°. Samples for transmission electron

microscopy (TEM) were prepared by slow evaporation of the micellar solutions analyzed by DLS on a formvar-coated copper grid. The excess of solution was removed with a filter paper. The samples were analyzed with a Philips CM100 microscope equipped with an Olympus camera, and the data were transferred to a computer equipped with the Megaview system.

3. Results and discussion

Synthesis of 2-(but-3-en-1-yloxy)-1,3,2 dioxaphospholane 2-oxide (BODOP)

2-(but-3-en-1-yloxy)-1,3,2 dioxaphospholane 2-oxide (BODOP) was synthesized by a procedure already reported in the literature for other functional alcohols[24]. Typically, an excess of 2-chloro-1,3,2-dioxaphospholane 2-oxide was reacted with 3-buten-1-ol in the presence of a stoechiometric amount of triethylamine as detailed in the experimental part. The final yield in this monomer after purification was 60%. The IR spectrum of the collected product showed characteristic absorption bands at 1643 and 1304 cm^{-1} typical of the C=C and P=O elongation, respectively. The ^{1}H NMR spectrum (Figure 1) confirmed the expected structure for BODOP.

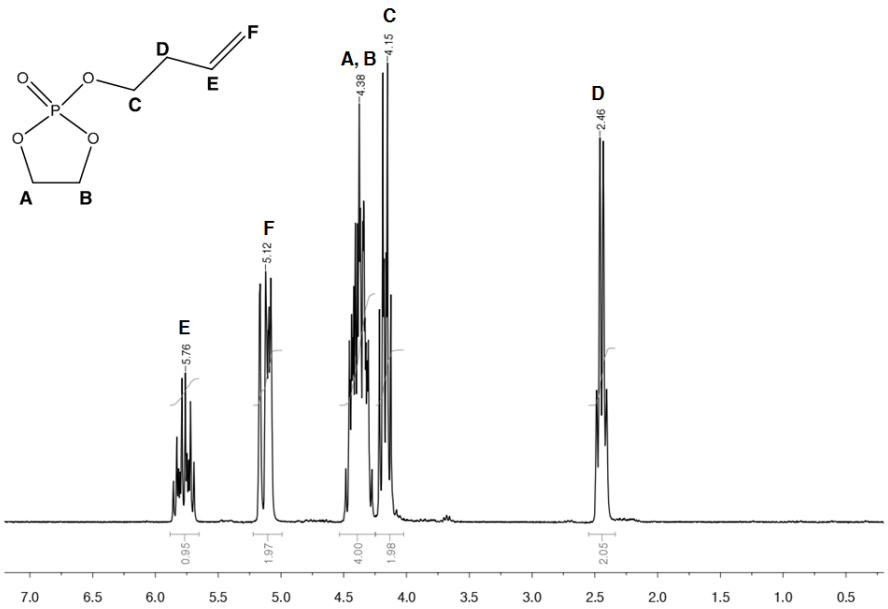

Figure 1. ^{1}H NMR spectrum of BODOP monomer

The 1:4 ratio for the intensity of peak E characteristic of the CH=C proton and peaks A and B typical of the intracyclic methylene protons was an experimental evidence for the quantitative addition of 3-buten-1-ol to the phosphate chloride. ^{31}P NMR analysis of the purified monomer was also carried out (Figure 2).

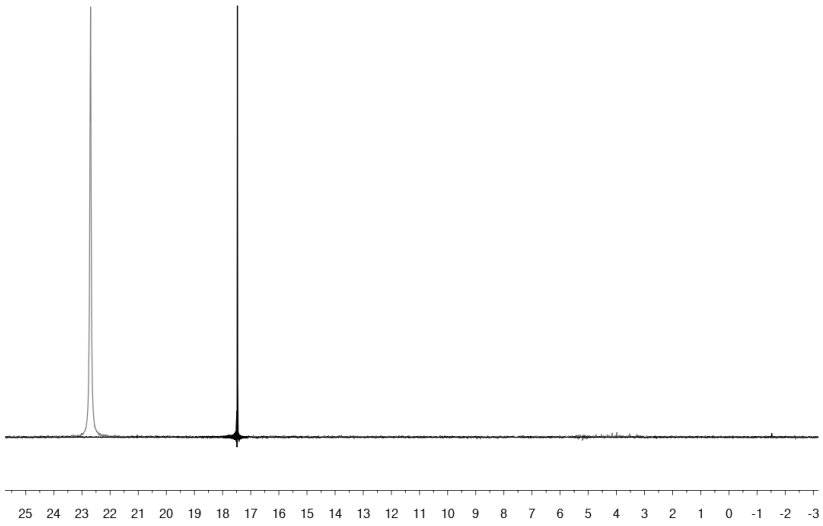

Figure 2. ^{31}P NMR spectrum of ClDOP (grey line) and BODOP monomer (black line)

The successful addition of 3-buten-1-ol onto ClDOP was again confirmed by the shift of the signal of ClDOP from 23 ppm (grey line) to 17.5 ppm (black line) after reaction. Moreover, the presence of a unique signal at 17.5 ppm (black curve) assessed the high purity of the monomer after only one run of fractionated distillation. ^{1}H-^{1}H COSY and ^{13}C-^{1}H HMQC also supported the structure of the monomer (Figures 3 and 4). The ^{1}H-^{1}H COSY spectrum allows to underline the correlation between the protons of the molecule; especially the coupling between protons separated by three bonds ($^{3}J_{HH}$) but also protons separated by four bonds ($^{4}J_{HH}$) when double bonds are concerned, as it is the case for the protons D and F. The ^{13}C-^{1}H HMQC correlates the protons to their corresponding atoms. These two analyses definitely confirm the structure of the new monomer.

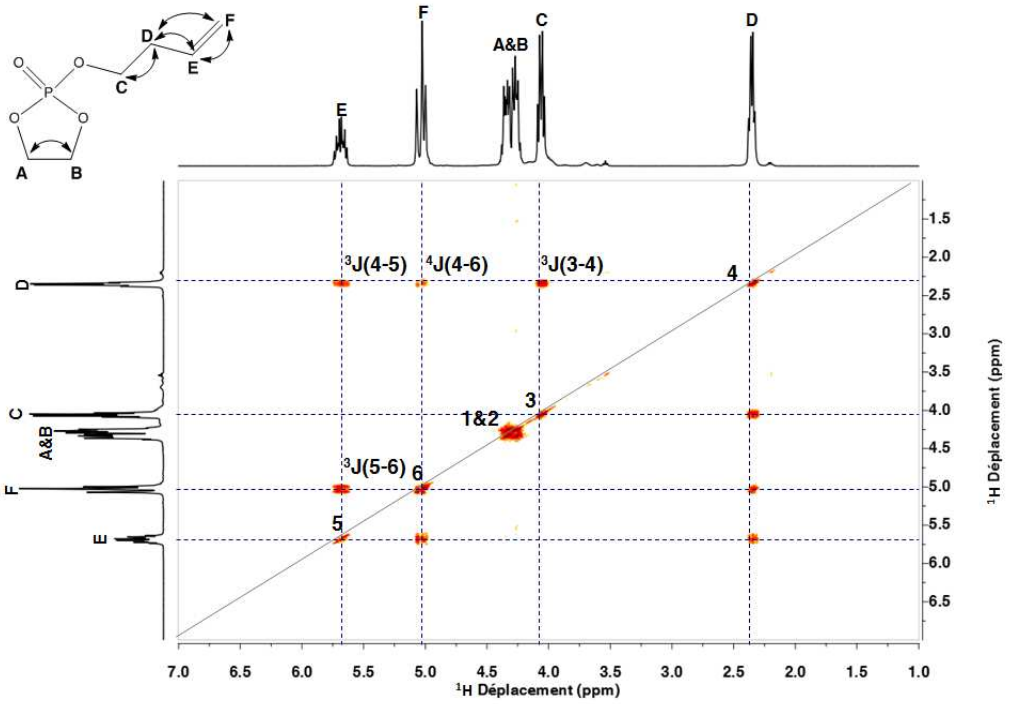

Figure 3. ^{1}H-^{1}H COSY spectrum of BODOP monomer

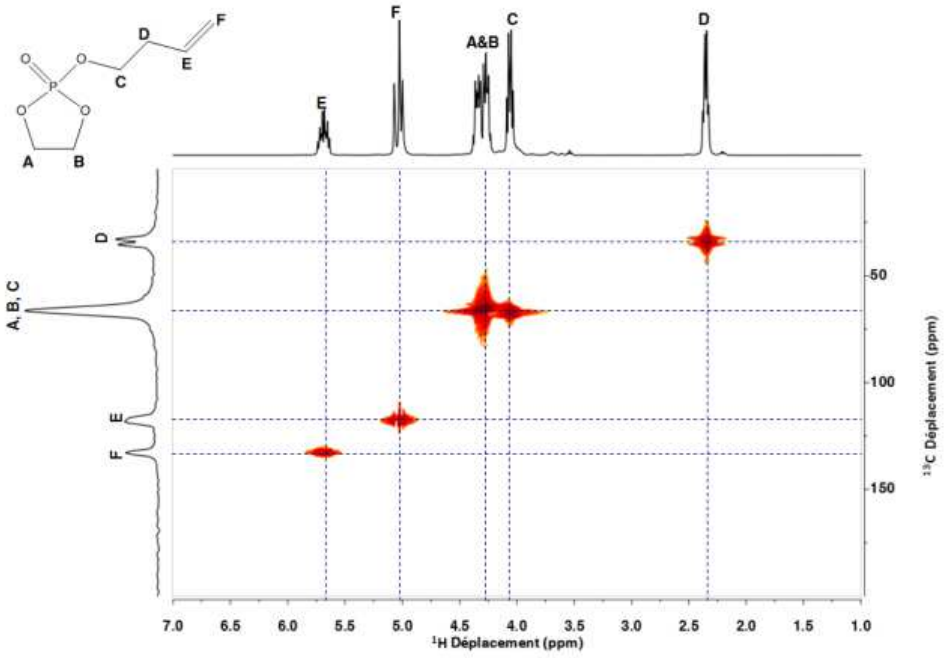

Figure 4. ^{13}C-^{1}H HMQC spectrum of PBODOP monomer

Stability of BODOP towards hydrolysis was investigated by ^{1}H NMR analysis of BODOP dissolved in D_2O. After only 30 min, this monomer was completely degraded as shown by the complete disappearance of the signals of BODOP in favor of new signals characteristic of 3-buten-1-ol and ethylene glycol. ^{31}P NMR analysis showed a single signal at 0 ppm, which was attributed to phosphoric acid. Thus, the expected high sensitivity of BODOP to hydrolysis was confirmed, which was the reason for keeping the monomer under an inert atmosphere. The monomer was also stored at low temperature in order to prevent thermal degradation.

Synthesis of poly(BODOP)

Polymerizability of BODOP was tested with benzylic alcohol as an initiator and $Sn(Oct)_2$ as a catalyst in toluene at 55°C, by the classical coordination –insertion mechanism previously described for the ring opening polymerization of lactones or lactides[25]. Progress of the polymerization was followed by ^{1}H and ^{31}P NMR analyses of the reacting solution. After 24 h of reaction, the intensity of the signal of the monomer at 4.4 ppm, corresponding to the two intracyclic methylene protons had decreased in contrast to peaks characteristic of poly(BODOP) at 4.3 ppm. The ^{31}P NMR spectrum also recorded after 24h of polymerization, confirmed the high conversion of BODOP by the appearance of a new signal of high intensity centered at -1.4 ppm, assigned to the phosphorous atom of poly(BODOP). The polyphosphate was purified by precipitation in cold diethyl ether, collected by decantation and dried in vacuo. Poly(BODOP) was amorphous with a T_g of -28°C as measured by DSC. The ^{1}H NMR spectrum of purified poly(BODOP) is shown in Figure 5.

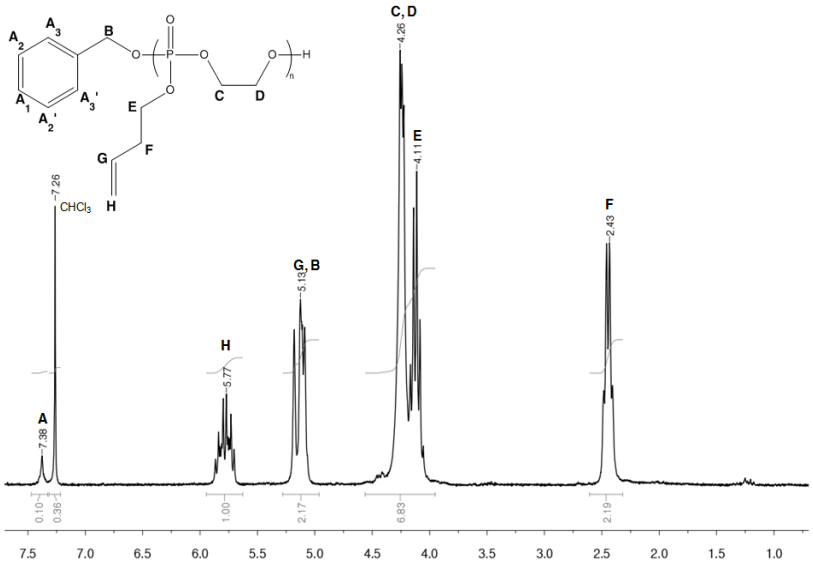

Figure 5. ^{1}H NMR spectrum of poly(BODOP)

The ^{1}H signal of the two intracyclic methylene groups (peaks A and B, Figure 2) was shifted from 4.38 ppm to 4.26 ppm (peaks C and D, Figure 5) as result of the opening of the cyclic phosphate upon the polymerization. The monomer conversion could not be determined because of both the overlapping of the monomer and the polymer signals. The ^{1}H signal of the benzyl end-group (protons A) at 7.38 ppm (initiator fragment) allowed the average polymerization degree (DP) and the average molar mass (M_n) of poly(BODOP) to be calculated according the following equations.

$$DP = \frac{I_{C,D,E}/6}{I_A/5} \qquad [1]$$

$$M_n = DP \times 178.1243 + 108.1378 \qquad [2]$$

Experimental DP was 50, thus lower than the theorical value of 56 calculated from the monomer to initiator molar ratio at complete conversion. From these data, and on the assumption of a living polymerization quantitatively initiated by the benzylic alcohol, the monomer conversion was estimated at 89%. This value was in rather good agreement with the

approximate value of 81% calculated from the intensity ratio of the monomer and polymer signals in the ^{31}P NMR spectrum (Figure 6) recorded after 24 h of polymerization.

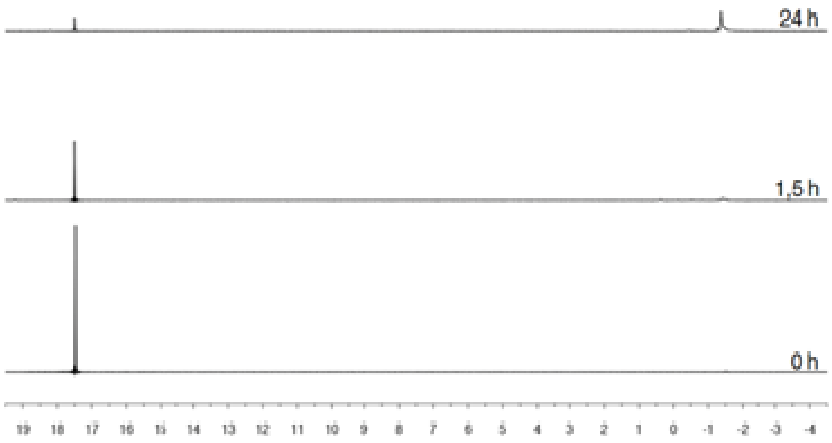

Figure 6. ^{31}P NMR spectrum of the homopolymerization of the BODOP vs. time

The SEC chromatogram showed a monomodal trace with a low polydispersity index of 1.15 (Figure 7). The results of BODOP homopolymerization are reported in table 1. It must be noted that a shoulder appear on the low molar mass side of the SEC chromatogram when the polymerization time exceeded 24 h, which is more likely the signature of transesterification side-reactions (Figure 7).

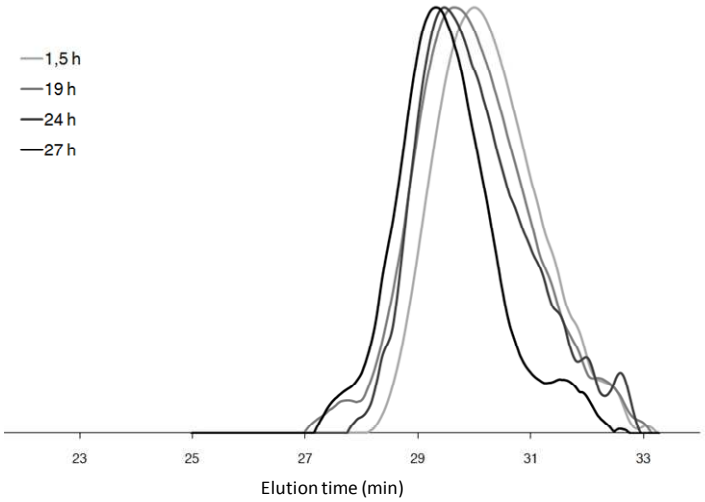

Figure 7. SEC traces of the homopolymerisation of the BODOP vs. time

Table 1. Cumulative results for the homopolymerization of BODOP

DP[a]	**M_n[b] (g/mol)**	**Conversion[c]**	**DP[d] (^{1}H NMR)**	**M_n[e] (^{1}H NMR) (g/mol)**	**M_w/M_n[f] (SEC)**
56	10 000	89 %	50	8 900	1.15

a: theoretical polymerization degree calculated from the initial [monomer]/[initiator] ratio at complete conversion

b: theoretical molar mass of the polymer calculated as M_n= DP x MM_{BODOP}

c: Conversion of the BODOP monomer

d: experimental polymerization degree determined by ^{1}H NMR according to equation 1

e: experimental molar mass determined by ^{1}H NMR according to equation 2

f: polydispersity index measured by SEC

Stability of poly(BODOP) was evaluated in two solvents, i.e. THF and a phosphate buffer (pH = 7.2). Solution of the polymer in THF and dispersion in the phosphate buffer were each transferred into a glass flask that were sealed and kept at room temperature (20°C). The SEC chromatogram was recorded at different times as shown in Figures 8 and 9. Sampling of the THF solution was directly injected in the chromatograph. In contrast, the polymer dispersed in the phosphate buffer, was recovered by water lyophilization, then dissolved in THF and analyzed by SEC.

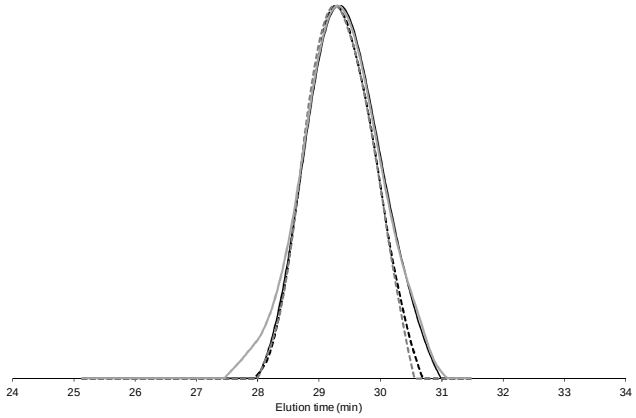

Figure 8. Stability of poly(BOBOP) in THF after 1 hours (—) , 1 week (- -), 1 month (—) and 2 months (- -).

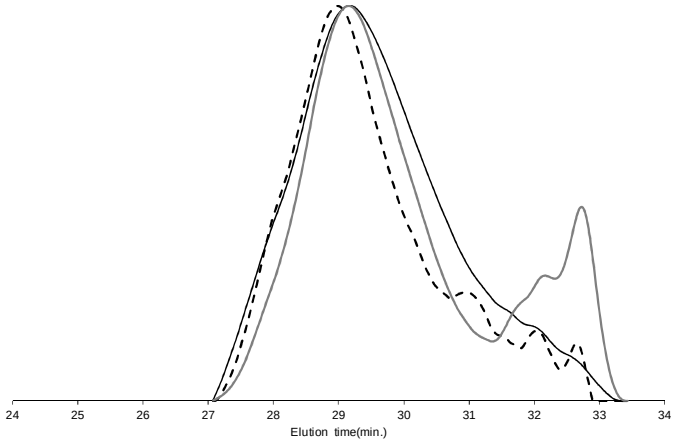

Figure 9. Stability of poly(BOBOP) in phosphate buffer (pH=7.2) after 1h (—), 3 days (- -) and 1 week (—).

Poly(BODOP) is thus reasonably stable in a polar solvent. Indeed, only a small increase in polydispersity beyond 1 week in THF is observed that could be accounted for transesterification reactions. Conversely, degradation was very pronounced after only 3 days of contact with the phosphate buffer, which proved that polyphosphate are more easily hydrolyzed compared to aliphatic polyesters, such as PCL, largely reported as building block of drug delivery vehicles.

Synthesis of MPEO-*b*-poly(BODOP)

Because polymerization of BODOP was successfully initiated by an alcohol, the synthesis of a novel amphiphilic PEO-*b*-poly(BODOP) block copolymer was tested by initiating the BODOP polymerization by a MPEO-OH macroinitiator under the same experimental conditions as for the homopolymerization from benzylic alcohol. Amphiphilic block copolymers with a hydrophilic-lipophilic balance (HLB) around 15 is usually recommended when the parent micelles are intended for drug delivery applications[26]. Indeed, when molecular weight of the hydrophilic block (PEO) is higher than the hydrophobic block (poly(BODOP)) (HLB > 10), amphiphilic copolymers are prone to form spherical micelles. In contrast, when the molecular weight of the hydrophobic block is higher than the hydrophilic one (HLB<10), the copolymer is rather used as stabilizer of nanoparticles. Therefore, because the molar mass of the PEO macroinitiator available for this study was 5000 g/mol, a molar mass of 2000 g/mol was targeted for the hydrophobic poly(BODOP) block. As for homopolymerization, a high monomer conversion of more than 90 percents was observed by ^{1}H NMR after 24 h in toluene at 55°C. After purification by precipitation in cold diethyl ether, the PEO-*b*-poly(BODOP) copolymer was analyzed by ^{1}H NMR.

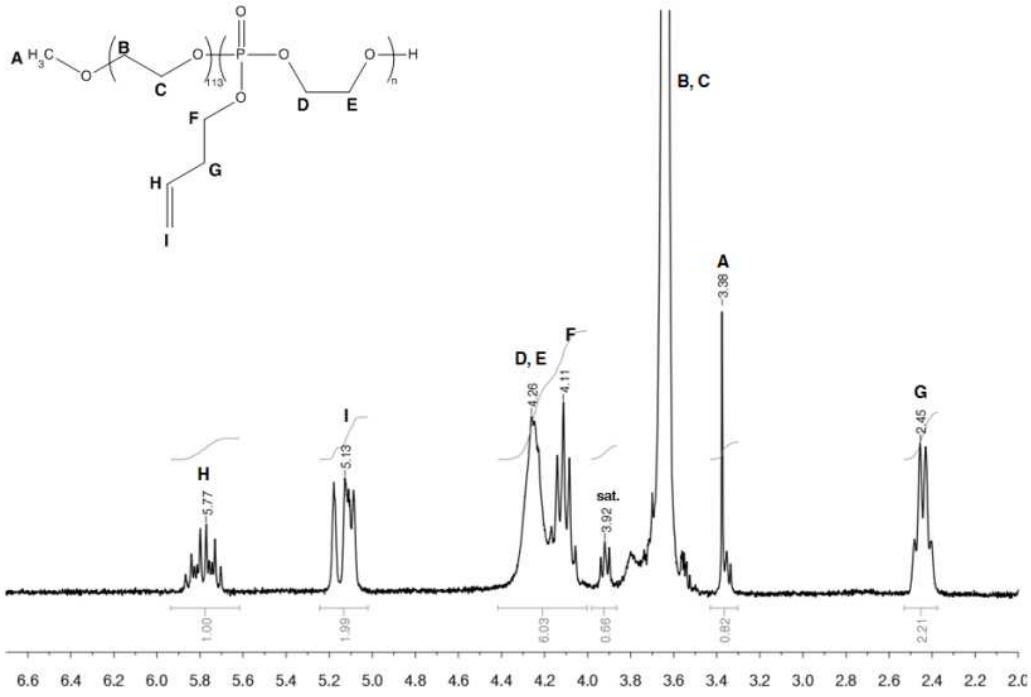

Figure 10. ^{1}H NMR spectrum of PEO-*b*-poly(BODOP) amphiphilic copolymer

The ^{1}H NMR spectrum (Figure 10) was the same as for the poly(BODOP), excepted for two additional signals characteristic of the PEO block at 3.6 ppm and 3.4 ppm assigned to the methyl protons of the ethylene oxide repeating units and the methoxy end-group, respectively. The molar mass of the poly(BODOP) block was calculated from the relative intensity of peaks (H+I) for the three olefinic protons and peak A typical of the methoxy end-group of the PEO block. However, the molar mass of the poly(BODOP) block (3200 g/mol) was higher than the targeted value of 2000 g/mol.

Table 2. Cumulative results for the synthesis of PEO-*b*-poly(BODOP)

DP[a]	**M_n[b] (g/mol)**	**Conversion[c]**	**DP[d] (^{1}H NMR)**	**M_n[e] (^{1}H NMR) (g/mol)**
11	2 000 g/mol	> 92 %	18	3 200 g/mol

a: theoretical polymerization degree calculated from the initial [monomer]/[initiator] ratio at 100% of conversion

b: theoretical molar mass of the polymer (M_n= DP x MM_{BODOP})

c: Conversion of BODOP monomer

d: experimental polymerization degree determined by ^{1}H NMR according to equation 1

e: experimental molar mass determined by ^{1}H NMR according to equation 2

Nevertheless, the success of the copolymerization could not be undoubtedly confirmed by the SEC analysis. Indeed, the SEC trace appears multimodal with a new peak at low elution time corresponding to chains of very high molecular mass, together with a peak close to the initial PEO macroinitiator but slightly shifted towards higher M_n, showing a more complex polymerization from the polymeric initiator as compared to benzylic alcohol (Figure 11). However, due to the high sensitivity of the polyphosphate towards hydrolysis, no further purification by dialysis was attempted and the material was thus used as such in the following.

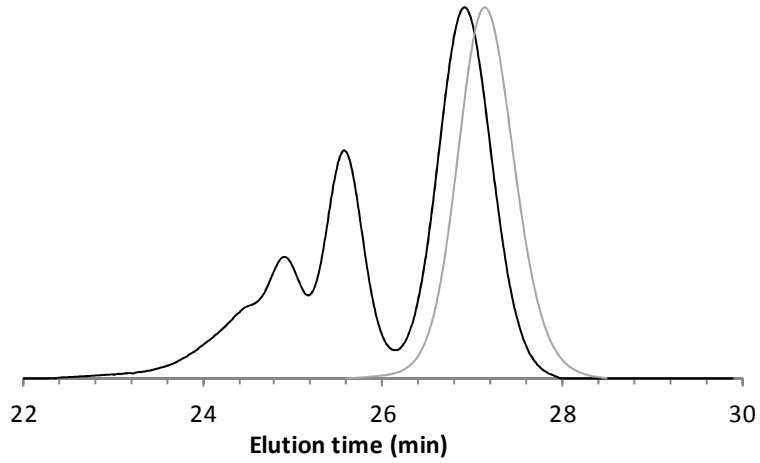

Figure 11. SEC traces of the PEO macroinitiator (grey line) and the PEO-*b*-poly(BODOP) copolymer (black line)

DSC analysis showed that the sample is semi-cristalline (T_g = -29,4°C and T_m = 54,3°C), showing that the amorphous poly(BODOP) block is unable to prevent PEO from

crystallizing. The thermal stability of the PEO-*b*-poly(BODOP) copolymer was investigated by TGA analysis. No weight loss was observed before 200°C showing a good thermal stability.

Micelles formation and cross-linking

Micellization of the amphiphilic PEO-*b*-poly(BODOP) block copolymer was carried out by a traditional method. Typically, the copolymer was dissolved in DMF, a good solvent for both the hydrophobic (poly(BODOP)) and the hydrophilic (PEO) blocks, followed by the rapid addition of water, a selective solvent of the PEO block, under vigorous stirring. After 2 h, DMF was removed by dialysis. Excepted for a small part kept as a reference, the micellar solution was submitted to UV irradiation in order to have the hydrophobic core cross-linking as result of the [2+2] cycloaddition of the side alkene groups into cyclobutane ones [27] (Figure 12). This reaction occurred in the presence of a photo-initiator, benzophenone, that was previously added to the copolymer solution in DMF. Upon water addition, the hydrophobic photoinitiator was expected to be located in the hydrophobic core of the micelles.

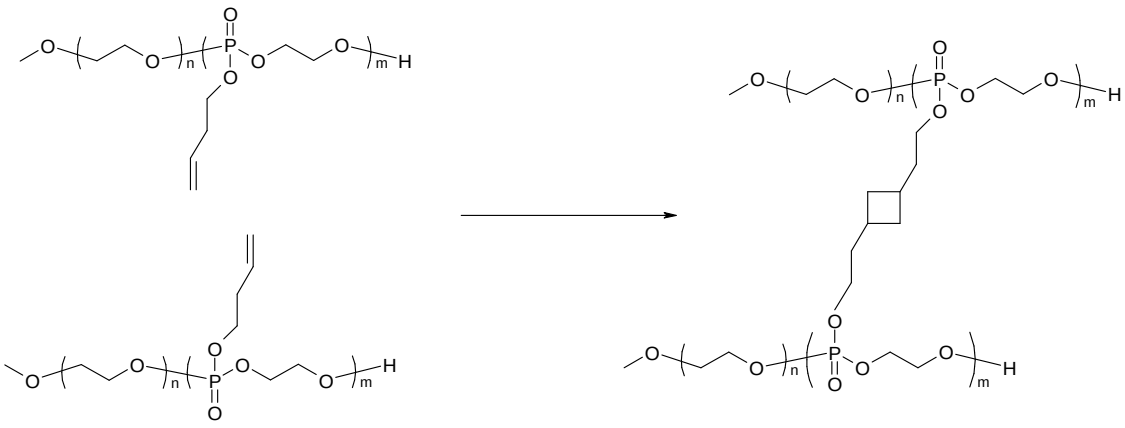

Figure 12. Cross-linking of the micelle core by a [2+2] cycloaddition reaction

The core cross-linked micelles were characterized by DLS comparatively to the reference micelles. The results are summarized in Table 3 and Figure 13.

Table 3. DLS data for the cross-linked and non cross-linked micelles of PEO-*b*-poly(BODOP) in water.

Copolymer	Non cross-linked micelles		Cross-linked micelles	
	$D_{h,\,app}$ (nm) [a]	PDI [b]	$D_{h,\,app}$ (nm) [a]	PDI [b]
PEO-*b*-PBODOP	100	0.2	90	0.2

[a] Apparent hydrodynamic diameter ; [b] polydispersity index determined by DLS

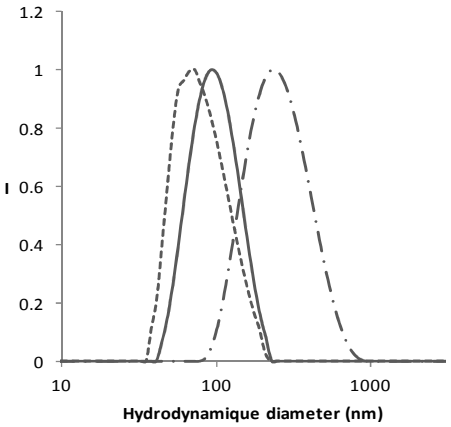

Figure 13. Size distribution of the non cross-linked PEO-*b*-PBODOP micelles in H_2O (———) and of the cross-linked PEO-*b*-poly(BODOP) micelles in H_2O (– –) and DMF (. —).

The average size ($D_{h,app}$) of the non cross-linked micelles in water was about 100 nm, thus twice the size (50 nm) of PEO-*b*-PCL micelles of comparable composition and DP[28]. This apparent hydrodynamic diameter decreased by 10 nm upon the core cross-linking, which suggests that the intermolecular cycloaddition reaction is responsible for a higher compactness of the poly(BODOP) chains in the core.

The spherical morphology of the previously dried cross-linked micelles was observed by TEM in agreement with the relative length of the blocks (Figure 14). The phosphorus

atoms in the hydrophobic core provided it with a high contrast, whereas the PEO corona was collapsed and this unobserved.

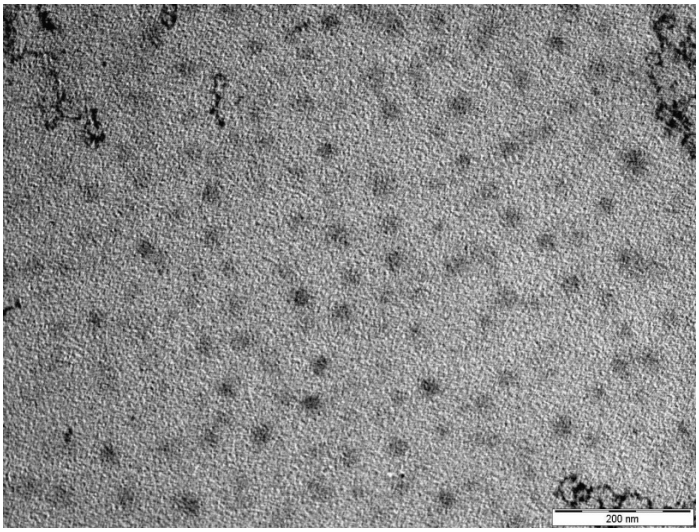

Figure 14. TEM picture of the cross-linked micelles of PEO-*b*-poly(BODOP)

The efficiency of the core cross-linking reaction was also assessed by the resistance of the micelles against solubilization in DMF, a good solvent for both the PEO and the poly(BODOP) blocks. Nevertheless, the cross-linked poly(BODOP) core was solvated by DMF, which accounts for a substantial increase in size, from 100 nm in water up to 230 nm in DMF (Figure 13). The reference micelles were extensively soluble, although not completely, in DMF. This observation strongly suggests that the cross-linking reaction may occur independently of a photoinitiator and UV irradiation.

Another evidence of the cross-linking of the core was given by NMR analysis of the micelles in D_2O before and after photo cross-linking (Figure 15). A decrease in intensity of the signals of the alkene protons (at 5.45 and 6.20 ppm) and the methylene protons in α-position of the alkene (at 2.75 ppm) was observed to the benefit of signals typical of the cyclobutane protons. Broadening of the signals of the core protons were observed as result of the restricted mobility of the chains in line with the cross-linking reaction. According to ^1H NMR, 80% of the alkenes were converted into cyclobutane.

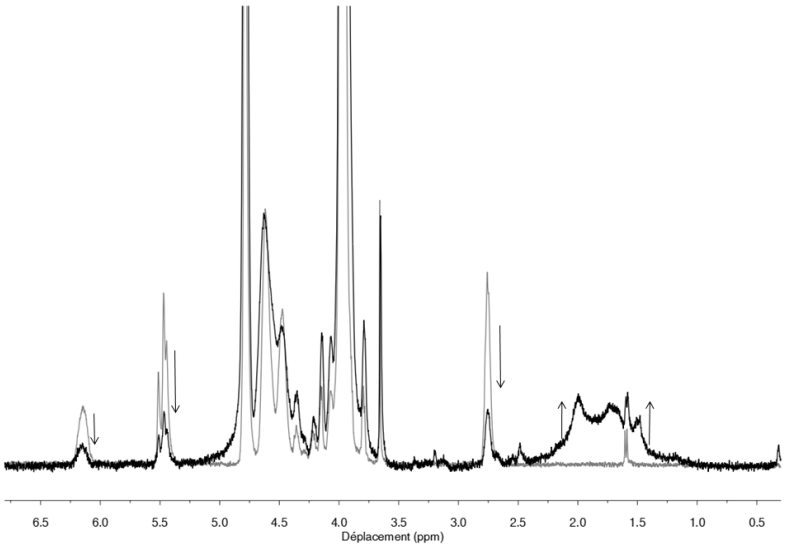

Figure 15. ^{1}H NMR spectrum of non cross-linked micelles (●) and cross-linked micelles (●) of PEO-*b*-poly(BODOP) in D_2O.

4. Conclusions

A new alkene containing cyclic phosphate (BODOP) was successfully synthesized by a straightforward one-step reaction of addition of 3-buten-1-ol onto 2-chloro-1,3,2-dioxaphospholane 2-oxide. After complete characterization by spectroscopic methods, polymerizability of this monomer was assessed by polymerization initiated by benzylic alcohol in presence of a catalytic amount of tin octoate in toluene at 55°C. The macromolecular parameters, determined by SEC and ^{1}H NMR analysis, were in good agreement with the theoretical values predicted in case of a living polymerization. With the purpose to synthesize a novel amphiphilic PEO-*b*-poly(BODOP) block copolymer, polymerization of the BODOP monomer was initiated by an α-methoxy, ω-hydroxyl-PEO macroinitiator. Even if this macroinitiator does not appear to prevent the BODOP polymerization as confirmed by NMR data, a relatively poor control of the polymerization initiated by this macromonomer was evidenced by SEC. Nevertheless, the recovered material

forms well-defined micelles in water which were analyzed by DLS and TEM. Micelles with an average diameter of 100 nm were observed. The micellar core could be cross-linked by UV irradiation, so accounting for resistance of the micelles in DMF, a good solvent for the two blocks. Moreover, an increase in the average diameter was measured in DMF as a result of the swelling of the cross-linked polyphosphate core.

As perspective, the unsaturations of the core of the micelles might be used not only for cross-linking purpose but also for having active molecules attached by a thiol-ene reaction within the prospect of sustained release. This widens the interest of such diblock copolymer. Nevertheless, the polymerization from the macroinitiator should be investigated further in order to optimize the synthesis of the desired diblock copolymer.

However, the very fast hydrolysis of the poly(phosphate) appears to us as a limiting point to the development of long-circulating drug delivery systems and the development of stimuli responsive nanocarriers. For these reasons, in the following of this thesis, we will rather focus on aliphatic polyesters and particularly on poly-ε-caprolactone as hydrolyzable hydrophobic partner to form well-defined core cross-linked micelles sensitive to a specific stimulus.

5. References

1. Rösler, A.; Vandermeulen, G. W. M.; Klok, H.-A. *Advanced Drug Delivery Reviews* **2001**, *53*, 95.

2. Letchford, K.; Burt, H. *European Journal of Pharmaceutics and Biopharmaceutics* **2007**, *65*, 259.

3. Hadjichristidis, N.; Pispas, S.; Floudas, G. In *Block Copolymers*; John Wiley & Sons, Inc.: 2003, p 255.

4. Hadjichristidis, N.; Pispas, S.; Floudas, G. In *Block Copolymers*; John Wiley & Sons, Inc.: 2003, p 268.

5. Aliabadi, H. M.; Mahmud, A.; Sharifabadi, A. D.; Lavasanifar, A. *J. Control. Release* **2005**, *104*, 301.

6. Jones, M.-C.; Leroux, J.-C. *European Journal of Pharmaceutics and Biopharmaceutics* **1999**, *48*, 101.

7. Gaucher, G.; Marchessault, R. H.; Leroux, J.-C. *J. Control. Release* **2010**, *143*, 2.

8. Barratt, G. *Cellular and Molecular Life Sciences* **2003**, *60*, 21.

9. Lee, J. H.; Lee, H. B.; Andrade, J. D. *Progress in Polymer Science* **1995**, *20*, 1043.

10. Maeda, H.; Bharate, G. Y.; Daruwalla, J. *European Journal of Pharmaceutics and Biopharmaceutics* **2009**, *71*, 409.

11. Jaracz, S.; Chen, J.; Kuznetsova, L. V.; Ojima, I. *Bioorganic & Medicinal Chemistry* **2005**, *13*, 5043.

12. Shin, H.-C.; Alani, A. W. G.; Rao, D. A.; Rockich, N. C.; Kwon, G. S. *J. Control. Release* **2009**, *140*, 294.

13. Dash, T. K.; Konkimalla, V. B. *J. Control. Release*.

14. Mikhail, A. S.; Allen, C. *Biomacromolecules* **2010**, *11*, 1273.

15. Yáñez, J.; Forrest, M.; Ohgami, Y.; Kwon, G.; Davies, N. *Cancer Chemotherapy and Pharmacology* **2008**, *61*, 133.

16. Vangeyte, P.; Leyh, B.; Heinrich, M.; Grandjean, J.; Bourgaux, C.; Jerome, R. *Langmuir* **2004**, *20*, 8442.

17. Cajot, S.; Lautram, N.; Passirani, C.; Jérôme, C. *J. Control. Release* **2011**, *152*, 30.

18. Jamróz-Piegza, M.; Wałach, W.; Dworak, A.; Trzebicka, B. *Journal of Colloid and Interface Science* **2008**, *325*, 141.

19. Xiong, M.-H.; Wu, J.; Wang, Y.-C.; Li, L.-S.; Liu, X.-B.; Zhang, G.-Z.; Yan, L.-F.; Wang, J. *Macromolecules* **2009**, *42*, 893.

20. O'Reilly, R. K.; Joralemon, M. J.; Wooley, K. L.; Hawker, C. J. *Chemistry of Materials* **2005**, *17*, 5976.

21. Lecomte, P.; Riva, R.; Jerome, C.; Jerome, R. *Macromolecular Rapid Communications* **2008**, *29*, 982.

22. Zhao, Z.; Wang, J.; Mao, H.-Q.; Leong, K. W. *Advanced Drug Delivery Reviews* **2003**, *55*, 483.

23. Wang, Y.-C.; Liu, X.-Q.; Sun, T.-M.; Xiong, M.-H.; Wang, J. *J. Control. Release* **2008**, *128*, 32.

24. Iwasaki, Y.; Akiyoshi, K. *Macromolecules* **2004**, *37*, 7637.

25. Lecomte, P. *Encyclopedia of Polymer Science and Technology* **2004**.

26. Cajot, S.; Riva, R.; Billiet, L.; Du Prez, F.; Alexandre, M.; Lecomte, P.; Jérôme, C. *Macromolecular Symposia* **2011**, *309/310*, 111.

27. Okay, O.; Kurz, M.; Lutz, K.; Funke, W. *Macromolecules* **1995**, *28*, 2728.

28. Vangeyte, P.; Gautier, S.; Jerome, R. *Colloids and Surfaces, A: Physicochemical and Engineering Aspects* **2004**, *242*, 203.

CHAPTER IV

Novel functional degradable block copolymers for the building of reactive micelles

S. Cajot, P. Lecomte, C.Jérôme, R. Riva

Polymer Chemistry, **2012**, submitted

Abstract

Amphiphilic biocompatible copolymers are promising materials for the elaboration of nanosystems for drug delivery applications. This paper aims at reporting on the synthesis of new functional amphiphilic copolymers based on biocompatible and bioeliminable blocks. Poly(ethylene oxide) was selected as the hydrophilic block, whereas an aliphatic polyester, i.e. poly(ε-caprolactone), or a polycarbonate, i.e. poly(trimethylene carbonate), were chosen as the degradable hydrophobic block. In order to allow a post-functionalization of the micelles core, azide groups were introduced on the hydrophobic segment to provide reactivity towards functional alkyne derivatives by the copper azide-alkyne cycloaddition (CuAAC). For this purpose, a functional lactone, i.e. α-chloro-ε-caprolactone was introduced during the polymerization of the hydrophobic block before being converted into azide on the preformed copolymer. Such reactivity of the block copolymers and their self-assemblies is of prime interest for drugs or fluorescent dyes grafting, so as for micelles cross-linking. The influence of the azides distribution along the degradable block on the micelles post-functionalization ability has been studied by using alkyne bearing fluorescent dyes as model for drugs. The hydrophilicity of the dye on the micelles post-functionalization efficiency has also been investigated.

1. Introduction

Micellar self-assemblies of biocompatible amphiphilic block copolymers have attracted an increasing interest in the field of nanomedecines since they appear as promising carriers to improve the bioavailability of hydrophobic drugs [1]. Indeed, the supramolecular self-organization in water of amphiphilic block copolymers having appropriate hydrophilic/lipophilic balance (HLB) leads to spherical core/shell micelles with a diameter of a few tens of nanometers able to encapsulate hydrophobic drugs in their core [2-4]. Aliphatic polyesters, such as poly(ε-caprolactone) (PCL), and polycarbonates, such as poly(trimethylene carbonate) (PTMC) are good candidates for the elaboration of the hydrophobic core of the micelles due to their remarkable degradable and biocompatible properties, while poly(ethylene oxide) (PEO) is usually desirable to form the hydrophilic shell. Such micelles of PEO-*b*-PCL and PEO-*b*-PTMC block copolymers [5-6] were found particularly well-suited to encapsulate hydrophobic poorly soluble drugs and to protect them against early elimination from the bloodstream [7]. Therefore, they are used today as therapeutic drug delivery systems that are able of passive targeting of tumor cells by the so-called enhanced permeability and retention (EPR) effect [8].

The post-functionalization of such micelles has been found particularly interesting. For example, the grafting, at the shell periphery of preformed micelles, of a specific pilot molecule for active targeting, has been recently reported [9-11] offering the advantage of minimum handling of the carrier once labeled with sometimes sensitive moieties (e.g. antibodies). Other examples lie in the chemical cross-linking of the micelles core or shell [12-13] which increases drastically the nanocarrier stability during the dilution upon injection.

On the other hand, the anchoring of a drug or of a labeling agent (e.g. a fluorescent dye) on the degradable polymer backbone is also an efficient way to direct and control the release of the drug by the polymer degradation rate or to follow the fate of the carrier by fluorescent techniques [14].

All these strategies rely on the synthesis of reactive copolymers as first step, the specific distribution of the reactive sites along the copolymer backbone directing the final location of the post-functionalization. For example, PEO-*b*-PCL chains bearing an aldehyde group at the α-chain-end can be synthesized by anionic polymerization of ethylene oxide initiated by an appropriate functional initiator and used to graft the targeting unit, e.g. amino-mannose by reductive amination, at the outer periphery of the resulting reactive micelles [11].

As far as reactivity should be imparted to the degradable segment, the ω-end chain, generally a hydroxyl group is available for functionalization or grafting. Nevertheless, several strategies are reported in the literature to increase the functionality by grafting reactive groups along the polyester backbone. For example, Vert *et al.* investigated the direct functionalization of PCL chains by a two-step anionic process, which relied on the capture of the α-carbonyl proton of the polymer chain with formation of the corresponding polyenolate, followed by the addition of an electrophile. Remarkably, no toxic residues, such as metal catalyst, are used during the reaction but an important degradation of the polyester chains was observed [15]. An alternative strategy based on the synthesis and the (co)polymerization of functional lactones was also reported. If the preparation of such functional monomers generally requires multi-step synthesis reducing the final yield [16-17], the copolymerization conditions allow to limit the polymer degradation which is determinant as far as well-defined architectures such as block copolymers are targeted. Recently, Emrick *et al.* described the synthesis of an alkyne bearing valerolactone with the purpose to functionalize PCL copolymers by the copper azide-alkyne cycloaddition (CuAAC) [18]. CuAAC is characterized by a high tolerance to many functional groups or water and oxygen and can be carried out under mild conditions, which is of prime importance when the functionalization of degradable polymers is concerned. By a similar strategy, Riva *et al.* copolymerized α-chloro-ε-caprolactone (αClεCL) with ε-caprolactone (εCL) [19] and used the hanging chloro atoms of poly(αClεCL-*co*-εCL) to introduce pendent hydroxyl or carboxylic acid groups by reaction with the corresponding alkene by an atom transfer radical addition (ATRA) process. Later on, the chloro hanging groups were judiciously converted into azide by reaction of the copolyester with sodium azide allowing a

functionalization by CuAAC. Compared to the ATRA strategy, the CuAAC is more efficient and more versatile with a less contamination of the final product by copper residues [20-21].

In this framework, the present paper aims at reporting on the synthesis of sets of novel amphiphilic block copolymers based on a PEO hydrophilic block and a degradable hydrophobic one based on PCL or PTMC which includes αClεCL as comonomer with the purpose to generate reactive sites selectively distributed along the hydrophobic backbone and available for post-functionalization. Two sets of reactive diblock or triblock copolymers have been targeted by copolymerizing either εCL or TMC with αClεCL as a mixture or sequentially, from a monomethoxy poly(ethylene oxide) (MPEO) macroinitiator (Scheme 1). The influence of the copolymer architecture on the properties of the nano-assemblies formed in water has been studied. The post-functionalization of these micelles by either hydrophilic or hydrophobic dyes via the CuAAC reaction has been particularly investigated and will be discussed.

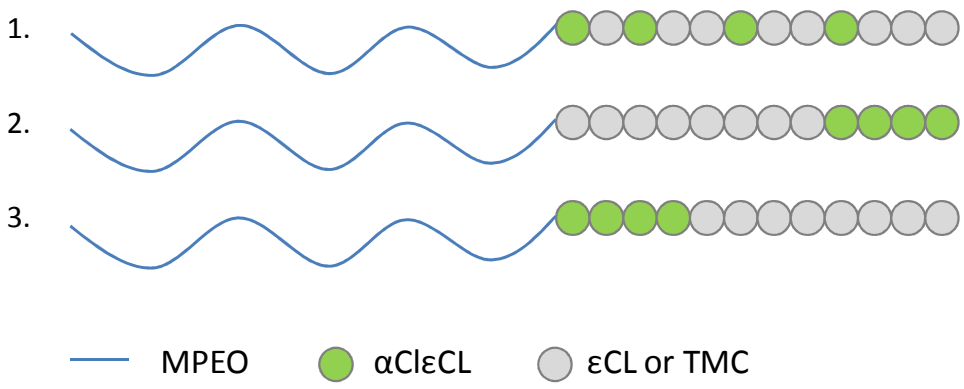

Scheme 1. Targeted architectures for the two sets of reactive amphiphilic copolymers based on either polyester or polycarbonate hydrophobic and degradable block.

2. Materials and methods

Materials

Monomethoxy poly(ethylene oxide) (MPEO, M_n = 5000 g/mol), 2-chlorocyclohexanone, *m*-chloroperoxybenzoic acid, 1-pyrenebutyric acid, propargylamine, rhodamine B thiocyanate, *N,N'*-dicyclohexylcarbodiimide (DCC), 4-dimethylaminopyridine (DMAP) triethylamine (NEt_3), copper sulfate ($CuSO_4$), and ascorbic acid sodium salt were purchased from Aldrich and used as received. ε-Caprolactone (εCL) (Janssen Chimica) was stirred over calcium hydride for 48 hours at room temperature and distilled under reduced pressure before use. Toluene (Chem-Lab) and tetrahydrofuran (Chem-Lab) were flown over molecular sieves in order to eliminate water. $SnOct_2$ (Alfa Aesar) was diluted in anhydrous toluene (0.06M) and stored under nitrogen. α-Chloro-ε-caprolactone (αClεCL) [22] and trimethylene carbonate (TMC) [23] were synthesized as already reported elsewhere.

Reactive copolymer synthesis

Synthesis of MPEO-b-poly(εCL-co-αClεCL) (1a)

Typically, 4.26 g of MPEO (0.85 mmol of terminal OH group) and 0.71 g of αClεCL (4.77 mmol) were dried by three azeotropic distillations with anhydrous toluene into two different glass reactors. In the αClεCL containing reactor, 1 g of εCL (8.77 mmol) and 5 ml of anhydrous toluene were added through a rubber septum via a stainless steel capillary. The monomer solution was then transferred into the glass reactor containing MPEO with a previously flamed stainless steel capillary. 2.8 mL of $SnOct_2$ 0.06 M (1.5 wt % in toluene) and 30 mL of anhydrous toluene were finally added and the reaction solution was refluxed for 24 hours. After polymerization, a drop of pure acetic acid was added, the solution was concentrated and the copolymer was recovered by precipitation in cold heptane.

M_n = 7100 g/mol (^{1}H NMR), M_w/M_n = 1.10 (SEC)

^{1}H NMR ($CDCl_3$) : δ (ppm), 1.2 to 1.8 (m, 6H, CO-CH_2-C***H***$_2$-C***H***$_2$-C***H***$_2$-CH_2-O- and m, 4H, CO-CH(Cl)-CH_2-C***H***$_2$-C***H***$_2$-CH_2-O-), 2 (m, 2H, CO-CH(Cl)-C***H***$_2$-CH_2-CH_2-CH_2-O-) , 2.4 (t, 2H, CO-C***H***$_2$-CH_2-CH_2-CH_2-CH_2-O-), 3.3 (s, 1H, C***H***$_3$-O-), 3.6 (m, 4H, O-C***H***$_2$-C***H***$_2$-O-), 4.1 (t, 2H, CO-CH_2-CH_2-CH_2-CH_2-C**H**$_2$-O-), 4.1 to 4.3 (m, 3H, CO-C***H***(Cl)-CH_2-CH_2-CH_2-C***H***$_2$-O-).

Synthesis of MPEO-b-PCL-b-poly(αClεCL)(2a)

Typically, 4.26 g of MPEO (0.85 mmol) was dried by three azeotropic distillations with anhydrous toluene before adding 1 g of εCL (8.77 mmol) and 2.8 ml of $SnOct_2$ solution (0.06 M) through a rubber septum with a syringe equipped with a stainless capillary. The reaction medium was stirred in bulk at 130°C for 72 hours. After polymerization, a drop of pure acetic acid was added and the solid was dissolved into toluene. The MPEO-*b*-PCL block copolymer was recovered by precipitation in cold heptane. After filtration and drying under vacuum, MPEO-*b*-PCL was dried by three azeotropic distillations with anhydrous toluene. 0.71 g of freshly dried αClεCL (4.77 mmol) dissolved into 5 ml of anhydrous toluene was added through the rubber septum to the glass reactor containing MPEO-*b*-PCL. 2.8 mL of $SnOct_2$ 0.06 M (1.5 wt%) and 30 mL of toluene were then added and the reaction solution was refluxed for 24 hours. After polymerization, a drop of pure acetic acid was added, the solution was concentrated and the copolymer was recovered by precipitation in cold heptane.

M_n= 7200 g/mol (^{1}H NMR), M_w/M_n = 1.10 (SEC)

^{1}H NMR ($CDCl_3$) : δ (ppm), 1.2 to 1.8 (m, 6H, CO-CH_2-C***H***$_2$-C***H***$_2$-C***H***$_2$-CH_2-O- and m, 4H, CO-CH(Cl)-CH_2-C***H***$_2$-C***H***$_2$-CH_2-O-), 2 (m, 2H, CO-CH(Cl)-C***H***$_2$-CH_2-CH_2-CH_2-O-) , 2.4 (t, 2H, CO-C***H***$_2$-CH_2-CH_2-CH_2-CH_2-O-), 3.3 (s, 1H, C***H***$_3$-O-), 3.6 (m, 4H, C***H***$_2$-C***H***$_2$-O-), 4.1 (t, 2H, CO-CH_2-CH_2-CH_2-CH_2-C**H**$_2$-O-), 4.1 to 4.3 (m, 3H, CO-C***H***(Cl)-CH_2-CH_2-CH_2-C***H***$_2$-O-).

Synthesis of MPEO-b-poly(αClεCL)-b-PCL (3a)

Typically, 4.26 g of MPEO (0.85 mmol) and 0.71 of αClεCL(4.77 mmol) were dried by three azeotropic distillations of anhydrous toluene in two different glass reactors. αClεCL was dissolved in 5 ml of anhydrous toluene and quantitatively transferred into the MPEO containing reactor via a stainless steel capillary. 2.8 mL of $SnOct_2$ 0.06 M (1.5 wt%) and 30 mL of anhydrous toluene were finally added and the reaction solution was refluxed for 24 hours. After complete conversion of the αClεCL, 1 g of εCL (8.77 mmol) was added to the solution for a second 24 hours of reflux. After polymerization, a drop of pure acetic acid was added, the solution was concentrated and the copolymer was recovered by precipitation in cold heptane.

M_n = 6900 g/mol (^{1}H NMR), M_w/M_n = 1.10 (SEC)

^{1}H NMR ($CDCl_3$) : δ (ppm), 1.2 to 1.8 (m, 6H, CO-CH_2-C***H***$_2$-C***H***$_2$-C***H***$_2$-CH_2-O- and m, 4H, CO-CH(Cl)-CH_2-C***H***$_2$-C***H***$_2$-CH_2-O-), 2 (m, 2H, CO-CH(Cl)-C***H***$_2$-CH_2-CH_2-CH_2-O-) , 2.4 (t, 2H, CO-C***H***$_2$-CH_2-CH_2-CH_2-CH_2-O-), 3.3 (s, 1H, C***H***$_3$-O-), 3.6 (m, 4H, C***H***$_2$-C***H***$_2$-O-), 4.1 (t, 2H, CO-CH_2-CH_2-CH_2-CH_2-C**H**$_2$-O-), 4.1 to 4.3 (m, 3H, CO-C***H***(Cl)-CH_2-CH_2-CH_2-C***H***$_2$-O-).

Synthesis of MPEO-b-poly(TMC-co-αClεCL) (1a')

Typically, 2.23 g MPEO (0.45 mmol), 0.40 g of αClεCL (2.7 mmol) and 0.50 g of freshly recrystallized TMC (4.9 mmol) were dried by three azeotropic distillations with anhydrous toluene into two different glass reactors. The αClεCL and TMC mixture was then dissolved in anhydrous toluene and added through a rubber septum via a stainless steel capillary to the glass reactor containing MPEO. 2 mL of $SnOct_2$ 0.06 M (2 wt % in toluene) and 20 mL of anhydrous toluene were added and the reaction solution was refluxed for 24 hours. After polymerization, a drop of pure acetic acid was added, the solution was concentrated and the copolymer was recovered by precipitation in cold heptane.

M_n= 6500 g/mol (^{1}H NMR), M_w/M_n = 1.05 (SEC)

^{1}H NMR ($CDCl_3$) : δ (ppm), 1.3 to 1.8 (m, 4H, CO-CH(Cl)-CH_2-C***H***$_2$-C***H***$_2$-CH_2-O-), 1.8 to 2.2 (m, 2H, CO-CH(Cl)-C***H***$_2$-CH_2-CH_2-CH_2-O- and m, 2H, CO-O-CH_2-C***H***$_2$-CH_2-O-), 3.3 (s, 1H, C***H***$_3$-O-), 3.6 (m, 4H, C***H***$_2$-C***H***$_2$-O-), 4.1 to 4.4 (t, 4H, CO-O-C***H***$_2$-CH_2-C***H***$_2$-O- and m, 3H, CO-C***H***(Cl)-CH_2-CH_2-CH_2-C***H***$_2$-O-).

Synthesis of MPEO*-b-*PTMC*-b-*poly(αClεCL) (2a')

Typically, 2.23 g of MPEO (0.45 mmol), 0.40 g of αClεCL (2.7 mmol) and 0.50 g of freshly recrystallized TMC (4.9 mmol) were previously dried by three azeotropic distillation with anhydrous toluene before polymerization. TMC was dissolved in anhydrous toluene and added through a rubber septum via a stainless steel capillary to the glass reactor containing MPEO. 2 mL of $SnOct_2$ 0.06 M (2 wt%) and 20 mL of anhydrous toluene were added and the reaction solution was refluxed for 24 hours. After complete conversion of TMC, αClεCL, dissolved into 5 ml of toluene, was added for a second 24 hours of refluxing. After polymerization, a drop of pure acetic acid was added, the solution was concentrated and the copolymer was recovered by precipitation in cold heptane.

M_n = 6800 g/mol (^{1}H NMR), M_w/M_n = 1.05 (SEC)

^{1}H NMR ($CDCl_3$) : δ (ppm), 1.3 to 1.8 (m, 4H, CO-CH(Cl)-CH_2-C***H***$_2$-C***H***$_2$-CH_2-O-), 1.8 to 2.2 (m, 2H, CO-CH(Cl)-C***H***$_2$-CH_2-CH_2-CH_2-O- and m, 2H, CO-O-CH_2-C***H***$_2$-CH_2-O-), 3.3 (s, 1H, C***H***$_3$-O-), 3.6 (m, 4H, C***H***$_2$-C***H***$_2$-O-), 4.1 to 4.4 (t, 4H, CO-O-C***H***$_2$-CH_2-C***H***$_2$-O- and m, 3H, CO-C***H***(Cl)-CH_2-CH_2-CH_2-C***H***$_2$-O-).

Synthesis of MPEO*-b-*poly(αClεCL)*-b-*PTMC (3a')

Typically, 2.23 g of MPEO (0.45 mmol), 0.4 g of αClεCL (2.7 mmol) and 0.50 g of freshly recrystallized TMC (4.9 mmol) were dried by three azeotropic distillations with anhydrous toluene before polymerization. αClεCL was dissolved into 2 ml of anhydrous toluene and transferred through a rubber septum via a stainless steel capillary into the glass

reactor containing MPEO. 1.7 mL of $SnOct_2$ 0.06 M (2 wt%) and 20 mL of anhydrous toluene were added and the reaction solution was refluxed for 15 hours. After polymerization, a drop of pure acetic acid was added, the solution was concentrated and the copolymer was recovered by precipitation in cold heptane. The MPEO-*b*-poly(αClεCL) block copolymer was dried by three azeotropic distillations with anhydrous toluene. TMC, dissolved into 5 ml of anhydrous toluene, was added through the rubber septum to the glass reactor containing MPEO-*b*-poly(αClεCL). 2 mL of $SnOct_2$ (2 wt%) in 10 ml of anhydrous toluene was added and the solution was refluxed for 15 hours. After polymerization, a drop of pure acetic acid was added, the solution was concentrated and the copolymer was recovered by precipitation in cold heptane.

M_n= 7000 g/mol (^{1}H NMR), M_w/M_n = 1.10 (SEC)

^{1}H NMR ($CDCl_3$) : δ (ppm), 1.3 to 1.8 (m, 4H, CO-CH(Cl)-CH_2-C***H***$_2$-C***H***$_2$-CH_2-O-), 1.8 to 2.2 (m, 2H, CO-CH(Cl)-C***H***$_2$-CH_2-CH_2-CH_2-O- and m, 2H, CO-O-CH_2-C***H***$_2$-CH_2-O-), 3.3 (s, 1H, C***H***$_3$-O-), 3.6 (m, 4H, C***H***$_2$-C***H***$_2$-O-), 4.1 to 4.4 (t, 4H, CO-O-C***H***$_2$-CH_2-C***H***$_2$-O- and m, 3H, CO-C***H***(Cl)-CH_2-CH_2-CH_2-C***H***$_2$-O-).

Substitution of chloro atoms into azide groups

2 g of MPEO-*b*-poly(TMC-*co*-αClεCL) (**1a'**) (0.305 mmol) (or MPEO-*b*-PTMC-*b*-poly(αClεCL) (**2a'**) or MPEO-*b*-poly(αClεCL)-*b*-PTMC (**3a'**)) was dissolved into 20 mL of DMF. 0.175 g of sodium azide (2.75 mmol, 150 mol % vs. chloro atoms) was added and the solution was stirred at room temperature overnight. The solvent was removed under vacuum and the resulting product was dissolved into toluene. Insoluble salts were removed by centrifugation (15k rpm, 15 min, rt). The azide bearing copolymer was recovered by precipitation in cold heptane. For copolymers based on polyester backbone (1a to 1c), a similar process already described in the literature has been pursued [24].

Synthesis of alkyne-pyrene and alkyne–rhodamine

Alkyne-pyrene: 0.5 g of 1-pyrenebutyric acid (3.5 mmol) and 0.134 ml of propargylamine (4.16 mmol) were dissolved in 5 ml of anhydrous THF. 0.43 g of DCC (4.16 mmol) and 4 mg of DMAP ($3.5 \cdot 10^{-2}$ mmol) were added to the solution and the reaction solution was stirred at room temperature for 72 hours. *N*,*N'*-dicyclohexylurea (DCU) formed during the reaction was eliminated by filtration and the alkyne-pyrene was purified by successive precipitations in cold heptane.

Alkyne-rhodamine: 0.2 g rhodamine B isothiocyanate (0.97mmol) and 0.744 ml of propargylamine (1.16 mmol) were dissolved into 3 mL of anhydrous THF. 10 µl of NEt_3 ($9.7 \cdot 10^{-2}$ mmol) was added to the solution and the reaction solution was stirred at room temperature for 72 hours. Both NEt_3 and the excess of propargylamine were removed by evaporation under vacuum and alkyne bearing rhodamine was precipitated in cold heptane.

Characterization methods

Size exclusion chromatography (SEC) was carried out in THF at 45 °C at a flow rate of 1 mL/min with a SFD S5200 auto sampler liquid chromatograph equipped with a SFD refractometer index detector 2000. The PL gel 5 µm (10^5 Å, 10^4 Å, 10^3 Å, and 100 Å) columns were calibrated with polystyrene standards. ^{1}H NMR spectra were recorded in $CDCl_3$ at 400 MHz in the FT mode with a Bruker AN 400 apparatus at 25°C. The infrared spectra were recorded with a Perkin-Elmer FT-IR 1720X. The samples for IR were prepared by slow evaporation of a solution in THF onto NaCl windows.

Micellization

Micellization of the azide bearing copolymers was obtained by a co-solvent process. A 1% stock solution of the copolymer (**1**, **2** or **3**) was prepared in DMF. 20 mL of Milli-Q water were added to 5 mL of this DMF solution under vigorous stirring for two hours. Polymer micelles were purified by dialysis overnight against 1L of water using cellulose dialysis membrane (Spectrapor, cut-off 3500). Dynamic light scattering measurements were performed using a Beckman Coulter Delsa Nano C Particle analyzer and the data were treated

by the Delsa Nano UI 2.21 software. All the measurements were carried out at 25°C at a measuring angle of 165°. The samples for transmission electron microscopy (TEM) were prepared by slow evaporation of the solutions after DLS analysis on a formvar-coated copper grid. The excess of solution was removed with a filter paper. The samples were analyzed with a Philips CM100 microscope equipped with an Olympus camera and transferred to a computer equipped with the Megaview system.

Post-functionalization of reactive micelles by alkyne-pyrene and alkyne rhodamine by CuAAC

An aqueous dispersion of micelles was prepared by addition of 20 mL of water to 5 mL stock solution of the corresponding azide bearing copolymers dissolved in DMF. After removing the remaining DMF by dialysis against water, alkyne–rhodamine (150 mol % vs. azide groups), $CuSO_4$ (25 mol %) and ascorbic acid sodium salt (25 mol %) were added to the aqueous micelle solution. The solution was stirred at 35°C during 24 hours. The micelles were then dialyzed against 1:4 (v:v) water:DMF to remove unreacted alkyne-rhodamine and finally against water.

The grafting of the alkyne-pyrene was performed in similar conditions but in presence of DMF. Indeed, after two hours of stirring of the aqueous dispersion of micelles prepared by addition of 20 mL of water to 5 mL of the DMF stock solution of the corresponding azide bearing copolymers, alkyne-pyrene (150 mol % vs. azide groups), $CuSO_4$ (25 mol %) and ascorbic acid sodium salt (25 mol %) were added to the aqueous micelle solution. The solution was stirred at 35°C during 24 hours. The micelles were then dialyzed against 1:4 (v:v) water:DMF to remove unreacted alkyne-pyrene and finally against water.

3. Results and discussion

Copolymer synthesis

The strategies for the synthesis of the different copolymers targeted in this work are detailed in Scheme 2.

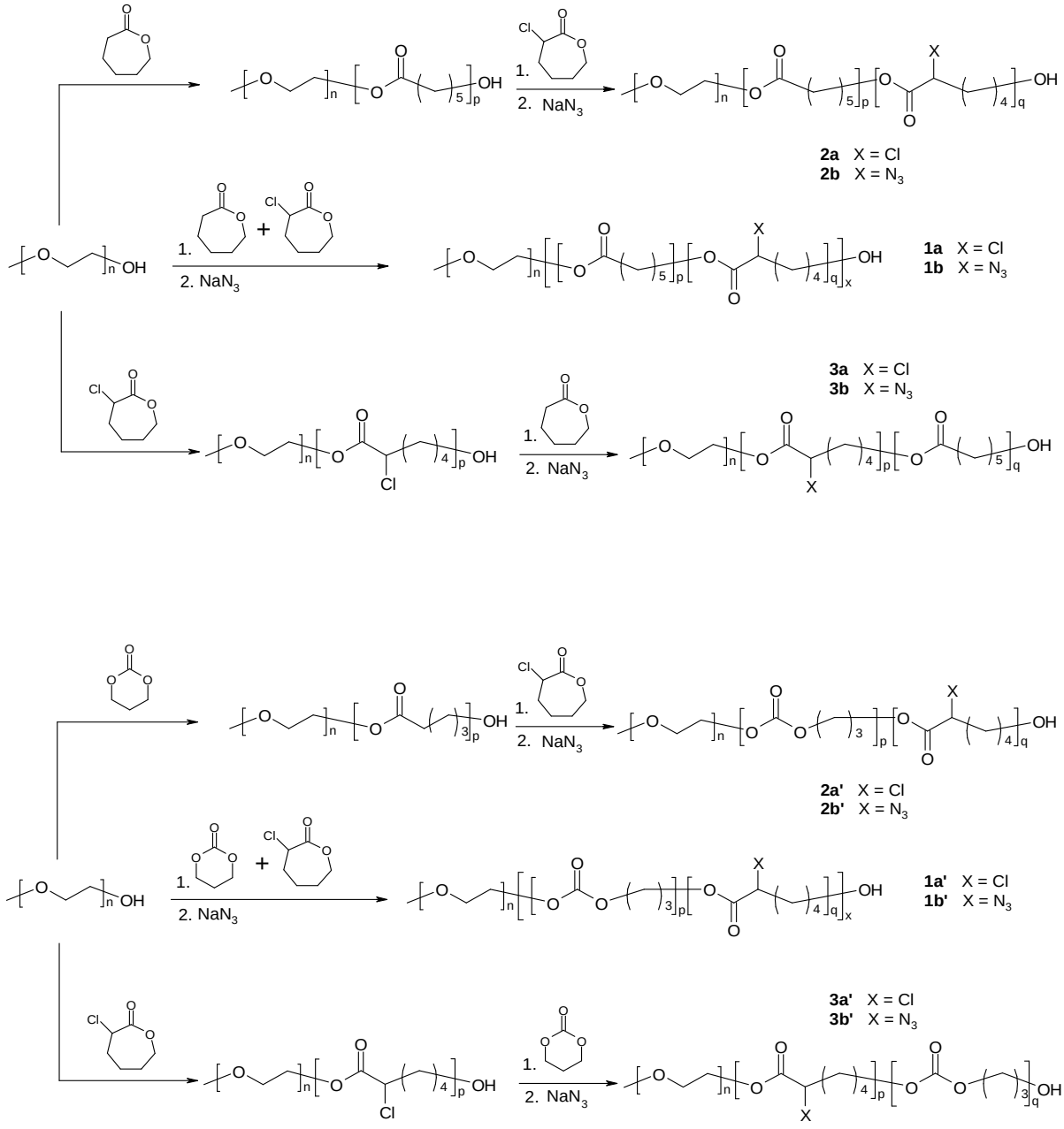

Scheme 2. Strategy for the synthesis of MPEO-*b*-poly(εCL-*co*-αN_3εCL] (**1b**), MPEO-*b*-poly(TMC-*co*-αN_3εCL] (**1b'**), MPEO-*b*-PCL-*b*-poly(αN_3εCL) (**2c**), MPEO-*b*-PTMC-*b*-poly(αN_3εCL) (**2c'**), MPEO-*b*-poly(αN_3εCL)-*b*-PCL (**3c**), MPEO-*b*-poly(αN_3εCL)-*b*-PTMC (**3c'**)

Copolymers based on PCL

The MPEO-*b*-poly(εCL-*co*-αClεCL) diblock copolymer (Scheme 1, **1a**) was synthesized by ring-opening polymerization (ROP) of a εCL and αClεCL mixture, initiated by a poly(ethylene oxide) bearing one hydroxyl group at the ω-chain end (MPEO) in presence of

tin octoate as catalyst. As demonstrated by Vangeyte *et al.* and later by Rieger *et al.*, a PEO_{114}-*b*-PCL_{16} gives stealthy and spherical micelles of about 35 nm [25-26]. A similar composition has thus been targeted in this work for the azide bearing copolymer. For this purpose, a MPEO macroinitiator with a molar mass of 5000 g/mol was selected and the amount of lactone monomers was adjusted to reach a polymerization degree (DP) of 16 at 100% conversion. In order to determine the influence of the molar fraction of $\alpha N_3\varepsilon CL$ in the copolymer, two copolymers, with a comonomer ratio (εCL:$\alpha Cl\varepsilon CL$) of 75:25 and 65:35 were synthesized leading to an average number of azide groups per polymer chain of 4 and 6 units respectively. In a previous paper, the conditions for the controlled copolymerization of εCL and αClεCL initiated by the dibutylstannadioxepane were reported [19]. Later on, Huang *et al.* successfully initiated the homopolymerization of αClεCL starting from a MPEO macroinitiator [27]. As this strategy was closer to this present work, these conditions were applied for the random copolymerization of εCL with αClεCL initiated from MPEO. Typically, the copolymerization occurred in toluene at reflux during 24 hours. As far as the triblock copolymer PEO-*b*-PCL-*b*-poly(αClεCL) (**2a**) is concerned, the diblock copolymer PEO-*b*-PCL formed after polymerization of the first monomer was purified by precipitation in heptane in order to completely remove traces of residual monomers able to generate a gradient copolymer during the synthesis of the third block. That purification step is not required for the triblock copolymer PEO-*b*-poly(αClεCL)-*b*-PCL (**3a**) whose the conversion of the αClεCL is quantitative. The composition and the molecular weight were kept constant for all of the synthesized copolymers. It is worth noting that a better control for the homopolymerization of εCL from the PEO macroinitiator was observed when the polymerization was performed in bulk instead of in toluene.

A complete conversion of both monomers was obtained after 24 hours of polymerization as confirmed by the absence of monomer signals in the ^1H NMR spectrum of the polymerization medium. The molar fraction in εCL and αClεCL in the final block copolymer was determined by comparison of the integral of one proton of the PCL and the poly(αClεCL) units of the copolymer according to equation 1 and 2, respectively.

$$F_{\varepsilon CL} = \frac{I_i}{I_i + I_e} \quad (1)$$

$$F_{\alpha Cl\varepsilon CL} = \frac{I_e}{I_i + I_e} \quad (2)$$

The molar fractions in both εCL ($F_{\varepsilon CL}$) and αClεCL ($F_{\alpha Cl\varepsilon CL}$) in the copolymers agreed with the composition in the comonomer feed (Table 1). The ^{1}H NMR spectrum of the copolymer MPEO-*b*-poly(αClεCL)-*b*-PCL (**3a**) is shown in Figure 1 as representative spectrum for all the PCL based copolymers prepared in this work. For each copolymer, the molar mass of the PCL and the poly(αClεCL) blocks were determined by the comparison of the relative intensity of the proton of the methoxy end group of the MPEO at 3.3 ppm (peak a, Figure 1) and the CH_2-C(O) protons at 2.3 ppm (peak i, Figure 1) of PCL or the CH_2-CHCl protons at 2.05 ppm (peak e, Figure 1) of poly(αClεCL), respectively. The calculated molar masses were in good agreement with the theoretical values for all the copolymers (Table 1).

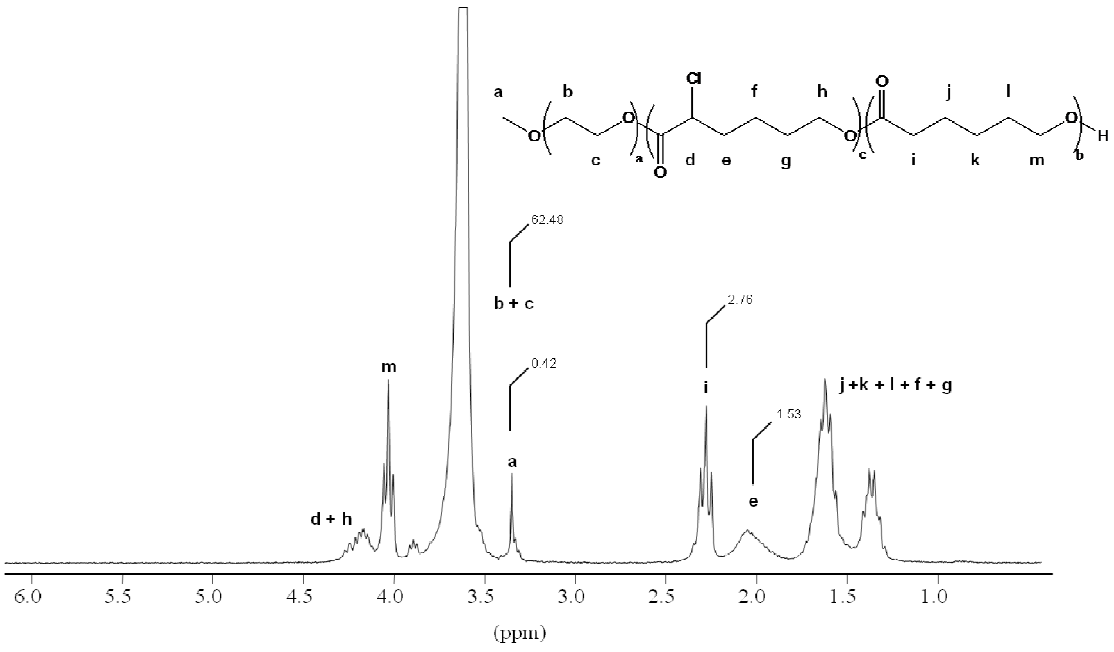

Figure 1. ^{1}H NMR spectrum in $CDCl_3$ of MPEO-*b*-poly(αClεCL)-*b*-PCL (**3a**)

Further analysis of the copolymers by SEC evidenced an increasing of the molar mass after polymerization by the shift towards lower elution time after each block addition with a narrow polydispersity (Figure 2). Moreover, the absence of residual MPEO was in agreement with a quantitative initiation by the PEO macroinitiator without transesterification reactions in line with reported data on the ROP (co)polymerization starting from small size initiators [19].

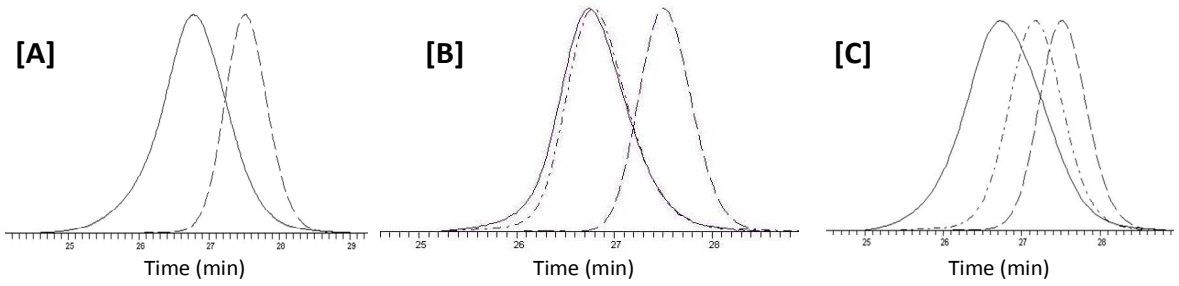

Figure 2. SEC traces recorded in THF for: [A] the MPEO macroinitiator (- - -) and MPEO-*b*-poly(εCL-*co*- αClεCL) (——) (**1a)**, [B] the MPEO macroinitiator (- - -), MPEO-*b*-PCL (-.-.-) and MPEO-*b*-PCL-*b*-poly(αClεCL) (**2a**) and [C] the MPEO macroinitiator (- - -), the MPEO-*b*-poly(αClεCL) (-.-.-) and the MPEO-*b*-poly(αClεCL)-*b*-PCL (——) (**3a**)

The macromolecular parameters of the obtained PCL based copolymers are summarized in table 1.

Table 1. Characteristics of the copolymers obtained by ROP of εCL and αClεCL initiated from MPEO M_n =5000 g/mol as presented in the Scheme 2.

Copolymer	$M_{n,\,th\ PCL}$ *(g/mol) (DP)*[a]	$M_{n,\,th\ poly(\alpha Cl\varepsilon CL)}$ *(g/mol) (DP)*[b]	$f_{\varepsilon CL}$ / $f_{\alpha Cl\varepsilon CL}$[c]	$M_{n,\,NMR\ PCL}$ *(g/mol) (DP)*[d]	$M_{n,\,NMR\ poly(\alpha Cl\varepsilon CL)}$ *(g/mol) (DP)*[e]	$F_{\varepsilon CL}$ / $F_{\alpha Cl\varepsilon CL}$[f]	M_w/M_n *(SEC)*[g]
1a-1	1370 (*12*)	590 (*4*)	75/25	1500 (*13*)	600 (*4*)	76/24	1.10
-2	1170 (*10*)	890 (6)	65/35	1100 (10)	1000 (7)	60/40	1.10
2a-1	1370 (*12*)	590 (*4*)	75/25	1400 (*12*)	400 (*3*)	80/20	1.05
-2	1170 (*10*)	890 (6)	65/35	*1300 (11)*	900 (6)	65/35	1.10
3a-1	1370 (*12*)	590 (*4*)	75/25	1400 (*12*)	700 (*5*)	70/30	1.05
-2	1170 (*10*)	890 (6)	65/35	1100 (10)	800 (5.5)	65/35	1.10

[a] Theoretical molar mass of the PCL block determined by the MPEO/εCL ratio

[b] Theoretical molar mass of the poly(αClεCL) block determined by the MPEO/αClεCL ratio
[c] Theoretical composition of the copolyester block determined by the αClεCL/εCL ratio
[d] Experimental molar mass of the PCL block determined by ^{1}H NMR based on the integration of peak l and a (Figure 1)
[e] Experimental molar mass of the poly(αClεCL) block determined by ^{1}H NMR based on the integration of peak e and a (Figure 1)
[f] Experimental composition of the copolyester block determined by the poly(αClεCL)/PCL ratio
[g] polydispersity index measured by SEC (polystyrene calibration)

Copolymers based on PTMC

The substitution of the PCL block by a PTMC block would allow the modulation of the physico-chemical properties of the copolymers and hence of the nanovectors formed in water. Indeed, in contrast to PCL, PTMC is an amorphous polymer, and hence known to high drug encapsulation abilities and appropriate release profile of the encapsulated drug [28]. Statistic copolymers of αClεCL and εCL are amorphous when the molar fraction in αClεCL was higher than 30 mol%, while poly(αClεCL) are totally non crystalline [19]. Data about the random copolymerization εCL and TMC initiated by a MPEO macroinitiator were already reported [28]. To our knowledge, no example of copolymerization of αClεCL with TMC is reported in the literature. Thereby, the ring-opening polymerization of the αClεCL and TMC initiated by a MPEO macroinitiatior in presence of a catalytic amount of $SnOct_2$ was performed under the same conditions as the ones reported above for the PCL based copolymers. Typically, random copolymerization of TMC with αClεCL required only 24 hours to reach high conversion of both monomers (complete conversion for the αClεCL and more than 80% for TMC) when performed in toluene. The homopolymerization of the αClεCL initiated by the MPEO macroinitiator was completed in 15 hours. Surprisingly, and unlike PCL based copolymers, a better control of the synthesis of the triblock copolymers PEO-*b*-poly(αClεCL)-*b*-PTMC (**3a'**) was obtained when a purification of the MEO-*b*-poly(αClεCL) diblock copolymer by precipitation into heptane was carried out before the synthesis of the PCL third block. Indeed, in order to favor the polymerization of TMC from this macroinitiator and avoid the poly(αClεCL) block degradation, a more concentrated solution of the PEO-*b*-poly(αClεCL) macroinitiator in anhydrous toluene was used and the polymerization time was reduced.

As representative example, the ^{1}H NMR spectrum of the MPEO-*b*-poly(αClεCL-*co*-TMC) (**1a'**) is presented at the Figure 3. As explained for the PCL based copolymers, the molar mass of the poly(αClεCL) block was easily calculated by the relative intensity of the methoxy protons of MPEO end-group at 3.3 ppm (peak a, Figure 3) and the intensity of the two CH_2 group of the poly(αClεCL) (peak i and j, Figure 3). In the case of PTMC block, the measurement of the molar mass was more difficult due to the overlap of the signal of PTMC with poly(αClεCL) around 4 ppm (I_{4ppm}). This problem was bypassed by the subtraction of the poly(αClεCL) contribution determined with the intensities of peaks i and j from this I_{4ppm} peak. Accordingly, the molar masses determined by ^{1}H NMR were in good agreement with the theoretical ones for each TMC based copolymer. The molar fractions in TMC and αClεCL in the final block copolymer were determined from I_{4ppm} according equation 3.

$$F_{TMC} = \frac{I_{4\,ppm} - \frac{3}{4}(I_i + I_j)}{I_{4\,ppm} + \frac{1}{4}(I_i + I_j)} \quad (3)$$

$$F_{\alpha Cl\varepsilon CL} = \frac{\frac{1}{4}(I_i + I_j)}{I_{4\,ppm} + \frac{1}{4}(I_i + I_j)} \quad (4)$$

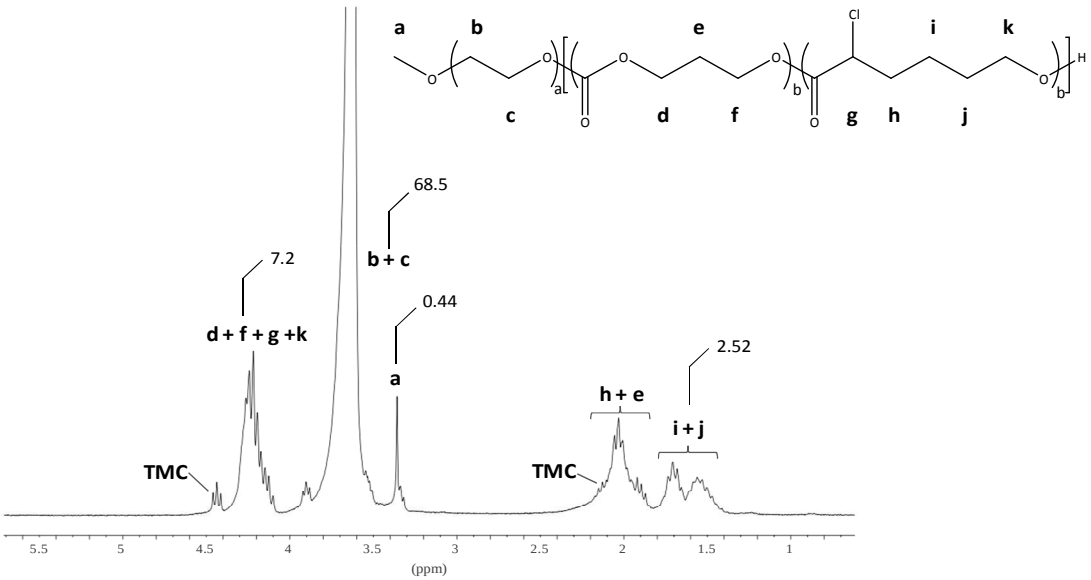

Figure 3. ^{1}H NMR spectrum in $CDCl_3$ of MPEO-*b*-poly(αClεCL-*co*-TMC) (**1a'**)

Further analysis of the copolymers by SEC evidenced an increase of the molar mass after polymerization by the shift towards lower elution time after each block addition with a narrow polydispersity (Figure 4).

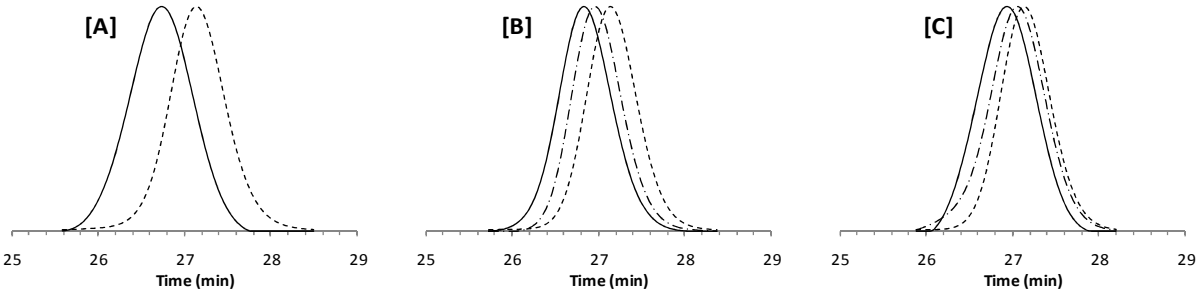

Figure 4. SEC traces recorded in THF for: [A] the MPEO macroinitiator (- - -) and MPEO-*b*-poly(TMC-*co*- αClεCL) (——) (**1a'**), [B] the MPEO macroinitiator (- - -), MPEO-*b*-PTMC (-.-.-) and MPEO-*b*-PTMC-*b*-poly(αClεCL) (**2a'**) and [C] the MPEO macroinitiator (- - -), the MPEO-*b*-poly(αClεCL) (-.-.-) and the MPEO-*b*-poly(αClεCL)-*b*-PTMC (——) (**3a'**)

The macromolecular parameters of the obtained TMC based copolymers are summarized in table 2.

Table 2. Characteristics of the copolymers obtained by ROP of TMC and αClεCL from MPEO M_n =5000 g/mol following the Scheme 2.

Copolymer	$M_{n,\,th\ PTMC}$ (g/mol) (DP)[a]	$M_{n,\,th\ poly(\alpha Cl\varepsilon CL)}$ (g/mol) (DP)[b]	$f_{TMC}/f_{\alpha Cl\varepsilon CL}$[c]	$M_{n,\,NMR\ PTMC}$ (g/mol) (DP)[d]	$M_{n,\,NMR\ poly(\alpha Cl\varepsilon CL)}$ (g/mol) (DP)[e]	$F_{TMC}/F_{(\alpha Cl\varepsilon CL)}$[f]	M_w/M_n (SEC)[g]
1a'	1120 (*11*)	890 (*6*)	65/35	900 (*9*)	600 (*4*)	69/31	1.05
2a'	1120 (*11*)	890 (*6*)	65/35	1000(*10*)	700 (*5*)	66/34	1.05
3a'	1120 (*11*)	890 (*6*)	65/35	1000 (*10*)	900 (*6*)	63/37	1.10

[a] Theoretical molar mass of the PTMC block determined by the MPEO/TMC ratio
[b] Theoretical molar mass of the poly(αClεCL) block determined by the MPEO/αClεCL ratio
[c] Theoretical composition of the copolyester block determined by the αClεCL/TMC ratio
[d] Experimental molar mass of the TMC block determined by ^{1}H NMR
[e] Experimental molar mass of the poly(αClεCL) block determined by ^{1}H NMR
[f] Experimental composition of the copolyester block determined by the αClεCL/TMC ratio
[g] polydispersity index measured by SEC (PS calibration)

Substitution of chloro atoms by azide groups

The copolymers structure and composition being confirmed, the hanging chloro atoms were converted into azide by a substitution reaction in order to allow the grafting of functional alkyne by a CuAAC process. The substitution reaction was performed in DMF, a good solvent for each block of the copolymers, in presence of sodium azide following the conditions reported in the literature for aliphatic polyesters [24]. This reaction occurred at room temperature under mild conditions to preserve the copolymers from degradation. An excess of 1.5 eq. of sodium azide compared to hanging chloro atoms was used to ensure a quantitative conversion. After substitution, FTIR analysis of the copolymers clearly showed the apparition of a new absorption band at 2106 cm^{-1} characteristic of the azide functions (Figure 5).

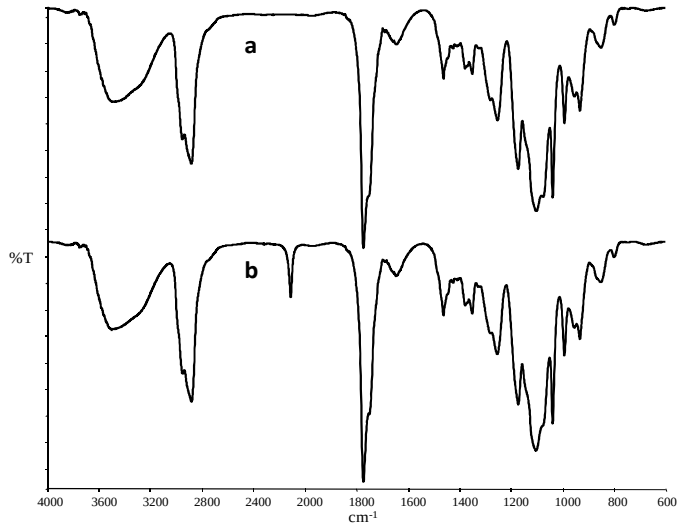

Figure 5. FTIR spectra of [**a**] PEO-*b*-PTMC-*b*-poly(αClεCL) (**2a'**) and [**b**] PEO-*b*-PTMC-*b*-poly($\alpha N_3\varepsilon$CL) (**2b'**)

The quantitative conversion of the chloro atoms into azide groups was confirmed by ^{1}H NMR (Figure 6) with the complete disappearance of the C*H*Cl signal at 4.25 ppm and the appearance of a new signal at 3.85 ppm (C*H*N_3). In addition, SEC shows that no degradation occurred during substitution. Indeed, although the elution time of the azide bearing-copolymer was smaller than the corresponding chloro bearing copolymer, due to a modification of the hydrodynamic volume, the polydispersity index remained quite narrow after substitution (Figure 7).

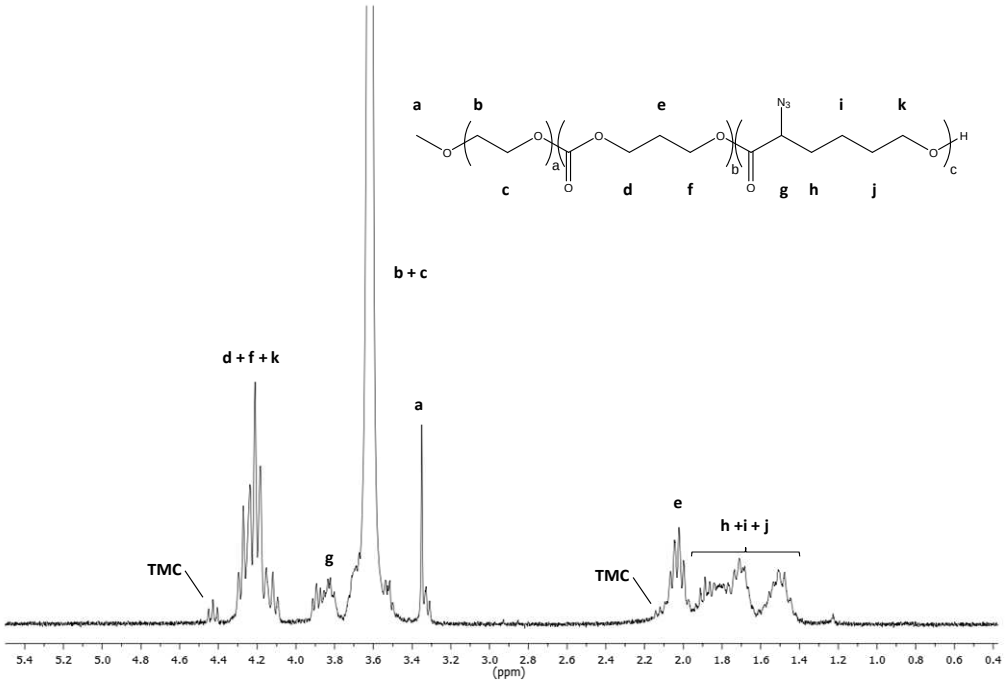

Figure 6. ^{1}H NMR spectrum in $CDCl_3$ of PEO-*b*-PTMC-*b*-poly(αN_3εCL) (**2b'**)

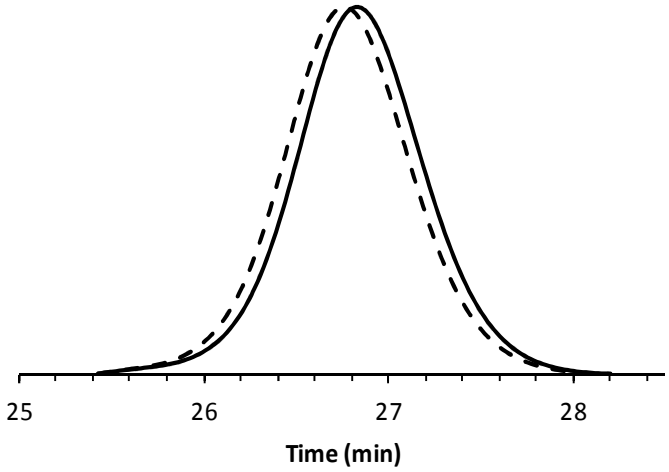

Figure 7. SEC traces in THF for the PEO-*b*-PTMC-*b*-poly(αClεCL) (——) (**2a'**) and the PEO-*b*-PTMC-*b*-poly(αN_3εCL) (- - -) (**2b'**)

Similar results of successful sodium azide substitution were obtained for the PCL based copolymers as expected from literature data reporting on statistic copolymers of poly(ε-caprolactone and poly(α-chloro-ε-caprolactone) [21].

Micellization

The ability of the different copolymers made available in this work, to self-assemble in spherical micelles in water and hence act as potential nanocarriers was then investigated. Well-defined micelles were achieved by dissolving first the copolymers into DMF, a good solvent of the hydrophilic and hydrophobic block followed by the rapid addition of a four times higher volume of water, a selective solvent of the hydrophilic block. After two hours of stirring, the solution was dialyzed against water to remove DMF. Probably due to the relatively high molecular mass of the semi-crystalline PEO, the use of a co-solvent (DMF) is required for the micelle formation of all the copolymers even based on PTMC block, in contrast with low molecular mass "liquid" terpolymers of PEO, PCL and PTMC which are able to self-assemble directly in water [28].

The size and polydispersity index of the micelles prepared with each copolymer were measured by DLS. All these data are collected in table 3. In case of polyester based copolymers, micelles with an apparent mean diameter of 30 nm were mainly observed with a low polydispersity, except for the amorphous random copolymer of higher size. These data are in agreement with previous study made on PEO_{114}-*b*-PCL_{16} [26]. In case of PTMC copolymers, larger micelles were observed probably due to the absence of crystallization, which generally increases the micellar core density and thus make the micelles more compact [29]. The spherical morphology was confirmed by TEM for all kinds of copolymer architectures as illustrated in Figure 8.

Table 3. DLS data of the micelles formed with the different reactive copolymers in water

Copolymers	Code [a]	$D_{h,\ app}$ (nm) [b]	PDI [c]
PEO_{114}-*b*-poly($\alpha N_3\varepsilon CL_4$-*co*-$CL_{13}$)	**1b -1**	41	0.23
PEO_{114}-*b*-poly($\alpha N_3\varepsilon CL_7$-*co*-$CL_{10}$)	**1b -2**	32	0.09
PEO_{114}-*b*-PCL_{12}-*b*-poly($\alpha N_3\varepsilon CL)_3$	**2b -1**	30	0.18
PEO_{114}-*b*-PCL_{11}-*b*-poly($\alpha N_3\varepsilon CL)_6$	**2b -2**	29	0.14
PEO_{114}-*b*-poly($\alpha N_3\varepsilon CL)_5$-*b*-$PCL_{12}$	**3b -1**	30	0.19
PEO_{114}-*b*-poly($\alpha N_3\varepsilon CL)_6$-*b*-$PCL_{10}$	**3b -2**	33	0.13
PEO_{114}-*b*-poly($\alpha N_3\varepsilon CL_4$-*co*-$TMC_9$)	**1b'**	45	0.22
PEO_{114}-*b*-$PTMC_{10}$-*b*-poly($\alpha N_3\varepsilon CL)_5$	**2b'**	53	0.23
PEO_{114}-*b*-poly($\alpha N_3\varepsilon CL)_6$-*b*-$PTMC_{10}$	**3b'**	57	0.22

(a) based on Scheme 2,

(b) apparent hydrodynamic diameter and (c) PDI as determined by DLS

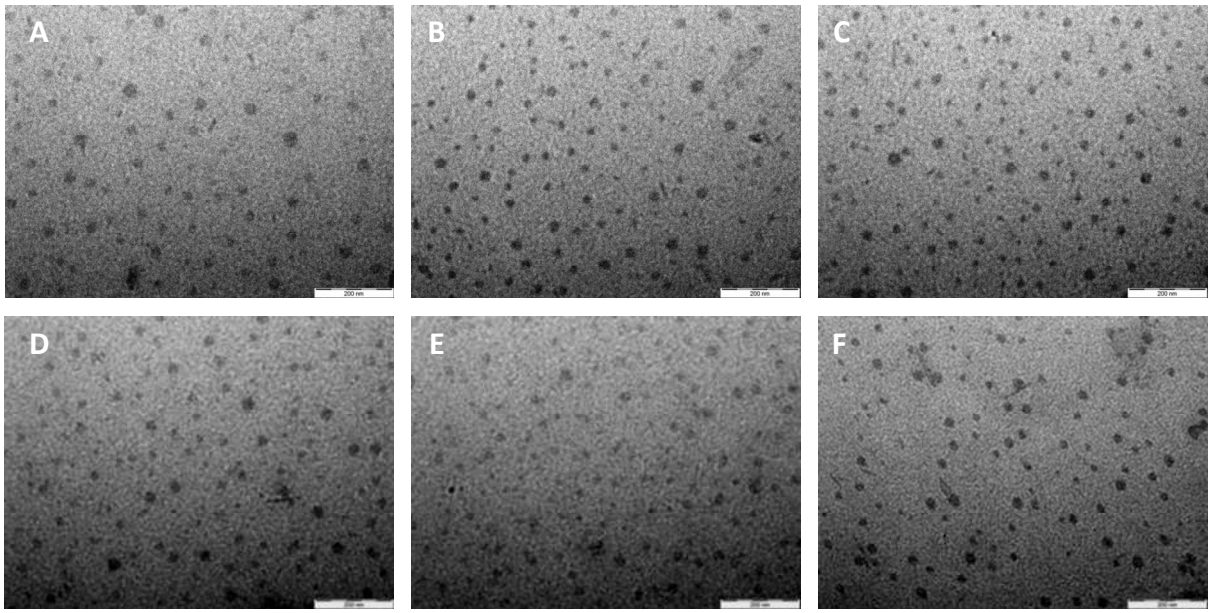

Figure 8. TEM images of micelles registered for copolymers: **A**. PEO-*b*-poly($\alpha N_3\varepsilon CL$-*co*-CL) (**1b-2**), **B**. PEO-*b*-PCL-*b*-poly($\alpha N_3\varepsilon CL$) (**2b-2**), **C**. PEO-*b*-poly($\alpha N_3\varepsilon CL$)-*b*-PCL (**3b-2**), **D**. PEO-*b*-poly($\alpha N_3\varepsilon CL$-*co*-TMC) (**1b'**), **E**. PEO-*b*-PTMC-*b*-poly($\alpha N_3\varepsilon CL$) (**2b'**), **F**. PEO-*b*-poly($\alpha N_3\varepsilon CL$)-*b*-PTMC (**3b'**)

Since these novel amphiphilic copolymers have been found able to self-assemble in water into spherical micelles, they appear thus as attractive candidates for the elaboration of

advanced drug delivery systems. Indeed, the presence of azide groups at different location within these micelles could be used to label them with a fluorescent dye for analytical purpose or to anchor a drug in order to sustain the release. In the last following section, we have been investigating the possibility to post-functionalize these micelles by CuAAC chemistry by using fluorescent dyes as model compounds. Two dyes have been used for this study, i.e. alkyne rhodamine, a hydrophilic and highly water soluble dye and alkyne-pyrene, a highly hydrophobic compound, in order to compare the efficiency of grafting on the various reactive micellar systems.

Post-functionalization of reactive micelles by alkyne-pyrene and alkyne-rhodamine by CuAAC

The functionalization of azide groups of the hydrophobic core of the micelles by the selected fluorescent dyes, i.e. pyrene or rhodamine, via the CuAAC requires firstly to attach an alkyne group to the dyes. These alkyne bearing fluorescent probes were synthesized by reaction of the isothiocyanate group of rhodamine B or the carboxylic acid group of the 1-pyrenebutyric acid with propargylamine as described in the experimental section.

These alkyne dyes were then used to study the coupling reactions with the azido functional micelles. Such micellar system being compartmentalized with highly swollen hydrophilic block and less mobile hydrophobic core, we were interested to compare on one hand the ability of a hydrophobic (pyrene) or a hydrophilic (rhodamine) dye to graft onto the micelles core knowing their reverse affinity for the water phase and micellar core which could be considered as a nanoreactor for CuAAC [12]. On the other hand, we were also curious of the possible effect of the location of the azide functions within the micelle core on the grafting efficiency. Indeed, as depicted on Scheme 3 which represents two extreme situations of the azide localization in the micelle core, depending on the selected copolymer architecture, the azide groups might be located at the periphery of the hydrophobic core of the micelles (a) or at the heart of the micelles (b). This was thus investigated by means of the previously prepared copolymers.

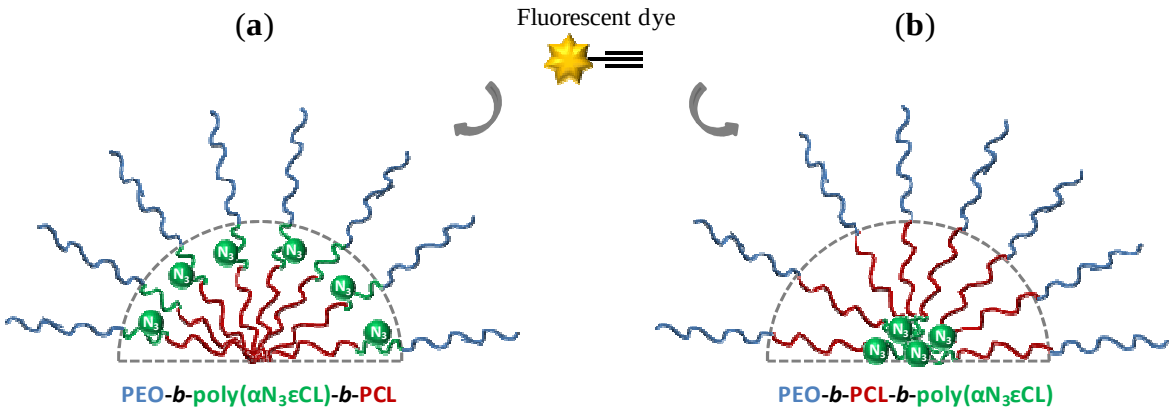

Scheme 3. Grafting of an alkyne bearing fluorescent dye on micelles of :

(**a**) PEO-*b*-poly(αN$_3$εCL)-*b*-PCL (**3b**) and (**b**) PEO-*b*-PCL-*b*-poly(αN$_3$εCL) (**2b**)

The CuAAC reaction was performed on freshly prepared micelles in water for the grafting of the hydrophilic rhodamine dye while micelles still in the mixture of H_2O and DMF were used for the grafting of the hydrophobic pyrene dye in order to provide some solubility of the hydrophobic dye in the medium. CuAAC was allowed to proceed for 24 hours at 35°C followed by exhaustive dialysis against DMF:H_2O (1:4) mixture and then water to remove quantitatively the unreacted alkyne bearing dyes added in excess. After functionalization, the DLS analysis showed a slight increase of the hydrodynamic diameter of about 4 nm for the micelles collected after purification. Micelles were lyophilized and dissolved into THF to be analyzed by FTIR and SEC.

An efficient grafting of alkyne-rhodamine dye in water was observed on the three different PCL-based copolymer micelles. Indeed, a complete disappearance of the azide band at 2106 cm^{-1} in the FTIR spectrum was observed for the micelles with the azide at the core periphery (system with the copolymer **3b**) and more than 80 % of decreased of the azide peak was measured for the two other systems. In contrast, significant differences were observed between the three PTMC-based copolymer micelles. If a decrease of about 80% of the azide band was observed for the micelles of **1b'** and **3b'** copolymers, only 50% of conversion of the azide was obtained for the micelles of **2b'** copolymer with the azide in the micelle heart. That difference is in line with a limited diffusion of the hydrophilic dye to the heart of the hydrophobic micelle core, immiscibility between PTMC and P(αClεCL) blocks favoring the

segregation and compartmentalization of the micellar core. A better miscibility between the different blocks of the PCL-based systems combined with the possible crystallization of the PCL block, could explain the better grafting efficiency on these systems by a more peripheric localization of the azide groups in these systems.

The rhodamine grafting was also evidenced by SEC by refractive index (RI) detection (Figure 9, black and dark grey curves) which shows a slight shift in the elution volume after grafting without modifying the profile of the trace meaning that no degradation occur during the grafting keeping narrow the polydispersity of the polymer sample. The coupling of the fluorescent dye on all the copolymer chains was also confirmed by comparin the SEC traces recorded by UV-vis detector (Figure 9, dotted dark grey curves) and RI detector for the same copolymer after rhodamine grafting (Figure 9, dark grey curve).The shift between RI and UV traces is typical of the experimental set-up, the UV detector being place before the RI one which induces the shift to lower elution time. However, the shape of the elugram and PDI measured from it are similar, evidencing the presence of the dye on all the chains. Moreover, the ^{1}H NMR spectrum of rhodamine-copolymers confirmed the grafting of the dyes by the disappearance of the signal of the CH-N_3 and the appearance of the characteristic peaks of the triazole ring and of the corresponding dye.

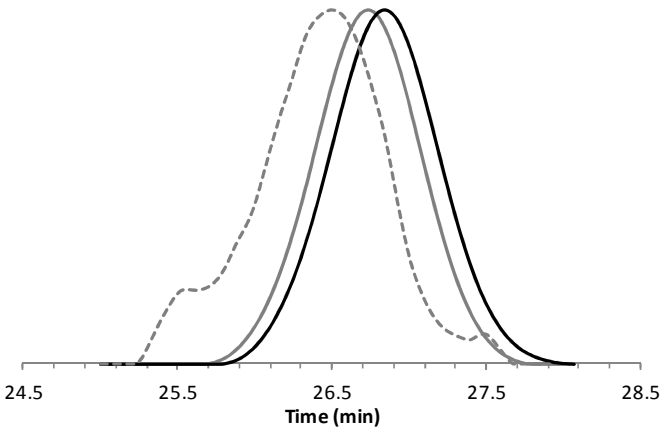

Figure 9. SEC traces recorded in THF of PEO-*b*-poly(CL-*co*-αN_3εCL) (**1b**): before the grafting reaction, RI detector (black) , after reaction with rhodamine in water, RI detector (dark grey) and UV-vis detector at 550 nm (dotted dark grey)

As far as the grafting of the hydrophobic pyrene dye is concerned, the reaction was performed in H_2O and DMF (4:1) mixture in order to insure enough solubility of the pyrene that is not water soluble. As expected, this mixture swells better the micelle core than pure water, since DMF is also a good solvent for the degradable blocks. Micelles of about 100 nm were observed under these conditions. After 24h of reaction and then purification, the complete disappearance of the azide band at 2106 cm^{-1} in the FTIR spectrum underlined the quantitative conversion of the azide functions. The coupling reaction was complete whatever the localization of the azide groups in the micelle core and whatever the copolymer system. Let us also mention that the grafting of the rhodamine dye in these conditions, i.e. the H_2O:DMF mixture, also led to quantitative grafting for all the systems. SEC traces (recorded in THF) of copolymers **2b** and **3b** after reaction in these conditions and recorded with UV-vis detector (Figure 10) clearly demonstrate the efficient grafting of pyrene and rhodamine without degradation of the copolymers. Let us mention that the peak at high elution volume on Figure 11A (dark grey trace) corresponds to some remaining free rhodamine in the sample.

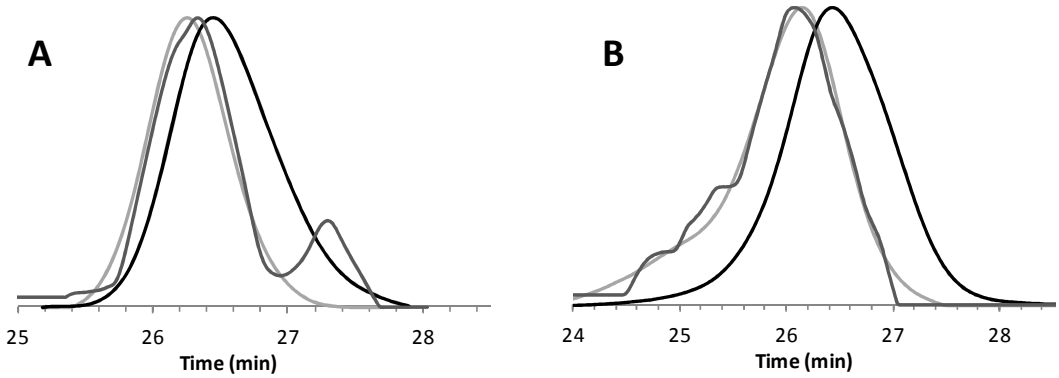

Figure 10. SEC traces of the grafting reaction performed in H_2O:DMF recorded in THF for

A - PEO-*b*-poly(αN_3εCL)-*b*-PCL (**3b**) (black) (RI), PEO-*b*-poly(αpyreneεCL)-*b*-PCL (grey) (UV-vis at 335 nm) and PEO-*b*-(αrhodaminεCL)-*b*-PCL (dark grey) (UV-vis at 550 nm)

B - PEO-*b*-PCL-*b*-poly(αN_3εCL) (**2b**) (black) (RI), PEO-*b*-PCL-*b*-poly(αpyreneεCL) (grey) (UV-vis at 335 nm) and PEO-*b*-PCL-*b*-poly(αrhodaminεCL) (dark grey) (UV-vis at 550 nm)

4. Conclusions

Azide bearing amphiphilic block copolymers based on PEO, PCL and PTMC have been successfully synthesized with a good control on the macromolecular parameters and with narrow molecular weight distribution for different molar ratios of PCL (or PTMC) and poly($\alpha N_3 \varepsilon CL$). The localization of the azide groups along these reactive copolymers was easily modulated by changing the addition sequence of the different comonomers. Of similar hydrophilic/hydrophobic balance (HLB), the selected copolymers proved to be able to form spherical micelles in water in all cases but with different localization of the azide groups depending if a polyester or a polycarbonate backbone is considered to form the hydrophobic core. Nevertheless, whatever the degradable copolymer system, conditions can be found where the azide groups can be efficiently reacted on the already self-assembled micellar dispersion in water and particularly in water:DMF mixture. Hydrophilic as well as hydrophobic fluorescent dyes could be grafted on the micelles leading to fluorescent labeled micelles of interest to follow the fate of the nanocarriers in interactions with living systems. These dyes might also be seen as model molecules for drugs that would be functionalized by an alkyne group. Finally, the demonstrated ability of post-functionalization of these micellar systems opens the door to the elaboration of cross-linked systems particularly attractive in drug delivery to prevent the nanocarrier destabilization by the high dilution (below CMC) generally occurring upon injection. Typically, the substitution of the alkyne-dye by a bis-alkyne would lead to the micelles cross-linking. This important aspect is the topic of a dedicated paper [30].

5. References

1. Soo, P. L.; Luo, L.; Maysinger, D.; Eisenberg, A. *Langmuir* **2002**, *18*, 9996.

2. Kataoka, K.; Harada, A.; Nagasaki, Y. *Advanced Drug Delivery Reviews* **2001**, *47*, 113.

3. Van Butsele, K.; Jerome, R.; Jerome, C. *Polymer* **2007**, *48*, 7431.

4. Kwon, G. S.; Okano, T. *Advanced Drug Delivery Reviews* **1996**, *21*, 107.

5. Kim, S. Y.; Lee, K. E.; Han, S. S.; Jeong, B. *Journal of Physical Chemistry B* **2008**, *112*, 7420.

6. Aliabadi, H. M.; Elhasi, S.; Mahmud, A.; Gulamhusein, R.; Mahdipoor, P.; Lavasanifar, A. *International Journal of Pharmaceutics* **2007**, *329*, 158.

7. Maeda, H.; Wu, J.; Sawa, T.; Matsumura, Y.; Hori, K. *Journal of Controlled Release* **2000**, *65*, 271.

8. Owens, D. E.; Peppas, N. A. *International Journal of Pharmaceutics* **2006**, *307*, 93.

9. Gref, R.; Couvreur, P.; Barratt, G.; Mysiakine, E. *Biomaterials* **2003**, *24*, 4529.

10. Rieger, J.; Freichels, H.; Imberty, A.; Putaux, J.-L.; Delair, T.; Jerome, C.; Auzely-Velty, R. *Biomacromolecules* **2009**, *10*, 651.

11. Freichels, H.; Auzely-Velty, R.; Lecomte, P.; Jérôme, C. *Polymer Chemistry* **2012**, *3*, 1436.

12. O'Reilly, R. K.; Joralemon, M. J.; Wooley, K. L.; Hawker, C. J. *Chemistry of Materials* **2005**, *17*, 5976.

13. Garg, S. M.; Xiong, X.-B.; Lu, C.; Lavasanifar, A. *Macromolecules (Washington, DC, United States)* **2011**, *44*, 2058.

14. Freichels, H.; Danhier, F.; Preat, V.; Lecomte, P.; Jerome, C. *International Journal of Artificial Organs* **2011**, *34*, 152.

15. Saulnier, B.; Ponsart, S.; Coudane, J.; Garreau, H.; Vert, M. *Macromolecular Bioscience* **2004**, *4*, 232.

16. Detrembleur, C.; Mazza, M.; Halleux, O.; Lecomte, P.; Mecerreyes, D.; Hedrick, J. L.; Jerome, R. *Macromolecules* **2000**, *33*, 14.

17. Stassin, F.; Halleux, O.; Dubois, P.; Detrembleur, C.; Lecomte, P.; Jerome, R. *Macromolecular Symposia* **2000**, *153*, 27.

18. Parrish, B.; Breitenkamp, R. B.; Emrick, T. *Journal of the American Chemical Society* **2005**, *127*, 7404.

19. Lenoir, S.; Riva, R.; Lou, X.; Detrembleur, C.; Jerome, R.; Lecomte, P. *Macromolecules* **2004**, *37*, 4055.

20. Riva, R.; Lenoir, S.; Jerome, R.; Lecomte, P. *Polymer* **2005**, *46*, 8511.

21. Riva, R.; Schmeits, S.; Stoffelbach, F.; Jerome, C.; Jerome, R.; Lecomte, P. *Chemical Communications (Cambridge, United Kingdom)* **2005**, 5334.

22. Lou, X.; Detrembleur, C.; Lecomte, P.; Jerome, R. *Journal of Polymer Science, Part A: Polymer Chemistry* **2002**, *40*, 2286.

23. Ariga, T.; Takata, T.; Endo, T. *Journal of Polymer Science, Part A: Polymer Chemistry* **1993**, *31*, 581.

24. Riva, R.; Schmeits, S.; Jerome, C.; Jerome, R.; Lecomte, P. *Macromolecules* **2007**, *40*, 796.

25. Rieger, J.; Passirani, C.; Benoit, J.-P.; Van Butsele, K.; Jerome, R.; Jerome, C. *Advanced Functional Materials* **2006**, *16*, 1506.

26. Vangeyte, P.; Gautier, S.; Jerome, R. *Colloids and Surfaces, A: Physicochemical and Engineering Aspects* **2004**, *242*, 203.

27. Lee, R.-S.; Huang, Y.-T. *Journal of Polymer Science, Part A: Polymer Chemistry* **2008**, *46*, 4320.

28. Ould-Ouali, L.; Arien, A.; Rosenblatt, J.; Nathan, A.; Twaddle, P.; Matalenas, T.; Borgia, M.; Arnold, S.; Leroy, D.; Dinguizli, M.; Rouxhet, L.; Brewster, M.; Preat, V. *Pharmaceutical Research* **2004**, *21*, 1581.

29. Du, Z.-X.; Xu, J.-T.; Fan, Z.-Q. *Macromol. Rapid Commun.* **2008**, *29*, 467.

30. Cajot, S.; Lautram, N.; Passirani, C.; Jerome, C. *Journal of Controlled Release* **2011**, *152*, 30.

CHAPTER V

Design of reversibly core cross-linked micelles sensitive to reductive environment

S. Cajot, N. Lautram, C. Passirani, C.Jérôme

Journal of Controlled Release, **2011**, 152, 30-36

Abstract

Azido-functional amphiphilic macromolecules based on a biodegradable aliphatic polyester (poly-ε-caprolactone, PCL) and a bioeliminable hydrophilic poly(ethylene oxide) (PEO) block have been used in order to build micellar drug delivery systems. Such azido groups being able to react by copper azide-alkyne cycloaddition (CuAAC) have been used further in order to cross-link the micelles via redox-sensitive disulfide bridges. This reversible cross-linking allows to prevent micelles dissociation at high dilution upon injection and to trigger their dissociation in more reductive environment, such as the cytosol. Copolymers having three different architectures, i.e. able to cross-link either the core or the shell of core-shell-corona system have been used to investigate their micellization, cross-linking and cross-linking reversibility. The stealthiness of these micelles cross-linked in the hydrophobic segment has also been studied *in vitro*.

1. Introduction

Nowadays, polymer micelles have attracted an increasing interest in pharmaceutical research because they could be used as efficient drug delivery systems. Micelles of amphiphilic block copolymers are supramolecular core-shell type assemblies of several tens of nanometers in diameter. In principle, the micelle core is usually constructed with biodegradable hydrophobic polymers such as aliphatic polyesters, e.g. poly(ε-caprolactone) (PCL), which serves as a reservoir for the incorporation of various lipophilic drugs. Water soluble poly(ethylene oxide) (PEO) is most frequently used to build the micelle corona because it is very efficient in preventing protein adsorption at surfaces and in stabilizing micelles in the blood compartment, making particles invisible to the body defence system [1-3]. The transport of macromolecular systems in the bloodstream is governed by diffusion and by convection. Indeed, the concentration gradient created during the injection ensures the diffusion transport. In the case of micellar systems, low critical micellar concentrations (CMC) are required in order to avoid destabilization of the carrier in the bloodstream caused by the dilution. On the other hand, the movement of fluids due to pressure gradients in the vessels insures transport by convection. The increased pressure gradient within the tumor tissue suggests the existence of a convective flow enabling the delivery of macromolecules. This is due to the morphology difference between the blood vessels in tumor and healthy tissues. Tumor tissues have a prominent vascular permeability through a non-continuous endothelium which allows the migration of nanoparticles or micelles. This effect is known as "EPR effect" (Enhanced Permeability and Retention effect) and helps to explain the accumulation of nanocarriers in tumor tissues (passive targeting) and high concentrations of these for long periods [4-5].

Even if micelles get a high stability in aqueous media thanks to their low critical micellar concentration, micelle dissociation is not always preserved when they are injected in the blood compartment. A way to provide the micelle stability during their administration is to cross-link them. Different kinds of cross-linked micelles can be investigated depending on the

localisation of the cross-linking. Wooley et *al*. have reported various systems of shell cross-linked micelles [6-7] or nanocage structures with a degradable core [8]. These kinds of shell cross-linked nanosystems have the great advantage to reach drug encapsulation with a high loading rate. However, cross-linking the hydrophilic shell may affect the stealthiness of the carrier. The present paper aims at reporting on the design of reversibly cross-linked micelles by introducing the cross-linking bridges in the hydrophobic segment of the block copolymer, rather than in the hydrophilic one, leading so to more internal cross-linking and thus preserving the mobility of the hydrophilic segment. Such internal but irreversible cross-linking of the micelle core has already been investigated to stabilize micelle structure, by photo-induced cross-linking [9-11], and also by click chemistry [12-13]. In the present paper, as depicted in Figure 1, three different localizations of the cross-linking will be targeted; (i) loose core cross-linking of a core-corona system (Figure 1a), (ii) tight core cross-linking of a core-shell-corona system (the shell and the core being both hydrophobic and the corona hydrophilic) (Figure 1b) and (iii) tight shell cross-linking of a similar core-shell-corona system (Figure 1c).

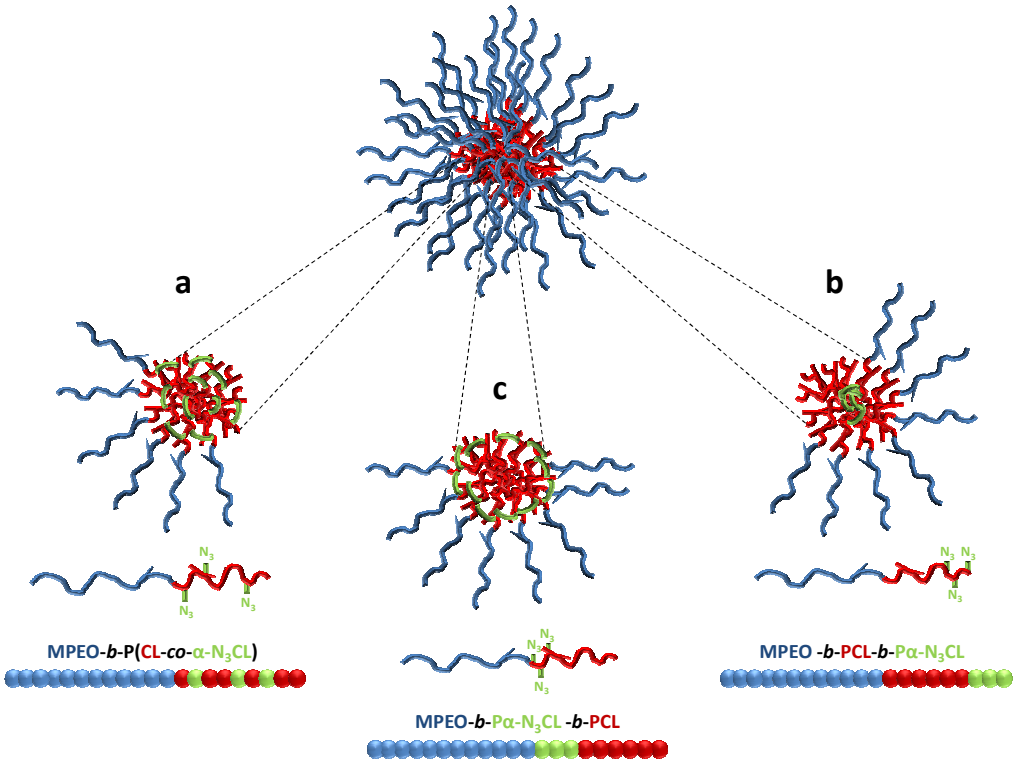

Figure 1. Structure of the cross-linked micelles versus macromolecular architecture.

To reach this goal, three types of amphiphilic copolymers have been used bearing pendent azide groups in the hydrophobic segment [14]. These copolymers have been obtained by starting the ring-opening polymerization of ε-CL and a functional CL, either as a mixture or sequentially from a poly(ethylene oxide) macroinitiator leading to the three targeted architectures (Figure 1). The azide groups located along the PCL backbone have then been used to cross-link the micelles by the copper azide-alkyne cycloaddition (CuAAC) with a bis-alkyne cross-linker. The choice of this cross-linker has also taken into account the requirement to make the cross-linking reversible. For that purpose, disulfide bridges have been selected in order to impart reversibility to the cross-linking by intracellular reduction. Indeed, the marked concentration difference of glutathione between extra- and intra-cellular environments has already been used to trigger drug release by intracellular disulfide bond cleavage [15-17]. Accordingly, a bis-alkyne disulfide molecule has been chosen as cross-linker. The micellization and cross-linking of these amphiphilic azido macromolecules have been studied. The reversibility of the cross-linking in reductive environment and the cross-linked micelles stealthiness have been tested.

2. Materials and methods

Materials

Copper sulfate, ascorbic acid sodium salt, dithiothreitol (DTT) and dimethylformamide (DMF) were purchased from Aldrich. Block copolymers have been synthesized by adapting conditions reported in the literature [14,18] for the homo and copolymerization of α-chloro-ε-caprolactone (αClCL) and ε-caprolactone (εCL) by using a poly(ethylene oxide) macroinitiator. The chloride groups were substituted by azide in a second step following the polymerization, by reaction with sodium azide. Details about the synthesis are reported elsewhere [19]. The characteristics of the copolymers used for this study are summarized in table 1.

PMMA nanoparticles were synthesized in aqueous suspension. After addition of the monomer, the polymerization was initiated by addition of potassium peroxymonosulfate and

heating to 70 °C. Submicronic particles, stable in the absence of added surfactant, were spontaneously formed [20]. The PMMA nanoparticles used in CH50 test as reference sample have been prepared by this process with a size of 150 nm.

The formulation of lipid nanocapsules was based on a phase inversion, from an oil-in-water to a water-in-oil emulsion. The process described elsewhere by Heurtault et *al.* [21] is leading to the formation of lipid nanocapsules with size from 20 to 100 nm, according to the respective amount of water, surfactants, and oil. The lipid nanocapsules used in CH50 test as reference sample have been prepared by this process with a size of 50nm.

Table 1. Characteristics of the copolymers obtained by ROP of εCL and αClCL from monomethoxy poly(ethylene glycol) (MPEO) M_n =5000 g/mol and then substituted by NaN_3.

Copolymer architectures[a]	***code***	***DP*[b] *PEO***	***DP*[b] *PCL***	***DP*[b] *N_3-PCL***	***CL/N_3CL ratio (%)***	***M_w/M_n (SEC)*[c]**
MPEO-*b*-poly(εCL-*co*-αN_3CL)	**1b-1**	114	*13*	*4*	76/24	1.08
	1b-2	114	10	7	60/40	1.08
MPEO-*b*-PCL-*b*-poly(αN_3CL)	**2b-1**	114	*12*	*3*	80/20	1.06
	2b-2	114	*11*	6	65/35	1.08
MPEO-*b*-poly(αN_3CL)-*b*-PCL	**3b-1**	114	*12*	*5*	70/30	1.05
	3b-2	114	10	5.5	65/35	1.08

[a] as schematized on figure 1

[b] DP: number of monomers unit per chain, determined by ^{1}H NMR

[c] by using PS calibration

Cross-linking of the micelles

Micellization of the azido-functional copolymers was obtained by co-solvent process. A 1% stock solution of the copolymer (**1b**, **2b** or **3b**) was prepared in DMF in presence of the cross-linker (0.6 mol equiv. vs. azide groups). 20 mL of Milli-Q water were added to 5 mL of this organic solution under vigorous stirring for one day. $CuSO_4$ (0.25 mol equiv. vs. azide groups) and ascorbic acid sodium salt (0.25 mol equiv. vs. azide groups) were added to the mixture. The cross-linking reaction was allowed to proceed for one day at room temperature. 2 mol equiv. vs. Cu of a solution of EDTA pH 7 were added to the solution to complex the

copper. Then, the cross-linked copolymer micelles were purified by dialysis overnight against 1L of water using cellulose dialysis membrane (Spectrapor, cut-off 3500).

Micelle characterization methods

The size distribution of the micelles was estimated by Photon Correlation Spectroscopy (PCS) using a particle-size analyser (Delsa Nano C, Particle Analyzer, Beckman Coulter) at 25°C. The intensity of scattered light was detected at 165° to an incident beam. Aqueous micellar solution was filtered with a microfilter having an average pore size of 0.2 µm. An average size distribution of aqueous micellar solution was determined based on CONTIN method.

Transmission Electron Microscopy (TEM) was performed with a Philips CM-100 microscope. Samples were prepared by spin-coating a drop of micellar solution on a copper grid coated with formvar.

Stability of the cross-linked micelles

The stability of cross-linked micelles has been studied by comparing them to non-cross-linked micelles. These were prepared in the same way as described above for cross-linked micelles except the addition of the cross-linker, $CuSO_4$ and ascorbic acid sodium salt. The micelle size was then followed by DLS over time and upon diluting below the CMC (~ 5.10^{-5} mol/L). In addition, the stability of the cross-linked micelles after 1 night of stirring at 37°C in water in the presence of a reducing agent (10 mM of DTT or glutathione) was similarly determined by comparing the DLS intensity at concentrations below and above CMC.

The sensitivity of the cross-linking towards DTT was also evaluated in DMF (a good solvent of both blocks) at high concentration (~0.15 mg/mL). Aqueous suspension of cross-linked and non-cross-linked micelles were diluted in DMF (10-fold) and stirred for one day at room temperature before determining the micelle size by DLS. Then, 10 mM of DTT were added, and the mixture was stirred for another night at 37°C before DLS investigation.

Complement Activation test (CH50)

Complement activation was measured as the lytic capacity of a normal human serum (NHS) towards antibody-sensitized sheep erythrocytes after exposure to the micelles. Aliquots of NHS were incubated with increasing concentrations of micelles. The amount of serum causing 50% haemolysis after exposure to the micelles was determined ("CH50 units") for each sample. NHS was provided by the "Etablissement Français du Sang" (Angers, France) and stored as aliquots at – 80°C until use. Veronal-buffered saline containing 0.15 mM Ca^{2+} and 0.5 mM Mg^{2+} (VBS^{++}) was prepared as reported elsewhere [22] . Firstly, sheep erythrocytes were sensitized by rabbit anti-sheep erythrocytes antibodies (Sérum hémolytique, Biomérieux, Marcy-l'Etoile, France) and diluted by the veronal-buffered saline at a final concentration of 2.10^9 cells/mL in VBS^{++}. Increasing amounts of micelles were added to NHS diluted in VBS^{++} such that the final dilution of NHS in the mixture was 1/4 (v/v) in a final volume of 1 mL. After 1 h of incubation at 37°C under gentle agitation, the suspension was diluted 1/25 (v/v) in VBS^{++}, and aliquots of 8 different dilutions were added to a given volume of sensitized sheep erythrocytes. After 45 min of incubation at 37°C, the reaction mixture was slightly centrifuged at 2000 rpm for 10 min. The absorption of the supernatant was determined at 414 nm with a microplate reader (Multiskan Anscent, Labsystems SA, Cergy-Pontoise, France) and compared to the results obtained with control serum in order to evaluate the amount of haemolyzed erythrocytes. Positive and negative controls were made in each series of experiments in order to account for any difference in the hemoglobin response from a given erythrocyte preparation. Furthermore, corrections for particle light-scattering and spontaneous erythrocyte haemolysis were estimated by UV/VIS measurements using blanks containing only particles and only erythrocytes, respectively. In order to compare micelles of different average diameters, their surface area was calculated as follows: $S = 3\ m/r\rho$, where S is the surface area [cm^2], m the weight [µg] in 1 mL nanosuspension, r the average radius [cm] determined by DLS, and ρ the density [$\mu g/cm^3$] of the micelles estimated at 10^6 $\mu g/cm^3$ [23-25]. The experimental data are the average of three independent experiments with a 10% standard deviation.

3. Results and discussion

Copolymer selection

Based on literature data, PEO_{114}-*b*-PCL_{16} amphiphilic copolymers are quite valuable diblock copolymers for building stealthy spherical micelles [26-28] and for loading them with hydrophobic drugs [29]. So, similar molecular weights for both the hydrophilic and the hydrophobic blocks have been selected for the azido-functionalized PEO-*b*-PCL based copolymers. In order to tune the density and the location of the cross-linking in the hydrophobic segment of the micelles, three kinds of amphiphilic azido-copolymers varying by the distribution of the azide along the PCL backbone have been selected in this work. As shown in Figure 1, PEO_{114}-*b*-poly(εCL-*co*-$\alpha N_3CL)_{17}$ diblock copolymer will lead to a core loosely cross-linked of a core-corona system (Figure 1a), PEO_{114}-*b*-(PCL_y-*b*-poly$(\alpha N_3CL)_x)_{16}$ triblock copolymer will lead to a tightly cross-linked core of a core-shell-corona system (the shell and the core being both hydrophobic and the corona hydrophilic) (Figure 1b), and PEO_{114}-*b*-(poly$(\alpha N_3CL)_x$-*b*-$PCL_y)_{16}$ triblock will give a tightly cross-linked shell of similar core-shell-corona system (Figure 1c).

These copolymers have been synthesized as reported elsewhere [19] with a good yield and well-defined macromolecular parameters (Table 1). Controlled composition of the azido copolymers was achieved. For each copolymer type, two different azide contents have been studied, i.e. about 25 and 35%. The composition of the prepared and used copolymers are summarized in Table 1 and are close to the targeted values. In addition, a narrow polydispersity (M_w/M_n, Table 1) was obtained for all the copolymers which is usually required to favor well-defined microstructuration of block copolymers [30]. This would be particularly important to differentiate core cross-linked micelles of type 1b and 1c (Figure 1) which relies on phase separation of the two PCL-based blocks.

Among all the possible functionalities that can be made available on a PCL backbone, the azide has been chosen since it is easily introduced without polymer degradation and it

reacts via a "click" reaction with alkyne derivatives by copper azide-alkyne cycloaddition [31]. This reaction can be performed in water or organic solvents and will be applied here for the micelle cross-linking.

Micelle formation and cross-linking

The well-defined azido-functional amphiphilic copolymers (Figure 1, table 1), i.e. MPEO-*b*-poly(εCL-*co*-αN_3CL) (**1b-1** and **1b-2**), MPEO-*b*-PCL-*b*-poly(αN_3CL) (**2b-1** and **2b-2**) and MPEO-*b*-poly(αN_3CL)-*b*-PCL (**3b-1** and **3b-2**) have then been micellized in water by first dissolving them in DMF, a good solvent of both the hydrophobic (PCL and poly(αN_3CL)) and the hydrophilic (PEO) blocks, followed by the addition of water, a selective solvent of the PEO block. In order to localize the cross-linker in the hydrophobic part of the micelles, an hydrophobic bis-alkyne molecule (Scheme 1), whose synthesis has already been described elsewhere [32], was added directly in the DMF solution together with the copolymer. Upon water addition, the cross-linker is expected to migrate to the hydrophobic part of the micelle core remaining swollen by DMF and to react by the click reaction following the addition of $CuSO_4$ and ascorbic acid sodium salt (Scheme 1). After reaction, an EDTA aqueous solution is added to the micelle solution to complex the copper and to remove it by dialysis so as the remaining DMF [33].

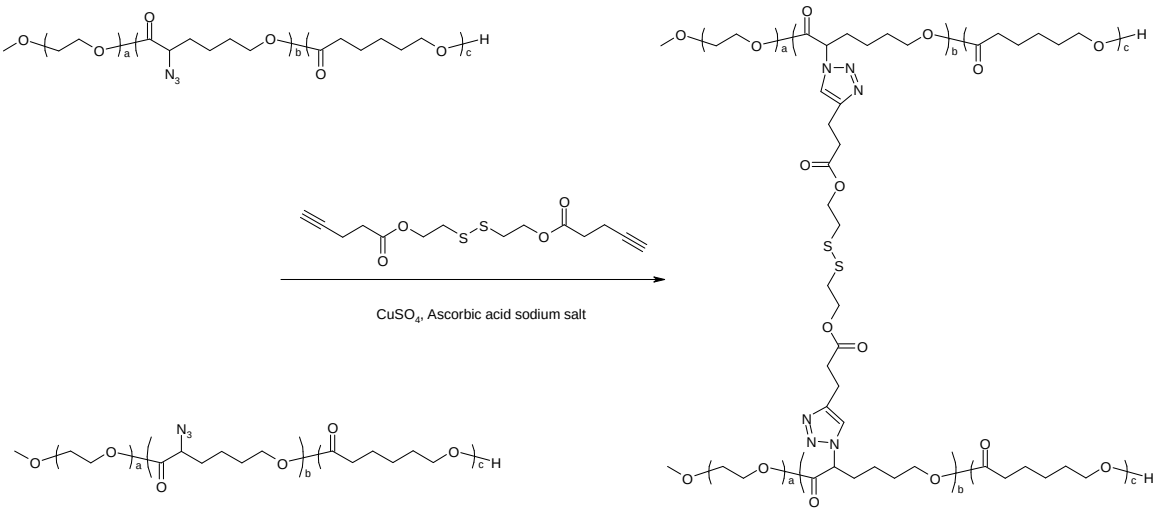

Scheme 1. Micelle cross-linking by Copper Azide-Alkyne Cycloaddition

The as-obtained cross-linked micelles were first characterized by dynamic light scattering (DLS) and were compared to the same micelles before the cross-linking step. These results are summarized in the table 2 and Figure 2.

Table 2. DLS data for cross-linked and non-cross-linked micelles of the various copolymers in water

Copolymers	**Non-cross-linked micelles**		**Cross-linked micelles**	
	$D_{h,app}$ (nm) [a]	**μ_2/Γ^2** [b]	**$D_{h,app}$ (nm)** [a]	**μ_2/Γ^2** [b]
1b-1	41	0.23	48	0.23
1b-2	32	0.09	37	0.07
2b-1	30	0.18	36	0.16
2b-2	29	0.14	43	0.16
3b-1	30	0.19	38	0.25
3b-2	33	0.13	36	0.11

[a] Apparent hydrodynamic diameter [a] and PDI [b] determined by DLS.

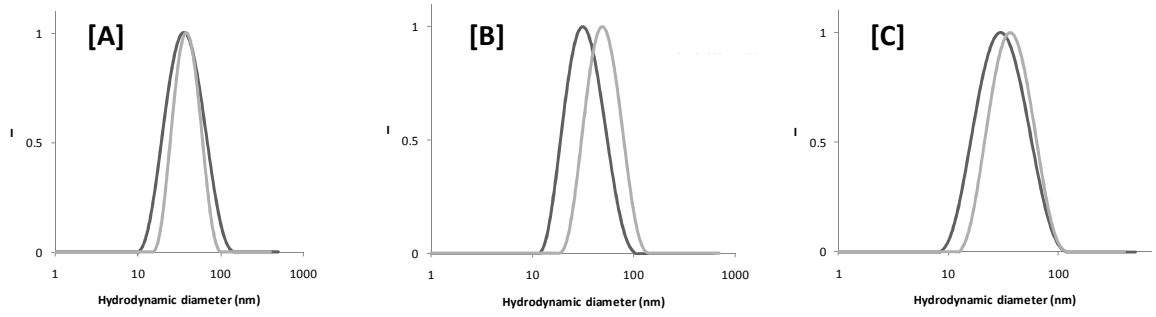

Figure 2. Size distribution of the cross-linked (——) and non-cross-linked micelles (**——)** of **1b-2** [A], **2b-2** [B] and **3b-2** [C] determined by DLS at an angle of 165°.

Non-cross-linked micelles of the azido-functional copolymers show similar sizes in water around 30 nanometers diameter which is in line with more conventional MPEO-*b*-PCL micelles of the same molecular weight [26]. After cross-linking, a size increase of about 5-7 nm

is observed which might be due to the inclusion of the cross-linker in the micelle core together with conformation rearrangements caused by the triazole ring formation during the cross-linking reaction leading to increased constrain of the chains. A spherical morphology of the cross-linked micelles was also confirmed by TEM for all the three types of copolymer architectures (Figure 3) with a size in agreement with DLS results. Nevertheless, the poor contrast resolution of the pictures brought by copper traces, does not allow evidencing the cross-linking location on these pictures.

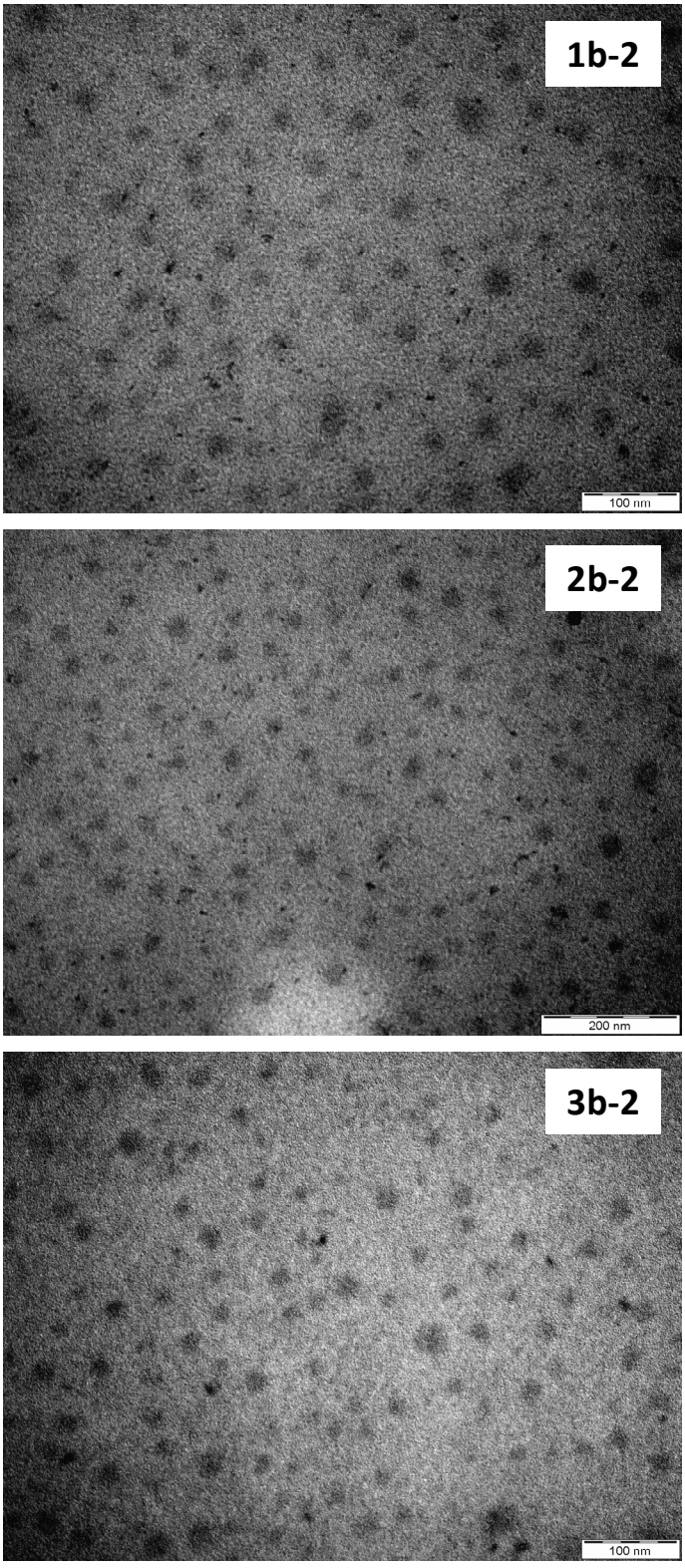

Figure 3. TEM images of cross-linked micelles obtained for copolymers: **1b-2**, **2b-2** and **3b-2**

The effectiveness of the cross-linking reaction was qualitatively evidenced by evaluating the micelle stability versus time (Figure 4). No variation of the hydrodynamic diameter of the cross-linked micelles is observed over period of at least 30 days, while aggregates are formed in solution of the non-cross-linked micelles as depicted by increasing hydrodynamic diameters with time. Interestingly, the micelles of **3b-2** copolymer exhibiting the azide groups in the shell appear more stable than the two other azido copolymers.

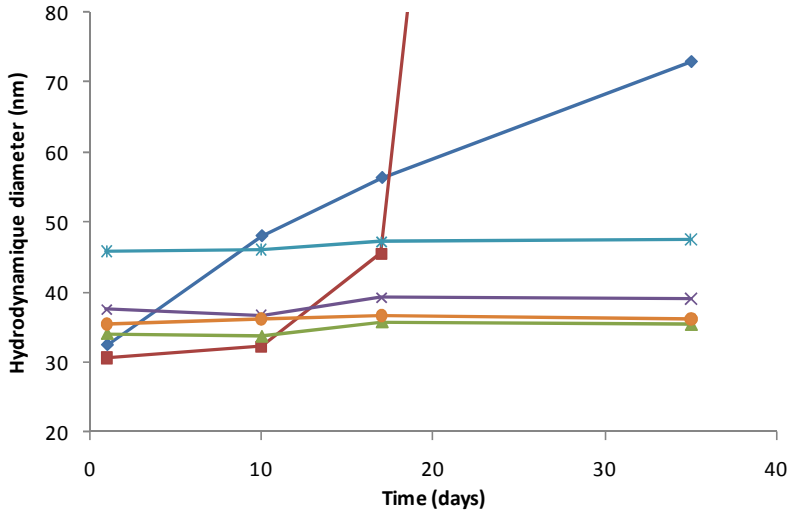

Figure 4. Size distribution vs. time of cross-linked micelles **1b-2** (—✕—), **2b-2** (—✳—), **3b-2** (—●—) and non-cross-linked micelles **1b-2** (—◆—), **2b-2** (—■—), **3b-2** (—▲—).

Another evidence of the cross-linking efficiency was also collected by high dilution of the aqueous solution below the CMC followed by DLS analysis. Well-defined nano-objects with a narrow polydispersity are still observed after a 100-fold dilution of the cross-linked micelles while these objects disappeared for the non-cross-linked system giving small-size unimers.

In addition, by keeping concentrated solutions that are easier to analyze by DLS, the micelle cross-linking was also confirmed by addition of a 10-fold excess of DMF, a good solvent for both PEO and PCL blocks. In case of cross-linked systems, the core of the micelles is able to swell giving objects of larger size than in water (about 400 nm diameter).

Again, in case of non-cross-linking micelles, dissociation is observed due to the solubilization of the azido-copolymers (Figure 5). Even if some traces of swollen micelles are still observed in DMF, the intensity of the diffuse signal is about 4-fold lower than in the case of cross-linked micelles which highlights the efficiency of the cross-linking.

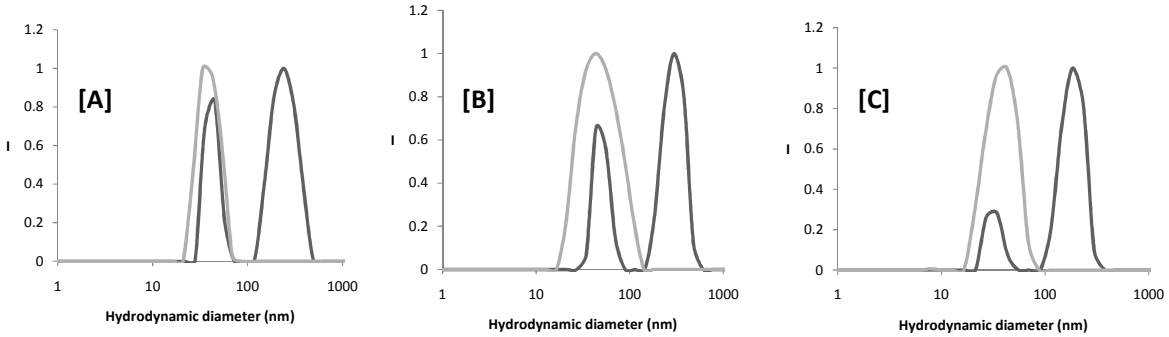

Figure 5. Size distribution of cross-linked micelles in water (——) against 10-fold dilution with DMF (——) of **1b-2** [A], **2b-2** [B] and **3b-2** [C] in terms of hydrodynamic diameter.

As mentioned in the introduction, a disulfide based cross-linker has been selected in order to get reversible cross-linking in the presence of a reductive medium. Glutathione is the main biological component that has been evidenced as responsible of intra-cellular cleavage of disulfide bonds that remain stable in extra-cellular media such as the bloodstream. Indeed, glutathione concentration is about 10 mM in the intra-cellular compartment, providing reductive environment in cells, while it is only 10 µM in the bloodstream [34]. The reversibility of the micelles cross-linking was thus tested by following the size of the objects in water in presence of DTT as reducing agent. As expected, above the CMC, the micelles size appears independent of the reducing agent content. On the other hand, at concentrations below the CMC, cross-linked micelles disappear forming unimers in presence of DTT as evidenced by the sharp decrease of the diffused signal in DLS in comparison to these micelles at the same dilution in absence of DTT. Indeed, micelles of higher size than unimers are more efficient scatterers so that at the same polymer concentration, a higher DLS intensity reflects the presence of bigger objects i.e. the presence of micelles rather than unimers. This gives a first

hint on the effect of cross-linking on the micelle stability. In order to work at higher concentration and recover a more intense DLS signal, similar experiments have been performed in DMF. This solvent being a good solvent of both blocks, individual chains are expected in non-cross-linked systems whatever the polymer concentration, only cross-linked micelles are giving rise to supramolecular assemblies. By using this solvent, the diffused intensity of cross-linked micelles becomes 5-fold smaller in presence of DTT indicating that the number of micelles in DMF is sharply decreased due to the reduction of the disulfide bridges. All these observations hold for the three copolymer architectures and both compositions showing the success of the cross-linking and its reversibility whatever the location of the cross-links in the hydrophobic core of the studied systems.

Similar conclusions on the reversibility of the micelle cross-linking can be drawn by substituting glutathione for DTT, even if in this case, the poor solubility of this reducing agent in DMF limited the experiments to aqueous media.

Stealth properties of the cross-linked micelles

The stealthiness of the cross-linked micelles is a key point since long-circulating micelles are targeted. The ability of micelles to resist protein adsorption has been studied by a quantitative analysis of the adsorption of human serum proteins on the micelles according to the so-called CH50 test [23]. Foreign bodies, like synthetic nanoparticles, when injected intravenously are indeed subject to the complement system, the most important mechanism of the immune system, which tries to remove them from the bloodstream. Nevertheless, opsonisation is usually limited by coating the particles by flexible and highly hydrophilic PEO chains leading to stealthy systems [22,35-36]. *In vitro* study of the activation of the complement by the cross-linked micelles was performed by the quantitative CH50 test. After incubation of the cross-linked micelles with human serum, the proteins remaining non-adsorbed on the micelles are quantified by the lysis of sensitived sheep erythrocytes added to the medium. The so-released heamoglobin is used as a dye for a colorimetric titration. The CH50 unit is the concentration expressed by mL of serum of complement units able to cause 50% heamolysis of a fixed volume of sheep red cells. The results are reported in terms of consumption of the

CH50 units for each cross-linked system (Figure 6) and compared to poly(methyl methacrylate) (PMMA) nanoparticles [37] and lipid nanocapsules [38] known for their high and low activation of the complement respectively. Figure 6 shows a slow increase of the CH50 consumption when the amount of micelles is increased in the serum whatever the type of micelles considered, as expected, when the surface area in contact with proteins is higher. This increase compares better to stealthy lipid nanocapsules rather than PMMA nanoparticles for which the protein adsorption occurs already for low exposed surface area. All the three kinds of cross-linked micelles show a similar low activation of the complement. Indeed, the PEO-corona is mainly responsible for the protein repellency - the high efficiency of PEO chains to repel proteins is known to be due to high hydrophilicity and high mobility of these chains - so that micelles differing by the cross-linked core are not expected to behave differently.

However, slightly faster complement activation is observed for micelles type **1b-1** as compared to **2b-1** and **3b-1**. This might be explained by a higher size of these micelles (48 nm as compared to 30 nm, table 2), rather than by a decrease of the PEO segments flexibility. Indeed, stealth behaviour is known to be improved by the reduction of the particle size [39]. Since the cross-linking reaction does not affect the external PEO-corona, an important decrease of the flexibility of these hydrophilic segments is not expected.

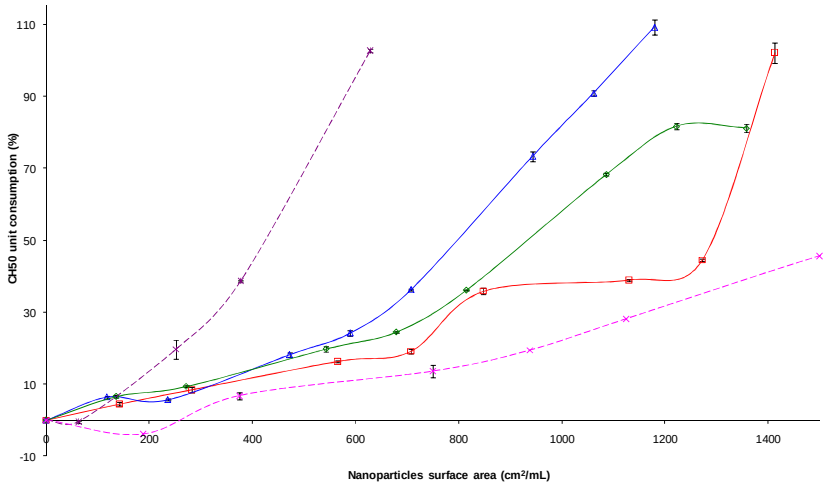

Figure 6. Consumption of CH50 units versus surface area of micelles **1b-1** (—△—), **2b-1** (—□—), **3b-1** (—◇—) compared to PMMA nanoparticles 150 nm (--✳--) and lipid nanocapsules 50 nm (--X--).

4. Conclusion

Amphiphilic and reactive well-defined block copolymers have been designed in order to build mainly hydrophobic core cross-linked micelles to be used as drug delivery vehicles. By the co-solvent micellization strategy, successful cross-linking of the micelles in aqueous media has been achieved. By the appropriate choice of the cross-linker functionality, reversible cross-linking triggered by reductive conditions has been achieved. Such novel reversible cross-linked micelles have been found stealthy which makes them quite promising for the elaboration of drug delivery systems. So far, the three studied macromolecular architectures exhibiting the functionality in the core or in the shell of core-shell-corona systems or randomly dispersed in the core of a core-shell system have not evidenced real differences; they were all successfully micellized, reversibly cross-linked and are stealthy, which shows the efficiency of the developed cross-linking process and offers a series of nanocarriers to be tested further. Drug encapsulation, as well as *in vitro* and *in vivo* release profiles by these various redox responsive cross-linked micelles are currently under investigations and will be the topic of a forthcoming paper.

5. References

1. Kataoka, K.; Harada, A.; Nagasaki, Y. *Advanced Drug Delivery Reviews* **2001**, *47*, 113.

2. Van Butsele, K.; Jerome, R.; Jerome, C. *Polymer* **2007**, *48*, 7431.

3. Kwon, G. S.; Okano, T. *Advanced Drug Delivery Reviews* **1996**, *21*, 107.

4. Takakura, Y.; Hashida, M. *Crit Rev Oncol Hematol* **1995**, *18*, 207.

5. Maeda, H.; Wu, J.; Sawa, T.; Matsumura, Y.; Hori, K. *Journal of Controlled Release* **2000**, *65*, 271.

6. Zhang, K.; Fang, H.; Wang, Z.; Taylor, J.-S. A.; Wooley, K. L. *Biomaterials* **2009**, *30*, 968.

7. Li, Y.; Du, W.; Sun, G.; Wooley, K. L. *Macromolecules (Washington, DC, United States)* **2008**, *41*, 6605.

8. Turner, J. L.; Wooley, K. L. *Nano Letters* **2004**, *4*, 683.

9. Prochazka, K.; Baloch, M. K.; Tuzar, Z. *Makromolekulare Chemie* **1979**, *180*, 2521.

10. Ishizu, K.; Saito, R. *Polymer-Plastics Technology and Engineering* **1992**, *31*, 607.

11. Guo, A.; Liu, G.; Tao, J. *Macromolecules* **1996**, *29*, 2487.

12. Jiang, X.; Zhang, J.; Zhou, Y.; Xu, J.; Liu, S. *Journal of Polymer Science, Part A: Polymer Chemistry* **2008**, *46*, 860.

13. Zhang, J.; Zhou, Y.; Zhu, Z.; Ge, Z.; Liu, S. *Macromolecules (Washington, DC, United States)* **2008**, *41*, 1444.

14. Riva, R.; Schmeits, S.; Jerome, C.; Jerome, R.; Lecomte, P. *Macromolecules* **2007**, *40*, 796.

15. Sun, H.; Guo, B.; Cheng, R.; Meng, F.; Liu, H.; Zhong, Z. *Biomaterials* **2009**, *30*, 6358.

16. Nasanit, R.; Iqbal, P.; Soliman, M.; Spencer, N.; Allen, S.; Davies, M. C.; Briggs, S. S.; Seymour, L. W.; Preece, J. A.; Alexander, C. *Molecular BioSystems* **2008**, *4*, 741.

17. Xu, Y.; Meng, F.; Cheng, R.; Zhong, Z. *Macromolecular Bioscience* **2009**, *9*, 1254.

18. Lee, R.-S.; Huang, Y.-T. *Journal of Polymer Science, Part A: Polymer Chemistry* **2008**, *46*, 4320.

19. S.Cajot; Riva, R.; Jérôme, C. **2010**.

20. Kreuter, J. *Colloidal Drum Deliverv Svstems, J. Kreuter (Eds), 219-342, Marcel Dekker,Inc., New York, USA* **1994**, 219.

21. Heurtault, B.; Saulnier, P.; Pech, B.; Proust, J.-E.; Benoit, J.-P. *Pharmaceutical Research* **2002**, *19*, 875.

22. Gref, R.; Luck, M.; Quellec, P.; Marchand, M.; Dellacherie, E.; Harnisch, S.; Blunk, T.; Muller, R. H. *Colloids and Surfaces, B: Biointerfaces* **2000**, *18*, 301.

23. Passirani, C.; Benoit, J.-P. *Biomaterials for Delivery and Targeting of Proteins and Nucleic Acids* **2005**, 187.

24. Kabat, E. A.; Mayer, M. M. *Experimental Immunochemistry. 2nd ed*, 1961.

25. Vittaz, M.; Bazile, D.; Spenlehauer, G.; Verrecchia, T.; Veillard, M.; Puisieux, F.; Labarre, D. *Biomaterials* **1996**, *17*, 1575.

26. Vangeyte, P.; Gautier, S.; Jerome, R. *Colloids and Surfaces, A: Physicochemical and Engineering Aspects* **2004**, *242*, 203.

27. Van Butsele, K.; Sibret, P.; Fustin, C. A.; Gohy, J. F.; Passirani, C.; Benoit, J. P.; Jerome, R.; Jerome, C. *Journal of Colloid and Interface Science* **2008**, *329*, 235.

28. Rieger, J.; Passirani, C.; Benoit, J.-P.; Van Butsele, K.; Jerome, R.; Jerome, C. *Advanced Functional Materials* **2006**, *16*, 1506.

29. Allen, C.; Yu, Y.; Maysinger, D.; Eisenberg, A. *Bioconjugate Chemistry* **1998**, *9*, 564.

30. Abetz, V.; Boschetti-de-Fierro, A.; Gohy, J.-F. *Controlled and Living Polymerizations* **2009**, 493.

31. Lecomte, P.; Riva, R.; Schmeits, S.; Rieger, J.; Van Butsele, K.; Jerome, C.; Jerome, R. *Macromolecular Symposia* **2006**, *240*, 157.

32. Gao, H.; Matyjaszewski, K. *Macromolecules* **2006**, *39*, 4960.

33. O'Reilly, R. K.; Joralemon, M. J.; Wooley, K. L.; Hawker, C. J. *Chemistry of Materials* **2005**, *17*, 5976.

34. Meister, A.; Anderson, M. E. *Annual Review of Biochemistry* **1983**, *52*, 711.

35. Vermette, P.; Meagher, L. *Colloids Surf., B* **2003**, *28*, 153.

36. Lee, J. H.; Oh, S. H. *Journal of Biomedical Materials Research* **2002**, *60*, 44.

37. Passirani, C.; Barratt, G.; Devissaguet, J.-P.; Labarre, D. *Life Sciences* **1998**, *62*, 775.

38. Vonarbourg, A.; Passirani, C.; Saulnier, P.; Simard, P.; Leroux, J. C.; Benoit, J. P. *Journal of Biomedical Materials Research, Part A* **2006**, *78A*, 620.

39. Vonarbourg, A.; Passirani, C.; Saulnier, P.; Benoit, J.-P. *Biomaterials* **2006**, *27*, 4356.

CHAPTER VI

In vitro investigations of smart drug delivery systems based on reversibly cross-linked micelles

S. Cajot, D. Schol, F. Danhier, V. Préat, M.-C. Gillet De Pauw, C. Jérôme

Acta Biomaterialia, **2012**, submitted

Abstract

Redox-sensitive micelles have been designed by using three block copolymers of different architectures composed of an hydrophilic block of poly(ethylene oxide) (PEO), and hydrophobic blocks of poly(ε-caprolactone) (PCL) and poly(α-azide-ε-caprolactone) (poly(αN_3CL)). Stability of these micelles was insured in diluted media by cross-linking their hydrophobic core via the addition of a bifunctional (bis-alkyne) cross-linker able to react with the azide functions of the micelles, while redox sensitivity was provided to these micelles by selecting a bis-alkyne cross-linker comprising a disulfide bridge. These smart cross-linked micelles are highly stable in the bloodstream whereas the reduction of the disulfide bridges in more reductive environments such as cells cytoplasm allows to trigger the intracellular drug delivery. The potential of these responsive micelles to be used as nanocarriers was studied in terms of cytotoxicity and cellular internalization. Moreover, the release profiles were also investigated in function of the environment reductive strength.

1. Introduction

These last years, nanoparticles, liposomes and polymer micelles have been largely investigated as drug nanocarriers [1-4]. The main common way of administration of these drug delivery systems is the direct systemic injection which already bypasses most of the natural barriers. Nevertheless, prolonged circulation time of nanocarriers is required to reach passive targeting of tumor tissues, i.e. the spontaneous accumulation of the nanoparticles in tumors by the Enhanced Permeability and Retention (EPR) effect [5-6]. Indeed, nanocarriers are generally rapidly recognized by the mononuclear phagocytic system (MPS) which removes foreign bodies of the bloodstream to direct them to the liver or the spleen [7-8]. The coating of the nanocarriers by poly(ethylene oxide) (PEO) prevents their too fast recognition by the macrophages and insures the stealthiness of the nanocarriers, due to its hydrophilic nature but also by its rapid conformational changes [9-10]. Moreover, the control of the nanocarrier size is essential to reach long circulating particles. Too small nanoparticles are rapidly removed from the body via the renal system while nanoparticles with larger radius than 200 nm are less stealthy and are rapidly directed to the liver.

Besides passive targeting, a more active targeting of the nanocarriers can be achieved by grafting targeting moieties exposed at the nanocarrier surface and able to recognize specific receptors over-expressed by cancer cells. This would fasten the internalization which is of prime importance since most of the drugs used to treat cancers act intracellularly [11]. However, the presence of a ligand at the surface of the nanocarriers is detrimental to the stealthiness [12]. The development of more complex and adaptive systems is thus today investigated, e.g. systems with a controlled exposition of the targeting units only in the surrounding of tumor cells [13-14].

The stability of the drug loaded nanocarriers is also a key point to avoid prematured release of the drug or Burst effect upon injection. For example, in case of micelles, when they are submitted to high dilutions, their destabilization might occur by crossing the critical micellar concentration (CMC) of the copolymers which causes the drug release before reaching the tumor site. In order to insure the nanocarrier stability against dilution and strong entrapment of the drug inside, polymer micelle systems are usually cross-linked. Nevertheless, after internalization by tumor cells, the drug needs to be released to perform its intracellular action. Thus, the development of reversibly cross-linked micelles was investigated over the recent years [15-17]. In this context, it was already shown that by using redox sensitive disulfide bridges to cross-link micelles, the stability of such nanocarrier is assured under a weakly reductive environment such as the bloodstream. In the cytoplasm, the higher level of glutathione (1000-fold more concentrated than in the bloodstream [18]), a tripeptide containing glutamic acid, cysteine, and glycine, the reduction of the disulfide bridges occurs hence the encapsulated drug is intracellularly delivered [19].

In this framework, some of us have already investigated reversibly core cross-linked micelles built from the three block copolymers, i.e. PEO-*b*-poly(CL-*co*-αN_3CL) (**1**), PEO-*b*-PCL-*b*-poly(αN_3CL) (**2**) and PEO-*b*-poly(αN_3CL)-*b*-PCL (**3**) (Scheme 1) that were cross-linked by a bis-alkyne containing a disulfide bridge as described in the Scheme 2 [20]. The interest of using three amphiphilic copolymers of the same composition but with different architectures (Scheme 1) lies in the possibility to modify the cross-linking location of the micellar core that can be rather peripheric with copolymer **3** or in the heart for copolymer **2** as depicted in Scheme 2. While the stealthiness of all these nanocarriers thanks to the hydrophilic PEO shell was previously demonstrated by CH50 test [21], their *in vitro* cytotoxicity and internalization properties are the purpose of the present paper. In addition, the controlled

release of a hydrophobic dye, chosen as a model for a drug, is also investigated here, in relation of the environment reductive strength and micelle structure.

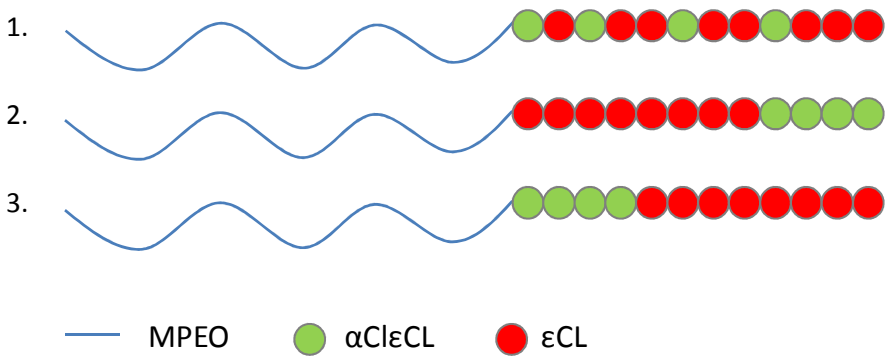

Scheme 1. Schematic architectures of the amphiphilic copolymers used to build the cross-linked micelles: (**1**) PEO-*b*-poly(CL-*co*-αN$_3$CL), (**2**) PEO-*b*-PCL-*b*-poly(αN$_3$CL) and (**3**) PEO-*b*-poly(αN$_3$CL)-*b*-PCL

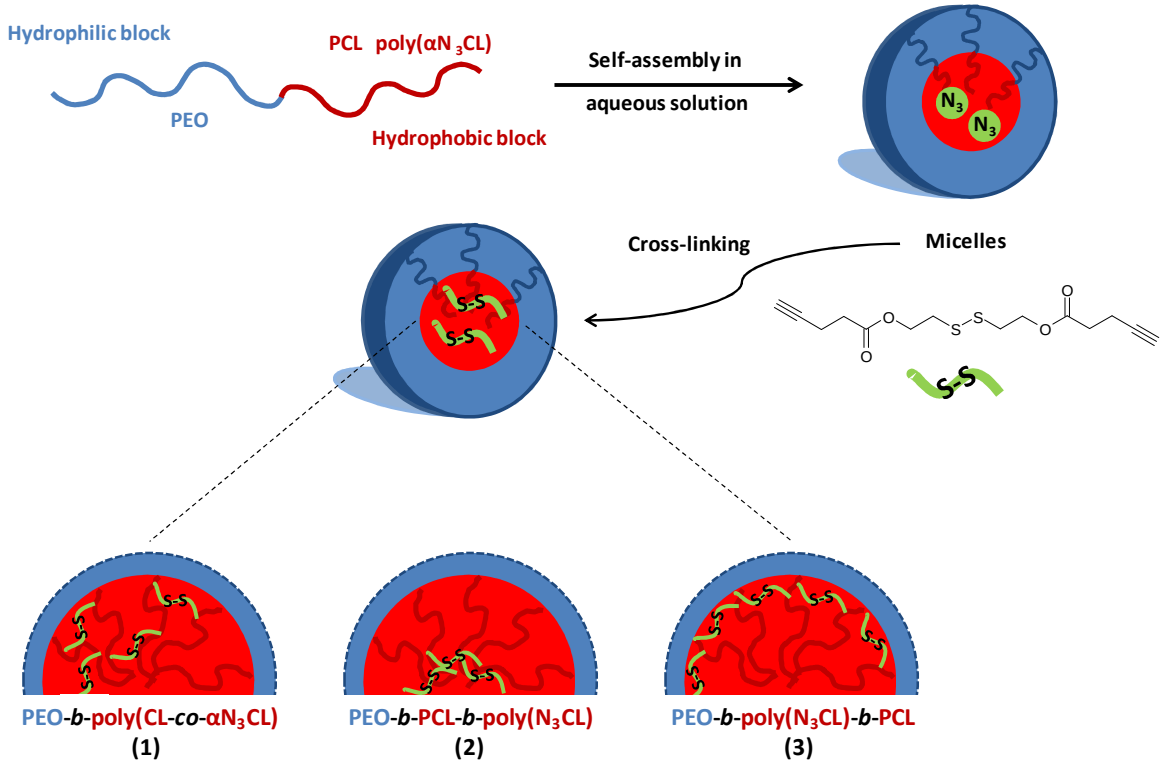

Scheme 2. Schematic representation of the formation of the core cross-linked micelles in aqueous solution.

2. Materials and methods

Materials

5-(and 6-)carboxyFluorescein succinimidyl ester (NHS-Fluorescein) was purchased from Thermo Scientific. 1,4-dithiothreitol (DTT) and Nile Red from Sigma Aldrich as ethylenediaminetetraacetic (EDTA) prepared in a solution of 0.5 M, pH 7. Dimethylformamide (DMF) were dried on molecular sieves. Deionized water was obtained from a Milli-Q plus system (Millipore). All other chemicals were used as received.

Copolymer synthesis

The block copolymers of PEO-*b*-poly(CL-*co*-αN_3CL), PEO-*b*-PCL-*b*-poly(αN_3CL) and PEO-*b*-poly(αN_3CL)-*b*-PCL were synthesized by ring-opening polymerization (ROP). Details of the copolymer synthesis were already reported elsewhere [20]. Briefly, ring-opening polymerization of ε-caprolactone (εCL) and α-chloro-ε-caprolactone (αClCL) was initiated from monomethoxy poly(ethylene oxide) macroinitiator in refluxing toluene for 48 hours in presence of a tin-based catalyst. For the random block copolymer, a mixture of the two lactones was copolymerized while a sequential monomer addition was followed for the synthesis of the two triblock architectures. The substitution of the chloride atoms by azide functions was carried out in presence of sodium azide in DMF for one night.

The molecular weight of the copolymers was calculated by ^{1}H-NMR spectroscopy while polydispersity index (M_w/M_n) was determined by size exclusion chromatography (Table 1).

Copolymer labeling

0.3 g of PEO-*b*-poly(CL-*co*-αN$_3$CL)-OH (M_n = 7100 g/mol, 4.2 10^{-5} mol) (or PEO-*b*-PCL-*b*-poly(αN$_3$CL)-OH or PEO-*b*-poly(αN$_3$CL)-*b*-PCL-OH) and 0.1 g NHS-Fluorescein (2.1 10^{-4} mol) were dissolved in 4 ml of anhydrous DMF and stirred for 48 hours at room temperature. The final product, PEO-*b*-poly(CL-*co*-αN$_3$CL)-Fluorescein were dialyzed against 50/50 water/DMF until a colorless dialysis medium as obtained and finally against water before recovery by lyophilization.

Micelle preparation and cross-linking

Aqueous dispersions of micelles were prepared by addition of water to the copolymer solution in an organic solvent (DMF) chosen as a good solvent for all the hydrophilic and hydrophobic blocks. Their cross-linking was simultaneously achieved by CuAAC of the pendant azide functions of the hydrophobic micelle core with a bis-alkyne disulfide cross-linker, i.e. a bis(alkyne-ethyl ester ethyl) disulfide following an already described process[21].

Briefly, a 1% stock solution of the copolymer was prepared in DMF in presence of the cross-linker (0.6 mol equiv. vs. azide groups). 10 mL of Milli-Q water were added to 2.5 mL of this organic solution under vigorous stirring for one day. $CuSO_4$ (0.25 mol equiv. vs. azide groups) and ascorbic acid sodium salt (0.25 mol equiv. vs. azide groups) were added to the mixture. The cross-linking reaction was allowed to proceed for one day at room temperature. 2 mol equiv. vs. Cu of solution of EDTA pH 7 was added to the solution to complex the copper. Then, the core cross-linked copolymer micelles were purified by dialysis overnight against 1L of water using cellulose dialysis membrane (Spectrapor, cut-off 3500).

In order to prepare fluorescent micelles, a mixed solution of Fluorescein-labeled and unlabeled copolymers (50/50) were used in the procedure described above.

In order to get dye loaded micelles, 2.5 mg of Nile Red were also added to the initial copolymer solution in DMF before following the same procedure of micellization and cross-linking.

The size distribution of the micelles was estimated by dynamic light scattering (DLS) using a particle-size analyser (Delsa Nano C, Particle Analyzer, Beckman Coulter) at 25 °C. The intensity of scattered light was detected at 165° of the incident beam. Aqueous micellar solution was filtered with a microfilter having an average pore size of 0.2 μm. An average size distribution of aqueous micellar solution was determined based on the CONTIN method.

Cell culture

The human melanoma line MEL-5 was obtained from De Giovani (University of Liege, Belgium). MEL-5 cells were grown at 37°C under humidified air containing 5% CO_2 in Dulbecco modified Eagle medium (DMEM) high glucose with 5% vol of Foetal Bovine Serum (FBS), 1% vol GlutaMax, 1% vol HEPES, 1% vol of penicillin/streptomycin (10,000 units of penicillin (base) and 10,000 units of streptomycin (base)/ml using penicillin G (sodium salt) and streptomycin sulfate in 0.85% saline).

The murine melanoma line B16 was obtained from ATCC. B16 cells were grown at 37°C under humidifier air containing 5% of CO_2 in Minimum Essential Medium (MEM) Alpha medium with 10% vol FBS, 1 % vol GlutaMax, 1 % vol penicillin/streptomycin.

Micelle cytotoxicity

The cytotoxicity of the micelles was evaluated by determining the viability of B16 and MEL-5 cells after incubation with different concentrations of micelles (from 0.5 to 2 mg/mL) for 24 and 48h. The number of viable cells was determined by estimation of their dehydrogenase activity using the tetrazolium-based colorimetric method (MTT conversion

test). B16 and MEL-5 cells were seeded in 96-well plates at the density of 6000 viable cells per well and incubated 24 h to allow cell attachment. At the end of incubation period with micelles, cells were incubated with 10 µL of a MTT solution (5 mg/mL) for at least 1h at 37°C until crystal formation. After rinsing, two hundred microliters of DMSO were then added in order to dissolve the formazan crystals. The absorbance of the solubilized formazan crystals was measured spectrophotometrically at 580 nm. Cell viability was expressed as the ratio between the amount of formazan determined for cells treated with the different micelles and for control non-treated cells. The optical density values were measured using Powerwave X multiwell-scanning spectrophotometer.

Internalization studies by flow cytometry

Nile Red loaded cross-linked micelles were diluted in culture media (final concentrations: from 1 to 0.25 mg/mL) and were incubated with MEL-5 cells for 1 and 4h. After incubation, removal of attached micelles was accomplished by washing cells two times with culture medium and two times with phosphate buffered saline solution (PBS without Ca^{2+} and Mg^{2+}). Cells were then detached by trypsinization (trypsin in PBS). After centrifugation, the pellet was suspended in a 4% formaldehyde PBS solution. Analyses of the internalized micelles were then performed using a FACS Canto II flow cytometer.

Internalization studies by fluorescence microscopy

MEL-5 and B16 cells were seeded in a twelve-well plate with 2 mL of culture medium. After 48h, medium was replaced by Fluorescein-labeled micelles loaded with Nile Red at a concentration of 0.5 mg/mL. After 0.5 hours of incubation, removal of attached micelles was accomplished by washing the cells with culture medium and twice with PBS. Cells were then fixed and nuclei stained with 4% formaldehyde/Hoechst (10 µM) in PBS

solution for 15 min at 4°C in the dark. Finally after aspiration, 0.5 mL of formaldehyde solution in PBS were added. Analyses of nuclei and internalized micelles were performed using fluorescent microscope Olympus IX81.

Internalization studies by fluorescence spectrometry

Fluorescein-labeled cross-linked micelles loaded with Nile Red were diluted in culture media (final concentration: 0.5 mg/mL) and were incubated with MEL-5 cells for 0.5 h. After incubation, removal of attached micelles was accomplished by washing cells two times with culture medium and two times with phosphate buffered saline solution (PBS without Ca^{2+} and Mg^{2+}). Cells were then detached by trypsinization (trypsin in PBS). After centrifugation the pellet was suspended in PBS. Analyses of the internalized micelles were then performed using a fluorescence spectrometer Perkin Elmer VICTOR^3 1420.

Statistical analyses

Cell culture experiments were performed in triplicates. Results are presented as mean ± standard deviation. Statistical analyses of the data were performed using the unpaired, two-tailed, Student's *t*-test. Statistical significance was determined at a $p < 0.01$.

Redox-dependent release of Nile Red from cross-linked micelles

Fluorescent Nile Red was used as an hydrophobic model molecule. For the determination of redox-dependent release profile of the cross-linked micelles, 5 ml of Nile red loaded micelles (1 mg/mL) were transferred into dialysis membranes (Spectrapor, cut-off 3500) which were then introduced into 1000 mL of phosphate buffer and incubated at 37°C in the dark. At predetermined time intervals, 100 µL of micelles were removed from the dialysis

membrane for measurement. The amount of dye remaining in the micelles was determined by fluorescence spectroscopy (Perkin Elmer VICTOR^3 1420).

In order to study the redox-release of Nile Red from the cross-linked micelles, DTT was added to the phosphate buffer to reach a concentration of 10 mM.

3. Results and discussion

Copolymer synthesis and core cross-linked micelle formation

In order to insure the stability of the PEO_{114}-*b*-PCL_{17} spherical micelles deeply studied and well-suited for drug delivery systems [22-24], the cross-linking of the PCL core was targeted by introducing some reactive azide groups along the hydrophobic segment, while keeping unchanged the hydrophilic/lipophilic balance. By the living ring-opening copolymerization of ε-caprolactone and α-choro-ε-caprolactone from a PEO macroinitiator, followed by the substitution of chloro atoms by azide groups, three kinds of amphiphilic copolymers were obtained (Scheme 1) and used to build up core cross-linked micelles. The core cross-linking of these micelles was achieved by copper mediated alkyne-azide cycloaddition (CuAAC) of a bis-alkyne cross-linker with the pendant azide functions during the micellization process. Depending on the localization of azide functions in the hydrophobic block, the cross-linking is expected to occur (i) loosely and randomly within the hydrophobic core for copolymer **1** (Scheme 2-1), (ii) more tightly and as a shell surrounding the core of a core–shell–corona system for copolymer **3** (the shell and the core being both hydrophobic and the corona hydrophilic) (Scheme 2-(3)) and (iii) very densely in the heart of the core for copolymer **2** (Scheme 2-(2)). The copolymer synthesis and cross-linking were previously reported in details [20-21]. The Table 1 summarizes the main characteristics of the copolymers used in the present study together with the size and size distribution of their corresponding cross-linked

micelles by bis(alkyne-ethyl ester ethyl) disulfide, the bis-alkyne cross-linker, that includes a disulfide bridge in order to provide redox reversible cross-linking. A quantitative cross-linking was obtained for the three different copolymers, leading to micelles of similar sizes for copolymers **1** and **3** with a diameter of about 37 nm while cross-linked micelles of copolymer **2** are slightly bigger with a size of 43 nm. Moreover, these last micelles were not as well defined as micelles of copolymers **1** and **3**. The inner localization of the cross-linkers with copolymer **2** might thus affect more the initial micellar structure than with the two other copolymers. After purification by dialysis, these cross-linked spherical micelles were then used for the following *in vitro* studies.

Table 1. Main characteristics of the copolymers used in this study and of the corresponding cross-linked micelles.

Copolymer architecture	$M_{n,\ total}$ (g/mol) [a]	M_w/M_n [b]	Micellization	
			D_h (nm) [c]	PDI [d]
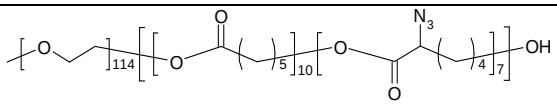 **PEO_{114}-*b*-poly(CL_{10}-*co*-αN_3εCL_7) (1)**	7100	1.08	37	0.07
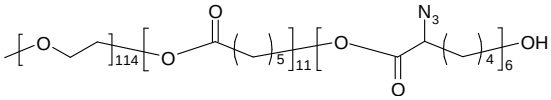 **PEO_{114}-*b*-PCL_{11}-*b*-poly(αN_3ε$CL)_6$ (2)**	7200	1.08	43	0.16
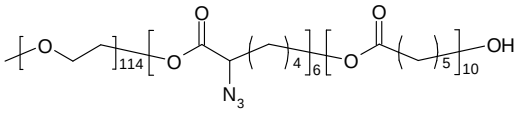 **PEO_{114}-*b*-poly(αN_3ε$CL)_6$-*b*-PCL_{10} (3)**	6900	1.08	36	0.11

[a] Experimental molar mass determined by ^{1}H NMR
[b] Polydispersity index measured in THF by Size Exclusion Chromatography (polystyrene calibration)
[c] Apparent hydrodynamic mean diameter of the micelles determined by DLS in water
[d] Polydispersity index measured by DLS

Cytotoxicity

To evaluate the *in vitro* cytotoxicity of the cross-linked micelles, MTT test was performed using B16 and MEL-5 melanoma cells. Figures 1a and b show the cell viability of

B16 cells treated with 0.5 to 2 mg/mL of the three kinds of micelles after 24 and 48 hours, and respectively, the same analyses on Figures 2a and b for MEL-5 cells. All these micelles showed similar *in vitro* cytotoxicity. A concentration for the micelles of 1 mg/mL leads to a percentage of survival of 40% to 60% after 24 hours while the ideal concentration of 0.5 mg/mL leads to very high level of survival of 80% to 100%. After 48 hours, the percentage of survival falls to about 30% for the concentration of 1 mg/mL while a diminution of cell viability (60-80%) was recorded for the concentration of 0.5 mg/mL. These cytotoxicity results are comparable to other polymer micelles of similar size benefiting of a PEO corona [25]. In accordance to literature data [26], the core cross-linked micelles benefit from a still flexible corona of poly(ethylene oxide) which keeps low their cytotoxicity [27]. From these first data, no cytotoxity really results from the core cross-linking process whatever the considered micellar system and for both kinds of studied cells lines.

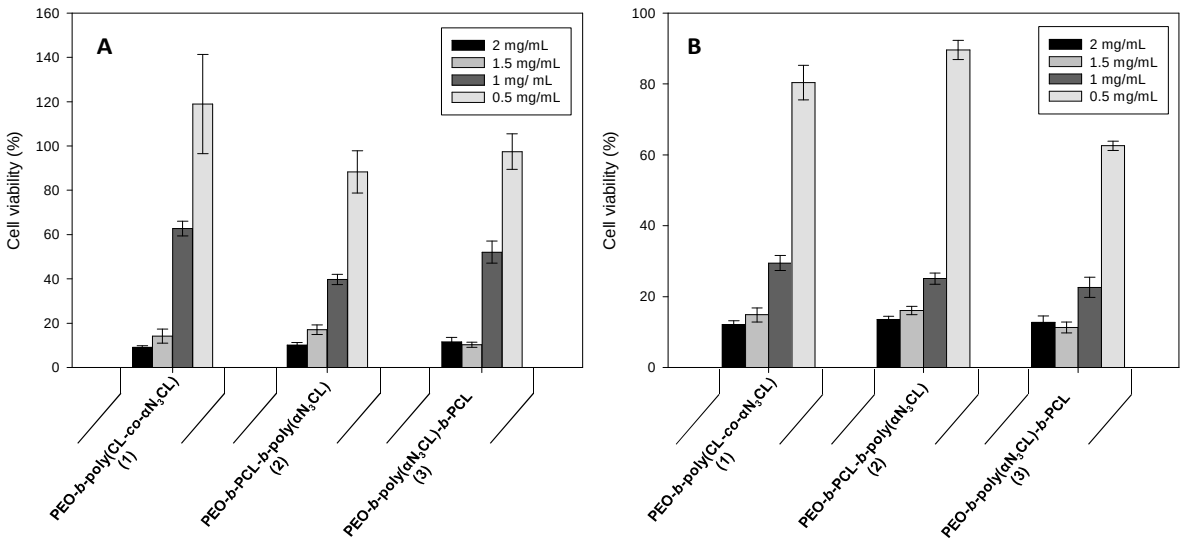

Figure 1. Cell viability in the presence of cross-linked micelles of copolymers **1**, **2** and **3** in B16 cell culture after (**a**) 24 and (**b**) 48 hours of incubation.

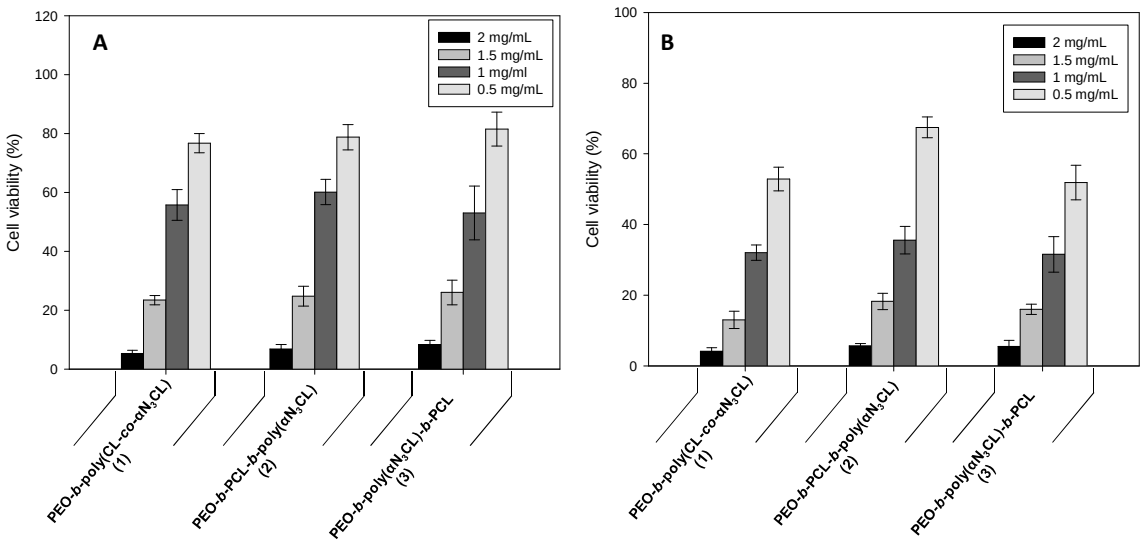

Figure 2. Cell viability in the presence of cross-linked micelles of copolymers **1**, **2** and **3** in MEL-5 cell culture after (**a**) 24 and (**b**) 48 hours of incubation.

Cytotoxicity of the cross-linked micelles was compared to the same micelles before cross-linking, i.e. on the azide bearing copolymers by using MEL-5 cells. The Figures 3a and b show the ratio of survival in function of the concentration. At lower concentrations (0.5 and 1 mg/mL), non cross-linked micelles exhibited a lower cytotoxicity than cross-linked ones after 24 hours of incubation. However, at higher concentration (1.5 mg/mL), no survival cells were observed for the non cross-linked micelles while about 20% were still observed for the corresponding cross-linked micelles. A similar tendency is observed after 48h of incubation, with a general increased cytotoxicity. As a rule, the non cross-linked micelles cytotoxicity increases much sharply with the concentration and with the incubation time than the cross-linked systems. Thus, it is difficult to make correlation between the azide functions or their substitution by disulfide bridges, when micelles are cross-linked, on MEL-5 cell viability. Nevertheless, the better stability of the cross-linked micelles versus the dilution may cause the difference of behavior at the lower concentrations after 24 hours of incubation. Indeed, under

these conditions, a larger proportion of unimers may be present for the non cross-linked micelles, compared to the cross-linked micelles, causing less toxic effects.

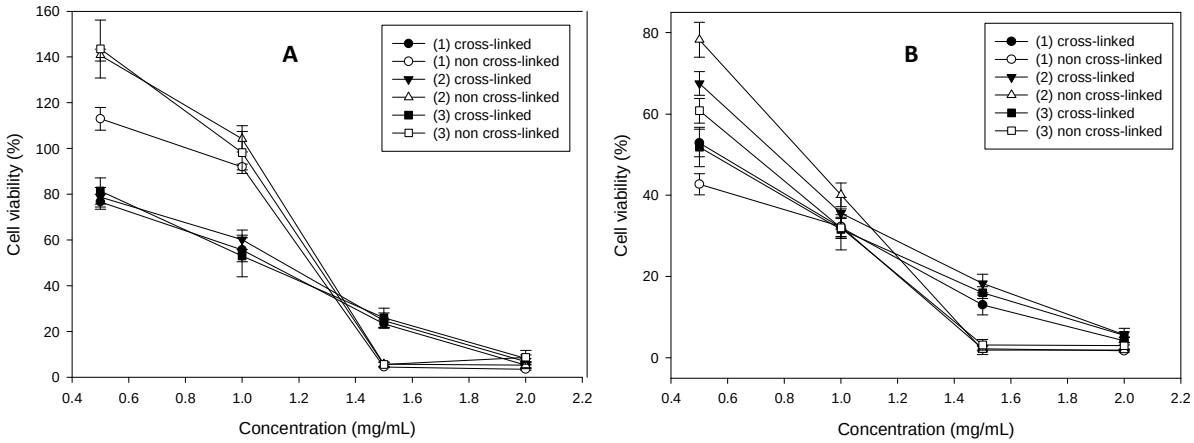

Figure 3. Cell viability in function of the concentration of cross-linked and non cross-linked micelles in MEL-5 cell culture after (**A**) 24 and (**B**) 48 hours of incubation.

Micelle uptake

The *in vitro* micelle uptake was evaluated on B16 and MEL-5 cells after different concentrations and incubation times. Firstly, in order to quantify by flow cytometry the cell uptake, the cross-linked micelles have been loaded before cross-linking with Nile Red, a fluorescent dye mimicking a poorly water-soluble drug, easily detected by the FACS.

Flow cytometry study was performed after 1 and 4 hours of incubation of Nile-Red loaded micelles at concentration of 1 mg/mL and 0.5 mg/mL on MEL-5 cells in order to quantify the uptake. Data obtained after 1 hour of incubation for the lower concentration of 0.5 mg/mL already confirmed the rapid internalization of the dye loaded micelles despite the absence of targeting moieties at the surface of the micelles. Indeed, 100 % of cells were positive to the Nile Red according to flow cytometry data whatever the type of cross-linked micelles used. The same results were obtained for a lower concentration of 0.25 mg/mL and for a reduced incubation time of 0.5 hours (Figure 4).

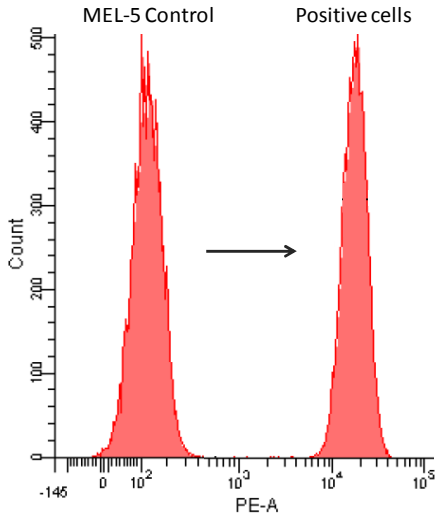

Figure 4. Cellular uptake of Nile Red loaded micelles of copolymer **1** analyzed by flow cytometry after 0.5 hours of incubation at a concentration of 0.25 mg/mL (Positive cells) compared to non-treated cells (MEL-5 control)

Nevertheless, if the flow cytometry allows a quantitative determination of the fluorescent cells, it does not clearly discern whether the dye is still in the micelles or not and if it is externally adsorbed at the cell surface or actually internalized. In order to clarify the situation, some Fluorescein-labeled copolymers were used to form the micelles loaded with Nile Red and cross-linked. Thus, having one encapsulated red dye and one green dye covalently attached to the copolymer micelles would afford information of the localization of both the micelles and the encapsulated dye, independently. Fluorescein-labeled cross-linked micelles loaded with Nile Red were thus incubated with B16 and MEL-5 cells at a concentration of 0.5 mg/mL for periods of time of 0.5 hours. Then, the cell nuclei were stained with Hoechst dye after fixation. Fluorescence microscopy observations of the fixed cells clearly show the successful internalization of the cross-linked micelles after short incubation times (Figures 5 and 6). The red image is the signature of Nile Red, while the green image is the one of the micelles labeled by the Fluorescein. The blue image shows the

cells nuclei. The Figure 5 compares the internalization of the three different kinds of copolymer micelles into B16 cells. Uniform distribution of the Nile Red was observed into the cytoplasm of the cells but not inside the nuclei. This was also observed for the green micelles except that the nuclei of the cells were also marked by the Fluorescein especially with the copolymer **3** where dense structures (nucleoli) in the nuclei are visible (Figure 5, **3-C**). Micelles of copolymer **2** lead to a high green and red fluorescence homogeneous in the cytoplasm and strong ring around nuclei. The presence of the Fluorescein in the cells allows confirming the internalization of the Nile Red loaded micelles and not only of free Nile Red previously released from the micelles. The fluorescence intensity of the Fluorescein needed to be increased comparing to the Hoechst and Nile red contributions in the Figures 5 and 6, due to the low content of Fluorescein on the polymer chains and the low concentration in the micelles.

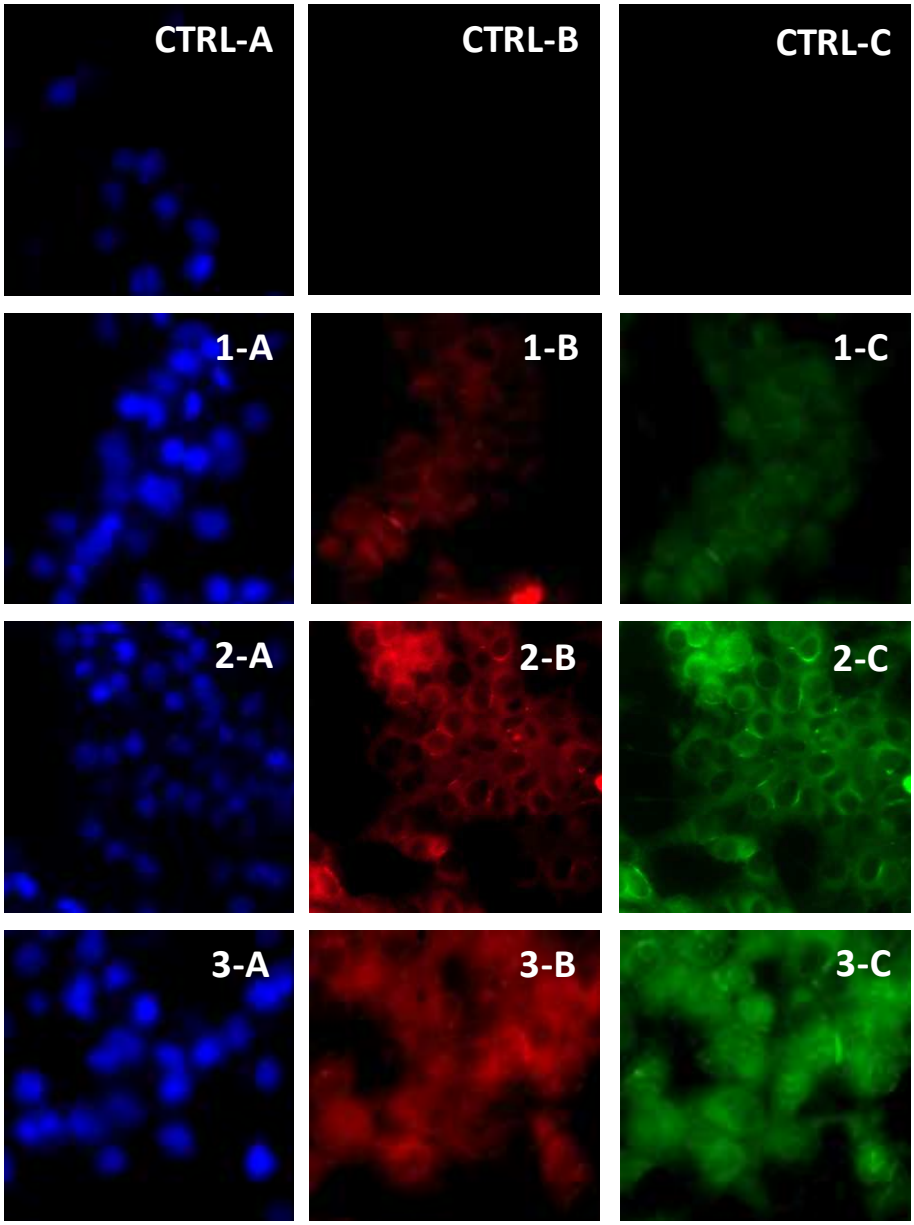

Figure 5. Fluorescence microscopy images of B16 cells incubated 0.5 hours with cross-linked micelles of copolymers **1**, **2** and **3** at a concentration of 0.5 mg/mL. Hoechst staining (**A**: blue filter, **B**: red filter and **C**: green filter) and the control (CTRL) cells incubated without micelles.

The same experiments performed on MEL-5 cells with the three kinds of core cross-linked micelles have led to similar conclusions. Results obtained with the cross-linked micelles of copolymer **3** on MEL-5 cell are illustrated in Figure 6 and allowed to highlight the difference of localization of the Nile Red dye and the Fluorescein-labeled copolymer. Indeed, the Nile Red is only localized in the cytoplasm of the cell (Figure 6, **3-A**) while Fluorescein is

also localized in the nuclei (Figure 6, **3-B**). That difference is mainly underlined on Figure 6, **3-D**, where the green and red filters are combined and compared to Figure 6, **3-C**. The substitution of the blue coloration by the green one confirms the presence of the copolymer in the cell nucleus. One possible explanation for this observation is that after the uptake of the loaded micelles by the cells, the reductive environment of the cytoplasm allows the reduction of the disulfide bridges which cross-linked the micelle core. As a consequence, the encapsulated Nile Red dye is released by destabilization of the micelles and freely diffuses in the cytoplasm. This hypothesis is supported by the uniform distribution of the Nile Red in the cytoplasm and the localization of the green copolymer in the nucleus independently of the Nile Red, which tend to confirm the micelles dissociation. The phenomenon appears mainly with micelles of copolymer **3**, i.e. with the most superficial cross-linking and thus probably the most sensitive to the reductive environment needed for the rupture of the disulfide cross-links.

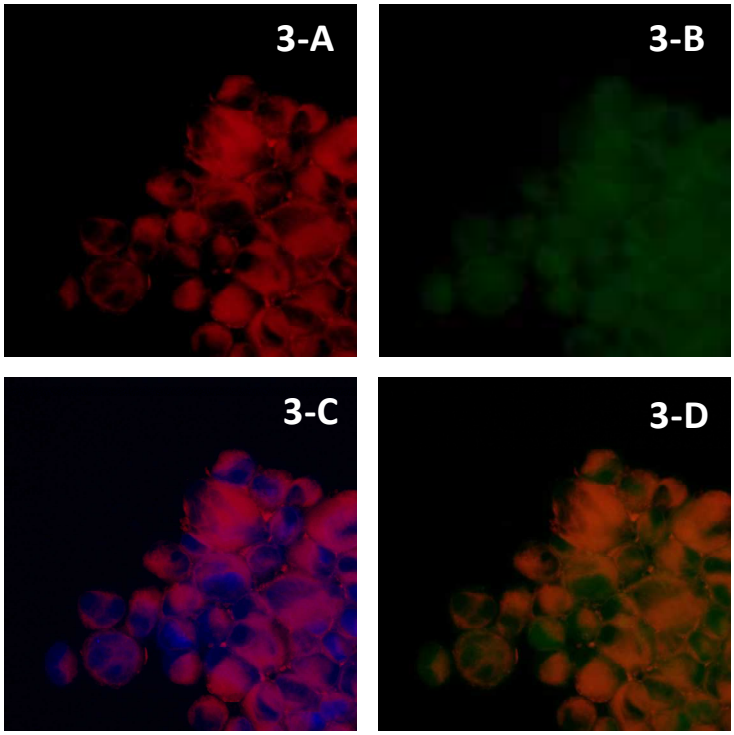

Figure 6. Fluorescence microscopy images of MEL-5 cells incubated 0.5 hours with Nile Red loaded cross-linked green micelles of copolymer **3** at a concentration of 0.5 mg/mL after Hoechst staining (**A**: red filter, **B**: green filter, **C**: blue and red filter and **D**: red and green filter).

Finally, the micelles uptake by MEL-5 cells was quantified by fluorescence spectrometry. The percentage of internalization was calculated from the fluorescence intensity of the cells after incubation in presence of Fluorescein-labeled cross-linked micelles loaded with Nile Red. Micelle uptake typical for micelles exhibiting a PEO shell at their external periphery [28] has been measured for the three systems, as reported in Figure 7 that shows the percentage of internalization after 0.5 hours of incubation at a concentration of 0.5 mg/mL. Similar values were obtained for the three kinds of copolymer micelles. This shows that they have all similar propensities to enter the cells, which is not surprising since they are all exhibiting the same PEO shell at their external periphery. Interestingly enough, different behaviors have been observed when the same experiment is performed on the Nile Red quantification. In that case, a significantly higher Nile Red internalization is measured on the

micelles of copolymer **2**, i.e. cross-linked at the heart of the hydrophobic core. That observation could be explained by the less efficient encapsulation of Nile Red in these micelles that are the most internally cross-linked and thus less efficiently preventing the red dye to diffuse out of the micelle core and hence leading to some release of the Nile Red before the micelle internalization. This free Nile Red internalized independently of the micelles would explain the higher red dye content as compared to the green micelles. Micelle internalization was also investigated after 1 hour of incubation and with a higher micelle concentration of 1 mg/mL. Increasing the incubation time keeps constant the percentage of internalization while increasing of the micellar concentration even decreases the percentage of internalization because similar amount of micelles are internalized for a higher concentration at the same incubation time. Internalization appears thus kinetically limited by the PEO external shell which would be improved by decorating with a specific ligand [29] or with positive charges [30].

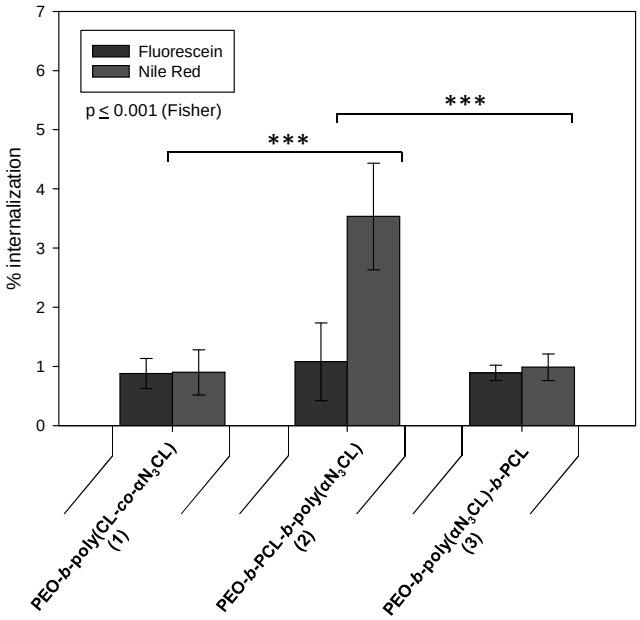

Figure 7. Micelle uptake by MEL-5 cells at a concentration of 0.5 mg/mL determined by fluorescent spectroscopy after 0.5 hours of incubation.

Redox-dependent release of Nile Red from cross-linked micelles

Redox-dependent release profile of the core cross-linked micelles was investigated using Nile Red as fluorescent probe, mimicking an hydrophobic drug. The Nile Red was encapsulated in the micelles by incubation with the micelles in DMF before the cross-linking step. The Nile Red loaded and cross-linked micelles were incubated in phosphate buffer at two different concentrations and in presence or not of dithiothreitol (DTT), a reducing agent for the disulfide bridges. The release of the dye was quantified vs. time by fluorescence spectrometry. Results are shown in Figures 8 and 9.

The Figure 8a compares the Nile Red release profiles of the three cross-linked micellar systems at high concentration (1mg/mL) against PBS buffer. At first look, the release profiles were quite similar for the three kinds of cross-linked micelle systems. A faster release of the Nile Red is however observed for the micelles of cross-linked copolymer **2** as compared to the two other systems. In line with the above explanation given for the Nile Red uptake, we can again conclude that for this inner cross-linked micellar system, the network when localized at the center of the micelles core does not efficiently entrap the dye which might diffuse out of the hydrophobic core, leading to faster release. Similar profiles with limited release of the dye is observed for the two other cross-linked systems showing that the cross-linking appears in these cases as an efficient barrier preventing diffusion and release of more than 75% of the dye. Figure 8b shows the same experiment performed at lower concentration (0.35mg/mL), i.e. a concentration that would lead to micelles destabilization if they would not be cross-linked by the disulfide bridges (the CMC of non cross-linked micelles is ~0.35 mg/mL). In these conditions, even if the release appears slightly faster than at higher concentration, it remains diffusion limited and below 50% after 1000 min. This clearly evidences the strong effect of the cross-linking on the release profile whatever the micellar systems. At very low

concentration, cross-linking keeps the compartimentalization of the systems which allows the capture of the dye by hydrophobic interactions with the micelle core avoiding Burst effect.

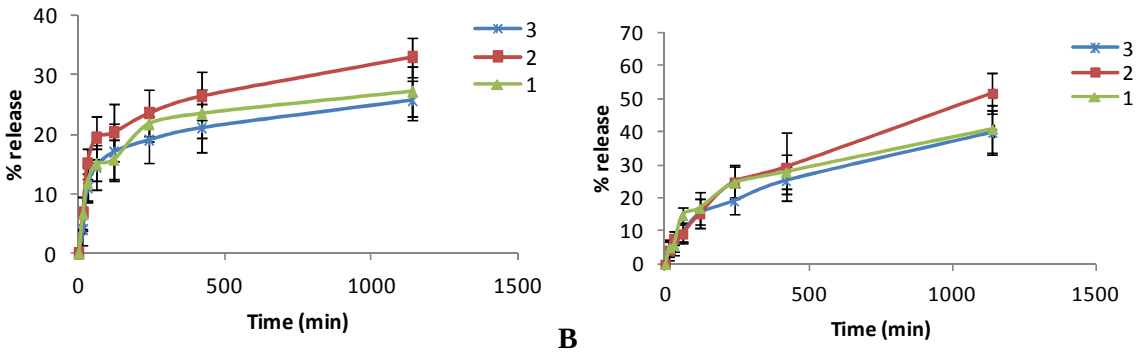

Figure 8. Nile Red release from cross-linked micelles of copolymers **1** (◆), **2** (■) and **3** (▲**)** at a concentration of 1 mg/mL (**A**) and 0.35 mg/mL (**B**) against PBS buffer.

Finally, the dye release profile studied against PBS was compared to the same experiment performed against PBS containing DTT as reducing agent (Figure 9). For all the three studied systems, the presence of DTT clearly triggers the Nile Red release in case of diluted solutions (0.35 mg/mL). A very fast release was observed that reached about 80% after 19 hours. In the reductive DTT environment, the reduction of the disulfide bridges is breaking the cross-links allowing the destabilization the micelles below the CMC and causing a rapid delivery of the Nile Red. It is noteworthy that the release profiles in reductive environment but at a concentration above the CMC (1 mg/mL) are similar for all the three systems and typical for a diffusion limited release from non cross-linked micelles.

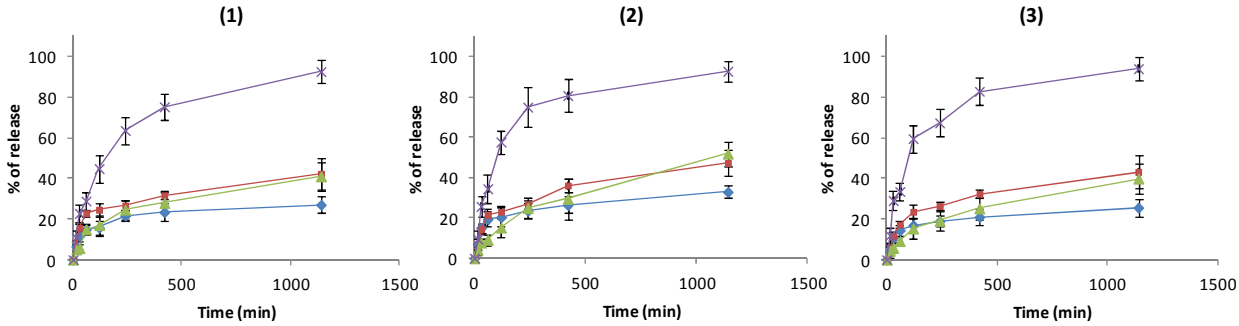

Figure 9. Nile Red release from cross-linked micelles of copolymers **1**, **2** and **3** at a concentration of 1 mg/mL against PBS (—◆—) and against PBS/10 mM DTT (—■—) and at lower concentration of 0.35 mg/mL against PBS (—▲—**)** and against PBS/10 mM DTT (—✳—**)**.

Figure 10 shows an overlay of the release profile in reduced environment of diluted micelles evidencing a quicker release of the dye from micelles of copolymer **3** as compared to copolymer **1**. This is in line with the conclusion of a faster micelle destabilisation observed for micelles of copolymer **3** after 30 min. of incubation in internalization experiments. The more external cross-linking location might be the reason why cleavage of the disulfide bridges is faster for these micelles made of copolymer **3**.

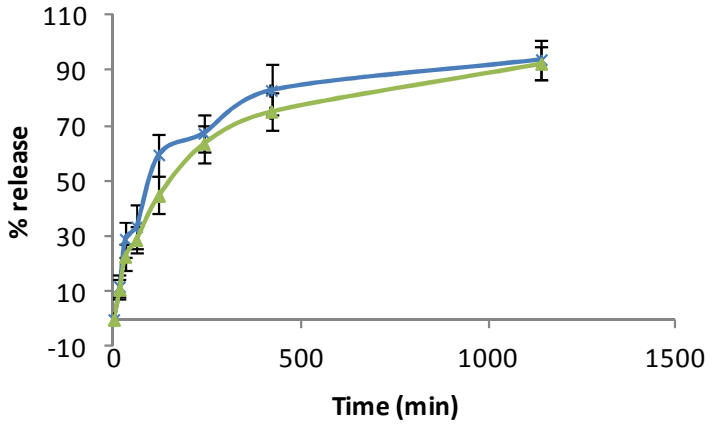

Figure 10. Nile Red release from cross-linked micelles of copolymers **1** (—▲—) and **3** (—◆—) at a concentration of 0.35 mg/mL against PBS/10 mM DTT.

In summary, these experiments evidenced that a fast drug release could be expected in the cell cytoplasm which is a more reductive environment than extracellular media. Moreover, it was demonstrated that micelle cross-linking not only insures high micelles stability in diluted environment but also offers an efficient barrier towards dye diffusion particularly in case of cross-linked micelles of copolymers **1** and **3**. These two systems appear thus quite relevant for the development of adaptative drug delivery systems. Particularly the system of copolymer **3** allows the rapid trigger of the drug release by fast disulfide cleavage in reductive environment thanks to the most external localization of the cross-links.

4. Conclusions

In this study, the potential of novel reversibly core cross-linked micelles to act as smart drug delivery systems has been demonstrated. Three kinds of cross-linked micelles differing by the cross-linking localization have been developed and compared. All the three systems exhibit *in vitro* low cytotoxicity and are able to be internalized without the presence of a targeting moiety. Thus, after their intravenous administration, these new nanocarriers would be able to be internalized in solid tumors by EPR effect. Moreover, the presence of the disulfide bridges insures the micelle stabilization in the bloodstream and limits the release of the encapsulated dye even at very low concentration, particularly in case of copolymers **1** and **3**. After their internalization, the reduction of these bridges triggers the release of the dye most rapidly in case of copolymer **3** that exhibits the cross-links at the most external periphery of the hydrophobic core. Based on these data, cross-linked micelles of the PEO_{114}-*b*-poly($\alpha N_3 \varepsilon CL)_6$-*b*-$PCL_{10}$ appear to us as the most promising candidate for drug delivery applications.

5. References

1. Van Butsele, K.; Jerome, R.; Jerome, C. *Polymer* **2007**, *48*, 7431.
2. Kwon, G. S.; Okano, T. *Advanced Drug Delivery Reviews* **1996**, *21*, 107.
3. Kataoka, K.; Harada, A.; Nagasaki, Y. *Advanced Drug Delivery Reviews* **2001**, *47*, 113.
4. Gabizon, A. A. *Advanced Drug Delivery Reviews* **1995**, *16*, 285.
5. Iyer, A. K.; Khaled, G.; Fang, J.; Maeda, H. *Drug Discovery Today* **2006**, *11*, 812.
6. Maeda, H.; Wu, J.; Sawa, Y.; Matsumura, Y.; Hori, K. *Journal of Controlled Release* **2000**, *65*, 271.
7. Owens, D. E.; Peppas, N. A. *International Journal of Pharmaceutics* **2006**, *307*, 93.
8. Belting, M.; Sandgren, S.; Wittrup, A. *Advanced drug delivery reviews* **2005**, *57*, 505.
9. Lee, J. H.; Lee, H. B.; Andrade, J. D. *Progress in Polymer Science* **1995**, *20*, 1043.
10. Vermette, P.; Meagher, L. *Colloids Surf., B* **2003**, *28*, 153.
11. Jaracz, S.; Chen, J.; Kuznetsova, L. V.; Ojima, I. *Bioorganic & Medicinal Chemistry* **2005**, *13*, 5043.
12. Allen, T. M.; Brandeis, E.; Hansen, C. B.; Kao, G. Y.; Zalipsky, S. *Biochimica et Biophysica Acta, Biomembranes* **1995**, *1237*, 99.
13. Torchilin, V. P. *European Journal of Pharmaceutics and Biopharmaceutics* **2008**.
14. Van Butsele, K.; Morille, M.; Passirani, C.; Legras, P.; Benoit, J. P.; Varshney, S. K.; Jerome, R.; Jerome, C. *Acta Biomaterialia* **2011**, *7*, 3700.
15. Bronich, T. K.; Keifer, P. A.; Shlyakhtenko, L. S.; Kabanov, A. V. *Journal of the American Chemical Society* **2005**, *127*, 8236.
16. Hu, X.; Chen, X.; Wei, J.; Liu, S.; Jing, X. *Macromolecular Bioscience* **2009**, *9*, 456.
17. Sandholzer, M.; Bichler, S.; Stelzer, F.; Slugovc, C. *Journal of Polymer Science, Part A: Polymer Chemistry* **2008**, *46*, 2402.
18. Meister, A.; Anderson, M. E. *Annual Review of Biochemistry* **1983**, *52*, 711.
19. Wang, Y.; Chen, P.; Shen, J. *Biomaterials* **2006**, *27*, 5292.

20. Cajot, S.; Lecomte, P.; Jérôme, C.; Riva, R. *in submission* **2012**.

21. Cajot, S.; Lautram, N.; Passirani, C.; Jerome, C. *Journal of Controlled Release* **2011**, *152*, 30.

22. Vangeyte, P.; Gautier, S.; Jerome, R. *Colloids and Surfaces, A: Physicochemical and Engineering Aspects* **2004**, *242*, 203.

23. Rieger, J.; Passirani, C.; Benoit, J.-P.; Van Butsele, K.; Jerome, R.; Jerome, C. *Advanced Functional Materials* **2006**, *16*, 1506.

24. Allen, C.; Yu, Y.; Maysinger, D.; Eisenberg, A. *Bioconjugate Chemistry* **1998**, *9*, 564.

25. Lin, W.-J.; Chen, Y.-C.; Lin, C.-C.; Chen, C.-F.; Chen, J.-W. *Journal of Biomedical Materials Research, Part B: Applied Biomaterials* **2006**, *77B*, 188.

26. Kunath, K.; von Harpe, A.; Petersen, H.; Fischer, D.; Voigt, K.; Kissel, T.; Bickel, U. *Pharmaceutical Research* **2002**, *19*, 810.

27. Fischer, D.; Li, Y.; Ahlemeyer, B.; Krieglstein, J.; Kissel, T. *Biomaterials* **2003**, *24*, 1121.

28. Allen, C.; Yu, Y.; Einsenberg, A.; Maysinger, D. *Biochimica et Biophysica Acta - Biomembranes* **1999**, *1421*, 32.

29. Sawant, R. M.; Hurley, J. P.; Salmaso, S.; Kale, A.; Tolcheva, E.; Levchenko, T. S.; Torchilin, V. P. *Bioconjugate Chemistry* **2006**, *17*, 943.

30. Gu, J.; Cheng, W.-P.; Liu, J.; Lo, S.-Y.; Smith, D.; Qu, X.; Yang, Z. *Biomacromolecules* **2008**, *9*, 255.

CHAPTER VII

Pegylated disulfide core cross-linked micelles based on poly(trimethylene carbonate) and functional poly(ε-caprolactone)

S. Cajot, N. Lautram, C. Passirani, M.-C. Gillet De Pauw, C. Jérôme

Acta Biomaterialia, **2012**, submitted

Abstract

In order to design smart drug delivery systems, three reactive block copolymers composed of an hydrophilic poly(ethylene oxide) block (PEO) and an hydrophobic segment based on trimethylene carbonate (TMC) and α-azido-ε-caprolactone (αN_3CL) copolymers have been investigated. The reactive azide groups variously distributed along the hydrophobic block depending on the simultaneous or sequential copolymerization of the two hydrophobic comonomers were then used to cross-link the micelle core of these copolymers by reaction with a bis-alkyne derivative. To insure the micelles stability in oxidative conditions, as in the bloodstream, but their dissociation in the intracellular compartment, a bis-alkyne cross-linker containing a disulfide bridge was purposely selected. The stability of the core cross-linked micelles was investigated in function of the copolymer concentration and the redox properties of their environment. The potential of these responsive micelles to be used as nanocarriers was studied in terms of stealthiness, cytotoxicity and cellular internalization.

1. Introduction

Particularly in case of tumors treatment, targeted delivery systems are highly desirable. The design of drug delivery systems able to adapt toward an evolutive environment [1-2] is therefore the topic of active recent researches [3-5]. In this framework, there is still a need for systems able to trigger the drug release intracellularly. Indeed, the therapeutic efficiency of many anticancer drugs takes place only when they are released in the cytoplasm or in the cells nuclei.

If long circulating nanocarriers can be obtained by decorating it with a poly(ethylene oxide) brush [6], their accumulation in the tumor might be achieved by Enhance Permeation and Retention (EPR) Effect characterized by a low bloodstream flow and a discontinuous epithelium [7-8]. This process is designated as passive targeting while active targeting needs the additional anchoring of specific ligands at the surface of the nanocarrier to allow their cell surface binding by recognition of specific receptors inducing then the internalization process [9-10].

Recent advances in the field of the polymer engineering have contributed to development of smart systems able to respond to environment variations [11-13]. Interestingly, pH-sensitive nanocarriers have been developed to target tumor cells by regulating the exposure of a ligand depending on the pH, which is known to be lower in the tumor surrounding as compared to normal tissues [14-15]. As a specific importance is addressed to the intracellular release of the nanocarrier content, advantage can be taken from the typically low pH values of the endosomal and lysosome compartments to trigger the carrier dissociation and consequently the release of its content [16].

Similarly, attention is paid to the development of redox-sensitive nanocarriers which may insure the drug release in the cytoplasm where the concentration of glutathione (10 mM) is higher, i.e. providing a more reductive environment (Scheme 1) [17-18] as compared to the extracellular compartment where the glutathione concentration falls to 10 µM. Indeed, this

tripeptide regulates the anti-oxidative capacity of the cells via the glutathione-thiol/glutathione-disulfide redox couple [19-20]. Thus, the dissociation of cross-linked nanocarriers via disulfide bridges is expected to specifically occur in the cytosol and to lead to the intracellular drug release.

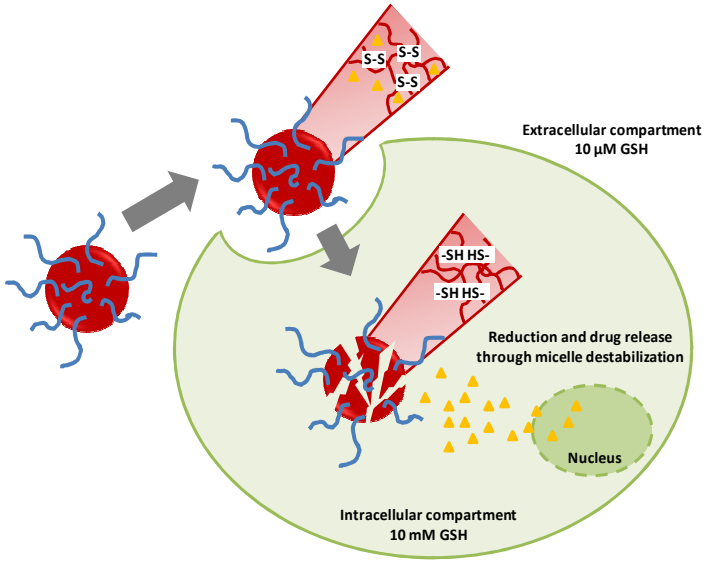

Scheme 1. Illustration of the intracellular drug release of disulfide core cross-linked nanocarriers

Amphiphilic block copolymers of poly(ethylene oxide) (PEO) and poly(ε-caprolactone) (PCL) are largely described in the literature due to their ability to be self-assembled in aqueous media and be used for the solubilization and the controlled release of hydrophobic drugs [21]. The cross-linking of that kind of micelles has been already described in the literature based on copolymers of an azido functional ε-caprolactone and ε-caprolactone [22].Their micellization, their reversible cross-linking and their *in vitro* properties were fully described [22-23]. More recently, biodegradable polycarbonates have been studied in order to reduce the crystalinity of the polyester by their copolymerization [24-25]. Thus, the synthesis of amphiphilic block copolymers based on a hydrophilic block of PEO and a hydrophobic block of poly(trimethylene carbonate) (PTMC) and azido functional poly(ε-caprolactone) lead to the formation of new cross-linked micelles whose crystalinity and degradability may favorably impact the behavior of the resulting micelles as compared to the better known poly(ε-caprolactone) based drug delivery systems.

The present work aims at reporting on reversibly core cross-linked micelles based on three novel reactive block copolymers: PEO-*b*-poly(TMC-*co*-αN_3CL) (**1**), PEO-*b*-PTMC-*b*-poly(αN_3CL) (**2**) and PEO-*b*-poly(αN_3CL)-*b*-PTMC (**3**) [26] (Scheme 2). The PEO hydrophilic block of these copolymers have been selected in order to insure stealthiness of their micelles. The hydrophobic segment bearing azide groups allows the hydrophobic core to be cross-linked by copper mediated azide-alkyne cycloaddition (CuAAC) with a bis-alkyne cross-linker. The cross-linking reversibility is insured by a disulfide bridge included within the cross-linker. Depending on the copolymer architecture, the cross-linking is expected to occur at different locations of the micellar core. The objective of this research is to evaluate the *in vitro* cytotoxicity and internalization properties of the cross-linked micelles in function of the architecture of the block copolymers having a comparable composition.

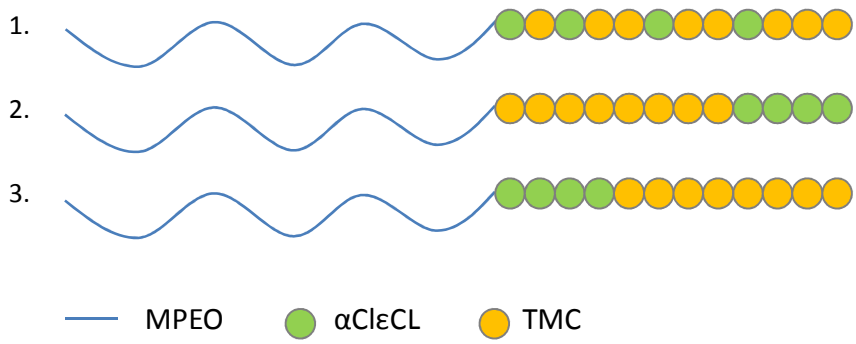

Scheme 2. Schematic architectures of the amphiphilic copolymers used to build the cross-linked micelles (**1**) PEO-*b*-poly(TMC-*co*-αN_3CL), (**2**) PEO-*b*-PTMC-*b*-poly(αN_3CL) and (**3**) PEO-*b*-poly(αN_3CL)-*b*-PTMC

2. Materials and methods

Materials

5-(and 6-)carboxyFluorescein succinimidyl ester (NHS-Fluorescein) was purchased from Thermo Scientific. 1,4-dithiothreitol (DTT) and Nile Red from Sigma Aldrich as ethylenediaminetetraacetic (EDTA) prepared in a solution of 0.5M, pH 7.

Dimethylformamide (DMF) was dried on molecular sieves. Deionized water was obtained from a Milli-Q plus system (Millipore). All other chemicals were used as received.

Copolymer synthesis

The synthesis of the PEO-*b*-poly(TMC-*co*-αN_3CL), PEO-*b*-PTMC-*b*-poly(αN_3CL) and PEO-*b*-poly(αN_3CL)-*b*-PTMC block copolymers was performed by ring opening polymerization (ROP), following an already reported procedure detailed elsewhere [26]. Briefly, the ring-opening polymerization of trimethylene carbonate (TMC) and α-choro-ε-caprolactone (αClεCL) was initiated from a monomethoxy poly(ethylene oxide) (M_n= 5000 g/mol, Aldrich) macroinitiator in refluxing toluene for 24 hours in presence of a tin-based catalyst for the random segment of the diblock copolymer while a sequential monomer addition was required for the synthesis of the two other triblock architectures. The substitution of the chloride atoms by azide functions was achieved in presence of sodium azide in DMF for one night.

The molecular weight of the copolymers was calculated by ^{1}H-NMR spectroscopy while polydispersity index (M_w/M_n) was determined by size exclusion chromatography (SEC) analysis.

Copolymer labeling

0.1 g of PEO-*b*-poly(TMC-*co*-αN_3CL)-OH (M_n = 6500 g/mol, 1.5 10^{-5} mol) (or PEO-*b*-PTMC-*b*-poly(αN_3CL)-OH and PEO-*b*-poly(αN_3CL)-*b*-PTMC-OH) and 0.018 g NHS-Fluorescein (3.8 10^{-5} mol) were dissolved in 2 mL of anhydrous DMF and stirred for 48 hours at room temperature. The final product, PEO-*b*-poly(TMC-*co*-αN_3CL)-Fluorescein were dialyzed against 50/50 water/DMF until obtaining colorless dialysis medium and finally against water before recovery by lyophilization.

Micelle preparation and cross-linking

Micellization of the azido-functional copolymers was performed by co-solvent process. A 1% stock solution of the copolymer (**1**, **2** or **3**) was prepared in DMF in presence of the bis-alkyne-disulfide cross-linker, i.e. a bis(alkyne-ethyl ester ethyl) disulfide following described in the literature [27], (0.6 mol equiv. vs. azide groups). 20 mL of Milli-Q water were added to 5 mL of this organic solution under vigorous stirring for one day. $CuSO_4$ (0.25 mol equiv. vs. azide groups) and ascorbic acid sodium salt (0.25 mol equiv. vs. azide groups) were added to the mixture. The cross-linking reaction was allowed to proceed for one day at room temperature. Then, 2 mol equiv. vs. Cu of a solution of EDTA at pH 7 were added to the solution to complex the copper. Finally, the cross-linked copolymer micelles were purified by overnight dialysis against 1L of water using cellulose dialysis membrane (Spectrapor, cut-off 3500) [22].

The stability of cross-linked micelles was studied by comparing them to non cross-linked micelles. These were prepared in the same way except for the addition of the cross-linker, $CuSO_4$ and ascorbic acid sodium salt. The micelle size was then followed by DLS upon diluting below the critical micellar concentration (CMC) (~10^{-5} g/mL). In addition, the stability of the cross-linked micelles after 1 night of stirring at 37 °C in water in the presence of a reducing agent (10 mM of DTT) was similarly determined by comparing the DLS intensity at concentrations below and above the CMC. The sensitivity of the cross-linking towards DTT was also evaluated in DMF (a good solvent for both blocks) at high concentration (~0.15 mg/mL). Aqueous suspensions of cross-linked and non cross-linked micelles were diluted in DMF (10-fold) and stirred for one day at room temperature before determining the micelle size by DLS. Then, 10 mM of DTT were added, and the mixture was stirred for another night at 37 °C before DLS investigation.

In order to prepare fluorescent micelles, a mixed solution of Fluorescein-labeled and unlabeled copolymers (50/50) were used in the procedure described above.

In order to get dye loaded micelles, 2.5 mg of Nile Red were also added to the initial copolymer solution in DMF before following the same procedure of micellization and cross-linking.

Micelle characterization methods

The size distribution of the micelles was measured by dynamic light scattering (DLS) using a particle-size analyser (Delsa Nano C, Particle Analyzer, Beckman Coulter) at 25°C. The intensity of scattered light was detected at 165° to an incident beam. Aqueous micellar solution was filtered with a microfilter having an average pore size of 0.2 µm. The average size distribution of the aqueous micellar solutions was determined based on the CONTIN method.

Transmission Electron Microscopy (TEM) was performed with a Philips CM-100 microscope. Samples were prepared by spin-coating a drop of the micellar solutions on a copper grid previously coated with formvar.

Complement Activation test (CH50)

Complement activation was measured as the lytic capacity of a normal human serum (NHS) towards antibody-sensitized sheep erythrocytes after exposure to the micelles. Aliquots of NHS were incubated with increasing concentrations of micelles. The amount of serum causing 50% haemolysis after exposure to the micelles was determined ("CH50 units") for each sample. NHS was provided by the "Etablissement Français du Sang" (Angers, France) and stored as aliquots at – 80°C until use. Veronal-buffered saline containing 0.15 mM Ca^{2+} and 0.5 mM Mg^{2+} (VBS^{++}) was prepared as reported elsewhere [28]. Firstly, sheep erythrocytes were sensitized by rabbit anti-sheep erythrocytes antibodies (Sérum hémolytique, Biomérieux, Marcy-l'Etoile, France) and diluted by the veronal-buffered saline at a final concentration of 2.10^9 cells/mL in VBS^{++}. Increasing amounts of micelles were added to NHS diluted in VBS^{++} such that the final dilution of NHS in the mixture was 1/4 (v/v) in a final volume of 1 mL. After 1 h of incubation at 37°C under gentle agitation, the suspension was diluted 1/25

(v/v) in VBS^{++}, and aliquots of 8 different dilutions were added to a given volume of sensitized sheep erythrocytes. After 45 min of incubation at 37°C, the reaction mixture was slightly centrifuged at 2000 rpm for 10 min. The absorption of the supernatant was determined at 414 nm with a microplate reader (Multiskan Anscent, Labsystems SA, Cergy-Pontoise, France) and compared to the results obtained with control serum in order to evaluate the amount of haemolyzed erythrocytes. Positive and negative controls were made in each series of experiments in order to account for any difference in the hemoglobin response from a given erythrocyte preparation. Furthermore, corrections for particle light-scattering and spontaneous erythrocyte haemolysis were estimated by UV/VIS measurements using blanks containing only particles and only erythrocytes, respectively. In order to compare micelles of different average diameters, their surface area was calculated as follows: $S = 3\ m/r\rho$, where S is the surface area [cm^2], m the weight [µg] in 1 mL nanosuspension, r the average radius [cm] determined by DLS, and ρ the density [$\mu g/cm^3$] of the micelles estimated at 10^6 $\mu g/cm^3$ [29-31]. The experimental data are the average of three independent experiments with a 10% standard deviation.

Cell culture

The human melanoma line MEL-5 was obtained from De Giovani (University of Liege, Belgium). MEL-5 cells were grown at 37°C under humidified air containing 5% CO_2 in Dulbecco modified Eagle medium (DMEM) high glucose with 5% vol of Foetal Bovine Serum (FBS), 1% vol GlutaMax, 1% vol HEPES, 1% vol of penicillin/streptomycin (10,000 units of penicillin (base) and 10,000 units of streptomycin (base)/ml utilizing penicillin G (sodium salt) and streptomycin sulfate in 0.85% saline).

Micelle cytotoxicity

The cytotoxicity of the micelles was evaluated by determining the viability of MEL-5 cells after incubation with different concentrations of micelles (from 0.5 to 2 mg/mL) for 24 and 48h. The number of viable cells was determined by estimation of their dehydrogenase

activity using the tetrazolium-based colorimetric method (MTT conversion test). MEL-5 cells were seeded in 96-well plates at the density of 6000 viable cells per well and incubated 24 h to allow cell attachment. At the end of incubation period with micelles, cells were incubated with 10 µL of a MTT solution (5 mg/mL) for at least 1h at 37°C until crystal formation. After rinsing, two hundred microliters of DMSO were then added in order to dissolve the formazan crystals. The absorbance of the solubilized formazan crystals was measured spectrophotometrically at 580 nm. Cell viability was expressed as the ratio between the amount of formazan determined for cells treated with the different micelles and for control non-treated cells. The optical density values were measured using Powerwave X multiwell-scanning spectrophotometer.

Internalization studies by fluorescence microscopy

MEL-5 cells were seeded in a twelve-well plate with 2 mL of culture medium. After 48h, medium was replaced by Fluorescein-labeled micelles loaded with Nile Red at a concentration of 0.5 mg/mL. After 0.5 hours of incubation, removal of attached micelles was accomplished by washing the cells with culture medium and twice with PBS. Cells were then fixed and nuclei stained with 4% formaldehyde/Hoechst (10 µM) in PBS solution for 15 min at 4°C in the dark. Finally after aspiration, 0.5 mL of formaldehyde solution in PBS was added. Analyses of nuclei and internalized micelles were performed using fluorescent microscope Olympus IX81.

Internalization studies by fluorescence spectrometry

Fluorescein-labeled cross-linked micelles loaded with Nile Red were diluted in culture media (final concentration: 0.5 mg/mL) and were incubated with MEL-5 cells for 0.5 h. After incubation, removal of attached micelles was accomplished by washing cells two times with culture medium and two times with phosphate buffered saline solution (PBS without Ca^{2+} and Mg^{2+}). Cells were then detached by trypsinization (trypsin in PBS). After centrifugation the

pellet was suspended in PBS. Analyses the internalized micelles were then performed using a fluorescence spectrometer Perkin Elmer VICTOR^3 1420.

Statistical analyses

Cell culture experiments were performed in triplicates. Results are presented as mean ± standard deviation. Statistical analyses of the data were performed using the unpaired, two-tailed, Student's *t*-test. Statistical significance was determined at a $p < 0.01$.

3. Results and discussion

Micelle formation and cross-linking

As previously described in the literature, amphiphilic block copolymers of PEO as hydrophilic shell and PTMC as hydrophobic core are frequently used in the building of stealthy nanocarriers [25]. In order to prevent the premature release of the encapsulated drug in the bloodstream due to high dilution, the core cross-linking of such micelles was considered. For this purpose, reactive copolymers have been used for micellization. Three reactive block copolymers with a similar composition but varying in their architecture, i.e. PEO-*b*-poly(TMC-*co*-$\alpha N_3\varepsilon$CL), PEO-*b*-PTMC-*b*-P($\alpha N_3\varepsilon$CL) and PEO-*b*-P($\alpha N_3\varepsilon$CL)-*b*-PTMC have thus been synthesized following a reported process. Their macromolecular characteristics are reported in Table 1 [26].

Table 1. Characteristics of the home-made reactive copolymers used in this study.

Copolymer architectures		*DP [a] PEO*	*DP [a] PTMC*	*DP [a]* P(αN$_3$CL)	*TMC/N$_3$-CL ratio (%)*	*M_w/M_n [b]*
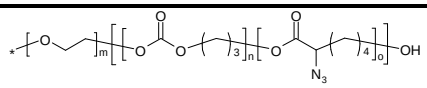 **PEO-*b*-poly(TMC-*co*-αN$_3$εCL)**	**(1)**	114	9	4	69/31	1.05
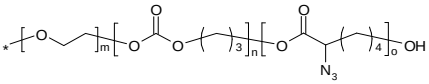 **PEO-*b*-PTMC-*b*-poly(αN$_3$εCL)**	**(2)**	114	10	5	66/34	1.05
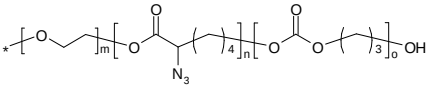 **PEO-*b*- poly(αN$_3$εCL)-*b*-PTMC**	**(3)**	114	10	6	63/37	1.10

[a] DP: number of monomers unit per chain, determined by ^{1}H NMR

[b] determined by SEC by using PS calibration

Well-defined copolymers have been obtained as evidenced by the narrow polydispersity, the controlled azide content and copolymer composition. By the introduction of the functional azido-caprolactone units, the hydrophobic PTMC block is easily made reactive. The three different localizations of the azide functions in the hydrophobic block will lead to three different core cross-linking: loose core cross-linking (i), tight core cross-linking (ii) and tight shell core-shell-corona system (iii) as it was the same for PCL based core cross-linked micelles [22].

The micellization of the three block copolymers was performed by dissolving them first in DMF, a good solvent for both the hydrophobic (PTMC and P(αN$_3$εCL)) and the hydrophilic (PEO) blocks followed by a rapidly addition of water which induces the micellization by precipitating selectively the hydrophobic blocks. After dialysis, the micelle size was characterized by dynamic light scattering (DLS). Results are summarized in table 2 and compared to PCL based copolymer micelles.

Table 2. DLS data for cross-linked and non cross-linked micelles of the various copolymers in water

	Copolymers	Non-cross-linked micelles		Cross-linked micelles	
		$D_{h,app}$ (nm) [a]	μ_2/Γ^2 [b]	$D_{h,app}$ (nm) [a]	μ_2/Γ^2 [b]
1	**PEO114-*b*-poly(TMC_9-*co*-$\alpha N_3\varepsilon CL_4$)**	44	0.22	58	0.16
2	**PEO114-*b*-$PTMC_{10}$-*b*-poly($\alpha N_3\varepsilon CL)_5$**	57	0.21	74	0.14
3	**PEO114-*b*-poly($\alpha N_3\varepsilon CL)_{10}$-*b*-$PTMC_6$**	52	0.23	60	0.16
	PEO_{114}-b-poly(CL_{10}-co-$\alpha N_3\varepsilon CL_7$)	32	0.09	37	0.07
	PEO_{114}-*b*-PCL_{11}-*b*-poly($\alpha N_3\varepsilon CL)_6$	29	0.14	43	0.16
	PEO_{114}-*b*-poly($\alpha N_3\varepsilon CL)_{10}$-*b*-$PCL_6$	33	0.13	36	0.11

Apparent hydrodynamic diameter [a] and PDI [b] determined by DLS

Micelles larger than those previously reported for PCL based copolymers of similar size and hydrophilic/lipophilic balance, were obtained. The immiscibility between the PTMC and the P($\alpha N_3\varepsilon CL$) blocks, together with the absence of dense crystalline zones, might account for this observation.

Then, the cross-linking of the azido functional hydrophobic core was carried out by copper mediated azide-alkyne cycloaddition (CuAAC) in similar condition similar to previously reported ones applied to PCL based copolymers [22]. The cross-linker, a bis alkyne molecule connected via a disulfide bridge [27], was directly added (0.6 mol equiv. vs. azide groups) to the DMF solution in order to be located in the hydrophobic core of the micelles swollen by the DMF. The click reaction, leading to the cross-linking of the micelles only occurs upon the addition of $CuSO_4$ and sodium ascorbate to the aqueous micellar solution. The effectiveness of the click reaction was firstly confirmed by the complete disappearance of the azide band at 2106 cm^{-1} in the IR spectrum which confirmed the good efficiency of the CuAAC reaction between the cross-linker and the azido functional micelles formed in the H_2O/DMF mixture. After reaction, copper is removed by complexation with EDTA followed by dialysis that also removes the remaining DMF.

As evidenced by DLS data reported in table 2, the micelle size increases of about 10-15 nm upon cross-linking in larger proportion than observed for the similar systems based on

PCL [22] rather than PTMC, and might be explained by the additional volume occupied by the cross-linker in the micelle core together with conformation modification caused by the triazole ring formation. Interestingly, larger micelle size and size increase were observed for the PTMC based micelles as compared to the PCL systems, which might be due to the more dynamic amorphous core of PTMC as compared to the denser semi-crystalline PCL cores [26]. The Figure 1 illustrates the well-defined distribution of the as-obtained cross-linked micelles and compared them to non-cross-linked micelles. Narrow polydispersities were recorded as summarized in the table 2.

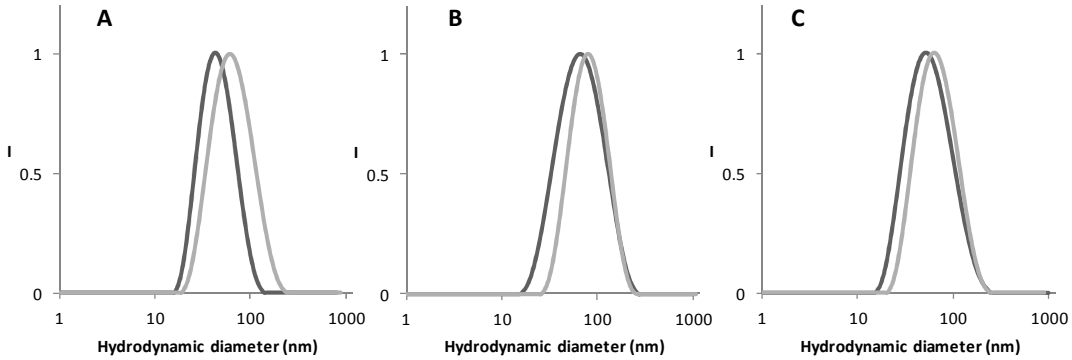

Figure 1. Size distribution of the cross-linked (grey) and non-cross-linked micelles (black) of copolymers **1** [A], **2** [B] and **3** [C] determined by DLS at an angle of 165° in water at a concentration of 1.5 mg/mL.

As illustrated in Figure 2, TEM images evidenced a spherical morphology for all the three different cross-linked micelles.

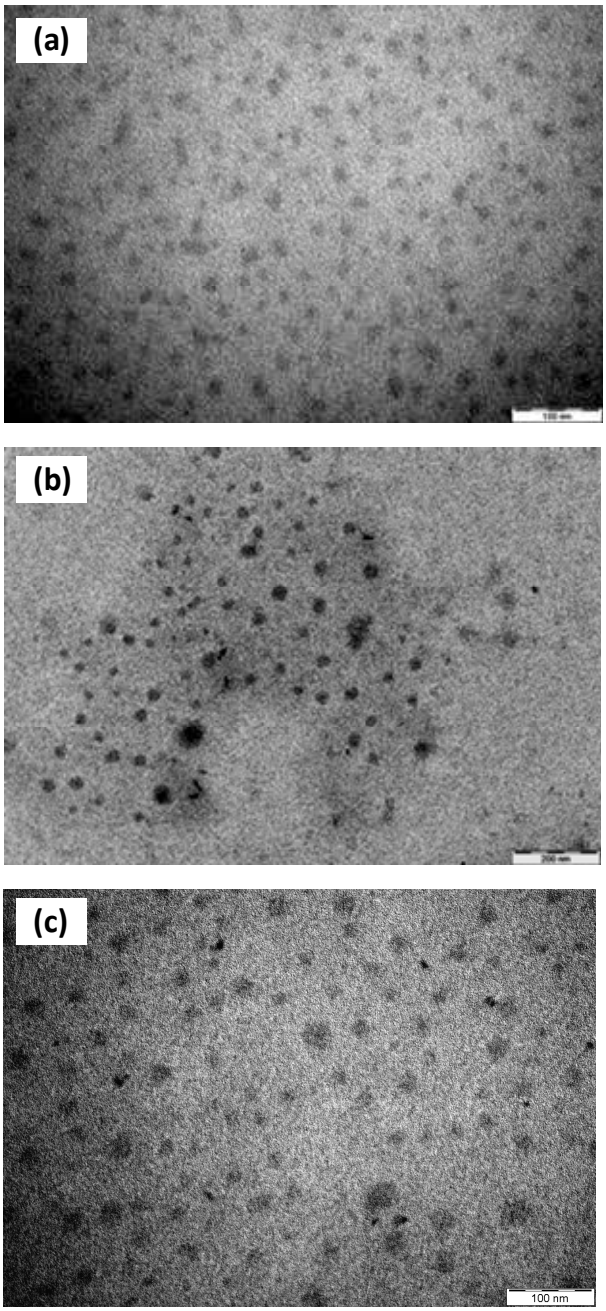

Figure 2. TEM images of cross-linked micelles obtained for copolymers **1** (a), **2** (b) and **3** (c**)**

Cross-linking efficiency was then evidenced by adding a 10-fold excess of DMF to the dialyzed systems. In these conditions, a complete dissociation was observed for the non cross-linked micelles due to the solubilization of both blocks of the azido-copolymers by DMF. In contrast, swollen nanogels are observed for the core cross-linked micelles with an average size ranging from 250 to 500 nm (Figure 3).

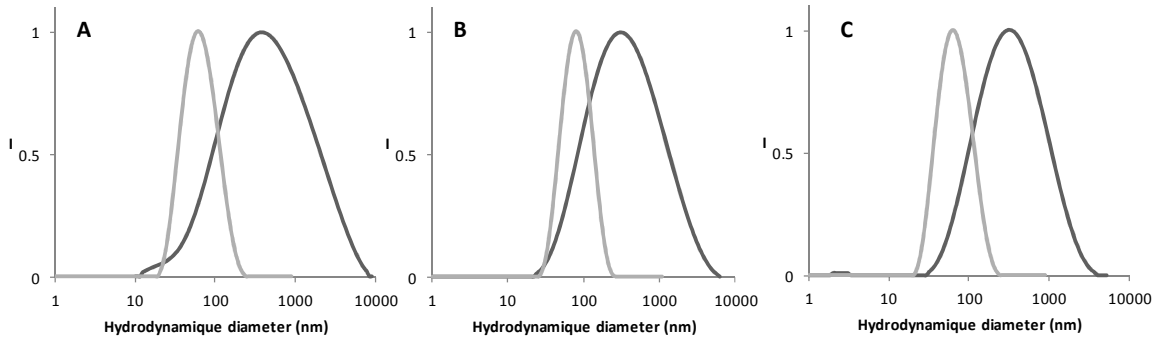

Figure 3. Size distribution of cross-linked micelles in water at a concentration of 1.5 mg/mL (grey) ; after 10-fold dilution with DMF (black) for copolymers **1** [A], **2** [B] and **3** [C].

In order to study the redox-reversibility of the cross-linking induced by the presence of the disulfide bridges, the behavior of the core cross-linked micelles was investigated in presence of DTT as a reducing agent. As expected, no significant change of size was observed upon DTT addition when the copolymer concentration remains above the CMC (in the range of 10^{-5} g/mL for PEO-*b*-P(CL-*co*-TMC) [24]), but the diffused light intensity measured by DLS decreases significantly in diluted media below the CMC. Similar observations were previously observed for PCL based core cross-linked micelles [22]. Moreover, the addition of DTT, working at high concentrations in DMF, provokes the nanogel destabilization even if not completely, as indicated by the reduction of the diffused intensity of about 3-folds. All these observations demonstrate the success of the cross-linking and its reversibility whatever the kind of investigated copolymers.

Stealth properties of the cross-linked micelles

In order to evaluate the foreseen long-circulating properties of the cross-linked micelles in the bloodstream, *in vitro* study of the complement activation by the cross-linked micelles was performed by the quantitative CH50 test [29]. Indeed, after their administration in the bloodstream, the immune system tries to remove foreign bodies by opsonisation. However, complement protein adsorption, the first step of this process, is expected to be limited on PEO decorated nanocarriers [28,32-33]. The complement consumption, i.e. the amount of complement protein adsorbed on the nanocarrier surface, was quantified by the lytic capacity of serum (amount of CH50 units) towards antibody-sensitized sheep erythrocytes after exposure to the micelles. After centrifugation of the unbroken erythrocytes, the released hemoglobin from the broken ones can be used as a dye for colorimetric titration. The CH50 unit is the concentration expressed by mL of serum of complement units able to cause 50% haemolysis of a fixed volume of sheep red cells. Experimental results are expressed as the percentage of the CH50 units consumed as a function of the micelle surface (Figure 4).

The three different types of core cross-linked micelles exhibit a slow activation of the complement. As expected, higher is surface area in contact with proteins, higher is the CH50 consumption. The protein repellency is mainly governed by the PEO corona, its rapid changes of conformation preventing their adsorption. So, it is not surprising that the different core cross-linked micelles exhibit a similar behavior since they mainly differ by their hydrophobic core rather than their hydrophilic PEO shell. The faster complement activation for the micelles of copolymer (**2)** as compared to the micelles of copolymers (**1)** and (**3)** is mainly explained by the higher size of these micelles. Similar results were previously observed for the PCL based cross-linked micelles [22].

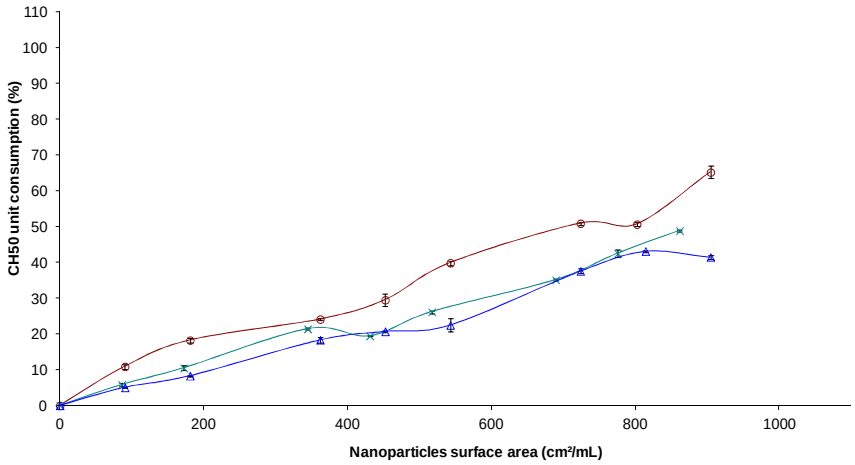

Figure 4. Consumption of CH50 versus surface area of cross-linked micelles of copolymers **1** (—×—), **2** (—o—) and **3** (—△—)

Cytotoxicity

The biocompatibility of the different micelles was evaluated *in vitro* by cytotoxicity tests (MTT) using MEL-5 melanoma cells. Figures 5 a and b show the percentage of survival cells treated with 0.5 to 2 mg/mL of the three kinds of micelles after 24 and 48 hours of incubation. All these cross-linked micelles show a low *in vitro* cytotoxicity at a concentration of 0.5 mg/mL where more than 70% of survival cells were still observed. The percentage of survival cells fall down to 20% when higher concentrations than 1.5 mg/mL were used. After 48 hours of incubation, the percentage of survival cells decreased to about 40% at the lower concentration of 0.5 mg/mL except for the copolymer **2** where still 70% of survival cells were still observed. These cytotoxicity results are comparable to other polymer micelles, which beneficiate of PEO corona to reduce cytotoxic effects and more particularly to the PCL-based core cross-linked micelles previously described [23,34].

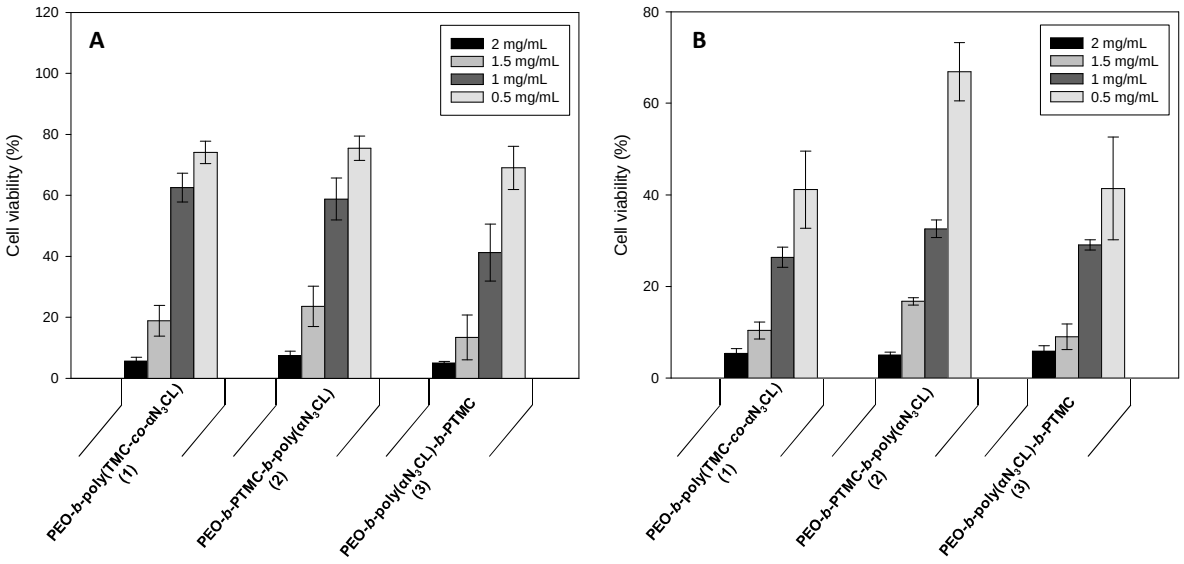

Figure 5. Cell viability in the presence of cross-linked micelles of copolymers **1**, **2** and **3** in MEL-5 cell culture after (**A**) 24 hours and (**B**) 48 hours of incubation

The Figure 6 compares the viability of MEL-5 cells treated with cross-linked and non cross-linked micelles after (**A**) 24 and (**B**) 48 hours of incubation. The substitution of the azide present in the micelle core does not increase the cytotoxicity of the nanocarriers cross-linked by CuAAC.

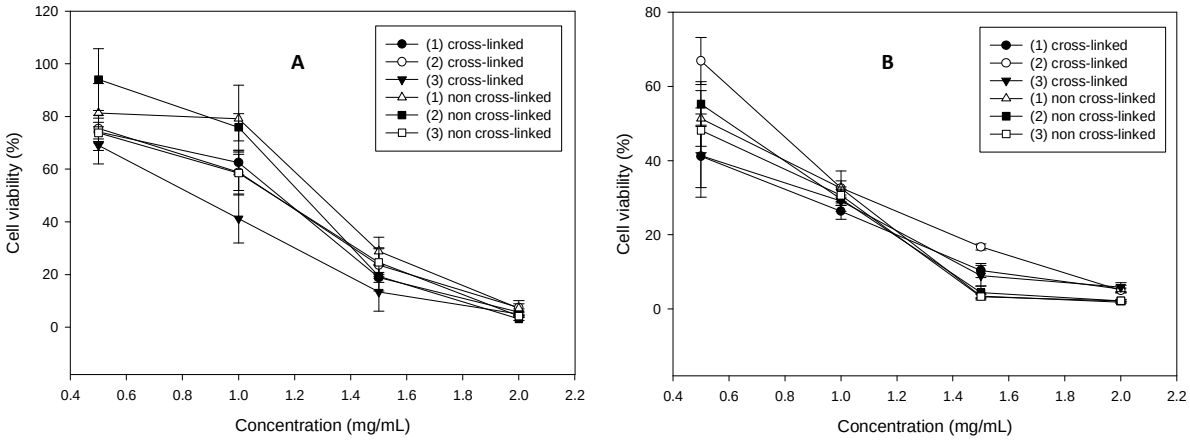

Figure 6. Cell viability in function of the concentration of cross-linked and non cross-linked micelles in MEL-5 cell culture after (**A**) 24 and (**B**) 48 hours of incubation

Micelle uptake

The *in vitro* micelle uptake was evaluated on MEL-5 cells at a concentration of 0.5 mg/mL and 0.5 hours of incubation. For this purpose, Fluorescein-labeled copolymers were used to form micelles and Nile Red was encapsulated in the hydrophobic core as model molecule of a poorly water soluble drug. Thus, the use of an encapsulated dye and another attached to the copolymer micelles would afford getting information on the localization of the release of the hypothetic drug encapsulated in the micelles and micelles themselves.

The micelle uptake on MEL-5 cells was quantified by fluorescence spectrometry. The percentage of internalization was calculated from the fluorescence intensity of the cells after incubation in presence of Fluorescein-labeled cross-linked micelles loaded with Nile Red. The Figure 7 shows the percentage of internalization after 0.5 hours of incubation at a concentration of 0.5 mg/mL. Comparative values were obtained for the three kinds of copolymer architecture. About 1% of internalization was observed when detecting at the Fluorescein emission wavelength. This low percentage of internalization is typical for pegylated systems without targeting moieties at the micelle surface presenting only neutral hydrophilic block of poly(ethylene oxide). Significant differences were observed when measuring at the Nile Red emission wavelength. In that case, about 8% of internalization was measured. That can be explained by internalization of free Nile Red independently of the micelles showing that even if the micelles are cross-linked, Nile Red can escape the micelles and rapidly enter the cells. Compared to PCL based cross-linked micelles previously studied, larger amount of Nile Red seems to be prematurely released from the PTMC cross-linked micelles for the three different macromolecular architectures as observed for the high percentage of internalization recorded when measuring at the Nile Red emission wavelength. Indeed, about 1 % of internalization was previously observed for the PCL cross-linked micelles at the Nile Red and Fluorescein emission wavelength excepted for the PEO-*b*-PCL-*b*-poly(αN_3CL) cross-linked system with about 3% of internalization [23]. Cross-linked PTMC-systems appear thus to retain less efficiently the Nile Red than the PCL systems.

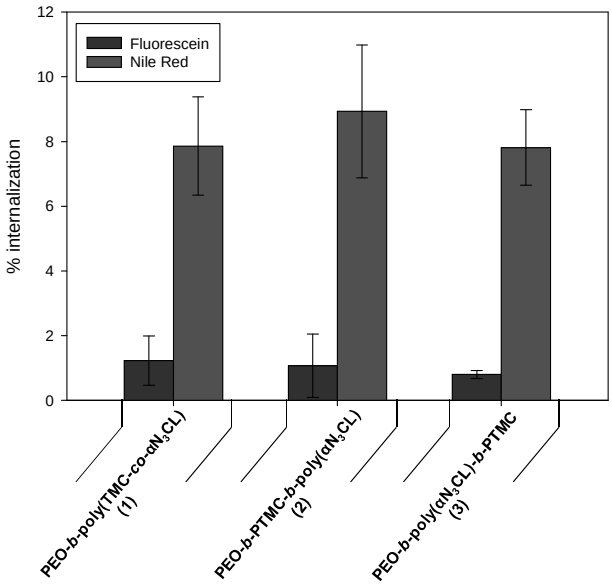

Figure 7. Micelle uptake by MEL-5 cells at a concentration of 0.5 mg/mL determined by fluorescent spectroscopy after 0.5 hours of incubation.

Fluorescence spectroscopy would afford getting information on the localization of the micelles and the dyes inside the cells and giving clarity whether the micelles are at the surface or are actually internalized. Fluorescence microscopy attests the successful internalization of the cross-linked micelles after limited concentration and time of incubation (Figure 8). The red area are due to the fluorescence emission of the Nile Red, the green ones are that of Fluorescein which labeled the copolymers while the cell nuclei has been stained in blue. Uniform distribution of the Nile Red is observed in the cytoplasm of the cells but not inside the nuclei. This is also observed for Fluorescein, except that the nuclei of the cells are also marked by the Fluorescein. Green fluorescence of the cells allows confirming the internalization of the micelles and not of Nile Red only. If free Nile Red can penetrate the cells, this experiment clearly demonstrate the presence of micelle intracellularly. The uniform repartition of the Nile Red in the cytoplasm as the presence of the Fluorescein labeled copolymer in the nuclei may indicated that the reductive environment of the cytoplasm allows the micelle dissociation by reduction of the disulfide bridges which leads to the release of the Nile Red. The dissociation of the micelles was also confirmed by the presence of the

Fluorescein-labeled copolymer in the nuclei independently of the Nile Red. These results are similar to those obtained with PCL based cross-linked micelles previously studied showing low but clear cell internalization of these three pegylated systems [23]. In case of PTMC, however, no significant differences are observed between the three different copolymers.

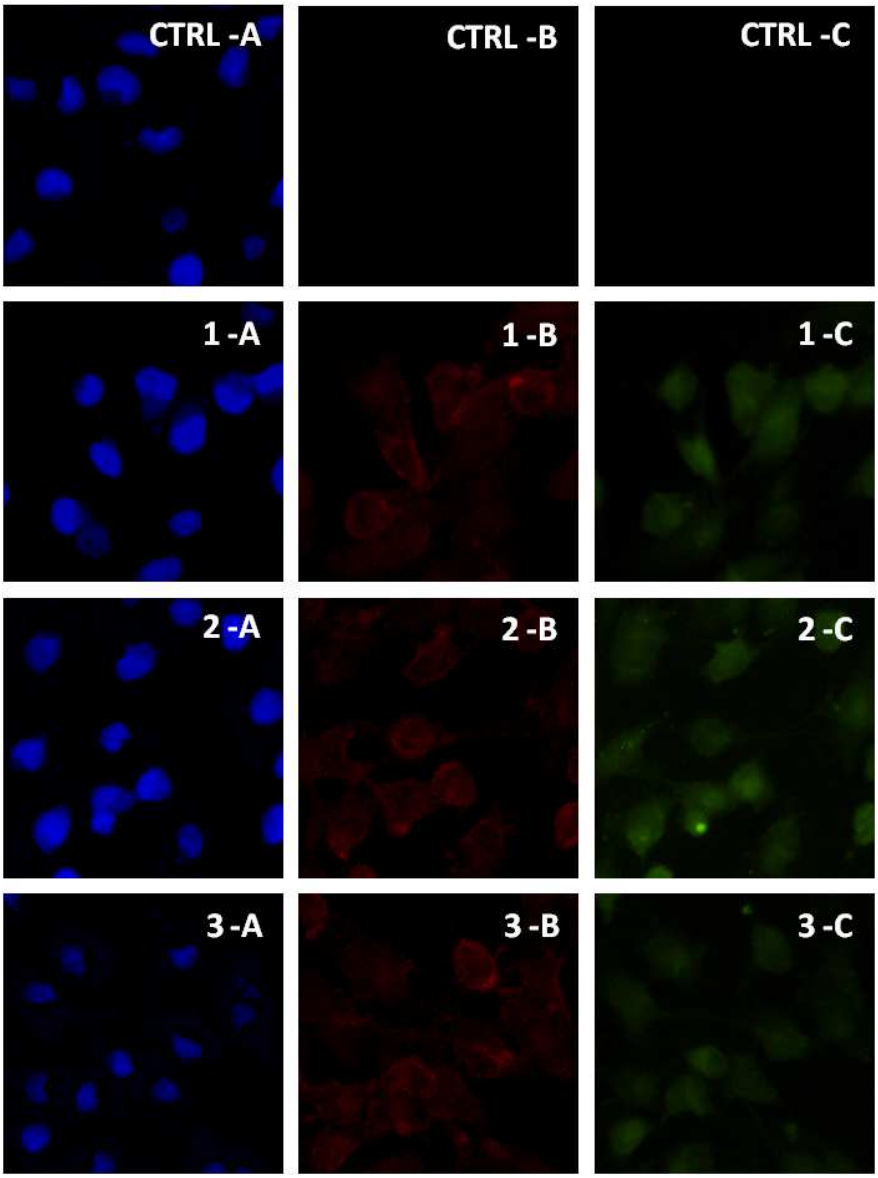

Figure 8. Fluorescence microscopy images of B16 cells incubated 0.5 hours with cross-linked micelles of copolymers **1**, **2** and **3** at a concentration of 0.5 mg/mL. Hoechst staining (**A**: blue filter, **B**: red filter and **C**: green filter) and the control (CTRL) incubated without micelles.

4. Conclusions

In this study, novel reversibly core cross-linked micelles based on poly(trimethylene carbonate) have been investigated as new smart drug delivery systems. Stable and reversible core cross-linked micelles were obtained by copper mediated alkyne azide cycloaddition of a disulfide bearing cross-linker with the azide groups present in the micelle core. Well-defined micelles were obtained and exhibited few interactions with proteins due to the presence of the PEO shell. Moreover, the three different kind of micelles designed present a low cytotoxicity and are able to be internalized in tumor cells without the presence of a targeting moiety. The immiscibility of the PTMC and the P($\alpha N_3 \varepsilon$CL) allows to form core cross-linked micelles with different properties in solution than more conventional PCL based micelles. Indeed, the stability of PTMC based-micelles seems to be lower than the one of PCL-based micelles of comparable HLB, as demonstrated by the premature release of Nile Red in the cellular-uptake studies. This could be accounted for lack of cristallinity of the micellar core in case of PTMC copolymers.

5. References

1. Sawant, R. M.; Hurley, J. P.; Salmaso, S.; Kale, A.; Tolcheva, E.; Levchenko, T. S.; Torchilin, V. P. *Bioconjugate Chemistry* **2006**, *17*, 943.

2. Lee, E. S.; Na, K.; Bae, Y. H. *Nano Letters* **2005**, *5*, 325.

3. Gabizon, A. A. *Advanced Drug Delivery Reviews* **1995**, *16*, 285.

4. Nishiyama, N.; Bae, Y.; Miyata, K.; Fukushima, S.; Kataoka, K. *Drug Discovery Today: Technologies* **2005**, *2*, 21.

5. Kwon, G. S.; Okano, T. *Advanced Drug Delivery Reviews* **1996**, *21*, 107.

6. Veronese, F. M.; Pasut, G. *Drug Discovery Today* **2005**, *10*, 1451.

7. Maeda, H.; Wu, J.; Sawa, T.; Matsumura, Y.; Hori, K. *Journal of Controlled Release* **2000**, *65*, 271.

8. Iyer, A. K.; Khaled, G.; Fang, J.; Maeda, H. *Drug Discovery Today* **2006**, *11*, 812.

9. Yoo, H. S.; Park, T. G. *Journal of Controlled Release* **2004**, *96*, 273.

10. Torchilin, V. P. *Cellular and Molecular Life Sciences* **2004**, *61*, 2549.

11. Van Butsele, K.; Fustin, C. A.; Gohy, J. F.; Jérôme, R.; Jérôme, C. *Langmuir* **2009**, *25*, 107.

12. Lee, S. C.; Kim, K. J.; Jeong, Y.-K.; Chang, J. H.; Choi, J. *Macromolecules* **2005**, *38*, 9291.

13. Gu, J.; Cheng, W.-P.; Liu, J.; Lo, S.-Y.; Smith, D.; Qu, X.; Yang, Z. *Biomacromolecules* **2008**, *9*, 255.

14. Lee, E. S.; Na, K.; Bae, Y. H. *Nano Letters* **2005**, *5*, 325.

15. Sawant, R. M.; Hurley, J. P.; Salmaso, S.; Kale, A.; Tolcheva, E.; Levchenko, T. S.; Torchilin, V. P. *Bioconjugate Chemistry* **2006**, *17*, 943.

16. Lee, E. S.; Shin, H. J.; Na, K.; Bae, Y. H. *Journal of Controlled Release* **2003**, *90*, 363.

17. Wang, Y.; Chen, P.; Shen, J. *Biomaterials* **2006**, *27*, 5292.

18. Kakizawa, Y.; Harada, A.; Kataoka, K. *Biomacromolecules* **2001**, *2*, 491.

19. Meister, A.; Anderson, M. E. *Annual Review of Biochemistry* **1983**, *52*, 711.

20. Saito, G.; Swanson, J. A.; Lee, K.-D. *Advanced Drug Delivery Reviews* **2003**, *55*, 199.

21. Aliabadi, H. M.; Elhasi, S.; Mahmud, A.; Gulamhusein, R.; Mahdipoor, P.; Lavasanifar, A. *International Journal of Pharmaceutics* **2007**, *329*, 158.

22. Cajot, S.; Lautram, N.; Passirani, C.; Jerome, C. *Journal of Controlled Release* **2011**, *152*, 30.

23. Cajot, S.; Schol, D.; Danhier, F.; Preat, V.; Gillet De pauw, M.-C.; Jérôme, C. *in submission* **2012**.

24. Ould-Ouali, L.; Arien, A.; Rosenblatt, J.; Nathan, A.; Twaddle, P.; Matalenas, T.; Borgia, M.; Arnold, S.; Leroy, D.; Dinguizli, M.; Rouxhet, L.; Brewster, M.; Preat, V. *Pharmaceutical Research* **2004**, *21*, 1581.

25. Ould-Ouali, L.; Noppe, M.; Langlois, X.; Willems, B.; Te Riele, P.; Timmerman, P.; Brewster, M. E.; Arien, A.; Preat, V. *Journal of Controlled Release* **2005**, *102*, 657.

26. Cajot, S.; Lecomte, P.; Jérôme, C.; Riva, R. *in submission* **2012**.

27. Gao, H.; Matyjaszewski, K. *Macromolecules* **2006**, *39*, 4960.

28. Gref, R.; Luck, M.; Quellec, P.; Marchand, M.; Dellacherie, E.; Harnisch, S.; Blunk, T.; Muller, R. H. *Colloids and Surfaces, B: Biointerfaces* **2000**, *18*, 301.

29. Passirani, C.; Benoit, J.-P. *Biomaterials for Delivery and Targeting of Proteins and Nucleic Acids* **2005**, 187.

30. Kabat, E. A.; Mayer, M. M. *Experimental Immunochemistry. 2nd ed*, 1961.

31. Vittaz, M.; Bazile, D.; Spenlehauer, G.; Verrecchia, T.; Veillard, M.; Puisieux, F.; Labarre, D. *Biomaterials* **1996**, *17*, 1575.

32. Vermette, P.; Meagher, L. *Colloids Surf., B* **2003**, *28*, 153.

33. Lee, J. H.; Oh, S. H. *Journal of Biomedical Materials Research* **2002**, *60*, 44.

34. Lin, W.-J.; Chen, Y.-C.; Lin, C.-C.; Chen, C.-F.; Chen, J.-W. *Journal of Biomedical Materials Research, Part B: Applied Biomaterials* **2006**, *77B*, 188.

GENERAL CONCLUSIONS AND PERSPECTIVES

General conclusions

Since few years, researches on the development of new drug delivery systems have a growing interest. Indeed, the last knowledges in the design of new macromolecular architectures but also their behaviors in the body have contributed to obtain systems with better therapeutic effects and a diminution of undesirable side effects. This thesis aims at reporting the synthesis of new macromolecular architectures in order to stabilize PLA nanoparticles or in order to form stabilized micelles by the core cross-linking (Scheme 1).

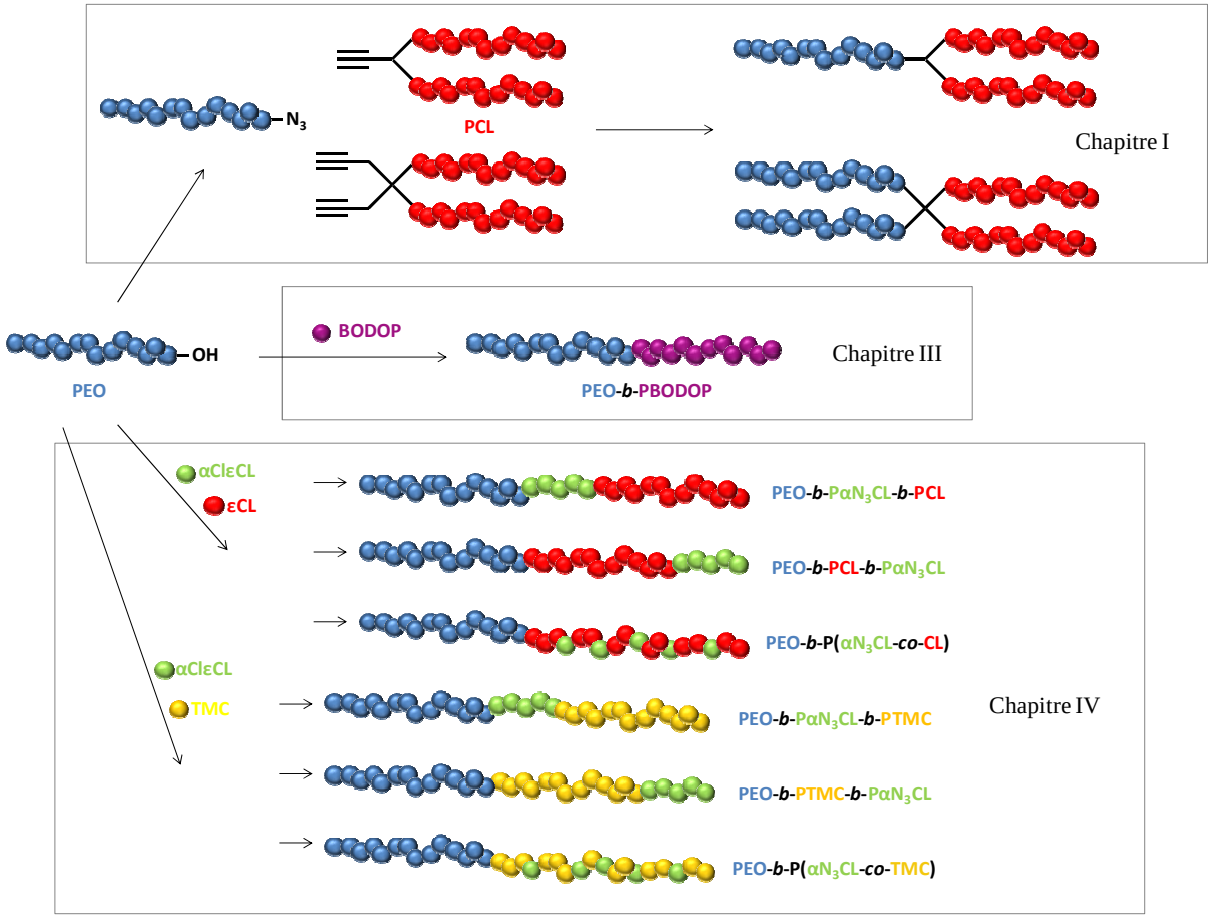

Scheme 1. Schematic illustration of new macromolecular architectures

In order to reach stealthy nanoparticles, all the designed macromolecular architectures are composed a hydrophilic block of poly(ethylene oxide) (PEO) well known for its ability to

repel proteins while the different hydrophobic blocks are combinations of polyesters as poly(ε-caprolactone) (PCL) or poly(α-chloro-ε-caprolactone) poly(αClεCL), of polyphosphate, the poly(2-(but-3-en-1-yloxy)-1,3,2 dioxaphospholane 2-oxide) (PBODOP) and of polycarbonate, the polytrimethylene carbonate (PTMC). These different hydrophobic polymers have been chosen due to their ability to be degraded in low acidic conditions and so, to prevent an accumulation of polymers in the body if repeated injections are required. The functional poly(αClεCL) and PBODOP have been used in order to easily functionalize the hydrophobic block and more particularly to cross-link this one.

The syntheses of the different macromolecular architectures described in the thesis are summarized in this section as their micellization in aqueous media. A major part of this work was dedicated to the development of reversibly core cross-linked micelles by the introduction of disulfide bridges in the hydrophobic block. Their increasing stability, as their reversibility in function of the redox environment, was investigated such as their long circulation properties, their cytotoxicity and the cellular uptake. The main results obtained are summarized here after.

Synthesis of amphiphilic mikto-arm star-shaped copolymers of PEO and PCL

Two different amphiphilic mikto-arm star-shaped copolymers were synthesized by controlled ring opening polymerization and composed of two arms of PCL (A) and one (A_2B_1) or two (A_2B_2) arms of PEO (B). Indeed, the polymerization of ε-caprolactone was initiated by two different diols functionalized by one and two alkyne functions to respectively reach mono-alkyne-PCL (PCL-$(alkyne)_1$) and bis-alkyne-PCL (PCL-$(alkyne)_2$). The final mikto-arm star-shaped copolymers $(PCL)_2$-PEO and $(PCL)_2$-$(PEO)_2$ were obtained by copper mediated alkyne azide cycloaddition (CuAAC) with a ω-azido terminated-poly(ethylene oxide). Expected molecular characteristics, narrow molecular weight distributions and quantitative coupling reactions were accordingly obtained and summarized in the table 1.

Synthesis of amphiphilic block copolymer of PEO and PBODOP

The amphiphilic block copolymer PEO-*b*-PBODOP were synthesized by ring opening polymerization of a new alkene bearing cyclic polyphosphate monomer, the BODOP, from a macroinitiator of monomethoxy poly(ethylene oxide). This new monomer was synthesized by the substitution of 2-chloro-1,3,2-dioxaphospholane 2-oxide by 3-buten-1-ol. Its well defined synthesis allows to obtain controlled homopolymers with expected molecular characteristics and narrow molecular weight distribution as summarized in the table 1. Nevertheless, a poor control of the copolymerization was obtained from the macro-initiator of PEO as presented on the SEC profile. More investigations will be required in the future to obtain a better control of the copolymerization.

Synthesis of various block copolymer architectures composed of PEO, PCL, PTMC and azido functional PCL

Three different block copolymer architectures composed of PEO, PCL and azido functional PCL were obtained by ring opening polymerization of ε-caprolactone and α-chloro-ε-caprolactone from a macroinitiator of monomethoxy poly(ethylene oxide). While a block copolymer composed of a hydrophilic block of PEO and a statistic hydrophobic block of PCL and P(αClεCL), PEO-*b*-poly(αClεCL-*co*-CL), was obtained when monomers are added at the same time, triblock copolymers PEO-*b*-PCL-*b*-poly(αClεCL) and PEO-*b*-poly(αClεCL)-*b*-PCL were obtained when monomers are sequentially added. Expected molecular characteristics and narrow molecular weight distributions were obtained in presence of tin based catalyst. Obtained copolymers are summarized in table 1.

A quantitative substitution of the chloride functions by azide was performed under mild conditions in presence of sodium azide preventing possible degradation of the previous synthesized copolymers.

The substitution of the PTMC for PCL allows obtaining similar block copolymer architectures with a same control of the macromolecular parameters as summarized in table 1.

Table 1. Macromolecular characteristics of the different copolymer architectures, PDI, HLB and DLS data.

Polymers	M_n PEO[a]	M_n PCL[a]	M_n PTMC[a]	M_n P(αClεCL)[a]	M_n PBODOP[a]	PDI[b]	HLB[c]	D_h (nm) un[d]	D_h (nm) cross[d]
$(PCL_9)_2$-$(PEO_{48})_1$	2100	2100	-	-	-	1.13	10	18.6	-
$(PCL_{10})_2$-$(PEO_{28})_2$	2500	2400	-	-	-	1.16	10.2	18.4	-
$(PCL_{10})_2$-$(PEO_{48})_2$	4200	2400	-	-	-	1.19	12.7	19.9	-
$PBODOP_{50}$	-	-	-	-	8900	1.15	-	-	-
$MPEO_{114}$-*b*-$PBODOP_{10}$	5000	-	-	-	3200	1.37	12.2	100	90
$MPEO_{114}$-*b*-poly(εCL$_{13}$-*co*-αClεCL$_4$)	5000	1500	-	600	-	1.10	14.1	41	48
$MPEO_{114}$-*b*-poly(εCL$_{10}$-*co*-αClεCL$_7$)	5000	1100	-	1000	-	1.10	14.1	32	37
$MPEO_{114}$-*b*-PCL_{12}-*b*-poly(αClεCL)$_3$	5000	1400	-	400	-	1.05	14.7	30	36
$MPEO_{114}$-*b*-PCL_{11}-*b*-poly(αClεCL)$_6$	5000	1300	-	900	-	1.10	13.9	29	43
$MPEO_{114}$-*b*- poly(αClεCL)$_5$-*b*-PCL_{12}	5000	1400	-	700	-	1.05	14.1	30	38
$MPEO_{114}$-*b*- poly(αClεCL)$_6$-*b*-PCL_{10}	5000	1100	-	800	-	1.10	14.5	33	36
$MPEO_{114}$-*b*-poly(αClεCL$_4$-*co*-TMC_9)	5000	-	900	600	-	1.05	15.4	44	58
$MPEO_{114}$-*b*-$PTMC_{10}$-*b*-poly(αClεCL)$_5$	5000	-	1000	700	-	1.05	14.9	57	74
$MPEO_{114}$-*b*-poly(αClεCL)$_6$-*b*-$PTMC_{10}$	5000	-	1000	900	-	1.10	14.5	52	60

[a] Experimental molar mass determined by ^{1}H NMR
[b] Polydispersity index measured by SEC (PS calibration)
[c] Hydrophilic-Lypophilic Balance
[d] Apparent hydrodynamic diameter determined by DLS

Formation of stealthy nano-objects in aqueous solution

The new macromolecular architectures designed along that thesis are not able to spontaneously self-assembly in water and require to be firstly dissolved in a common solvent of the hydrophilic and hydrophobic blocks of the amphiphilic copolymers considered to allow their dissolution.

Additionally to their micellization, and despite of the lack of functionalization of their structure, amphiphilic mikto-arm star-shaped copolymers based on PEO and PCL described in that thesis are also able to stabilize PLA nanoparticles (Chapter I).

In order to increase the stability of the micelles formed in solution, a specific attention was paid to the cross-linking of the micelle core. Due to the presence of vinyl groups along the hydrophobic block of the PEO-*b*-PBODOP amphiphilic block copolymers, a photo cross-linking of the micelle core was investigated under UV irradiation (Chapter III). Another strategy was investigated for the azido-functional copolymers in order to reversibly cross-link the micelle core by the addition of a cross-linker bearing disulfide bridges which could be reduced in a second time to destabilize the micelle in the specific condition of the cytoplasm (Chapter V and VII).

Long-circulation properties, release profile, cytotoxicity and cellular internalization

The evaluation of the long-circulation properties of the cross-linked azido-PCL and PTMC based copolymer micelles were investigated by the *in vitro* CH50 test. Due to the presence of a PEO shell, the core cross-linked micelles exhibited few interactions with complement proteins making these micelles stealthy.

The ability of the core cross-linked PCL based micelles to be destabilized in reductive environment was evaluated by the release of a hydrophobic dye, the Nile Red. At high concentration, micelles remain stables and limit the release of the dye while a rapid release was observed at lower concentration (below the CMC) due to the destabilization of the micelles after the de-cross-linking.

The low *in vitro* cytotoxicity of the PCL and PTMC based cross-linked micelles confirmed their ability to be safely used for biomedical applications. Moreover, cellular

uptake studies allow to confirm the possible internalization of the concerned cross-linked micelles in cancer cells after their accumulation in solid tumors by the EPR effect even if they do not beneficiate of targeting moieties at their surface.

Perspectives

In addition to the results reported in this thesis, some improvements could be mentioned, especially on the design of the reversibly core-cross-linked micelles, in order to reach better therapeutic activities. Some important prospects are mentioned hereafter.

- A first study of tumor growth was performed on mice in order to study the ability of reversibly core cross-linked micelles to passively target tumor and intracellularly control the release of a drug. Paclitaxel, a mitotic inhibitor used in cancer chemotherapy, was encapsulated in the core of PCL-based cross-linked micelles and were intravenously administrated in mice. Results obtained were compared to non cross-linked Paclitaxel charged micelles and uncharged non cross-linked micelles. While no mice death was observed along the test due to the good biocompatibility of the studied micelles, no diminution of the tumor size and no significant results were observed due to the too low content of Paclitaxel charged in micelles which was lower than the therapeutic dose. So, it would be interesting to increase the content of Paclitaxel in the micelles by an increasing of the molecular weight of the hydrophobic block of the cross-linked micelles.
- It was shown that the percentages of internalized micelles in tumor cells are quite low. Indeed, the absence of targeting moieties is responsible of that observation. It would be interesting to add a targeting moiety at the periphery of the core cross-linked micelles whose exposition would be pH-dependant. Thereby, a specific targeting of tumor would be possible due to the lower pH in the surrounding of the tumor. The Scheme 2 describes the use of a hydrolysable linker on a nanocarrier whose the diminution of the pH allows the de-shielding of the targeting moieties at the surface of

the nanocarrier while these ones are not exposed at physiological pH. Moreover, the reduction of the disulfide bridges present in the core of the nanocarrier allows their dissociation in the cytoplasm of the cell in order to release the encapsulated drug. Experiments were carried out on the synthesis of a block copolymer of PEO-*b*-PCL bearing an imine benzoic group as hydrolysable linker at the interface of the hydrophilic and hydrophobic blocks. However, this copolymer lacks of stability and requires the synthesis of a second copolymer of PEO-*b*-PCL bearing a functional group at the α position in order to graft the targeting moiety. This step is quite touchy and requires protective and deprotective reactions.

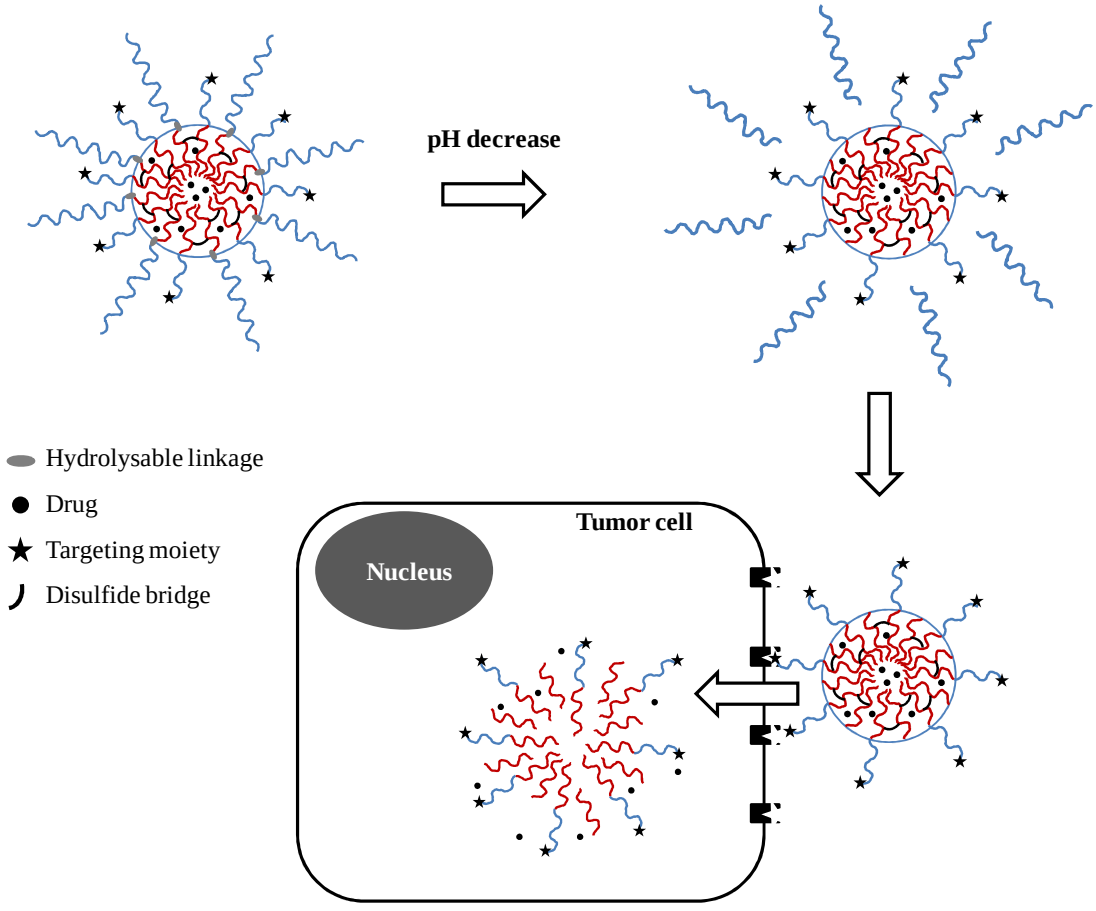

Scheme 2. Schematic illustration of pH-sensitive disulfide core cross-linked micelles.

- According to internalization microscopy data, it seems that the copolymer manage to reach nuclei of tumor cells. It would be interesting to link a drug to the copolymer, used as a prodrug, which could directly act in the nucleus. A mixed system combining

an encapsulated drug and another one linked to the copolymer could be interesting to obtain a double action, one in the cytoplasm and one in the nucleus.

* * *